THE EFF
MODEL
ON ELAST

This thesis

nden scattering at e

mance (E_π = 100-

investigates the effect

ating on resonant ela

sidered are ^{3}He, ^{12}C

The basic app

the exact numerical

proximations which

ce numerical results.

ained which contain

Nucleon model

e independent parti

ously. This exact

with three existing mod

The existing models all

ld one of them give

nerical model. By s

ABSTRACT

THE EFFECT OF INTERNAL NUCLEON
MOTION AND NUCLEAR BINDING
ON ELASTIC PION-NUCLEUS SCATTERING

By

Kenneth E. Gilbert

This thesis is a theoretical study of elastic pion-nucleus scattering at energies near the pion-nucleon (3,3) resonance (E_π = 100-300 MeV). Specifically, the work investigates the effect of internal nucleon motion and nuclear binding on resonant elastic pion-nucleus scattering. The nuclei considered are ^{4}He, ^{12}C, and ^{16}O.

The basic approach is first to calculate the effects using exact numerical methods and then to develop analytic approximations which take into account the main features of the numerical results. In all cases, an optical potential is obtained which contains no adjustable parameters.

Nucleon motion effects are calculated exactly using an independent particle model for ^{4}He and the free pion-nucleon t-matrix. This exact model, which is numerical, is compared with three existing models for pion-nucleus elastic scattering. The existing models all treat nucleon motion in an ad hoc way and none of them give satisfactory agreement with the exact numerical model. By systematically approximating the multiple

impels required in t

developed. The impr

with the exact num

required understandi

The nucleon n

use of ^{12}C and ^{16}O an

ta for all three nucl

in triplet equivalen

for the ^{4}He data and

We conclude

it should be accumulat

lar to spurious reac

Nuclear blurr

ual for ^{4}He. The tar

le nucleus by an s-wa

ual state at -20 Mev

tively small and

ivals. By extending

d states, an up

the individual lin

at about twice as lar

After generat

of ^{12}C and ^{16}O, the re

tively small blurr

und to be compatible

integrals required in the exact model, an improved analytic model is developed. The improved analytic model gives excellent agreement with the exact numerical model and, in addition, allows a transparent understanding of the main effects of nucleon motion.

The nucleon motion model for ^{4}He is generalized for the cases of ^{12}C and ^{16}O and a comparison is made with experimental data for all three nuclei. Both the exact numerical model and its analytic equivalent give significantly improved agreement with the ^{4}He data and good agreement with the ^{12}C and ^{16}O data.

We conclude that nucleon motion effects are significant and should be accurately accounted for since ad hoc treatments can lead to spurious results.

Nuclear binding effects are calculated using a 3-body model for ^{4}He. The target nucleon is bound to the rest of the ^{4}He nucleus by an s-wave separable potential which has a single bound state at -20 MeV. In this model, binding effects are relatively small and can be approximated with a simple analytic formula. By extending the formula to include an infinite number of bound states, an upper limit on binding effects is estimated. In this unphysical limiting case, the effects of nuclear binding are about twice as large as in the single-state case.

After generalizing the ^{4}He 3-body model for the cases of ^{12}C and ^{16}O, the results are compared with experiment. The relatively small binding effect in the single-state model is found to be compatible with the experimental data. However,

the empirical poi

our agreement with

We conclu

effect in resonant

the unphysical model with an infinite number of bound states gives poor agreement with experiment.

We conclude that nuclear binding is a relatively small effect in resonant elastic pion-nucleus scattering.

THE E

V.T

OF ELAC

V

D

1

THE EFFECT OF INTERNAL NUCLEON MOTION AND NUCLEAR BINDING ON ELASTIC PION-NUCLEUS SCATTERING

By

Kenneth E. Gilbert

A THESIS

Submitted to
Michigan State University
in partial fulfillment of the requirements
for the degree of

DOCTOR OF PHILOSOPHY

Department of Physics

1976

I would li

Remington, for s

rough some difficu

ist of Professors J

ful suggestions.

I gratefu

puting facilities

laboratory and the s

I also thank Drs. P.

ip with computer c

The Center

or printing the thr

Most of t

ssistance and unders

ACKNOWLEDGMENTS

I would like to thank my advisor, Professor J. H. Hetherington, for suggesting this problem and for helping me through some difficult periods in the work. I am grateful also to Professors J. Borysowicz and H. McManus for many helpful suggestions.

I gratefully acknowledge the use of the excellent computing facilities of the Michigan State University Cyclotron Laboratory and the able assistance of the computer staff. I also thank Drs. R. R. Doering and W. F. Steele for generous help with computer codes.

The Center for Naval Analyses is very much thanked for printing the thesis.

Most of all I want to thank my wife, Lynn, for her patience and understanding. This thesis is dedicated to her.

TABLE OF CONTENTS

Chapter

APPENDICES

APPENDICES

Table

5. A compar
in the c
modified
Rutgerwald

LIST OF TABLES

Figure

5.1 The relati
momenta in
momentum

5.2 Graphical
mations wo
(SSA), mod
the Kujawsk
for $|\underset{\sim}{P}_T|$

5.3 The real a
pion-nucle
of the scat
angle calc
the effect
tion of th
dash line,
(c) (dot-da
(MSA). Th
is 110 MeV

5.4 As in Figu
strong dow
part of th

5.5 As in Figu

5.6 The real a
nucleon in
cosine of
calculate
effective
of the in
the Kujaw
case (a),
is 110 Me

5.7 As in Fig

5.8 As in Fig

LIST OF FIGURES

Figure

7.1 The real
plot-mic
of the c
angle ca
the effe
integrat
(b) (lar
case (a)
plot is

7.2 As in Fi
at backw
higher a
angle co
the ener

7.3 As in Fig

7.4 The real
of the p
quantity
C.M. ener
is the co

8.1 Diagramma

8.2 An Argand

$\langle P'_{\pi} |$

and

$\langle P'_{\pi} |$

The solid
line is t
At a given
and the da

8.3 The real a
shown in F
These curve

of $\langle P'_{\pi}$

Note that
impulse ap

Figure

1. The real and

$\langle p' | K^0 | t$

calculated t
result using
the single s
The solid li

2. Three differ
nucleon inte
integrated
the single s
(SSAB); (c)
binding effe
of the pion

3. As in Figure

4. As in Figure

5. The elastic
resulting fr
nucleon impu
the fully-in
(b) (short da
(SSA); (c)
approximate
laboratory k

6. The elastic
calculated b
fully-impuls
the quadrupl
energies cho
the pion.

7. The elastic
calculated
integrated
Kujawski-Wa
shown are

8. The elastic
resulting
interaction
impulse ap
state appro
dash line)
The energie
the pion.

Figure

III.5 The elast
resulting
nucleon in
the fully-
(short das
(SSA); (c
approximat
laboratory

III.6 As in Fig

III.7 As in Fig

III.8 As in Fig

III.9 The elast
calculated
fully-inte
(dashed li
to case (a
kinetic en

III.10 As in Fig

III.11 As in Fig

III.12 As in Fig

III.13 The elast
calculated
fully-inte
(dashed li
approximat
tory kine

III.14 As in Fig

III.15 As in Fig

III.16 As in Fig

III.17 The elast
resulting
nucleon i
fully-in
(short da
for bind
the clos
energies
of the p

Figure

11.18 As in Fig

11.19 As in Fig

11.20 As in Fig

11.21 The elast
resulting
nucleon i
the fully-
(short da
(SSA); (
approxima
laboratory

11.22 As in Fig

11.23 As in Fig

11.24 The elast
calculate
the fully-
(dashed l
to case (a
tory kinet

11.25 As in Figu

11.26 As in Figu

11.27 The elast
calculated
the fully-
(dashed l
approxima
tory kinet

11.28 As in Figu

11.29 As in Figu

11.30 The elast
resulting
nucleon in
integrated
line) the
effects (S
limit for
shown are

1. The π-Meson

It is c

uld be used to

d deeper) to

d electrons. T

ch make them p

ee three charge

harge is possi

be described by "c

a single free

experiments may y

clei inside t

e non-nucleon

the well-known

possible to vary

---

[1] The qua

π: (isospin) =

total angular m

parity of the [illegible]

CHAPTER I

INTRODUCTION

1. The Pi-Meson As a Nuclear Probe

It is certainly reasonable to ask why pi-mesons (pions) should be used to probe the nucleus. After all, it is much easier (and cheaper) to use more conventional projectiles such as protons and electrons. The answer is that pions have some unique properties which make them particularly useful as nuclear probes. First, pions have three charge states (π^+, π^-, π^0) so that double charge exchange is possible. Second, pions are bosons and therefore can be absorbed by "clusters" of nucleons in the nucleus. (Absorption by a single free nucleon cannot occur.) Hence, pion absorption experiments may yield new information about correlations among nucleons inside the nucleus. Third, and perhaps most important, the pion-nucleon interaction is dominated in the 100-300 MeV region by the well-known (3,3) resonance.[1] The (3,3) resonance makes it possible to vary the strength of the pion-nucleus interaction by

---

[1] The quantum numbers associated with the (3,3) resonance are I (isospin) = 3/2, J (total angular momentum) = 3/2, and L (orbital angular momentum) = 1. At resonance, the laboratory kinetic energy of the incident pion is about 190 MeV.

ve that an order of m

incident pion beam.

rough is not present

terms. Fourth, the

sitive pions interac

inner mainly with n

bincoming proton a

ght and relatively sm

rmerical analysis o

1. Elastic Scattering

When an ener

cides with a nucle

ny cases, inelastic c

the elastic wave fu

he inelastic scatteri

ave function as impl

udy of elastic scat

mplete description

ons, elastic pion-n

by both experimental

[1] One such

"distorted-wave" Born

more than an order of magnitude simply by varying the energy of the incident pion beam. This convenient "knob" on the interaction strength is not present with conventional probes such as protons and electrons. Fourth, the (3,3) resonance has total isospin 3/2 so that positive pions interact mainly with protons and negative pions interact mainly with neutrons. Pions should therefore be useful in determining proton and neutron distributions. Finally, the zero spin and relatively small mass of the pion considerably simplify theoretical analysis of pion-nucleus scattering.

2. Elastic Scattering of Pions from Nuclei

When an energetic particle such as a 100-300 MeV pion collides with a nucleus it usually scatters elastically, so in many cases, inelastic scattering can be treated as a small perturbation on the elastic wave function.[1] In order to use a perturbative method for inelastic scattering, it is necessary to have an accurate elastic wave function as input. A careful experimental and theoretical study of elastic scattering is therefore the first step toward a complete description of pion-nucleus scattering. Hence, in recent years, elastic pion-nucleus scattering has received increased attention by both experimentalists and theorists.

---

[1] One such perturbative approach is the well-known "distorted-wave" Born approximation (DWBA).

3. The Present Experimental Situation

The present experimental situation in pion-nucleus physics is a bit strange. Several "meson factories" have recently become operational and should produce high quality pion-nucleus scattering data in the very near future. But, so far, no results from the meson factories have been published and the only data presently available come from older accelerators which were not designed for pion-nucleus scattering. While these data are not of the quality expected from the meson factories, some fairly good elastic scattering measurements have been made for light nuclei. Binon et. al. have measured differential cross sections for elastic π^--^{12}C scattering at 120, 150, 180, 200, 230, 260 and 280 MeV (Bin70). The same group has reported preliminary results for elastic π^--^{4}He scattering at 110, 150, 180, 220 and 260 MeV (Bin71). Bercaw et. al. have measured elastic differential cross sections for π^--^{16}O scattering at 160, 170, 220, 230 and 240 MeV (Ber72). Other data have been reported [1] but the ^{4}He, ^{12}C and ^{16}O data cited here are the most systematic data available at present in the (3,3) resonance region (100-300 MeV).

4. Previous Calculations

Many theoretical calculations have been done to explain the π^--^{12}C and π^--^{16}O data[2] and a few have been done to explain the π^--^{4}He data (Mac73, Ger73, Fra74). Most of the calculations use

---

[1] For a listing of experimental results see Kol70, Cer74.

[2] It is impractical to give a complete list here. Some more recent results can be found in Lan73, Pha73, Kis74, Kuj74.

from the Glauber the

ained from Watson's

hese calculations dec

egardless of the mode

ata.

A survey of

ws that while multi

ingle scattering dom

multiple scatterin

lso showed strong sh

nvolving in this ca

fairly good agreement

th the ^{4}He data. A

nvolving do not dep

equally accurate no

ve fairly good agre

ppeared that a more

on was needed for a

nvolving data.

5. The Calculation

The objecti

^{4}He, π^{-} ^{12}C and

nance region, wh

---

[1] However, t

ata at 120 and 150

ngles (Mac??).

either the Glauber theory (Gla67) or an optical potential model derived from Watson's multiple scattering theory (Wat53, Ker59). These calculations describe the π^--^{12}C and π^--^{16}O data fairly well, regardless of the model, but are in poor agreement with the π^--^4He data.[1]

A survey of the pion-nucleus scattering data indicated to us that while multiple scattering is important in ^{12}C and ^{16}O, single scattering dominates in ^4He. Our preliminary calculations and multiple scattering calculations by Charlton and Eisenberg (Cha71) also showed strong single scattering in ^4He. The dominance of single scattering in this case explains why most "standard" models give fairly good agreement with the ^{12}C and ^{16}O data, but poor agreement with the ^4He data. Apparently, the gross features of multiple scattering do not depend much on the details of the model so that marginally accurate models which give poor results for ^4He can still give fairly good agreement with the ^{12}C and ^{16}O data. Hence, it appeared that a more careful calculation of the single scattering term was needed for a good description of the π^--^4He elastic scattering data.

5. This Calculation

The objective of the present investigation to explain the π^--^4He, π^--^{12}C and π^--^{16}O elastic scattering data in the (3,3) resonance region, using a theoretical optical potential which contains

---

[1] However, R. Mach obtains good agreement with the π^--^4He data at 110 and 150 MeV. He does not report results at higher energies (Mac73).

a adjustable parameter

ion can be fit fairly

is directed toward a

generalize our $\pi^- - {}^7$H

for ^{12}C and ^{16}O.

In the optic

the single scattering

potential. Hence, a

to ^{4}He is equivalent

potential. In this

factors which we expe

1) internal motion

effects. Both of the

of the strong energy

the 100-300 MeV reg

The motion

misses the pion-nucl

a range of about 100

to a distribution of

absence of the (3,3

effect of nucleon

neglected entirely

calculation we make

using an independen

difference between

models. However, w

no adjustable parameters. Since the existing $\pi^- - {}^{12}C$ and $\pi^- - {}^{16}O$ data can be fit fairly well with almost any model, most of our effort is directed toward a more accurate optical potential for ^4He. We then generalize our $\pi^- - {}^4He$ optical potential to obtain optical potentials for ^{12}C and ^{16}O.

In the optical potential formalism used in this calculation, the single scattering term is given by the momentum-space optical potential. Hence, a more careful evaluation of single scattering in ^4He is equivalent to a better calculation of the $\pi^- - {}^4He$ optical potential. In this work we make a careful investigation of two factors which we expected to affect the $\pi^- - {}^4He$ optical potential: 1) internal motion of the target nucleons; 2) nuclear "binding" effects. Both of these effects were expected to be important because of the strong energy dependence of the pion-nucleon interaction in the 100-300 MeV region.

The motion of the target nucleons inside the nucleus causes the pion-nucleon center-of-mass energy to be "smeared" over a range of about 100 MeV. This C.M. energy distribution gives rise to a distribution of pion-nucleon interaction strengths due to the presence of the (3,3) resonance. In most previous calculations the effect of nucleon motion in pion-nucleus scattering has been either neglected entirely or else treated in some arbitrary way. In this calculation we make an exact numerical treatment of nucleon motion using an independent particle model for ^4He. We find considerable difference between the predictions of our model and typical "standard" models. However, we find that it is possible to accurately approximate

n exact numerical

exact numerical model

proved agreement w

an ^{16}O data.

We investi

y-body model. In o

otential well. Th

ed also with a bind

e large in the (3,

ransition is stron

as fairly small eve

the binding effect

the resonance regio

way from the recon

In order

ken in this work,

hapter.

In Chapte

ormalism and give

We also discuss the

^{8}Be, ^{12}C and ^{16}O da

ptical potential

the multiple scat

than in ^{12}C and ^{16}

hence, we argue th

ram (i.e., the op

ion of π^{-}-^{4}He s

our exact numerical result with a simple analytic model. Both our exact numerical model and its analytic approximation give significantly improved agreement with the ^{4}He data and good agreement with the ^{12}C and ^{16}O data.

We investigate nuclear binding effects using a simple 3-body model. In our model a single target nucleon is bound in a potential well. The nucleon thus interacts with the incident pion and also with a binding potential. We expected binding effects to be large in the (3,3) resonance region because the pion-nucleon interaction is strong there. However, we find that binding effects are fairly small even quite near the resonance. Our model predicts that binding effects weaken the optical potential by 10 - 20 % in the resonance region and that the effect is considerably smaller away from the resonance region.

In order to provide a more detailed outline of the approach taken in this work, we now discuss the main points contained in each chapter.

In Chapter II we outline the Watson optical potential formalism and give the major approximations used in our calculation. We also discuss the motivation for the calculation in light of the ^{4}He, ^{12}C and ^{16}O data and the qualitative features of the Watson optical potential formalism. Both the data and the formalism suggest that multiple scattering effects are significantly smaller in ^{4}He than in ^{12}C and ^{16}O. (Numerical calculations confirm this conjecture.) Hence, we argue that an accurate evaluation of the single scattering term (i.e., the optical potential) is necessary for a good description of π^--^{4}He scattering.

In Chapter

ntial potential.

ciple separable p

In most of this wor

the free pion-nuc

ation.) Our object

cleons so that the

matrix are accurat

calculating the p

"vector brackets" (s

of the pion-nucleon

Yukawsky or oscilla

ave functions are s

scillator wave func

siderably reduce

owever, even with t

perform non-trivial

Chapter IV

"factored form" of t

pproximations for ob

involves writing the

interaction factor a

aluation for the

ultiple integrals

convenient separa

interaction effects

In Chapter III we discuss our calculation of the $\pi^- - {}^4He$ optical potential. We use an independent particle model for ^4He and a simple separable parameterization of the free pion-nucleon t-matrix. (In most of this work we take the basic pion-nucleon interaction to be the free pion-nucleon t-matrix, i.e., we use the impulse approximation.) Our objective is to properly treat the motion of the target nucleons so that the essential features of the free pion-nucleon t-matrix are accurately represented in the pion-^4He optical potential. In calculating the pion-^4He optical potential we use the method of "vector brackets" (see Appendix D) to take advantage of the separability of the pion-nucleon t-matrix. (Vector brackets are the same as Moshinsky or oscillator brackets except the coordinate-space radial wave functions are spherical Bessel functions instead of harmonic oscillator wave functions.) The vector bracket method is shown to considerably reduce the computational effort required in the calculation. However, even with the vector bracket method, it is necessary to perform non-trivial multiple integrals.

Chapter IV is devoted to a discussion of the so-called "factored form" of the optical potential and to two typical ad hoc prescriptions for obtaining a factored form. The factored form involves writing the optical potential as the product of a pion-nucleon interaction factor and a nuclear ground state form factor. The motivation for the factored form is twofold. First, one avoids the multiple integrals discussed in Chapter III and, second, one obtains a convenient separation of nuclear structure effects from pion-nucleon interaction effects. However, most "standard" versions of the

formed form treat ru

ssential features of

epresented in the op

In Chapter

ich is a significan

hapter IV. However,

is as arbitrary as

time model is inclu

In Chapter VI we take

ism of the optical p

In Chapter

tromoleon impulse

The optical poter

In addition allows

partial and at the

ation. We compare c

interaction with the

V and V and find the

In Chapter

ation for the exact

hapter VI. By comp

several different

very good represen

lated to apply th

lows us to easily

effective impulse t

factored form treat nucleon motion in an arbitrary way so that the essential features of the pion-nucleon interaction are not accurately represented in the optical potential.

In Chapter V we discuss a recently published impulse model which is a significant improvement over the models discussed in Chapter IV. However, the derivation of this more recent model is just as arbitrary as the two models in Chapter IV. This recent ad hoc model is included in this study for the sake of completeness. In Chapter VI we take a more systematic approach to the factored form of the optical potential.

In Chapter VI we make a definition for an "effective" pion-nucleon impulse interaction in terms of the fully integrated $\pi^- - {}^4He$ optical potential which is calculated in Chapter III. Our definition allows us to have a factored form for the optical potential and at the same time to make an exact treatment of nucleon motion. We compare our "exact" or fully-integrated effective impulse interaction with the "standard" prescriptions discussed in Chapters IV and V and find there are significant differences.

In Chapter VII we develop a simple but accurate approximation for the exact or fully-integrated impulse interaction of Chapter VI. By comparing our approximation with the exact result at several different energies, we show that our approximation gives a very good representation of the exact result. While no more complicated to apply than the "standard" approximations, our approximation allows us to easily understand the differences between the exact effective impulse interaction and the standard prescriptions.

the zero approximation.

the role of nucleon

In Chapter VI

approximation using a

the nucleon that is

to just the nucleon a

with s-wave separab

affix that the "bind

all. The main effec

raph of the optical

cannot a simple ana

agreement with the exa

better to estimate a

n approximation to a

bound states (a separa

with that the effects

ave.

In Chapte

of the elastic sc

we give the ground

input for a Lippma

The calcu

^{4}He, ^{12}C and ^{16}O are

nucleus, the discuss

ation results and

we find that the fi

(2.4) gives satisfa

Using our approximation as a guide we give a qualitative discussion of the role of nucleon motion in the effective impulse interaction.

In Chapter VIII we consider corrections to the impulse approximation using a 3-body model. In our model the pion scatters from a nucleon that is bound in a potential well. The pion interacts with just the nucleon and not with the potential well itself. We use an s-wave separable potential to represent the potential well and find that the "binding" effects of the potential well are relatively small. The main effect in our model is a 10 - 20 % reduction in the strength of the optical potential near the (3,3) resonance. We also construct a simple analytic approximation which gives fairly good agreement with the exact numerical calculation for binding effects. In order to estimate an upper limit on the binding effects we extend our approximation to a potential well with an infinite number of bound states (a separable potential can produce only one bound state) and find the effects are about twice as large as with a single bound state.

In Chapter IX we discuss the details of the calculation of the elastic differential cross sections for ^{4}He, ^{12}C and ^{16}O. We give the ground state form factors and indicate how we obtain the imput for a Lippmann-Schwinger scattering equation.

The calculated elastic differential cross sections for ^{4}He, ^{12}C and ^{16}O are compared to the data in Chapter X. For each nucleus, the discussion is divided into two parts: 1) impulse interaction results and 2) impulse-plus-binding correction results. We find that the fully-integrated impulse model (and good approximations to it) gives satisfactory agreement for all three nuclei, and that

ther models do not.

ween the various m

The relativ

ax model is found

e larger correction

ber of bound state

Chapter XI c

other models do not. In ^{12}C and ^{16}O the data do not distinguish between the various models.

The relatively small binding correction given by the single state model is found to be compatible with the experimental data. The larger correction given by an (unrealistic) model with an infinite number of bound states overestimates the binding effects.

Chapter XI contains a summary and our conclusions.

THE OF
AND PION

1. Formal Theory

Watson et.al

scribe the scatterin

ms of a two-body op

otential" operator (w

essential elements of

given by Kerman, McMan

We assume a

(2.1) $H_{\pi\nu} = H$

where H_ν is the

energy operator and

(2.2) $V_{\pi\nu} = \sum$

is the sum of two bo

nucleons.

CHAPTER II

THE OPTICAL POTENTIAL FORMALISM AND PION-NUCLEUS ELASTIC SCATTERING

1. Formal Theory

Watson et.al. have shown that it is possible to formally describe the scattering of a projectile from a nucleus exactly in terms of a two-body operator which is commonly called the "optical" potential" operator (Wat53). In this section, we present the essential elements of the Watson optical potential formalism as given by Kerman, McManus, and Thaler (Ker59).

We assume a Hamiltonian of the form

$$H_{\pi\nu} = H_{\nu} + K_{\pi} + V_{\pi\nu} \tag{2.1}$$

where H_{ν} is the nuclear Hamiltonian, K_{π} is the pion kinetic energy operator and

$$V_{\pi\nu} = \sum_{j=1}^{A} v_{\pi N}(j) \tag{2.2}$$

is the sum of two body interactions between the pion and the target nucleons.

The pion-nu

given by

(3.3) $T_{\pi\nu}(E) =$

where E is the ki

ground state energy.[1]

$T_{\pi\nu}(E)$ betwe

matrix elements $\langle m'$

$|m\rangle$ and $|m'$

matrix element

independent of the la

(3.4) $T_{\pi\nu}(E) =$

where A is the num

$Q(E - H_$

projection operator

We now defi

for a pion from a bou

---

[1] Throughou

which do not include

that is. For exampl

ω_k is E

The pion-nucleus scattering operator $T_{\pi\nu}(E)$ is given by

$$(2.3)\quad T_{\pi\nu}(E) = V_{\pi\nu} + V_{\pi\nu}\left(E - H_\nu - K_\pi + i\epsilon\right)^{-1} T_{\pi\nu}(E)$$

where E is the kinetic energy of the pion plus the nuclear ground state energy.[1] In calculating the matrix elements of $T_{\pi\nu}(E)$ between antisymmetrized nuclear states we need to calculate $\langle n' | \sum_j v_{\pi N}(j) | n \rangle$ where $|n\rangle$ and $|n'\rangle$ denote the nuclear states. Since the matrix element $\langle n' | v_{\pi N}(j) | n \rangle$ is independent of the label j, we can write equation (2.3) as

$$(2.4)\quad T_{\pi\nu}(E) = A v_{\pi N} + A v_{\pi N} G(E) T_{\pi\nu}(E).$$

Here A is the number of target nucleons, and $G(E) = Q\left(E - H_\nu - K_\pi + i\epsilon\right)^{-1}$, where Q is a projection operator for completely antisymmetric nuclear states.

We now define the t-matrix $t_{\pi N}(E)$ for scattering of a pion from a bound nucleon;

---

[1] Throughout this work, we use E's to denote energies which do not include rest mass energy, and ω's for energies that do. For example, E_π means the kinetic energy of the pion and ω_π is $E_\pi + m_\pi c^2$.

(3.5) $\uparrow_{\pi N}(E) =$

he operator $\uparrow_{\pi N}$
emely difficult t
$\uparrow_{\pi N}$ with the t-
blem. The free pi

(3.6) $t_{\pi N}(E) =$

here $q_0(E) =$
$\uparrow_{\pi N}$ to $t_{\pi N}$
$t_{\pi N}$ and subs
the operator alge

(3.7) $\uparrow_{\pi N}(E$

ere E does n
is an arbitrary pa
hapter VIII, for
We consi
get $\uparrow_{\pi N}$ in

$$(2.5)\quad \hat{T}_{\pi N}(E) = \hat{V}_{\pi N} + \hat{V}_{\pi N} G(E) \hat{T}_{\pi N}(E).$$

The operator $\hat{T}_{\pi N}$ is a many-body operator and therefore extremely difficult to evaluate, so we will later approximate $\hat{T}_{\pi N}$ with the t-matrix for scattering of a pion from a free nucleon. The free pion-nucleon t-matrix is given by

$$(2.6)\quad t_{\pi N}(e) = \hat{V}_{\pi N} + \hat{V}_{\pi N} g_0(e) t_{\pi N}(e)$$

where $g_0(e) = (e - K_N - K_\pi + i\epsilon)^{-1}$. We can relate $\hat{T}_{\pi N}$ to $t_{\pi N}$ by using equation (2.6) to get $\hat{V}_{\pi N}$ in terms of $t_{\pi N}$ and substituting the result into equation (2.5). After some operator algebra we obtain

$$(2.7)\quad \hat{T}_{\pi N}(E) = t_{\pi N}(e) + t_{\pi N}(e)\left[G(E) - g_0(e)\right]\hat{T}_{\pi N}(E).$$

Note e does not necessarily equal E and that in fact e is an arbitrary parameter. We shall return to this point in Chapter VIII. For now we shall assume $e \cong E$.

We continue the formal development by using equation (2.5) to get $\hat{V}_{\pi N}$ in terms of $\hat{T}_{\pi N}$ so that we can write the

...nucleus scatte...

...) $T_{\pi D} = A$

...hereafter suppr...

...the above equation ...

...defining an auxil...

...) $T'_{\pi N} \equiv [$

...the operator T ...
...equation

...) $T'_{\pi N} =$

...The auxiliary scatte...
...multiple scatter...
...the target nucleon...
...we would have

At this ...
potential equation
$(A-1)T_{\pi N}$ ...
...ions excited int...

pion-nucleus scattering operator as

$$(2.8)\quad T_{\pi\nu} = A\hat{T}_{\pi N} + (A-1)\hat{T}_{\pi N} G T_{\pi\nu} .$$

(We hereafter suppress the variable E in the scattering operators.)

The above equation for $T_{\pi\nu}$ can be put in a more symmetric form by defining an auxillary scattering operator $T'_{\pi\nu}$:

$$(2.9)\quad T'_{\pi\nu} \equiv [(A-1)/A]\, T_{\pi\nu} .$$

The operator $T'_{\pi\nu}$ is given by the more symmetric integral equation

$$(2.10)\quad T'_{\pi\nu} = (A-1)\hat{T}_{\pi N} + (A-1)\hat{T}_{\pi N} G T'_{\pi\nu} .$$

The auxillary scattering operator $T'_{\pi\nu}$ can be thought of as a "multiple scattering" operator. For example, if there were just one target nucleon (A = 1) then there would be no multiple scattering and we would have $T'_{\pi\nu} = 0$ and $T_{\pi\nu} = \hat{T}_{\pi N}$.

At this point, equation (2.10) is in the form of an optical potential equation where the optical potential is taken to be $(A-1)\hat{T}_{\pi N}$. However, the propagator in equation (2.10) allows excited intermediate nuclear states so that the equation

will be extremely di

imal remedy is to f

f the optical poten

perator $U^{o}_{\pi\nu}$ a

(2.11) $U^{o}_{\pi\nu} = U$

th the complete op

(2.12) $U_{\pi\nu} = U$

here $|o\rangle$ repre

perator $T'_{\pi\nu}$

$U_{\pi\nu}$, is

(2.13) $T'_{\pi\nu} = U$

here E is the k

he to motion of th

nleus C.M. frame)

perator for transl

nlear degrees of

n be easily solv

would be extremely difficult (if not impossible) to solve. The formal remedy is to put the excited nuclear states into the definition of the optical potential. We define a "first order" optical potential operator $U^{o}_{\pi\nu}$ as

$$U^{o}_{\pi\nu} = (A-1)\hat{T}_{\pi N} \tag{2.11}$$

with the complete optical potential operator being given by

$$U_{\pi\nu} = U^{o}_{\pi\nu} + U^{o}_{\pi\nu}(1-|0\rangle\langle 0|)G\,U_{\pi\nu} \tag{2.12}$$

where $|0\rangle$ represents the nuclear ground state. The scattering operator $T'_{\pi\nu}$ written in terms of the complete optical potential, $U_{\pi\nu}$, is

$$T'_{\pi\nu} = U_{\pi\nu} + U_{\pi\nu}\frac{|0\rangle\langle 0|}{E-K_{\nu}-K_{\pi}+i\epsilon}T'_{\pi\nu}. \tag{2.13}$$

Here E is the kinetic energy of the pion plus the kinetic energy due to motion of the nucleus as a whole (for example, in the pion-nucleus C.M. frame) and the operator K_{ν} is the kinetic energy operator for translation of the nucleus as a whole. With the internal nuclear degrees of freedom removed, we have a two-body equation which can be easily solved.

For elastic scattering we want to calculate

$\langle \underset{\sim}{p}'_\pi | \langle 0 | T'_{\pi\nu} | 0 \rangle | \underset{\sim}{p}_\pi \rangle$, where the kets $| \underset{\sim}{p}_\pi \rangle$ and $| \underset{\sim}{p}'_\pi \rangle$ describe respectively the initial and final pion states in the pion-nucleus C.M. frame. Writing

$\langle \underset{\sim}{p}'_\pi | \langle 0 | T'_{\pi\nu} | 0 \rangle | \underset{\sim}{p}_\pi \rangle$ as $T'_{\pi\nu}(E, \underset{\sim}{p}'_\pi, \underset{\sim}{p}_\pi)$

and $\langle \underset{\sim}{p}'_\pi | \langle 0 | U_{\pi\nu} | 0 \rangle | \underset{\sim}{p}_\pi \rangle$ as $U_{\pi\nu}(\underset{\sim}{p}'_\pi \underset{\sim}{p}_\pi)$

we have

$$T'_{\pi\nu}(E, \underset{\sim}{p}'_\pi, \underset{\sim}{p}_\pi) = U_{\pi\nu}(\underset{\sim}{p}'_\pi \underset{\sim}{p}_\pi) + \int \frac{U_{\pi\nu}(\underset{\sim}{p}'_\pi \underset{\sim}{p}''_\pi) T'_{\pi\nu}(E, \underset{\sim}{p}''_\pi, \underset{\sim}{p}_\pi)}{E - K_\nu(p''_\pi) - K_\pi(p''_\pi) + i\epsilon} \frac{d^3 \underset{\sim}{p}''_\pi}{(2\pi)^3} . \tag{2.14}$$

Equation (2.14) involves only the pion coordinates and gives an exact description of elastic pion-nucleus scattering. However, it is clearly just as difficult to calculate the complete optical $U_{\pi\nu}$ as it is to solve the original equation for $T_{\pi\nu}$. The value of the optical potential formalism is that it allows us to relate the pion-nucleus scattering operator $T_{\pi\nu}$ to the pion-nucleon scattering operators $\hat{T}_{\pi N}$ and $t_{\pi N}$ in a systematic way.

In order t

ntaining approximati

a) The Col

w

optical

order

approxi

interm

b) The I

T

separa

approx

operat

ing the above appr

ntial potential op

ng) $U_{\pi\nu} =$

Most of our calcu

ndent optical po

n the impulse appr

We remark

potential here is b

ntaining operators

In order to actually calculate $T_{\pi\nu}$ we make the following approximations:

a) The Coherent Approximation:

We approximate the complete pion-nucleus optical potential $U_{\pi\nu}$ with the first order optical potential $U^{o}_{\pi\nu}$. The coherent approximation is equivalent to neglecting excited intermediate nuclear states in equation (2.10).

b) The Impulse Approximation:

The scattering operator $\hat{t}_{\pi N}$ for scattering of a pion from a bound nucleon is approximated by the free pion-nucleon scattering operator, $t_{\pi N}$.

Using the above approximations, we obtain for the pion-nucleus optical potential operator

$$U_{\pi\nu} = (A-1)t_{\pi N} . \tag{2.15}$$

In most of our calculations we use equation (2.15) for the pion-nucleus optical potential. In Chapter VIII we investigate corrections to the impulse approximation in a simple 3-body model.

We remark finally that the optical potential formalism presented here is by no means unique. There are many other ways of defining operators and grouping terms. The reason for using the

implies described

the pion-nucleon in

a pion-nucleus opt

mainly to would of

are grouped.

1. Collective Pen

In this se

a pion-nucleus opt

is indicate how ther

ent.

If we writ

$T'_{\pi\nu}$, as a po

$$T'_{\pi\nu} =$$

taking $U_{\pi\nu}$ to be

$$T'_{\pi\nu} = U$$

Hence, the Born ap

$[A/(A-1)] U_{\pi}$

approximation. For

is Born or single

nuclei such as ^{12}C

formalism described here is to put the resonant character of the free pion-nucleon interaction directly into the approximation for the pion-nucleus optical potential. If we could solve the problem exactly it would of course be irrelevant how the various terms were grouped.

2. Qualitative Remarks

In this section we discuss some qualitative features of the pion-nucleus optical potential and pion-nucleus scattering. We indicate how these features motivated the approach taken in this work.

If we write the auxillary pion-nucleus scattering operator, $T'_{\pi\nu}$, as a power series in $U_{\pi\nu}$, the first few terms are

$$(2.16)\quad T'_{\pi\nu} = U_{\pi\nu} + \frac{|0\rangle\langle 0|}{E - K_\pi - K_\nu + i\epsilon} U_{\pi\nu} + \cdots .$$

Taking $U_{\pi\nu}$ to be $(A-1)t_{\pi N}$, we have

$$(2.17)\quad T'_{\pi\nu} = (A-1)t_{\pi N} + (A-1)^2 t_{\pi N} \frac{|0\rangle\langle 0|}{E - K_\pi - K_\nu + i\epsilon} t_{\pi N} + \cdots .$$

Hence, the Born approximation for $T_{\pi\nu}$ is $T_{\pi\nu} = [A/(A-1)]\, U_{\pi\nu} = A\, t_{\pi N}$, i.e., the single scattering approximation. For a small nucleus such as ^{4}He it is plausible that the Born or single scattering term is more dominant than in larger nuclei such as ^{12}C or ^{16}O where multiple scattering is stronger.

ions we might expect

ppearing to be more

$\pi^{-12}C$ or $\pi^{-16}C$

ase when one compare

^4He, ^{12}C, and ^{16}O in

figure 10.1 and Figur

p-wave character of

nadronary minimum in

of in the π^{-} ^4He c

n minima appear to

energy. In ^{12}C and

interaction are appar

while in ^4He the Born

p-wave minima.

The fact t

approximation give r

greement for ^4He, c

sections have a defi

a more accurate tre

optical potential)

It was expected tha

generalized for lar

the ^{12}C and ^{16}O da

Hence we might expect the characteristic features of pion-nucleon scattering to be more prominent in $\pi^- - {}^4He$ scattering than in $\pi^- - {}^{12}C$ or $\pi^- - {}^{16}O$ scattering. Indeed, this appears to be the case when one compares the elastic differential cross sections for ${}^4He$, ${}^{12}C$, and ${}^{16}O$ in the 100-300 MeV region. (See, for example, Figure 10.1 and Figures 10.5 - 10.8 in Chapter X.) The strongly p -wave character of the pion-nucleon interaction causes a nearly stationary minimum in the $\pi^- - {}^4He$ elastic cross section at about 75° in the $\pi^- - {}^4He$ C.M. frame. In ${}^{12}C$ and ${}^{16}O$, on the other hand, the minima appear to be diffractive, moving inward with increasing energy. In ${}^{12}O$ and ${}^{16}O$ the details of the pion-nucleon p -wave interaction are apparently masked by multiple scattering effects, while in ${}^4He$ the Born term dominates, producing a characteristic p -wave minima.

The fact that optical potential models based on the impulse approximation give reasonable agreement for ${}^{12}C$ and ${}^{16}O$, but poor agreement for ${}^4He$, coupled with the fact that the $\pi^- - {}^4He$ cross sections have a definite p -wave minimum led us to conclude that a more accurate treatment of the single scattering term (i.e., the optical potential) was needed in the case of $\pi^- - {}^4He$ scattering. It was expected that an improved ${}^4He$ optical, when appropriately generalized for larger nuclei, would also give better agreement with the ${}^{12}C$ and ${}^{16}O$ data.

CALCULATION OF
INTEGRATION

It was sho

ultiple approxima

m form

$$U_{\pi\gamma}(\vec{p}_\pi', \vec{p}_\pi)$$

where the kets $|\vec{p}_\pi\rangle$

ion states in the

$|\Psi_{GS}\rangle$ describe

in the free pion-nu

aper we discuss

π-^{4}He scattering.

An Independent

We want t

account in a simple

for ^{4}He. In this

the π-^{4}He optic

CHAPTER III

CALCULATION OF THE π^- - ^{4}He OPTICAL POTENTIAL: INTEGRATION OVER THE TARGET NUCLEON MOMENTA

It was shown in Chapter II that the coherent approximation and impulse approximation give a pion-nucleus optical potential of the form

$$(3.1)\quad U_{\pi\nu}(\underset{\sim}{p}'_\pi, \underset{\sim}{p}_\pi) = (A-1)\langle \underset{\sim}{p}'_\pi | \langle \psi_{GS} | t_{\pi N} | \psi_{GS} \rangle | \underset{\sim}{p}_\pi \rangle$$

where the kets $|\underset{\sim}{p}_\pi\rangle$ and $|\underset{\sim}{p}'_\pi\rangle$ describe respectively the pion states in the pion-nucleus C.M. frame ($\pi\nu$CM frame) and $|\psi_{GS}\rangle$ describes the nuclear ground state. The operator $t_{\pi N}$ is the free pion-nucleon t-matrix in the $\pi\nu$CM frame. In this chapter we discuss the explicit evaluation of equation (3.1) for π^- - ^{4}He scattering.

1. An Independent Particle Model for ^{4}He

We want to take the main effects of nucleon motion into account in a simple way so we assume an independent particle model for ^{4}He. In this model equation (3.1) gives a very simple form for the π^- - ^{4}He optical potential

(42)

$$U_{\pi\nu}(p'_{\pi}$$

$$(A-1)\int \Psi$$

In equation (3.2),

two-nucleon t-matrix

ave function for T

mpulsed vector (

ed k' are respe

omentum, and final

TNCM frame),

in the C.M. frame o

the momentum trans

iderations involvi

4. Some Numerical

Although

ible tedious to

can be done to ob

integral is requir

$U_{\pi\nu}(p'_{\pi}\, p_{\pi}$

(3.2)

$$U_{\pi\nu}(\underset{\sim}{p}'_{\pi}\,\underset{\sim}{p}_{\pi}) =$$

$$(A-1)\int \psi^*(\underset{\sim}{p}_{4N} + \frac{A-1}{A}\underset{\sim}{q})\psi(\underset{\sim}{p}_{4N})\,\bar{t}_{\pi N}(\underset{\sim}{\omega})\,\frac{d^3 p_{4N}}{(2\pi)^3}\,.$$

In equation (3.2), $\bar{t}_{\pi N}$ is the spin-isospin averaged free pion-nucleon t-matrix and ψ is a single particle ground state wave function for ^{4}He. The vector $\underset{\sim}{\omega}$ is defined as the seven component vector (ω_{cm} , $\underset{\sim}{k}$, $\underset{\sim}{k}'$) where ω_{cm} , $\underset{\sim}{k}$ and $\underset{\sim}{k}'$ are respectively the collision energy, initial pion momentum, and final pion momentum,all in the pion-nucleon C.M. frame (πNCM frame). The vector $\underset{\sim}{p}_{4N}$ is the nucleon momentum in the C.M. frame of the ^{4}He nucleus alone and the vector $\underset{\sim}{q}$ is the 3-momentum transfer, $\underset{\sim}{p}_{\pi} - \underset{\sim}{p}'_{\pi}$. The reference frames and kinematics involved here are discussed in Appendix A.

2. Some Numerical Considerations

Although equation (3.2) is very simple in form, it is quite tedious to evaluate numerically. First, a 3-dimensional integral must be done to obtain $U_{\pi\nu}(\underset{\sim}{p}'_{\pi}, \underset{\sim}{p}_{\pi})$. Then another integral is required to obtain a partial wave decomposition of $U_{\pi\nu}(\underset{\sim}{p}'_{\pi}\,\underset{\sim}{p}_{\pi})$ for use in a scattering equation.

ion for each value
integral must be done
ation of multiple int
ation for the free
variables $\underset{\sim}{k}$ a
uation the complica
Euler" technique i
rate calculation of
-dimensional integr
quation (3.2) using
ion itself is rather
ation.

Determination of
Potential Matrix

In this
initial potential
matrix D_i. Our
matrix and also
matrix allows a
determination
matrix elements
ation.

We want

(3.3) $U_{\pi\nu}(p'_{\pi}$

Hence for each value of $|\underset{\sim}{p}_\pi|$ and $|\underset{\sim}{p}'_\pi|$, a 4-dimensional integral must be done, so that one is faced with calculating a large number of multiple integrals. In Appendix B we give a parameterization for the free pion-nucleon t-matrix which is separable in the coordinates $\underset{\sim}{k}$ and $\underset{\sim}{k}'$. We can exploit this separability to reduce the computational task considerably. Using the "vector bracket" technique described in Appendix D, we reduce the problem to the calculation of many 2-dimensional integrals rather than many 4-dimensional integrals. Obtaining the final algebraic form of equation (3.2) using vector brackets is tedious although the final form itself is rather simple. A derivation is given in the next section.

3. Derivation of the $\pi^- - {}^4$He Optical Potential Using Vector Brackets

In this section we give a derivation of the $\pi^- - {}^4$He optical potential using the vector bracket method described in Appendix D. Our derivation serves as an example of the use of vector brackets and also shows how the separability of the pion-nucleon t-matrix allows a considerable reduction in computational effort. The derivation itself is not essential for an understanding of the remaining chapters so this section can be skipped over by the casual reader.

We want to calculate the matrix element

$$(3.3)\quad U_{\pi\nu}(\underset{\sim}{p}'_\pi \underset{\sim}{p}_\pi) = (A-1)\langle \underset{\sim}{p}'_\pi | \langle 0 | \bar{t}_{\pi N} | 0 \rangle | \underset{\sim}{p}_\pi \rangle .$$

$$U_{\pi N}($$

$$(A-1)$$

$$\times \langle p'_{\pi} |$$

$$\psi(p_{\pi}$$

$$\langle 0 | p'_{A\pi} \rangle$$

$$\psi(p_{A\pi}$$

$$| p_{\pi} \rangle =$$

Inserting a complete set of nucleon momentum states on both sides of $\bar{t}_{\pi N}$ we obtain

(3.4)

$$U_{\pi\nu}(\underset{\sim}{p}'_{\pi}\,\underset{\sim}{p}_{\pi}) =$$

$$(A-1)\iint \frac{d^3p'_{4N}}{(2\pi)^3}\,\frac{d^3p_{4N}}{(2\pi)^3}\,\psi^*(\underset{\sim}{p}'_{4N})\psi(\underset{\sim}{p}_{4N})$$

$$\times \langle \underset{\sim}{p}'_{\pi}|\langle \underset{\sim}{p}'_{4N}|\bar{t}_{\pi N}|\underset{\sim}{p}_{4N}\rangle|\underset{\sim}{p}_{\pi}\rangle$$

where $\psi(\underset{\sim}{p}_{4N})$ and $\psi^*(\underset{\sim}{p}'_{4N})$ are $\langle \underset{\sim}{p}_{4N}|0\rangle$ and $\langle 0|\underset{\sim}{p}'_{4N}\rangle$ respectively.

We make the following definitions (see Appendix C for details concerning the notation):

$$(3.5)\quad \psi(\underset{\sim}{p}_{4N}) \equiv R(p_{4N})Y_{00}(\hat{p}_{4N})$$

$$(3.6)\quad |\underset{\sim}{p}_{\pi}\rangle \equiv \sum_{L_\pi M_\pi} Y^*_{L_\pi M_\pi}(\hat{p}_\pi)\,|p_\pi L_\pi M_\pi\rangle$$

with a similar definition for $|\underset{\sim}{p}'_{\pi}\rangle$.

Now we define

(3.7) $|P_{\pi N}\rangle \equiv$

and a similar definit

the equation (3.4) b

(3.8) $U_{\pi N}(P'_{\pi}$

$\times R(P'_{\pi N}$

$\times \langle P'_{\pi} L'_{\pi}$

The next operator i

which the relati

(3.

$1 = |\psi''$

Also, we define

$$(3.7)\quad |\underset{\sim}{P}_{4N}\rangle \equiv \sum_{L_N M_N} Y^*_{L_N M_N}(\hat{P}_{4N})\,|P_{4N}\,L_N\,M_N\rangle$$

with a similar definition for $|\underset{\sim}{P}'_{4N}\rangle$.

Now equation (3.4) can be written

$$(3.8)\quad U_{\pi N}(\underset{\sim}{P}'_{\pi}\,\underset{\sim}{P}_{\pi}) = (A-1)\iint \frac{P'^2_{4N}\,dP'_{4N}}{(2\pi)^3}\,\frac{P^2_{4N}\,dP_{4N}}{(2\pi)^3}$$

$$\times R(P'_{4N})R(P_{4N}) \times \sum_{\substack{L_\pi M_\pi \\ L'_\pi M'_\pi}} Y_{L'_\pi M'_\pi}(\hat{P}'_\pi)\,Y^*_{L_\pi M_\pi}(\hat{P}_\pi)$$

$$\times \langle P'_\pi L'_\pi M'_\pi K P'_{4N}\,L'_N=0\,M'_N=0|\bar{t}_{\pi N}|\,P_{4N}\,L_N=0\,M_N=0\rangle |P_\pi L_\pi M_\pi\rangle$$

The unit operator in terms of the πNCM coordinates (or equivalently, the relative and center-of-mass coordinates) is given by

(3.9)

$$1 = |\underset{\sim}{k}''\rangle|\underset{\sim}{x}''\rangle \int \frac{d^3k''}{(2\pi)^3}\int \frac{d^3x''}{(2\pi)^3}\langle \underset{\sim}{x}''|\langle \underset{\sim}{k}''|$$

or in terms of "coupled" angular momenta

(3.10)

$$1 =$$

$$|k''\chi''\ell''m''l_k''l_\chi''\rangle \sum_{\substack{\ell''m'' \\ l_k''l_\chi''}} \iint \frac{k''^2 dk''}{(2\pi)^3} \frac{\chi''^2 d\chi''}{(2\pi)^3} \langle k''\chi''\ell''m''l_k''l_\chi''| \, .$$

Inserting the unit vector of equation (3.10) on both sides of $\bar{t}_{\pi N}$ we have (The "coupled state" $|k''\chi''\ell''m''l_k''l_\chi''\rangle$ is defined in Appendix C.)

$$(3.11)\quad U_{\pi\nu}(\underset{\sim}{P'_\pi}\,\underset{\sim}{P_\pi}) = (A-1) \sum_{\substack{L_\pi M_\pi \\ L'_\pi M'_\pi}} \sum_{\substack{\ell''m'' \\ \ell'''m'''}} Y_{L'_\pi M'_\pi}(\hat{P}'_\pi)\, Y^*_{L_\pi M_\pi}(\hat{P}_\pi)$$

$$\times \int \frac{P'^2_{qN}\, dP'_{qN}}{(2\pi)^3} \int \frac{P^2_{qN}\, dP_{qN}}{(2\pi)^3} \int \frac{k'''^2\, dk'''}{(2\pi)^3} \int \frac{k''^2 dk''}{(2\pi)^3} \int \frac{\chi''^2 d\chi''}{(2\pi)^3} \int \frac{\chi'''^2 d\chi'''}{(2\pi)^3}$$

$$\times R(P'_{qN})\, R(P_{qN}) \langle P'_\pi P'_{qN} \ell' m' L_\pi L_N = 0 | k''\chi''\ell''m''l_k''l_\chi''\rangle$$

$$\times \langle k''\chi''\ell''m''l_k''l_\chi''| \bar{t}_{\pi N} | k'''\chi'''\ell'''m'''l_k'''l_\chi'''\rangle$$

$$\times \langle k'''\chi'''\ell'''m'''l_k'''l_\chi'''| P_\pi P_{qN} \ell m L_\pi L_N = 0\rangle$$

ere the states $|P$

nd $|P_\pi' P_{aa}'$ γ

re just $|P_\pi L_\pi M$

nd $|P_\pi' L_\pi' M_\pi'$

me that $\underset{\sim}{\alpha} = \underset{\sim}{\alpha}$

e now need the matri

ms and also the ove

πNCM kets. (

he matrix elements

(3.12)

$$\langle k'' \kappa'' \alpha'' \pi$$

$$= (2\pi)^3 \delta($$

$$\times \frac{1}{6} \sum_{HJ} (2$$

here

(3.13)

$$t_{IJ l_{k''}}(\omega_{CM},$$

where the states $|P_\pi P_{qN} \mathcal{L} \mathcal{M} L_\pi L_N = 0\rangle$

and $|P_\pi' P_{qN}' \mathcal{L}' \mathcal{M}' L_\pi' L_N' = 0\rangle$

are just $|P_\pi L_\pi M_\pi\rangle |P_{qN} L_N = 0 \; M_N = 0\rangle$

and $|P_\pi' L_\pi' M_\pi'\rangle |P_{qN}' L_N' = 0 \; M_N' = 0\rangle$ respectively.

Note that $\underset{\sim}{\mathcal{L}} = \underset{\sim}{\mathcal{L}}' = \underset{\sim}{L_\pi} = \underset{\sim}{L_\pi'}$ since $\underset{\sim}{L_N} = \underset{\sim}{L_N'} = 0$.

We now need the matrix elements of $\bar{t}_{\pi N}$ between the $\pi N C M$ kets and also the overlaps between the $\pi N C M$ kets and the $\pi \nu C M$ kets. (These overlaps are the so-called "vector brackets".)

The matrix elements of $\bar{t}_{\pi N}$ are given by

(3.12)

$$\langle k'' \chi'' \mathcal{L}'' \mathcal{M}'' l_{k''} l_{\chi''} | \bar{t}_{\pi N} | k''' \chi''' \mathcal{L}''' \mathcal{M}''' l_{k'''} l_{\chi'''} \rangle$$

$$= (2\pi)^3 \frac{\delta(\chi'' - \chi''')}{\chi''^2} \delta(\mathcal{L}'' \mathcal{L}''') \delta(\mathcal{M}'' \mathcal{M}''') \delta(l_{k''} l_{k'''}) \delta(l_{\chi''} l_{\chi'''})$$

$$\times \frac{1}{6} \sum_{IJ} \frac{(2I+1)(2J+1)}{2 l_{k''} + 1} t_{IJ l_{k''}}(\omega_{CM}, k', k)$$

where

(3.13)

$$t_{IJ l_{k''}}(\omega_{CM}, k', k) = \gamma \, t_{IJ l_{k''}}(\omega_{CM}, k_0, k_0) \frac{q(k') \, q(k) \; g_{IJ l_{k''}} \; g_{IJ l_{k''}}}{q^2(k_0) \; g_{IJ l_{k''}}}$$

and

(3.14)

$$t_{IJ\ell_k''}(\omega_{cm}, k_o, k_o) = \frac{-8\pi^2\hbar^2c^2}{\mu_R}\left[\frac{\eta_{IJ\ell_k''}\, e^{2i\delta_{IJ\ell_k''}} - 1}{2ik_o}\right].$$

A more complete discussion of the parameterization of $\bar{t}_{\pi N}$ is given in Appendix B. The vector bracket expressions are of the form (See Appendix D for a detailed discussion of the various factors in equation (3.15).)

(3.15)

$$\langle k'''\chi'''\mathcal{L}'''\mathcal{M}'''\ell_{k'''}\ell_{\chi'''} \mid P_\pi P_{4N}\mathcal{L}\mathcal{M}L_\pi L_N\rangle$$

$$= (2\pi)^3(4\pi)^2\delta(\mathcal{L}'''\mathcal{L})\delta(\mathcal{M}'''\mathcal{M})\delta(W)\,\theta_1\theta_2$$

$$\times \frac{1}{2\mathcal{L}+1}\frac{1}{k'''\chi'''P_\pi P_{4N}}\sum_{\mathcal{M}''=-\mathcal{L}}^{\mathcal{L}}\left\{\left[\sum_{\substack{m_k\\ m_\chi}}\langle \ell_{\chi'''}\ell_{k'''}m_\chi m_k\mid \mathcal{L}\mathcal{M}''\rangle\right.\right.$$

$$\left.\left.\times Y_{\ell_{\chi'''}m_\chi}(\hat{\chi})\,Y_{\ell_{k'''}m_k}(\hat{k})\right]^*\left[\sum_{M_N M_\pi}\langle L_N L_\pi M_N M_\pi\mid \mathcal{L}\mathcal{M}''\rangle Y_{L_\pi M_\pi}(\hat{P}_\pi)\,Y_{L_N M_N}(\hat{P}_{4N})\right]\right\}.$$

n factors to note

functions. These i

n $\bar{t}_{\pi N}$ (equa

onsiderably. For

we have $L_{\underset{\sim}{\pi}} =$

we can eliminate th

(L'_π, M'_π). Al

he sum over M_π

is independent of

The kine

llow us to elimina

liminate P_{4N}

liminated using th

leaving us with kn

rom equation (A.1

$\left(\underset{\sim}{k}''\right)^2 = \left(\underset{\sim}{p}'_\pi -\right.$

$\left(\underset{\sim}{k}'''\right)^2 = \left(\underset{\sim}{p}_\pi\right.$

he integrals over

nd X''' where

his eliminates

forward substitut

ion-nucleon t-ma

The factors to note in the vector bracket expression are the delta functions. These delta functions, together with the delta functions in $\bar{t}_{\pi N}$ (equation (3.12)), allow us to simplify things considerably. For example, since $L'_\pi = \ell'$ and $L_\pi = \ell$, we have $L_\pi = L'_\pi = \ell'' = \ell'''$. Hence, in equation (3.11), we can eliminate the sums over (ℓ'', m''), (ℓ''', m'''), and (L'_π, M'_π). Also, we have $\ell_{k''} = \ell_{k'''}$ and $\ell_{\chi''} = \ell_{\chi'''}$. The sum over M_π can be done trivially since the final result is independent of m, and $m = M_\pi$.

The kinetic energy conserving delta functions $\delta(w)$ and $\delta(w')$ allow us to eliminate two of the momentum integrations. (We eliminate P_{4N} and P'_{4N}.) The integral over χ''' is eliminated using the delta function $\delta(\chi'' - \chi''')$ in equation (3.12), leaving us with integrals over just χ'', k'', and k'''. From equation (A.10) in Appendix A, we obtain the relationships

$$(\underset{\sim}{k}'')^2 = \left(\underset{\sim}{P}'_\pi - \frac{\omega^\circ_\pi}{\omega^\circ}\underset{\sim}{q}''\right)^2$$

and

$$(\underset{\sim}{k}''')^2 = \left(\underset{\sim}{P}_\pi - \frac{\omega^\circ_\pi}{\omega^\circ}\underset{\sim}{q}''\right)^2$$

. We then write the integrals over $\underset{\sim}{k}''$ and $\underset{\sim}{k}'''$ as integrals over χ'' and χ''' where $\chi'' = \hat{P}'_\pi \cdot \hat{q}''$ and $\chi''' = \hat{P}_\pi \cdot \hat{q}''$. (This eliminates the need for the θ functions.) A straightforward substitution of the vector bracket expressions and the pion-nucleon t-matrix expression into equation (3.11) now gives

$$U_{\pi\nu}$$

(A-1)

$$\times \int \chi''^2 d\chi'' \left[\right.$$

$$\int_{-1}^{1} d\chi'' g_H$$

$$\times \sum_{m=-L_\pi}^{L_\pi} \left\{ \left[\sum_{M_\ell} \right. \right.$$

$$(3.16)\qquad U_{\pi N}(\underset{\sim}{p}'_{\pi}\,\underset{\sim}{p}_{\pi}) =$$

$$(A-1)\frac{1}{6}\sum_{\substack{L_\pi \ell_{\chi''} \\ I,J,\ell_{k''}}} \frac{(2I+1)(2J+1)}{(2L_\pi+1)(2\ell_{k''}+1)}\, P_{L_\pi}(\hat{p}'_{\pi}\cdot\hat{p}_{\pi})$$

$$\times\int \chi''^2 d\chi'' \left[\frac{t^{(\omega_{cm},k_o,k_o)}_{IJ\ell_{k''}}}{g^2(k_o)_{IJ\ell_{k''}}}\right] \mathcal{I}(p'_{\pi}\chi''L_\pi\ell_{\chi''})\,\mathcal{I}(p_{\pi}\chi''L_\pi\ell_{\chi''})$$

where

$$(3.17)\qquad \mathcal{I}_{IJ\ell_{k''}}(p_{\pi}\chi''L_\pi\ell_{\chi''}) =$$

$$\int_{-1}^{1} d\chi''\, g(k'')_{IJ\ell_{k''}}\, R(p'_{4N})\left[\frac{\omega_\pi(k'')\,\omega_N(k'')}{\omega_\pi(p'_\pi)\,\omega_N(p'_N)}\right]^{1/2}$$

$$\times\sum_{M=-L_\pi}^{L_\pi}\left\{\left[\sum_{m_k m_\chi}\langle \ell_{\chi''}\ell_{k''}m_\chi m_k|L_\pi M\rangle Y_{\ell_{k''}m_k}(\hat{k}'')\,Y_{\ell_{\chi''}m_\chi}(\hat{\chi}'')\right]^*\right.$$

$$\left.\times\left[Y_{L_\pi M}(\hat{p}_\pi)\,Y_{00}(\hat{p}'_{4N})\right]\right\}.$$

he square root factor

tion in equation (3

discussion of the

on (3.17), the vecto

$\underset{\sim}{p}_\pi$ and $\underset{\sim}{k}''$

$\underset{\sim}{k}'' = \underset{\sim}{p}'_\pi$ -

and $\underset{\sim}{p}'_\pi = \underset{\sim}{p}'_{4\pi}$

we use

(3.18) $\left(\underset{\sim}{k}''\right)^2 =$

$\left(\underset{\sim}{p}'_\pi\right)^2 +$

where

(3.19) $X'' =$

the similar expre

definition of the

may be drawn as

Figure 3.1 - The
of the $\pi\nu$cm
reaction $\underset{\sim}{k}''$

The square root factor in $\mathcal{J}_{IJl k''}$ comes from the γ factor in equation (3.13). (See equation (B.5) in Appendix B for a discussion of the γ factor.) In the integrals in equation (3.16) and (3.17), the vectors $\underset{\sim}{k}''$, $\underset{\sim}{P}_N'$ and $\underset{\sim}{P}_{4N}'$ are related to $\underset{\sim}{P}_\pi$ and $\underset{\sim}{\chi}''$ via the equations

$$\underset{\sim}{k}'' = \underset{\sim}{P}_\pi' - (\omega_\pi^\circ/\omega^\circ)\underset{\sim}{\chi}'' \quad , \quad \underset{\sim}{\chi}'' = \underset{\sim}{P}_\pi' + \underset{\sim}{P}_N'$$

and $\underset{\sim}{P}_N' = \underset{\sim}{P}_{4N}' - \frac{1}{A}\underset{\sim}{P}_\pi'$ (see Appendix A). For example, we use

$$(3.18)\quad (\underset{\sim}{k}'')^2 = (\underset{\sim}{P}_\pi')^2 + (\omega_\pi^\circ/\omega^\circ)^2(\underset{\sim}{\chi}'')^2 - (2\omega_\pi^\circ/\omega^\circ)|\underset{\sim}{P}_\pi'||\underset{\sim}{\chi}''|x''$$

where

$$(3.19)\quad x'' = \hat{P}_\pi' \cdot \hat{\chi}''$$

with similar expressions for $(\underset{\sim}{P}_N')^2$ and $(\underset{\sim}{P}_{4N}')^2$. The orientation of the vectors $\underset{\sim}{P}_\pi'$, $\underset{\sim}{P}_N'$, $\underset{\sim}{k}$ and $\underset{\sim}{\chi}$ can be drawn as shown in Figure 3.1.

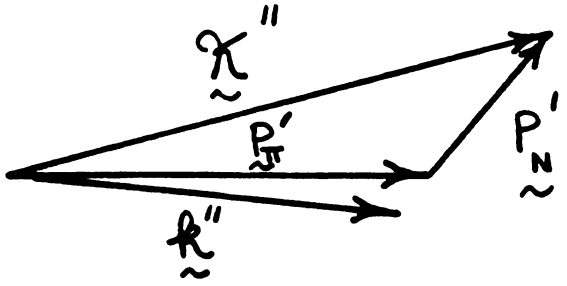

Figure 3.1 - The relationship between the pion and nucleon momenta in the πN CM frame and the total momentum $\underset{\sim}{\chi}''$ and relative momentum $\underset{\sim}{k}''$.

In the numer

integration is in the

we take the pion-

nuclei, i.e., we ta

in the (3,3) resonan

of $\int_{IJl_k}$.

The advant

these brackets allo

pion-nucleon t-matri

$\int_{IJl_k}$ and

calculated in equa

than a partial wav

the computational ef

tion (equation (3.2)

In the numerical calculation we assume the pion-nucleon interaction is in the (3,3) channel only ($I=3/2$, $J=3/2$, $\ell_{k''}=1$), and we take the pion-nucleon t-matrix to be the same off-shell as on-shell, i.e., we take $g_{IJ\ell_{k''}} \equiv 1$. We have found the results in the (3,3) resonance region to be rather insensitive to the choice of $g_{IJ\ell_{k''}}$.

The advantage of using vector brackets should now be clear. Vector brackets allow us to take advantage of the separability of the pion-nucleon t-matrix, so we just have to calculate the function $\mathcal{F}_{IJ\ell_{k''}}$ and integrate it with $t_{IJ\ell_{k''}} / g^2_{IJ\ell_{k''}}$ as indicated in equation (3.16). In addition, we automatically obtain a partial wave decomposition of the optical potential. Hence, the computational effort is considerably less than in the original form (equation (3.2)) where 4-dimensional integrals are required.

THE FA

In this

mels for the fa

mmonly popular

ther, however, w

ow the assumpti

potential.

A. Definition of

In orde

alculating the

he "factored fo

$t_{\pi N}(\Omega)$

the "effective"

ver the nucleon

as $\bar{t}$ and u

We have

(4.2) $V_{\pi\nu}($

CHAPTER IV

THE FACTORED FORM OF THE π - ^{4}He OPTICAL POTENTIAL: TWO AD HOC MODELS

In this chapter we review some of the conventional ad hoc models for the factored pion-nucleus optical potential that are currently popular and show the shortcomings inherent in these models. First, however, we need to consider the factored form in general and show the assumptions which are necessary to obtain a factored optical potential.

1. Definition of the Factored Form

In order to avoid the multiple integrals involved in calculating the fully integrated optical potential (equation (3.2)) the "factored form" of the optical potential is often used (Lan73, Kuj74, Mil74). In the factored form, the pion-nucleon t-matrix $\bar{t}_{\pi N}(\underset{\sim}{\Omega})$ (recall $\underset{\sim}{\Omega} \equiv (\omega_{cm}, \underset{\sim}{k}, \underset{\sim}{k}')$) is evaluated at some "effective" value of $\underset{\sim}{\Omega}$ and taken outside of the integral over the nucleon momenta. Denoting the effective value of $\underset{\sim}{\Omega}$ as $\underset{\sim}{\bar{\Omega}}$ and using the factored form for the ^{4}He optical potential we have

$$U_{\pi\nu}(\underset{\sim}{p}'_\pi, \underset{\sim}{p}_\pi) = (A-1)\bar{t}_{\pi N}(\underset{\sim}{\bar{\Omega}})\,\rho(q) \tag{4.1}$$

where $\rho(\mathbf{r})$ is gi

$$\rho(\mathbf{r}) =$$

The quantity $\rho(\mathbf{r})$

the Fourier transfo

$$\rho(\mathbf{r})$$

is spherical form

with a form factor

function.

4. The Ad Hoc Mod

The ad

In this chapter a

is that $\tilde{\Omega}$

description. T

purposes and do

π - The optica

take some correc

where $\rho(q)$ is given by

$$\rho(q) = \int \psi^*(P_{4N} + \frac{A-1}{A} q)\psi(P_{4N}) \frac{d^3P_{4N}}{(2\pi)^3} . \tag{4.2}$$

The quantity $\rho(q)$ is the ground state form factor and is just the Fourier transform of the ground state density $\rho(r)$:

$$\rho(q) = \int e^{iq\cdot r} \rho(r)\, d^3r . \tag{4.3}$$

An empirical form factor is usually used in equation (4.1) rather than a form factor obtained from some assumed ground state wave function.

2. The Ad Hoc Models

The ad hoc versions of the factored form which we consider in this chapter are typical of the models found in the literature in that $\bar{\Omega}$ is obtained by some plausible but rather arbitrary prescription. These models are presented solely for pedigodical purposes and do not give good agreement with the fully-integrated π^--^{4}He optical potential of Chapter III. Our objective is to make some connection with the work of other workers and not to give

exhaustive accoun

Chapter VII we g

sults from a syste

blem moments.

In our di

re there are actual

factored optical

a) The

b) The

c) The
(acc

ction (a) is in

this useful $\underset{\sim}{r}$ -

pecial class of

uch as the Kirchh

We use a simple n

throughout this

we isolate probl

Our

with the facto

fully integrable

most typical a

ever, the preci

approximating th

ation for $\underset{\sim}{\Omega}$

I_{Our}

(acyclic) indica

essentially the

an exhaustive account of the various (incorrect) choices for $\bar{\underset{\sim}{\Omega}}$. In Chapter VII we give our own version of the factored form which results from a systematic approximation to the integrals over the nucleon momenta.

In our discussion we consider just the choice of $\bar{\underset{\sim}{\Omega}}$, but there are actually three distinct problems involved in generating a factored optical potential from first principles:

a) The off-shell parameterization of $\bar{t}_{\pi N}(\underset{\sim}{q})$

b) The choice of $\bar{\underset{\sim}{q}}$

c) The $\underset{\sim}{r}$ -space form of the optical potential (assuming the calculation is done in $\underset{\sim}{r}$ -space)

Problem (a) is in practice often closely connected to problem (c) since useful $\underset{\sim}{r}$ -space optical potentials are obtained only for a special class of unphysical divergent off-shell parameterizations such as the Kisslinger and "local" parameterizations (Lan73, Lan74b). We use a simple non-divergent zero-range separable parameterization throughout this study and work entirely in momentum space so that we isolate problem (b), the choice of $\bar{\underset{\sim}{\Omega}}$.[1]

Our criteria for a "good" choice of $\bar{\underset{\sim}{\Omega}}$ is one for which the factored form is in good agreement with the exact or fully integrated optical potential of Chapter III. As will be shown, most typical ad hoc models involve "bad" choices for $\bar{\underset{\sim}{\Omega}}$. However, the prescription we obtain in Chapter VII by systematically approximating the integrals over the nucleon momenta gives a "good" choice for $\bar{\underset{\sim}{\Omega}}$.

---

[1] Our calculations and the work of Landau and Tabakin (Lan74b) indicate that a non-divergent zero-range t-matrix gives essentially the same results as a short-range t-matrix.

...ngle Transformat...

The proble...

...ntroduced conside...

...k_{CM}, k_{LAB}, ω_{LAB}, ...

...ken in the choice ...

...ikely connected t...

...menta $\underset{\sim}{k}$ and $\underset{\sim}{k}'$...

...ken for the work...

...ame for $\bar{\omega}_{CM}$ (th...

...used in much deta...

...ormed with the ...

The purp...

...ormer the "mappi...

...n the πN_{CM} fram...

...ne-to-one mapping...

...Schnider (Dedrick) a...

...transformation o...

...ed they proposed

$$\cos\theta_{\pi N} = a +$$

---

1. The re...
...maximum verbosity ...

$$\cos\theta_{\pi N} = \underset{\sim}{k}'\cdot$$

2. ...howeve...
...Lee and McManu...
...ngle transformat...
...Lee and McMan...
...Schnider and Fall...

3. Angle Transformations

The problem of choosing a value for $\bar{\Omega}$ in equation (4.1) has received considerable attention in recent years (Ded71, Fal72, Lan73, Kuj74, Mil74). For the most part, however, the emphasis has been on the choice of the so-called "angle transformation" which is closely connected to the choice of effective values for the πNCM momenta k and k' (which we denote as $\bar{k}$ and $\bar{k}'$ respectively). Except for the work of Landau et.al. (Lan73), the question of a good value for $\bar{\omega}_{CM}$ (the effective collision energy) has not been discussed in much detail in the literature. Hence, we shall mainly be concerned with the various angle transformations currectly in vogue.

The purpose of the angle transformation is to take into account the "mapping" of the scattering angle from the πNCM frame to the $\pi\nu$CM frame. In the early work of Kisslinger (Kis55), a one-to-one mapping was used so that $\cos\theta_{\pi\nu} = \cos\theta_{\pi N}$.[1] Dedonder (Ded71) and Faldt(Fal72) were the first to point out that a transformation of angles is important in pion-nucleus scattering and they proposed a linear angle transformation of the form $\cos\theta_{\pi N} = a + b\cos\theta_{\pi\nu}$.[2] An angle transformation similar

---

[1]The relation between the cosines and the associated momentum vectors is

$$\cos\theta_{\pi N} = \bar{k}'\cdot\bar{k}/|\bar{k}||\bar{k}'| \quad , \quad \cos\theta_{\pi\nu} = P_\pi\cdot P'_\pi/|P_\pi||P'_\pi|$$

[2]However, to our knowledge, the "local"optical potential of Lee and McManus (Lee71) was the first model to actually take the angle transformation into account. The angle transformation implied by Lee and McManus is the same on-shell as the one proposed by Dedonder and Faldt.

n that of Dedonder

plication of Lan

f discussion we c

ation" - this r

$\cos\theta_{\pi\gamma}$) and

ngle mappings; (

incorporates a li

and is representa

f Dedonder and F

. The Simple S

Our qu

mesons and π

for the details

(

$\underset{\sim}{k}$ =

(

$\underset{\sim}{k}'$

If we assume th

then we have

$\underset{\sim}{k}$ and $\underset{\sim}{k}'$

(

$|\underset{\sim}{k}$

to that of Dedonder and Faldt was later used in the momentum space calculation of Landau, Phatak, and Tabakin. Hence, for purposes of discussion we consider two models: (a) a "simple static approximation" - this model uses a one-to-one transformation ($\cos\theta_{\pi N} = \cos\theta_{\pi\gamma}$) and is representative of the early Kisslinger-type angle mappings; (b) a "modified static approximation" - this model incorporates a linear mapping of the form $\cos\theta_{\pi N} = a + b\cos\theta_{\pi\gamma}$ and is representative of models incorporating the angle transformation of Dedonder and Faldt.

4. The Simple Static Approximation

Our quasi-relativistic kinematics relate the $\pi\gamma$CM momenta and πNCM momenta by (see equation A.13 in Appendix A for the details of the kinematics) by

$$\underset{\sim}{k} = \underset{\sim}{P}_{\pi}\left[1 - \left(\frac{A-1}{A}\right)\omega^{\circ}_{\pi}/\omega^{\circ}\right] - \left(\omega^{\circ}_{\pi}/\omega^{\circ}\right)\underset{\sim}{P}_{4N} \tag{4.4}$$

$$\underset{\sim}{k}' = \underset{\sim}{P}'_{\pi}\left[1 - \left(\frac{A-1}{A}\right)\omega^{\circ}_{\pi}/\omega^{\circ}\right] - \left(\omega^{\circ}_{\pi}/\omega^{\circ}\right)\underset{\sim}{P}'_{4N}\,. \tag{4.5}$$

If we assume the struck nucleon remains "frozen" in the ^{4}He nucleus then we have $\underset{\sim}{P}_{4N} = \underset{\sim}{P}'_{4N} = 0$ and the effective values of $\underset{\sim}{k}$ and $\underset{\sim}{k}'$ are

$$\underset{\sim}{\bar{k}} = \underset{\sim}{P}_{\pi}\left[1 - \left(\frac{A-1}{A}\right)\omega^{\circ}_{\pi}/\omega^{\circ}\right] \tag{4.6}$$

$\bar{k}' =$

equations (4.4) -

the relativistic

ase that the simp

$\cos\theta_{\pi y}$.

The Modified S-

The modi

ople static appr

n the $\pi\nu$CM ang

$a+b\cos\theta_{\pi y}$.

mentia are taken

Hence, we have

(4.8)

(4.9)

(4.10)

Co

$$\bar{\underset{\sim}{k}}' = \underset{\sim}{p}_\pi' \left[1 - \left(\frac{A-1}{A}\right)\omega_\pi^\circ / \omega^\circ\right] . \tag{4.7}$$

In equations (4.4) - (4.7), $\omega_\pi^\circ / \omega^\circ$ is essentially the ratio of the relativistic pion mass to the nucleon mass. It should be clear that the simple static approximation implies $\cos\theta_{\pi N} = \cos\theta_{\pi\nu}$.

5. The Modified Static Approximation

The modified static approximation is the same as the simple static approximation except the πNCM angles are related to the $\pi\nu$CM angles via a transformation of the form $\cos\theta_{\pi N} = a + b\cos\theta_{\pi\nu}$. The relations between the magnitudes of the momenta are taken to be the same as in the simple static approximation. Hence, we have for the modified static approximation

$$|\bar{\underset{\sim}{k}}| = |\underset{\sim}{p}_\pi| \left[1 - \left(\frac{A-1}{A}\right)\omega_\pi^\circ / \omega^\circ\right] \tag{4.8}$$

$$|\bar{\underset{\sim}{k}}'| = |\underset{\sim}{p}_\pi'| \left[1 - \left(\frac{A-1}{A}\right)\omega_\pi^\circ / \omega^\circ\right] \tag{4.9}$$

$$\cos\theta_{\pi N} = a + b\cos\theta_{\pi\nu} . \tag{4.10}$$

Numerous

in choosing the "a

We shall use here a

measure. We sha

calculations becaus

between $\cos\theta_{\pi N}$

relationship is obt

is neglected. For

(4.11) (

or

(4.12) $\cos\theta$

$$\left[(k^2 + k'^2$$

where k denotes

due to the recoil

and $|k'|$ actua

represents a norm

(4.12) is often

to be independen

is obtained. Fo

suggest taking t

Numerous prescriptions have been given in the literature for choosing the "a" and "b" in equation (4.10) (Ded71, Fal72, Lan73). We shall use here a prescription that is typical of those in the literature. We shall not be concerned with the details of previous calculations because, as we shall see later, the proper relationship between $\cos\theta_{\pi N}$ and $\cos\theta_{\pi\nu}$ is, in fact, nonlinear. A linear relationship is obtained only if the recoil of the struck nucleon is neglected. For example, our quasi-relativistic kinematics give

$$(\underset{\sim}{k} - \underset{\sim}{k}')^2 = (\underset{\sim}{p}_\pi - \underset{\sim}{p}'_\pi)^2 \tag{4.11}$$

or

$$\cos\theta_{\pi N} = \left[(k^2 + k'^2 - p_\pi^2 - p_\pi'^2)/2kk'\right] + \left(p_\pi p_\pi'/2kk'\right)\cos\theta_{\pi\nu} \tag{4.12}$$

where k denotes $|\underset{\sim}{k}|$, etc..

Due to the recoil of the struck nucleon, the quantities $|\underset{\sim}{k}|$ and $|\underset{\sim}{k}'|$ actually depend on $\cos\theta_{\pi\nu}$ so equation (4.12) represents a nonlinear angle transformation. However, as equation (4.12) is often used (Fal72, Lan73), $|\underset{\sim}{k}|$ and $|\underset{\sim}{k}'|$ are taken to be independent of $\cos\theta_{\pi\nu}$ and a linear angle transformation is obtained. For instance, Landau, Phatak, and Tabakin (Lan73) suggest taking the momenta on-shell and calculating $|\underset{\sim}{k}|$ and $|\underset{\sim}{k}'|$

ssuming a nucleon

$|\underset{\sim}{k}'| = k_0$. U

e take $|f$

$|\underset{\sim}{k}| = |\underset{\sim}{k}'$

bstituting these

quation (4.12) we

(4.13) $\cos\theta$

Hence, in equation

$b = (P_\pi^0 / k_0)^2$

here no momentum

ncorrect at other

$|\cos\theta_{\pi N}|$ to

alues of $\cos\theta$

otential. As we

static approximat

is very poor at b

6. The effectiv

So far,

the ad hoc mo

se a value of U

ks 74). Hence,

n Chapter VII w

assuming a nucleon which remains frozen in the nucleus so $|\underset{\sim}{k}| = |\underset{\sim}{k}'| \equiv k_0$. Using the ansatz of Landau, Phatak, and Tabakin we take $|\underset{\sim}{p}_\pi| = |\underset{\sim}{p}'_\pi| \equiv p^0_\pi$ so that

$$|\underset{\sim}{k}| = |\underset{\sim}{k}'| = \left[1 - \left(\frac{A-1}{A}\right)\omega^0_\pi/\omega^0\right] p^0_\pi \equiv k_0$$

Substituting these values for the magnitudes of the momenta in equation (4.12) we get the transformation

$$\cos\theta_{\pi N} = 1 - (p^0_\pi/k_0)^2 + (p^0_\pi/k_0)^2 \cos\theta_{\pi\nu}. \tag{4.13}$$

Hence, in equation (4.10), we have $a = 1 - (p^0_\pi/k_0)^2$ and $b = (p^0_\pi/k_0)^2$. Equation (4.13) is valid for forward scattering where no momentum is transferred to the struck nucleon but is incorrect at other angles. For example, equation (4.13) allows $|\cos\theta_{\pi N}|$ to exceed 1 at backward angles. These unphysical values of $\cos\theta_{\pi N}$ introduce serious discrepancies into the optical potential. As we shall see later, the agreement between the modified static approximation and the fully integrated optical potential is very poor at backward angles.

6. The Effective Collision Energy

So far, nothing has been said about the choice of $\overline{\omega}_{CM}$ in the *ad hoc* models we have discussed. In general, most workers use a value of $\overline{\omega}_{CM}$ that is plausible for forward scattering (Lan73, Kis 74). Hence, for our study we use the value of $\overline{\omega}_{CM}$ obtained in Chapter VII with our systematic approximation, but evaluated for

toward on-shell sca

structure of the mod

result is[2]

(4.12) $\bar{\omega}_{cM} = \omega^0$

In equation (4.12),

average of $\underset{\sim}{p}^2_{4N}$ (

in the relativistic

We take the energy

(4.13) $\omega^0 = \omega$

This expression f

that plus the gro

energy (neglectin

(4.14) $\omega^0 = (p$

where $\langle \underset{\sim}{p}^2_N \rangle$

1 The

is, at most, a

2 The

nation" (equati

$\omega\theta_{NN} = 1$

forward on-shell scattering. This choice is intended to be representative of the models found in the literature.[1] The explicit result is[2]

$$(4.14)\quad \bar{\omega}_{CM} = \omega^0 - (\hbar^2c^2/2\omega^0)\left[\left(\frac{A-1}{A}\right)^2 p_\pi^{0\,2} + \langle \underset{\sim}{p}_{4N}^{\,2} \rangle\right].$$

In equation (4.14), the quantity $\langle \underset{\sim}{p}_{4N}^{\,2} \rangle$ is the ground state average of $\underset{\sim}{p}_{4N}^{\,2}$ (we use $\langle \underset{\sim}{p}_{4N}^{\,2} \rangle = 1\ \mathrm{fm}^{-2}$). The variable p_π^0 is the relativistic momentum of the incident pion in the πNCM frame. We take the energy parameter ω^0 to be

$$(4.15)\quad \omega^0 = \omega_\pi^0 + m_N c^2 + (\hbar^2c^2/2m_Nc^2)\left[\langle \underset{\sim}{p}_{4N}^{\,2} \rangle + (p_\pi^0/A)^2\right].$$

This expression for ω^0 is just the relativistic energy of the pion plus the ground state average of the relativistic nucleon energy (neglecting the potential energy). That is, ω^0 is

$$(4.16)\quad \omega^0 = (\hbar^2c^2 p_\pi^{0\,2} + m_\pi^2 c^4)^{1/2} + m_N c^2 + (\hbar^2c^2/2m_Nc^2)\langle \underset{\sim}{p}_N^{\,2} \rangle$$

where $\langle \underset{\sim}{p}_N^{\,2} \rangle = \langle \underset{\sim}{p}_{4N}^{\,2} \rangle + (p_\pi^0/A)^2$.

---

[1] The difference between equation (4.14) and typical choices is, at most, a few MeV. (See, for example, (Lan73)).

[2] The result given here is obtained from the "linear approximation" (equation (7.6) of Chapter VII) for $|\underset{\sim}{p}_\pi| = |\underset{\sim}{p}'_\pi| = p_\pi^0$ and $\cos\theta_{\pi N} = 1$.

THE FAC
POT

When our

(1[illegible]), Miller (M

formulors which ta

will not discuss

In Chapter VII we

variables (ω_{c}

easy to use as any

However, for compl

prescriptions.

Instead

ingle transformati

we could have calc

value for P_{N}

(5.1) $\underset{\sim}{k} = P_{\underset{\sim}{k}}$

[1]See A

CHAPTER V

THE FACTORED FORM OF THE π - ^{4}He OPTICAL POTENTIAL: A RECENT <u>AD HOC</u> MODEL

When our work was nearing completion, Kujawski and Miller (Kuj74), Miller (Mil74), and Landau (Lan74) proposed angle transformations which take into account the recoil of the nucleon. We shall not discuss these recent developments in great detail since in Chapter VII we present a more systematic choice for all of the variables $(\omega_{cm}, \underset{\sim}{k}, \underset{\sim}{k}') = \underset{\sim}{\Omega}$ which is just as easy to use as any of these more recent <u>ad hoc</u> prescriptions. However, for completeness, we shall give the general form of these prescriptions.

Instead of assuming $|\underset{\sim}{k}| = |\underset{\sim}{k}'| \equiv k_0$ as in the angle transformation used in the modified static approximation, we could have calculated $|\underset{\sim}{k}|$ and $|\underset{\sim}{k}'|$ by assuming some value for $\underset{\sim}{P}_N$ in the quasi-relativistic relations[1]

$$(5.1)\quad \underset{\sim}{k} = \underset{\sim}{P}_\pi - (\omega_\pi^0/\omega^0)\underset{\sim}{\chi}\ , \quad \underset{\sim}{k}' = \underset{\sim}{P}_\pi' - (\omega_\pi^0/\omega^0)\underset{\sim}{\chi}$$

---

[1]See Appendix A for a discussion of kinematics.

here $\underset{\sim}{\kappa} = \underset{\sim}{\kappa}'$

blem. The value

of the value used

th either of thes

elation between

nalizing optical

fully integrated o

f Chapter IV. In

nsformation tha

ne systematic app

potential.

A conven

Miller, and Landau

ratic approximat

(MLA) is to set

nd expand the tra

keeping terms up t

rocedure, we get

e compare these

$(E_R = 188$

nsformations h

lso have the sa

1The fo

form given by Ku

2To or

Miller, and Land

where $\underset{\sim}{K} = \underset{\sim}{K}' = \underset{\sim}{p}_\pi + \underset{\sim}{p}_N = \underset{\sim}{p}'_\pi + \underset{\sim}{p}'_N$ for a free nucleon. The value for $\underset{\sim}{p}_N$ used by Miller[1] is $\underset{\sim}{p}_N = 0$ and the value used by Landau is $\underset{\sim}{p}_N = -\frac{1}{2}(\underset{\sim}{p}_\pi - \underset{\sim}{p}'_\pi)$. With either of these choices, equation (5.1) leads to a non-linear relation between $\cos\theta_{\pi N}$ and $\cos\theta_{\pi\nu}$ and the resulting optical potential is in much better agreement with the fully integrated optical potential than the two older ad hoc models of Chapter IV. In fact, the choice made by Landau gives an angle transformation that is almost identical to the one we obtain in our systematic approximation to the fully integrated optical potential.

A convenient way to compare the transformation of Kujawski, Miller, and Landau (KML) with the transformations of the simple static approximation (SSA) and the modified static approximation (MSA) is to set $|\underset{\sim}{p}_\pi| = |\underset{\sim}{p}'_\pi| = p^0_\pi$ (i.e., on-shell) and expand the transformation formulas in powers of $\omega^0_\pi/\omega^0 \cong 1/5$ keeping terms up to the first power in ω^0_π/ω^0. With this procedure, we get the results shown in Table 5.1.[2] In Figure (5.1) we compare these transformations graphically for $p^0_\pi = 1.5\ fm^{-1}$ $(E_\pi = 188\ MeV)$. At $\theta_{\pi\nu} = 0^\circ$, all three transformations have the same value. The MSA and KLM approximations also have the same slope at $\theta_{\pi\nu} = 0^\circ$. At $\theta_{\pi\nu} = 180^\circ$ the

---

[1] The form given by Miller is equivalent on-shell to the form given by Kujawski and Miller.

[2] To order ω^0_π/ω^0, the transformations of Kujawski, Miller, and Landau are the same for $|\underset{\sim}{p}_\pi| = |\underset{\sim}{p}'_\pi| = p^0_\pi$.

XIII 5.1—A comparis
with approximation
by Lyaskd-Miller-I

$\cos\theta_{\pi N}$ =	
$\cos\theta_{\pi N}$ =	
$\cos\theta_{\pi N}$ =	

TABLE 5.1--A comparison of the angle transformations used in the simple static approximation (SSA), the modified static approximation (MSA), and the Kujawski-Miller-Landau approximation (KML).

SSA:	$\cos\theta_{\pi N} = \cos\theta_{\pi\nu}$
MSA:	$\cos\theta_{\pi N} = -2\omega_\pi^\circ/\omega^\circ + (1 + 2\omega_\pi^\circ/\omega^\circ)\cos\theta_{\pi\nu}$
KML:	$\cos\theta_{\pi N} = -\omega_\pi^\circ/\omega^\circ + \cos\theta_{\pi\nu} + (\omega_\pi^\circ/\omega^\circ)\cos^2\theta_{\pi\nu}$

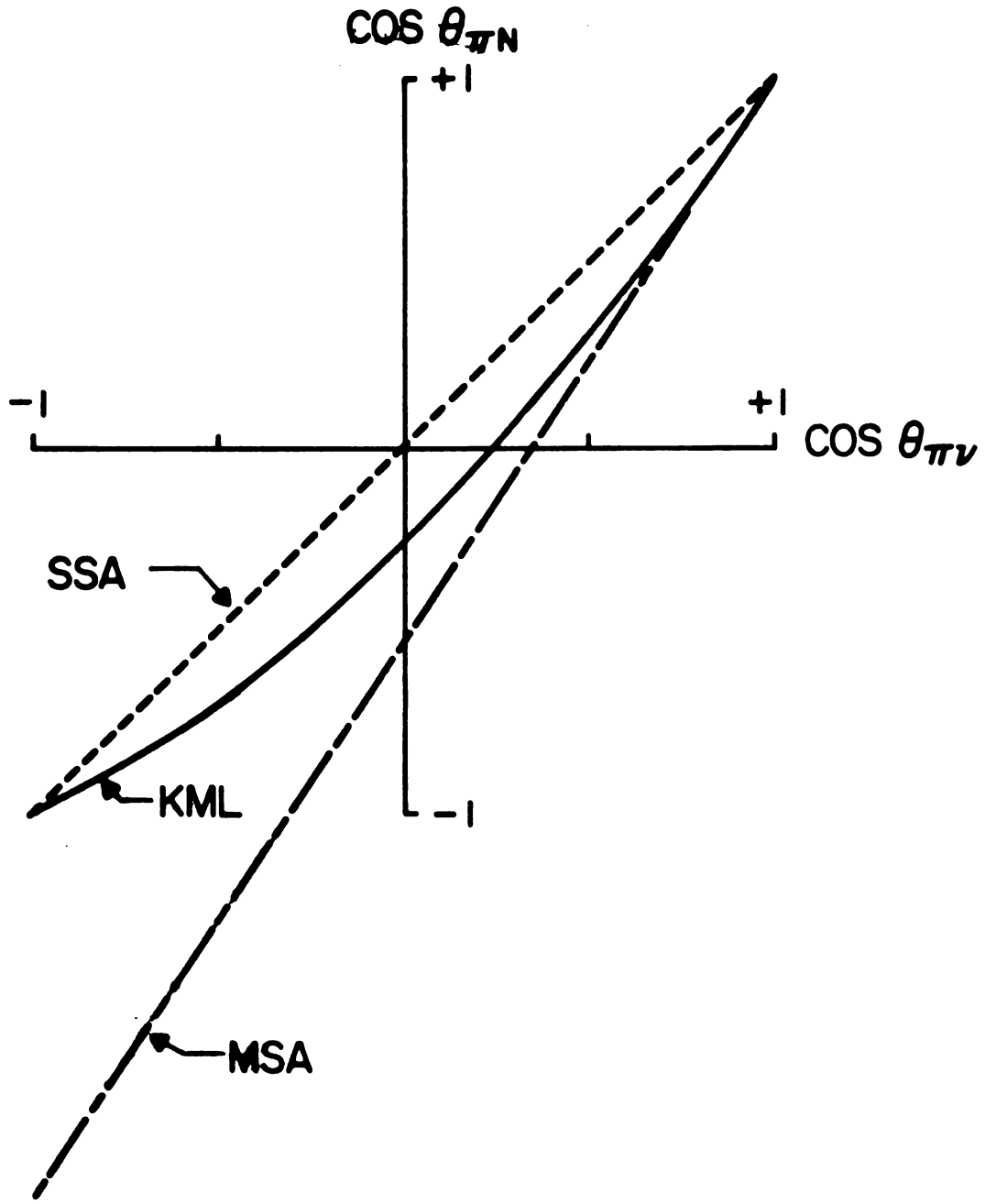

FIGURE 5.1--Graphical representation of the angle transformations used in the simple static approximation (SSA), modified static approximation (MSA), and the Kujawski-Miller-Landau approximation (KML) for $|\vec{p}_J| = |\vec{p}'_J| = p^*_\pi = 1.5$ fm^{-1}

SA and KLM approxi

e MSA gives $\cos\theta_{\pi N}$

apers, the unphy

ained with the M

partial. The KLM

ich cancels the

ut $\cos\theta_{\pi N}$

he inclusion of n

apparently remedie

atic approximati

Although

ucleon recoil are

epresented by the

atic approximati

pproach to the fi

ightforwardness by

fully integrated

ion allows some

scattering.

In Chap

ransformation o

integrated recul

eatures of the

he choice of

SSA and KLM approximation both give $\cos\theta_{\pi N} = -1$ while the MSA gives $\cos\theta_{\pi N} \cong -2$. As discussed in previous chapters, the unphysical backward angle values for $\cos\theta_{\pi N}$ obtained with the MSA leads to large discrepancies in the optical potential. The KLM transformation has a $\cos^2\theta_{\pi\nu}$ term which cancels the constant term for $\theta_{\pi\nu} \to 0^\circ$ or 180° so that $\cos\theta_{\pi N}$ varies nonlinearly between + 1 and - 1 . The inclusion of nucleon recoil via the KML angle transformation apparently remedies most of the problems associated with the simple static approximation and modified static approximation.

Although the more recent prescriptions which include nucleon recoil are certainly an improvement over the prescriptions represented by the simple static approximation and the modified static approximation, they are no less arbitrary. Our systematic approach to the factored form in Chapter VII eliminates this arbitrariness by relating the prescription for $\underset{\sim}{\overline{\Omega}}$ to the fully integrated result and perhaps more importantly, our prescription allows some insight into the physics of elastic pion-nucleus scattering.

In Chapters VI and X we show results using the angle transformation of KML. The general agreement with the fully integrated result is surprisingly good although some important features of the fully-integrated result (which are associated with the choice of $\overline{\omega}_{cm}$) are not given by the KML ansatz.

THE FACTORED F
THE EFFECTI

1. Definition of th

Writing th

ion allows a conve

from the pion-nucle

that the pion-nucle

state form factor

The interaction fa

it should contain

to clear a priori

static approximati

a posteriori they

impulse interacti

potential in the

(4.1) U

1 Howe

better agreemen

single static a

CHAPTER VI

THE FACTORED FORM OF THE π - ^{4}He OPTICAL POTENTIAL: THE EFFECTIVE PION-NUCLEON IMPULSE INTERACTION

1. Definition of the Effective Impulse Interaction

Writing the π - ^{4}He optical potential in a factored form allows a convenient separation of nuclear structure effects from the pion-nucleon interaction effects; however, we must realize that the pion-nucleon interaction factor which multiplies the ground state form factor is actually an effective pion-nucleon interaction. The interaction factor is a function of just the pion coordinates but should contain the effects of internal nucleon motion. It is not clear *a priori* that the simple static approximation or modified static approximation properly represent the nucleon motion effects (*a posteriori* they do not[1]) so we *define* an effective pion-nucleon impulse interaction by writing the fully-integrated π -He optical potential in the form

$$(6.1)\quad U_{\pi A}(\underset{\sim}{p}'_\pi, \underset{\sim}{p}_\pi) \equiv (A-1)\langle t_{\pi N}\rangle \rho(\underset{\sim}{q})$$

---

[1] However, the more recent KML approximation gives much better agreement with the fully-integrated result than either the simple static approximation or the modified static approximation.

n

(6.2) $\langle t_{\pi N} \rangle$

ere $\langle t_{\pi N} \rangle$

d $U_{\pi\nu}$ is

ulated as desc

$\langle t_{\pi N} \rangle$ a

otential without

w focus our atte

otential itself.

It shoul

n cases where ρ

an be written exp

$\langle t_{\pi N} \rangle$ d

uclear wave funct

$N_0 \exp(-\frac{1}{3}$

ables results in

is well defined.

aussian wave fu

for $\langle t_{\pi N} \rangle$

ext section we

$\langle t_{\pi N} \rangle$

ation and the n

or

$$(6.2)\quad \langle t_{\pi N} \rangle \equiv \left[(A-1)\rho(\underset{\sim}{q}) \right]^{-1} U_{\pi\nu}(\underset{\sim}{p}'_{\pi}\, \underset{\sim}{p}_{\pi})$$

where $\langle t_{\pi N} \rangle$ is the effective pion-nucleon impulse interaction and $U_{\pi\nu}$ is the fully-integrated π - ^{4}He optical potential calculated as described in Chapter III. The above definition for $\langle t_{\pi N} \rangle$ allows us to have a factored form for the optical potential without making any arbitrary choice for $\underset{\sim}{\Omega}$. We can now focus our attention on $\langle t_{\pi N} \rangle$ rather than the optical potential itself.

It should be noted that $\langle t_{\pi N} \rangle$ is well defined only in cases where $\rho(\underset{\sim}{q})$ has no zeros or where $U_{\pi\nu}(\underset{\sim}{p}'_{\pi}\, \underset{\sim}{p}_{\pi})$ can be written explicitly in factored form. Since we expect that $\langle t_{\pi N} \rangle$ does not depend strongly on the details of the nuclear wave function, we take $\psi(\underset{\sim}{p}_{4N})$ to be of the form $N_0 \exp(-\frac{1}{3} R_0^2 \underset{\sim}{p}_{4N}^2)$ with $R_0 \cong 1.5$ fm . This choice results in a gaussian form factor so that $\langle t_{\pi N} \rangle$ is well defined. We calculate $U_{\pi\nu}(\underset{\sim}{p}'_{\pi}\, \underset{\sim}{p}_{\pi})$ using the gaussian wave function and then obtain the fully-integrated result for $\langle t_{\pi N} \rangle$ via the definition in equation (5.2). In the next section we compare the exact or fully-integrated result for $\langle t_{\pi N} \rangle$ with the result given by the simple static approximation and the modified static approximation.

4. The Fully-Inte
Single Static A

The two

factored form of

garded as approxi

mpulse interactio

where $\bar{t}$ is gi

nsider the simpl

pproximation to b

emainder of our d

In Figu

the following case

from a numerical e

efinition in equ

static approximat

static approximat

ucleon interacti

the following zer

(6.3) $\bar{t}_{\pi N}$

The above form

with $I = 3/2$

is hence $(1/3\pi$

It is

gnificant dif

2. The Fully-Integrated Impulse Interaction Compared to the Simple Static Approximation and the Modified Static Approximation

The two *ad hoc* approximations used in Chapter IV to obtain a factored form of the π - ^{4}He optical potential can now be regarded as approximations for the exact or fully-integrated effective impulse interaction, i.e., $\langle t_{\pi N} \rangle \cong \bar{t}_{\pi N}(\underset{\sim}{\bar{\Omega}})$ where $\underset{\sim}{\bar{\Omega}}$ is given by the prescriptions in Chapter IV. We will consider the simple static approximation and the modified static approximation to be approximations for $\langle t_{\pi N} \rangle$ in the remainder of our discussions.

In Figures 6.1 - 6.3 we show on-shell $\langle t_{\pi N} \rangle$ for the following cases: (a) the fully-integrated result obtained from a numerical evaluation of $U_{\pi\nu}(p'_{\pi}\, p_{\pi})$ and the definition in equation 6.2; (b) the result obtained from the simple static approximation; (c) the result obtained from the modified static approximation. In all three cases we have assumed the pion-nucleon interaction is in the (3,3) channel only and we have used the following zero-range form for $\bar{t}_{\pi N}(\underset{\sim}{\Omega})$:

$$\bar{t}_{\pi N}(\underset{\sim}{\Omega}) = \gamma \alpha_{33}(\omega_{cm})\, \hat{k}' \cdot \hat{k} . \tag{6.3}$$

The above form is just the parameterization described in Appendix B with $I = 3/2, J = 3/2$, and $L = 1$. The factor α_{33} is hence $(1/3\pi)\, t_{IJL}$.

It is apparent from Figures 6.1 - 6.3 that there are significant differences between the fully-integrated result for

FIGURE 6.1-- The real and imaginary parts of the effective pion-nucleon impulse interaction as a function of the cosine of the pion-nucleus C.M. scattering angle calculated by three methods: (a) (solid line) the effective interaction resulting from full integration of the impulse approximation (FIA); (b) (short dash line) the simple static approximation (SSA); (c) (dot-dash line) the modified static approximation (MSA). The laboratory kinetic energy of the pion is 110 MeV.

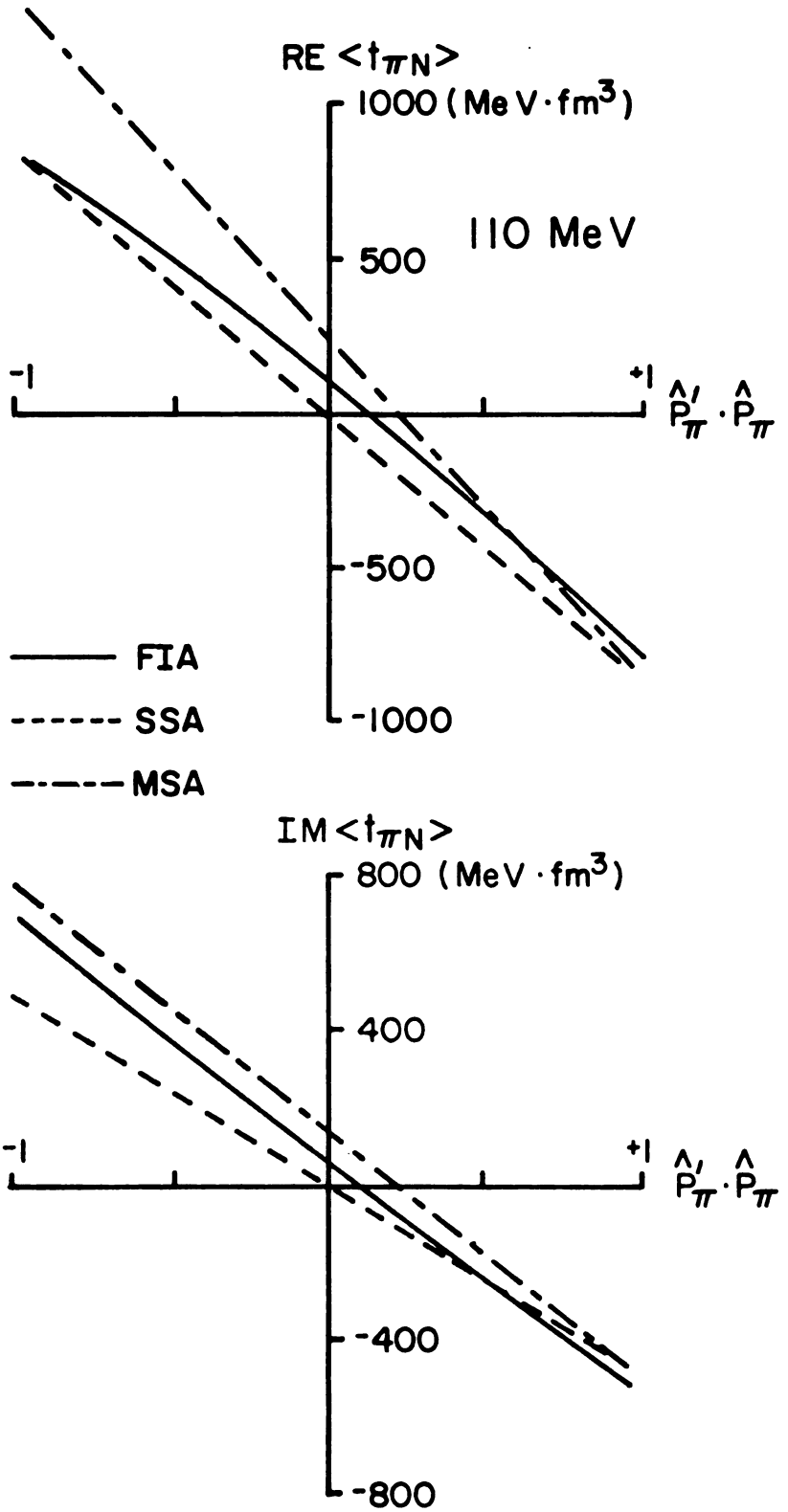
RE $<t_{\pi N}>$
1000 (MeV·fm^3)
110 MeV
500
-500
-1000
-1
+1
$\hat{P}'_\pi \cdot \hat{P}_\pi$
FIA
SSA
MSA
IM $<t_{\pi N}>$
800 (MeV·fm^3)
400
-400
-800
-1
+1
$\hat{P}'_\pi \cdot \hat{P}_\pi$

FIGURE 6.1.

ure 6.2--As t
ur bending at
tegrated impl

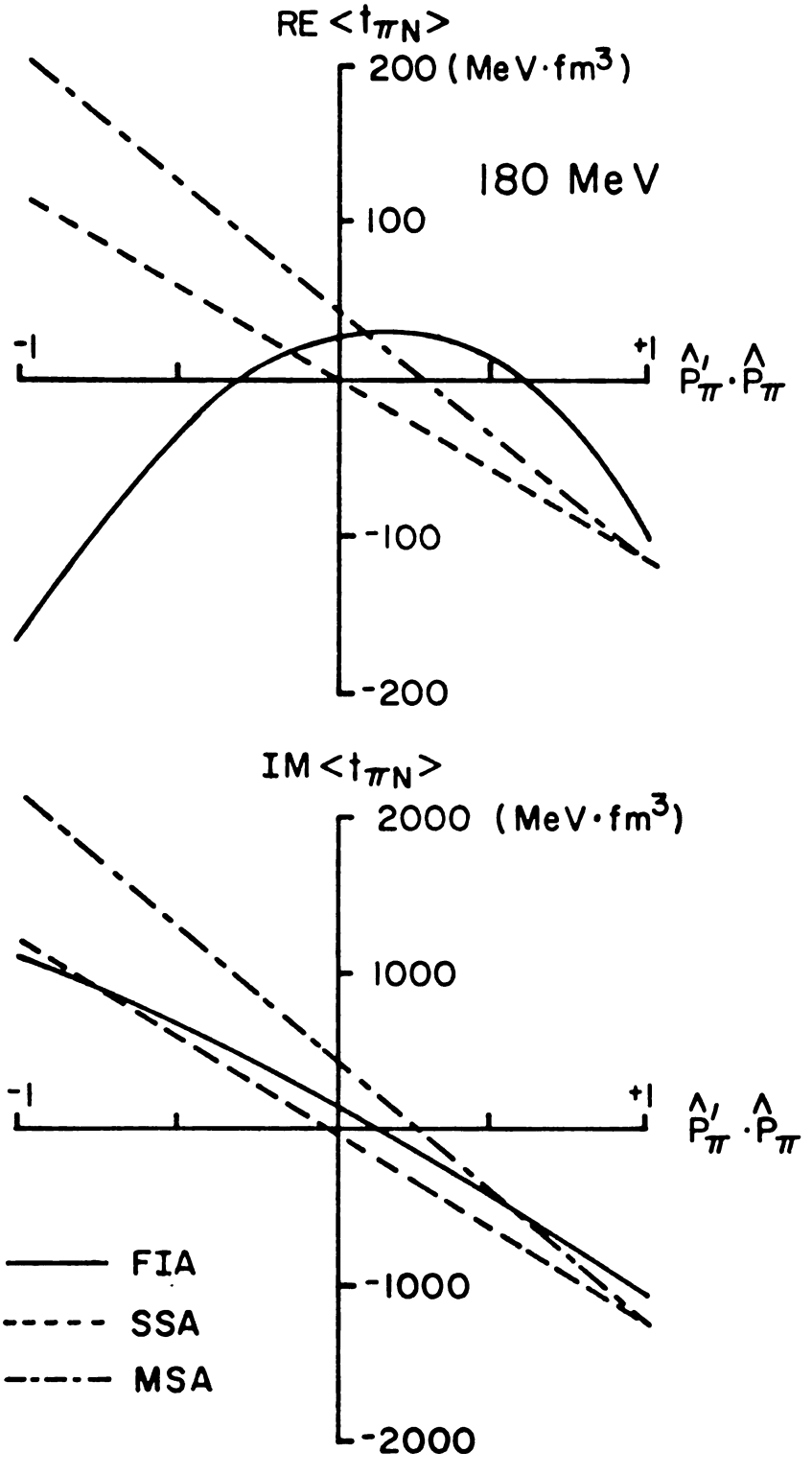

FIGURE 6.2--As in Figure 6.1 except at 180 MeV. Note the strong down bending at backward angles in the real part of the fully-integrated impulse interaction (FIA).

260

-1

FIG 6.3--A

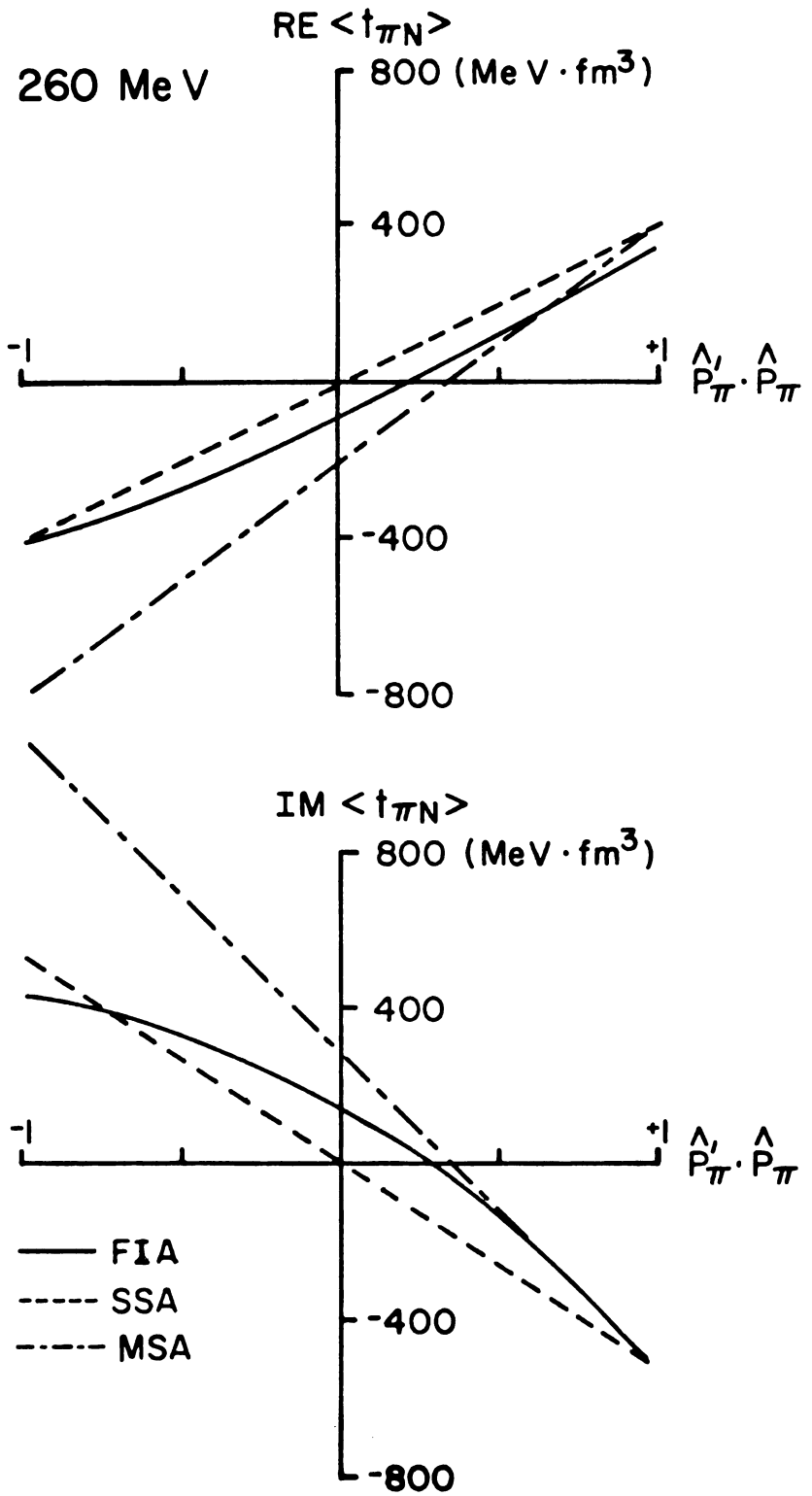

FIGURE 6.3--As in Figure 6.1 except at 260 MeV.

$\langle t_{\pi N} \rangle$ and t

d the modified s

ese differences

$\langle t_{\pi N} \rangle$ whi

which allows us t

d nucleon motion

n prescription

). Comparison of
with the Hu

As men

mined, the ne

egan to come in

alculated $\langle t$

Paper V. The

he PL approxi-

tegrated recoil

me significant

It is

pproximation f

pproximations)

$\cos\theta_{\pi N}$

n Table 5.1.

pproximation a

ucleon recoil

$\langle t_{\pi N} \rangle$ and the results given by the simple static approximation and the modified static approximation. In trying to understand these differences we have arrived at a simple prescription for $\langle t_{\pi N} \rangle$ which is in good agreement with the exact result and which allows us to understand in a transparent way the main effects of nucleon motion in elastic pion-nucleus scattering. We present our prescription for $\langle t_{\pi N} \rangle$ in Chapter VII.

3. Comparison of the Fully-Integrated Impulse Interaction with the Kujawski-Miller-Landau Model

As mentioned in Chapter V, when our study was nearly finished, the newer models which take nucleon recoil into account began to come into use. For the sake of completeness, we have calculated $\langle t_{\pi N} \rangle$ using the KML angle transformation in Chapter V. The results are shown in Figures 6.4 - 6.6. Clearly, the KML approximation is a much better representation of the fully-integrated result for $\langle t_{\pi N} \rangle$, although there are still some significant discrepancies.

It is important to note that at each energy the KML approximation for $\langle t_{\pi N} \rangle$ (as well as the other two *ad hoc* approximations) is just a complex constant times the function for $\cos\theta_{\pi N}$ given by the associated angle transformation in Table 5.1. The surprisingly good agreement between the KML approximation and the fully-integrated result thus indicates that nucleon recoil is an important effect in $\langle t_{\pi N} \rangle$.

FIGURE 6.4--The real and imaginary parts of the effective pion-nucleon impulse interaction as a function of the cosine of the pion-nucleus C.M. scattering angle calculated by two methods: (a) (solid line) the effective interaction resulting from full integration of the impulse approximation (FIA); (b) (large dots) the Kujawski-Miller-Landau approximation (KML) to case (a). The laboratory kinetic energy of the pion is 110 MeV.

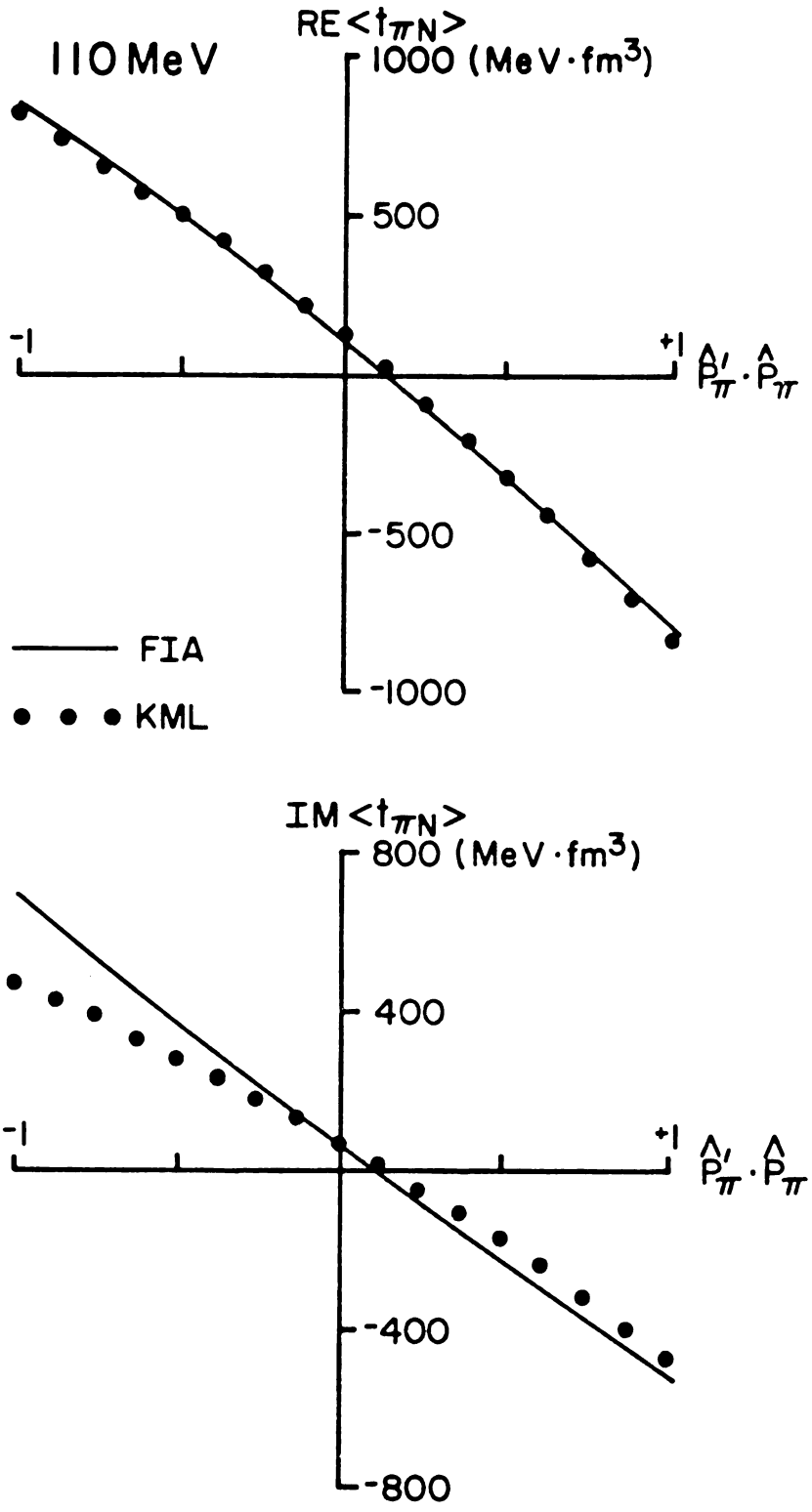
RE<$t_{\pi N}$>
110 MeV
1000 (MeV·fm^3)
500
-500
-1000
-1
+1
$\hat{p}'_\pi \cdot \hat{p}_\pi$
FIA
KML
IM<$t_{\pi N}$>
800 (MeV·fm^3)
400
-400
-800
-1
+1
$\hat{p}'_\pi \cdot \hat{p}_\pi$

FIGURE 6.4.

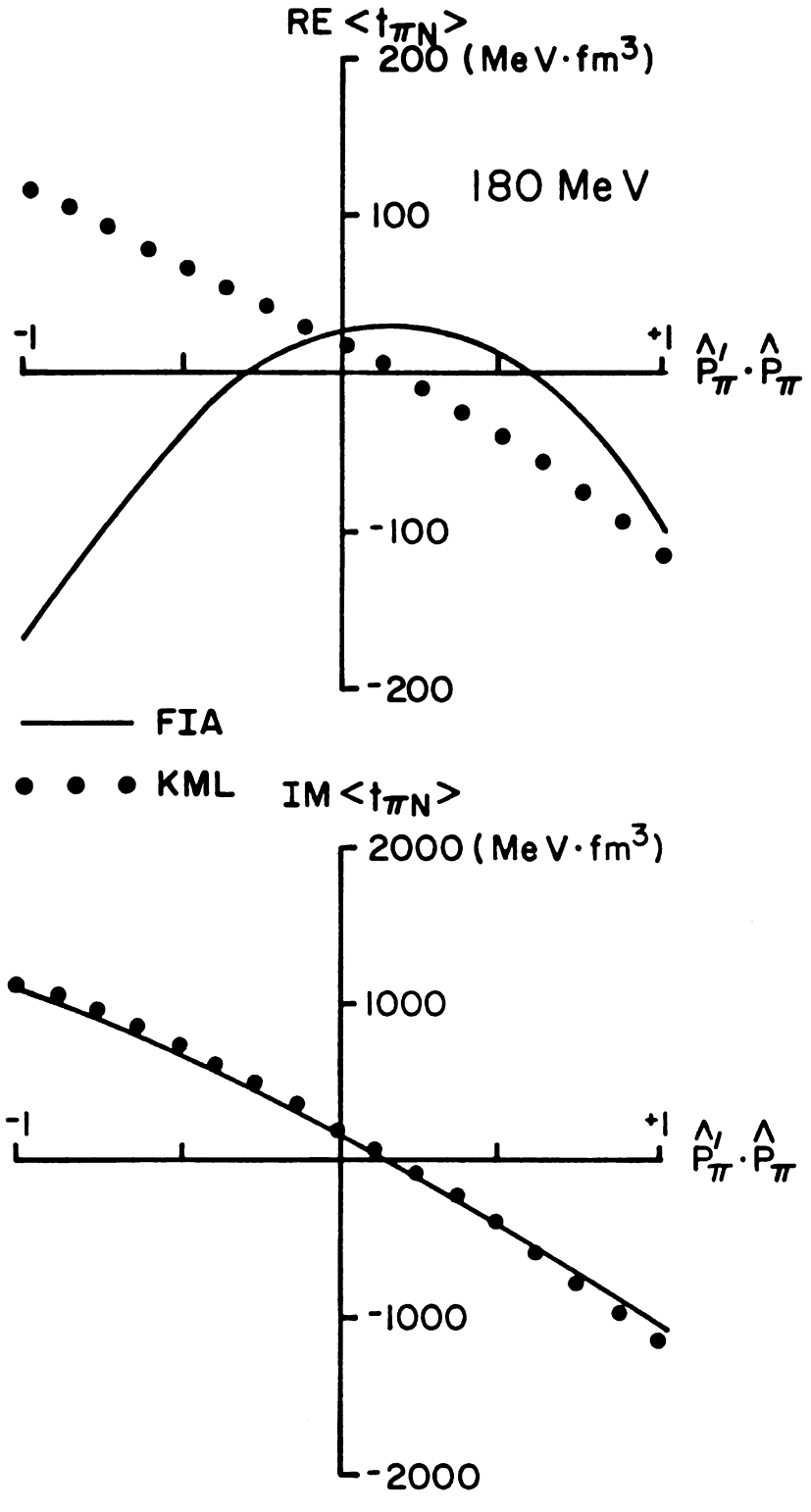

FIGURE 6.5--As in Figure 6.4 except at 180 MeV.

260

-1

-1

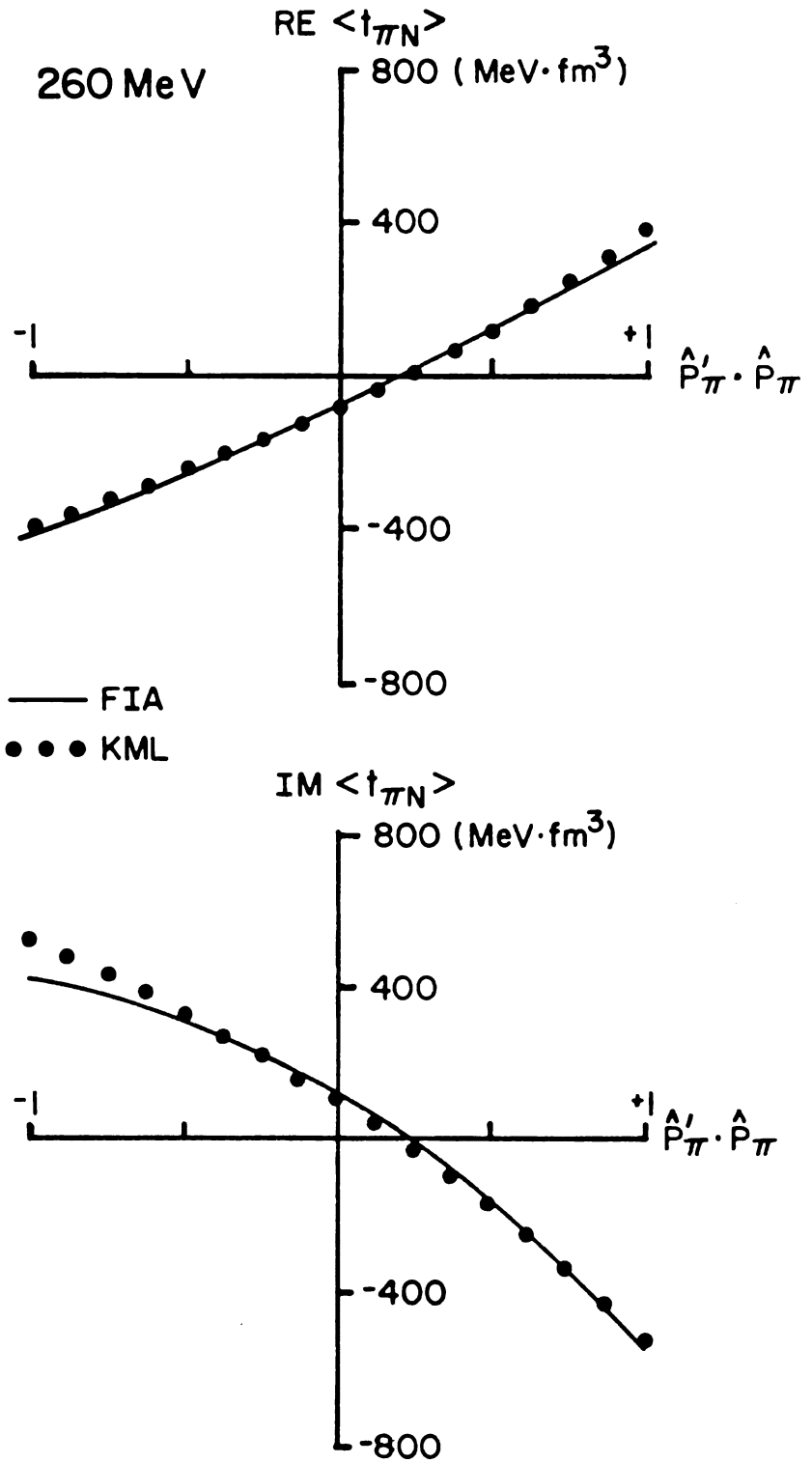

FIGURE 6.6--As in Figure 6.4 except at 260 MeV.

A SYST
Fl

In thi
ematic appro
interaction.

1. A linear A

We a
molecu motion
obtaining for

(2.1) <t

x

ized in
R. Feynma

CHAPTER VII

A SYSTEMATIC APPROXIMATION FOR THE EFFECTIVE PION-NUCLEON IMPULSE INTERACTION

In this chapter we outline a method for obtaining a systematic approximation for the effective pion-nucleon impulse interaction.

1. A Linear Approximation

We assume the fluctuations in $\bar{t}_{\pi N}(\underset{\sim}{\Omega})$ due to nucleon motion are small and make a linear expansion of $\bar{t}_{\pi N}(\underset{\sim}{\Omega})$ obtaining for $\langle t_{\pi N} \rangle$ [1]

$$\langle t_{\pi N} \rangle \cong \rho(\underset{\sim}{q})^{-1} \int \psi^*(\underset{\sim}{p}_{4N} + \tfrac{A-1}{A}\underset{\sim}{q})\psi(\underset{\sim}{p}_{4N}) \times \left[\bar{t}_{\pi N}(\underset{\sim}{\bar{\Omega}}) + \left(\underset{\sim}{\nabla}_{\underset{\sim}{q}} \bar{t}_{\pi N}\right)_{\underset{\sim}{\bar{\Omega}}} \cdot (\underset{\sim}{\Omega} - \underset{\sim}{\bar{\Omega}})\right] \frac{d^3 p_{4N}}{(2\pi)^3} \tag{7.1}$$

---

[1] It turns out a similar approach has previously been used in nucleon-nucleus scattering (Kow63, Ade72). We thank R. Landau for bringing these calculations to our attention.

use the expansi

if we choose $\vec{r}$

$$\vec{r} = \rho \quad (12)$$

the linear term

$$\langle t_F \quad (13)$$

where $\vec{r}$ is

description of

In c

we use the gau

take a change

$$\vec{r} = \quad (14)$$

The form fac

$\exp(-R_0^2 q^2$

$$\vec{r} \quad (15)$$

where the expansion point $\underset{\sim}{\bar{\Omega}}$ is arbitrary at this time. Clearly if we choose $\underset{\sim}{\bar{\Omega}}$ to be

$$(7.2)\quad \underset{\sim}{\bar{\Omega}} = \rho(q)^{-1}\int \underset{\sim}{\Omega}\, \psi^*\left(p_{4N} + \frac{A-1}{A}\, q\right)\psi(p_{4N})\,\frac{d^3p_{4N}}{(2\pi)^3}$$

the linear term vanishes so that we obtain the simple prescription

$$(7.3)\quad \langle t_{\pi N}\rangle \cong \bar{t}_{\pi N}(\underset{\sim}{\bar{\Omega}})$$

where $\underset{\sim}{\bar{\Omega}}$ is defined in equation (7.2). We call the above prescription the "linear approximation" for $\langle t_{\pi N}\rangle$.

In order to obtain an explicit expression for $\langle t_{\pi N}\rangle$ we use the gaussian form for $\psi(p_{4N})$ given in Chapter VI and make a change of variable $p_{4N} \rightarrow p^* - \frac{A-1}{2A}\, q$ so we have

$$(7.4)\quad \underset{\sim}{\bar{\Omega}} = \rho(q)^{-1}\exp(-R_0^2 q^2/6) \times \int \underset{\sim}{\Omega}\, N_0^2 \exp(-2R_0^2 p^{*2}/3)\,\frac{d^3p^*}{(2\pi)^3}$$

The form factor associated with our gaussian wave function is $\exp(-R_0^2 q^2/6)$ so we have finally

$$(7.5)\quad \underset{\sim}{\bar{\Omega}} = \int \underset{\sim}{\Omega}\, N_0^2 \exp(-2R_0^2 p^{*2}/3)\,\frac{d^3p^*}{(2\pi)^3}\,.$$

use the quasi-pa

ain for $\bar{k}$

(18) $\bar{\omega}_{cm} =$

(17) $\bar{k} =$

(18) $\bar{k}' =$

equations (

the initial an

The quantity

$(\omega_\pi^0 = (\hbar$

ual ground

ω^0 is

nucleon ene

(19)

We use the quasi-relativistic kinematics given in Appendix A and obtain for $\underset{\sim}{\bar{k}}$ [1]

$$(7.6)\quad \bar{\omega}_{CM} = \omega^0 - \frac{\hbar^2 c^2}{2\omega^0}\left[\left(\frac{A-1}{2A}\right)^2 \left(\underset{\sim}{P}_\pi + \underset{\sim}{P}'_\pi\right)^2 + \langle \underset{\sim}{P}^2_{4N} \rangle\right]$$

$$(7.7)\quad \underset{\sim}{\bar{k}} = \underset{\sim}{P}_\pi - \left(\omega^0_\pi/\omega^0\right)\left(\frac{A-1}{2A}\right)\left(\underset{\sim}{P}_\pi + \underset{\sim}{P}'_\pi\right)$$

$$(7.8)\quad \underset{\sim}{\bar{k}'} = \underset{\sim}{P}'_\pi - \left(\omega^0_\pi/\omega^0\right)\left(\frac{A-1}{2A}\right)\left(\underset{\sim}{P}_\pi + \underset{\sim}{P}'_\pi\right) .$$

In equations (7.6) - (7.8), $\underset{\sim}{P}_\pi$ and $\underset{\sim}{P}'_\pi$ are respectively the initial and final momentum of the pion in the πNCM frame. The quantity ω^0_π is the relativistic energy of the incident pion $\left(\omega^0_\pi = \left(\hbar^2 c^2 P^{02}_\pi + m^2_\pi c^4\right)^{1/2}\right)$ and $\langle \underset{\sim}{P}^2_{4N} \rangle$ is the usual ground state average of $\underset{\sim}{P}^2_{4N}$. The energy parameter ω^0 is ω^0_π plus the ground state average of the relativistic nucleon energy (neglecting the potential energy), i.e.,

$$(7.9)\quad \omega^0 = \omega^0_\pi + M_N c^2 + \left(\hbar^2 c^2/2M_N c^2\right)\langle P^2_N \rangle$$

---

[1] We could use fully relativistic kinematics just as easily. For purposes of comparison we consistently use the quasi-relativistic kinematics of Appendix A.

ware $\langle p_N^2 \rangle = \langle$

ur for on-shell

ture prescription

e the simple and

In Figur

for $\langle t_{\pi N} \rangle$

I. A Quadratic A

A smoot

for $\langle t_{\pi N} \rangle$

lapse for $\bar{t}_{\pi N}$

expansion of

n $d_{33}(\omega_{CM}$

e thus expand

ther order in

ay of accounti

dence in $\bar{t}_{\pi N}$

In Fi

region $(m_\pi +$

n regions whe

teraction, we w

effect. For e

$\omega_{CM} - (m$

ewhat with

$\bar{t}$

where $\langle p_N^2 \rangle = \langle p_{4N}^2 \rangle + \left(p_\pi^0/A\right)^2$. It should be noted that for on-shell values of p_π and p_π' and $\theta_{\pi\nu} = 0^\circ$, the above prescription for $\langle t_{\pi N} \rangle$ reduces to the prescriptions in the simple and modified static approximations.

In Figures 7.1 - 7.3 we compare the linear approximation for $\langle t_{\pi N} \rangle$ with the fully-integrated result.

2. A Quadratic Approximation

A smoothing effect is missing in our linear approximation for $\langle t_{\pi N} \rangle$ that can be included by using energy averaged input for $\bar{t}_{\pi N}$ or by including higher order terms in the expansion of $\bar{t}_{\pi N}$. We consider here a quadratic approximation to $\alpha_{33}(\omega_{cm})$ in the zero-range t-matrix of equation (6.3).[1] We thus expand $\bar{t}_{\pi N}$ to second order in ω_{cm} but only to first order in k and k'. This procedure provides a simple way of accounting for the main part of the nonlinear energy dependence in $\bar{t}_{\pi N}$.

In Figure 7.4 we show $\alpha_{33}(\omega_{cm})$ in the energy region $(m_\pi + m_N)c^2$ to $(m_\pi + m_N)c^2 + 400$ MeV. In regions where $\alpha_{33}(\omega_{cm})$ shows strong nonlinear behavior, we want our quadratic approximation to produce an averaging effect. For example, the peak in $IM(\alpha_{33})$ at $\omega_{cm} - (m_\pi + m_N)c^2 \cong 150$ MeV should be lowered somewhat with a quadratic approximation.

---

[1] The parameterization in equation (6.3) is

$$\bar{t}_{\pi N}(q) = \gamma\, \alpha_{33}(\omega_{cm})\, \hat{k}' \cdot \hat{k} \ .$$

FIGURE 7.1--The real and imaginary parts of the effective pion-nucleon impulse interaction as a function of the cosine of the pion-nucleus C.M. scattering angle calculated by two methods: (a) (solid line) the effective interaction resulting from full integration of the impulse approximation (FIA); (b) (large dots) the linear approximation (LA) to case (a). The laboratory kinetic energy of the pion is 110 MeV.

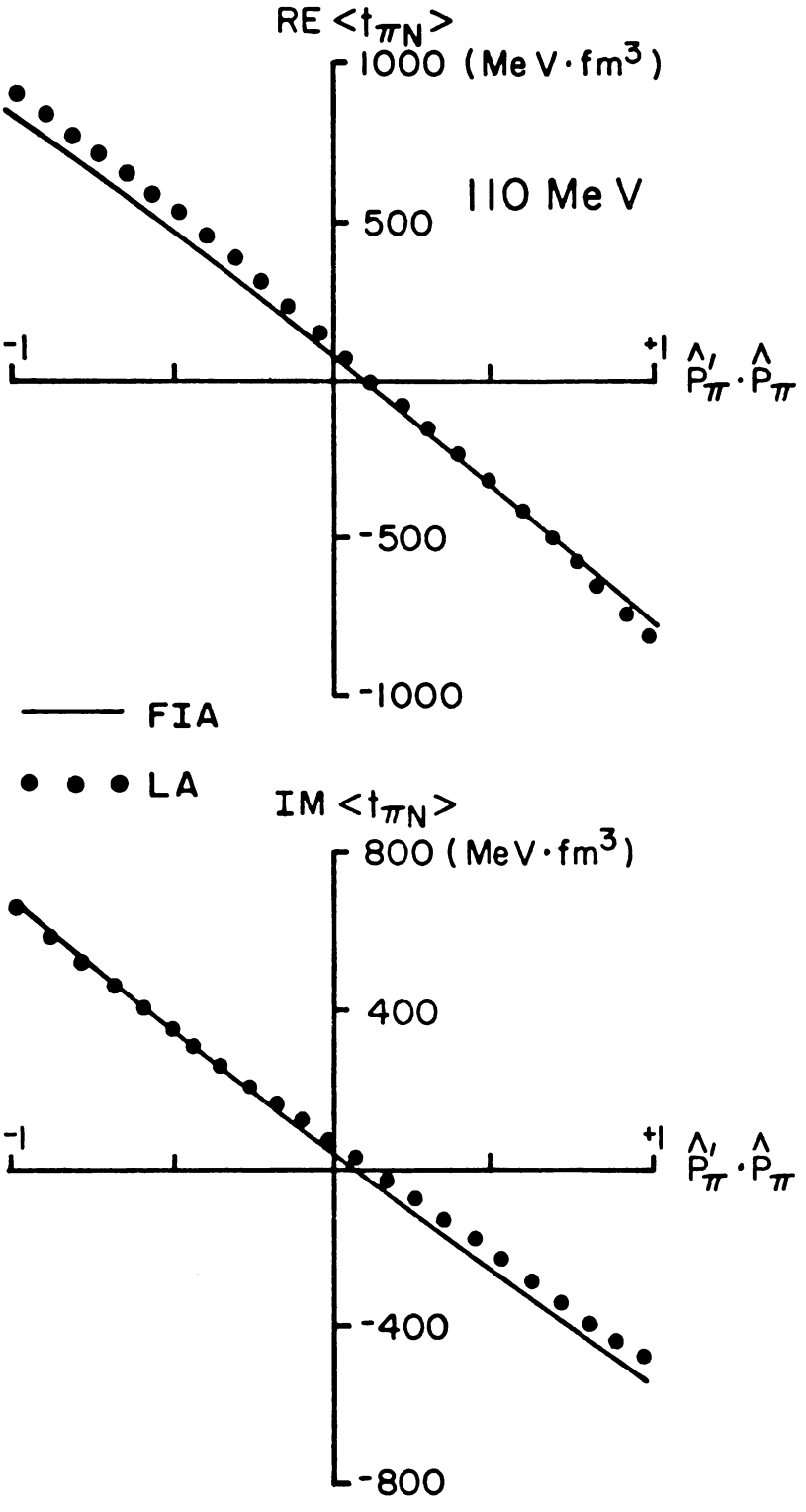
RE $<t_{\pi N}>$
1000 (MeV·fm^3)
110 MeV
500
-500
-1000
-1
+1
$\hat{P}'_\pi \cdot \hat{P}_\pi$
FIA
LA
IM $<t_{\pi N}>$
800 (MeV·fm^3)
400
-400
-800
-1
+1
$\hat{P}'_\pi \cdot \hat{P}_\pi$

FIGURE 7.1.

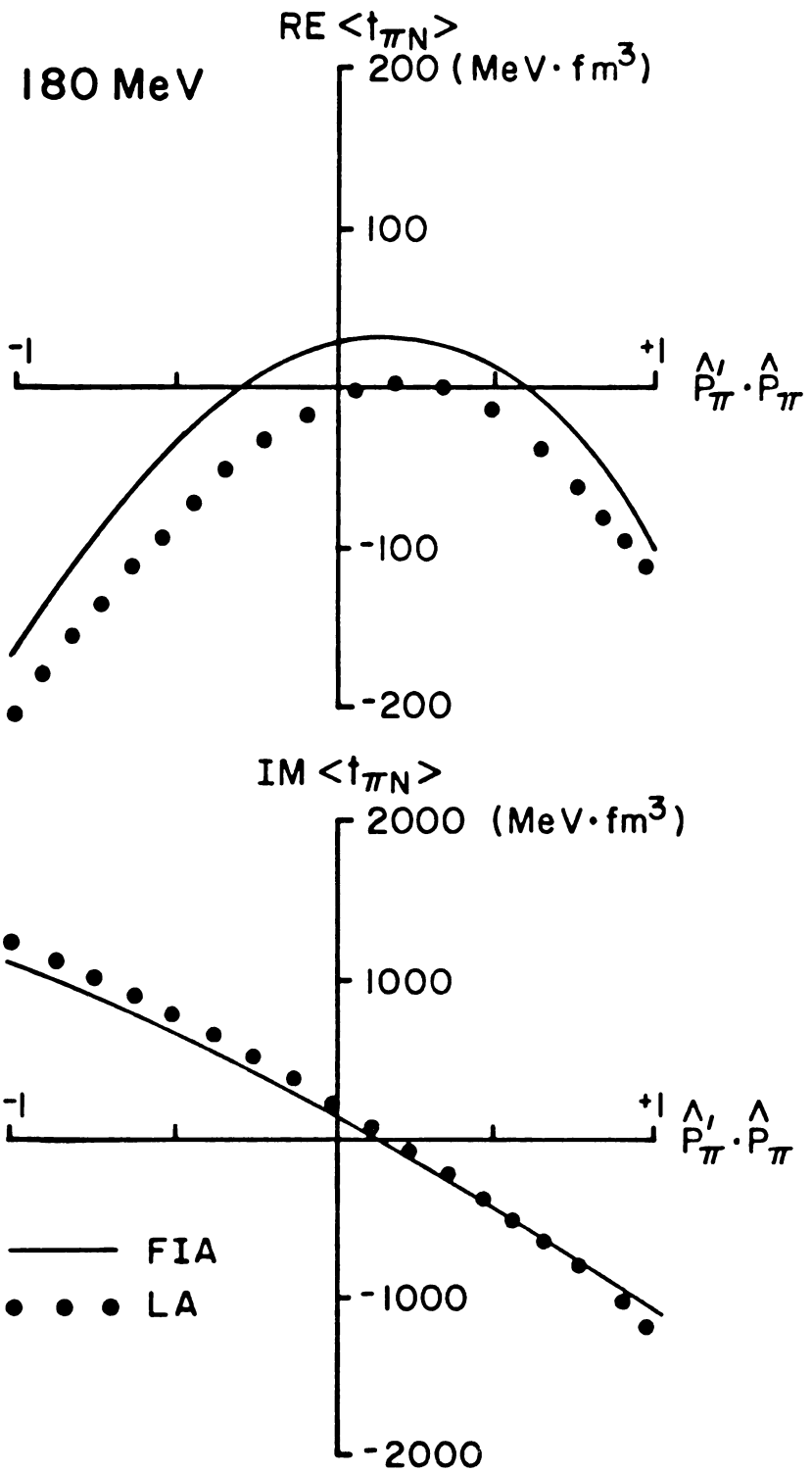

FIGURE 7.2--As in Figure 7.1 except at 180 MeV. The down bending at backward angles in the real part is due to the higher average two-body scattering energy for large angle scattering, which for this case actually raises the energy from below to above resonance.

-1

FIGURE 7.3--As

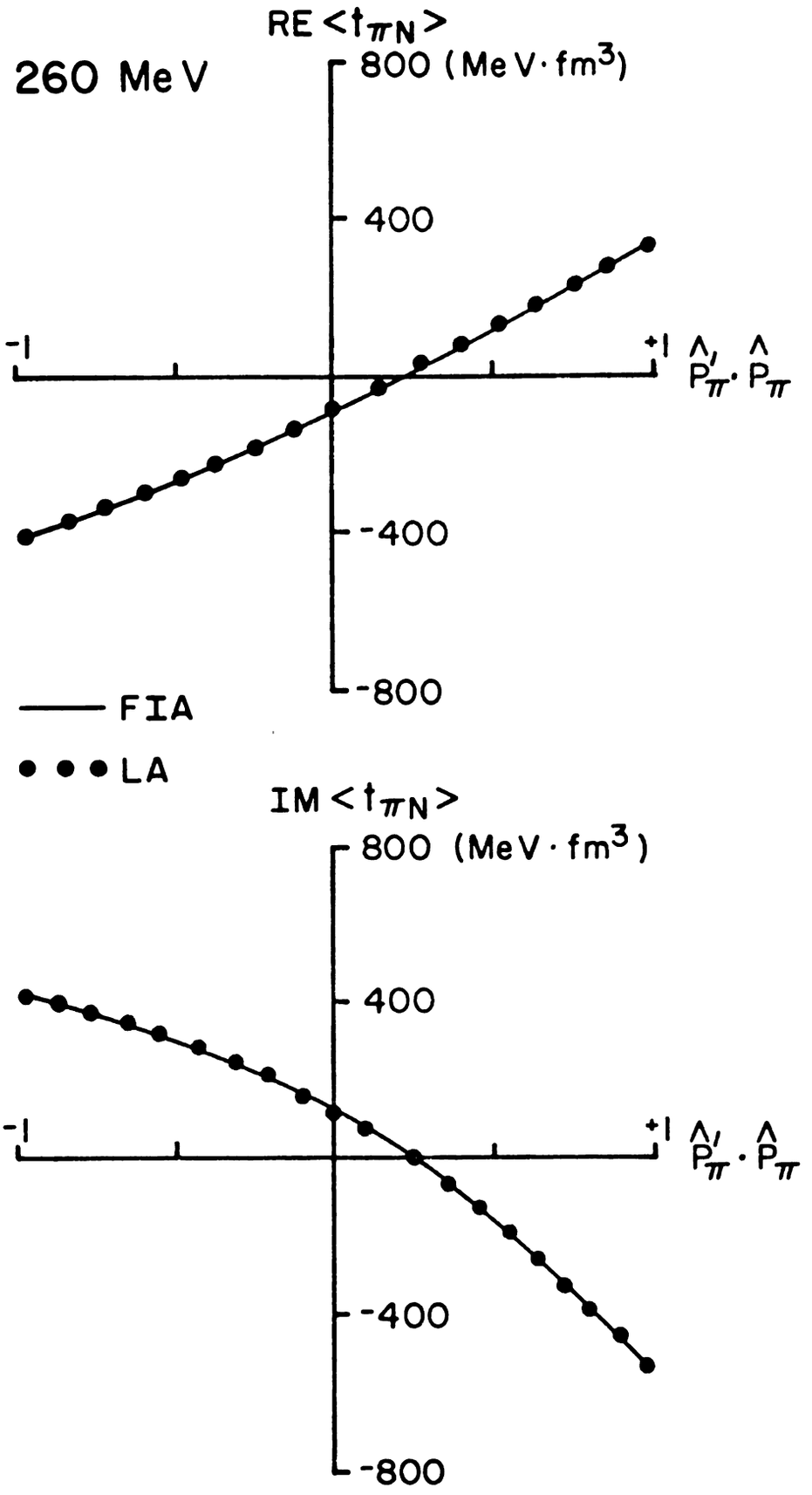

FIGURE 7.3--As in Figure 7.1 except at 260 MeV.

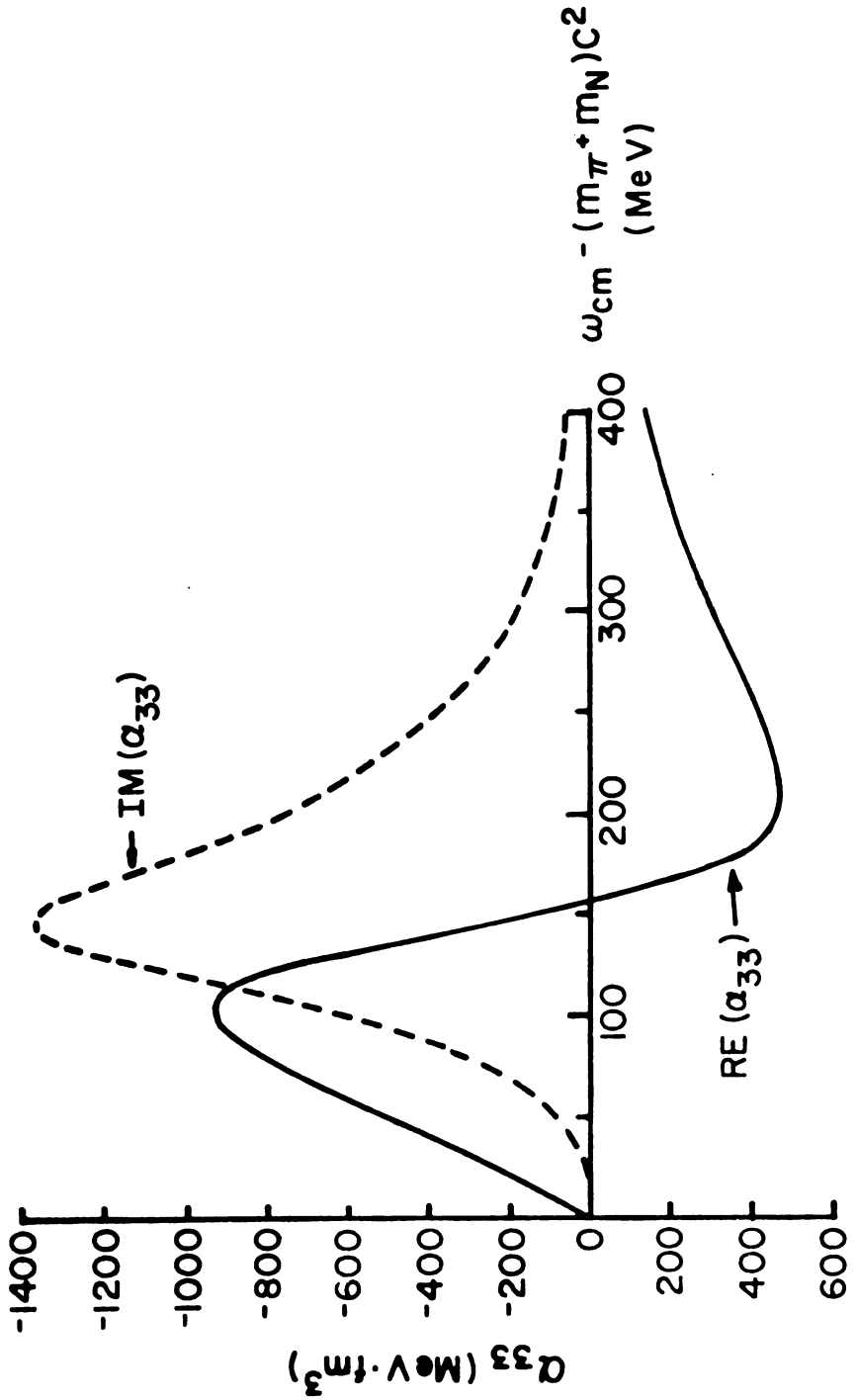

FIGURE 7.4--The real and imaginary parts of a_{33} as a function of the pion-nucleon C.M. kinetic energy. The quantity ω_{cm} is the total relativistic pion-nucleon C.M. energy so that $\omega_{cm} - (m_\pi + m_N)c^2$ is the corresponding kinetic energy.

We choose $\alpha_{33}(\omega_{cm})$ to be of the form

$$(7.9)\quad \alpha_{33}(\omega_{cm}) = a_0 + a_1(\omega_{cm} - \bar{\omega}_{cm}) + a_2(\omega_{cm} - \bar{\omega}_{cm})^2$$

where $\bar{\omega}_{cm}$ is given in equation (7.6). We require that equation (7.9) be exact at the points $\bar{\omega}_{cm}$, $\bar{\omega}_{cm} \pm \sigma_\omega$ where σ_ω^2 is the average value of $(\omega_{cm} - \bar{\omega}_{cm})^2$ calculated from equation (7.5). The explicit result for σ_ω^2 is[1]

$$(7.10)\quad \sigma_\omega^2 = \left(\frac{\hbar^2 c^2}{2\omega^0}\right)^2 \left[\langle p_{4N}^4 \rangle - \langle p_{4N}^2 \rangle^2 + \frac{4}{3}\left(\frac{A-1}{2A}\right)^2 (p_\pi + p'_\pi)^2 \langle p_{4N}^2 \rangle\right].$$

(Note σ_ω^2 depends on the scattering angle, being larger at forward angles.) Using the above quadratic form for α_{33} and proceeding as with the linear case, we obtain

$$(7.11)\quad \langle t_{\pi N} \rangle = \frac{1}{2}\left[\bar{t}_{\pi N}(\bar{\Omega}^+) + \bar{t}_{\pi N}(\bar{\Omega}^-)\right]$$

---

[1] We use equation (7.5) with $\Omega \to (\omega_{cm} - \bar{\omega}_{cm})^2$ to define σ_ω^2. For $R_0 = 1.5$ fm we have $\langle p_{4N}^2 \rangle \cong 1\ \text{fm}^{-2}$ and $\langle p_{4N}^4 \rangle \cong 5/3\ \text{fm}^{-4}$, so $\sigma_\omega\big|_{\theta_{\pi N} = 0^\circ}$ is about 30 MeV near the (3,3) resonance.

where

$$(7.12)\quad \underset{\sim}{\bar{\mathcal{L}}}^{\pm} = \left(\bar{\omega}_{CM} \pm \sigma_{\omega} \, , \, \underset{\sim}{\bar{k}} \, , \, \underset{\sim}{\bar{k}'} \right) .$$

The difference between the quadratic approximation and the linear approximation is fairly small, but there is a slight improvement so we use the quadratic approximation in the actual calculation of elastic scattering cross sections.

3. Qualitative Effects of Nucleon Motion in the Effective Impulse Interaction

The linear approximation for $\langle t_{\pi N} \rangle$ contains the main features of the fully-integrated result (see Figures 7.1 - 7.3) so we can use the simple form in equation (7.3) to understand how the effects of internal nucleon motion enter into the effective pion-nucleon impulse interaction. First, however, we need to understand the properties of $\underset{\sim}{\bar{\mathcal{L}}}$. The dependence of $\underset{\sim}{\bar{\mathcal{L}}}$ on $\underset{\sim}{p}_{\pi}$ and $\underset{\sim}{p}_{\pi}'$ shown in equations (7.6) - (7.8) is due to the fact that the average value of $\underset{\sim}{P}_{4N}$ is $-\left(\frac{A-1}{2A}\right)\underset{\sim}{q}$ and not zero (we define "average" here by using equation (7.5) with $\underset{\sim}{\mathcal{L}} \rightarrow \underset{\sim}{P}_{4N}$). This result for $\underset{\sim}{P}_{4N}$ is valid for any single particle wave function of definite parity. Due simply to momentum conservation the average value of the final 4NCM nucleon momentum is $\underset{\sim}{\bar{P}}_{4N}' = \underset{\sim}{\bar{P}}_{4N} + \frac{A-1}{A}\underset{\sim}{q} = \frac{A-1}{2A}\underset{\sim}{q}$. Thus for elastic scattering (viewed in the 4NCM frame) where the nucleon "absorbs" momentum $\frac{A-1}{A}\underset{\sim}{q}$ but no energy, the nucleon wave function favors collisions where the nucleon momentum vector is

reversed without changing magnitude. The effect of this momentum "selection rule" is to make $\bar{\omega}_{CM}$, $\bar{k}$ and $\bar{k}'$ all larger for large angle scattering than for small angle scattering. (We assume $|\bar{p}_\pi| = |\bar{p}'_\pi|$ here for purposes of discussion.)

Let us now examine how the properties of $\bar{q}$ are reflected in the behavior of $\bar{t}_{\pi N}(\bar{q})$. We consider only the parameterization of equation (6.3), but the main effects should be present in any parameterization. First, in the angle factor, our prescription for $\bar{k}$ and $\bar{k}'$ generates an effective angle transformation from the πNCM frame to the πNCM frame. This angle transformation is essentially the same as the Kujawski-Miller-Landau (KML) angle transformation given in Table 5.1 and shown in Figure 5.1 in Chapter V. In the limit $\frac{A-1}{A} \to 1$ our transformation is identical with Landau's. (The $(A-1)/A$ factor arises in our transformation because we take into account the (small) effect of the recoil of the nucleus as well as the recoil of the nucleon.) Hence, in our transformation $\cos\theta_{\pi N} \equiv \bar{k} \cdot \bar{k}' / |\bar{k}| |\bar{k}'|$ varies nonlinearly between $+1$ and -1 as $\cos\theta_{\pi\nu} = \hat{p}_\pi \cdot \hat{p}'_\pi$ varies between $+1$ and -1. It is interesting to note that for $|\bar{p}'_\pi| = |\bar{p}_\pi|$, Miller's choice $(\bar{p}_N = 0)$ gives $|\bar{k}'| \neq |\bar{k}|$, while Landau's choice $\left(\bar{p}_N = -\frac{1}{2}(\bar{p}_\pi - \bar{p}'_\pi)\right)$ and our result $\left(\bar{p}_{4N} = \frac{A-1}{2A}(\bar{p}_\pi - \bar{p}'_\pi)\right)$ both give $|\bar{k}'| = |\bar{k}|$. Hence, elastic scattering in the $\pi\nu$CM frame corresponds (on the average) to elastic scattering also in the πNCM frame when nucleon motion is taken into account correctly.[1]

---

[1] There is actually a different πNCM frame for each component of the nucleon momentum. We really mean the "average" πNCM frame when we speak of "the" πNCM frame in elastic pion-nucleus scattering.

Next, the factor γ in equation (7.3) (see Appendix B for an explicit form) has a nonneglible dependence on $\underset{\sim}{p}_\pi$ and $\underset{\sim}{p}'_\pi$. This factor has previously been treated as a constant for each scattering energy. (Lan73, Kuj74). At backward angles γ is approximately 1, whereas at forward angles γ is about .8 or .9 for the energies we consider.

Third, the most interesting feature of the effective impulse interaction is the dependence of $\alpha_{33}(\bar{\omega}_{cm})$ on $\underset{\sim}{p}_\pi$ and $\underset{\sim}{p}'_\pi$. In energy regions where the free pion-nucleon scattering amplitude (Re or Im part) is increasing with energy, the factor $\alpha_{33}(\bar{\omega}_{cm})$ (Re or Im part) is larger at backward angles because $\bar{\omega}_{cm}$ is larger there. The reverse is true in energy regions where the free scattering amplitude is decreasing with increasing energy. This effect is quite evident in the real part of $\langle t_{\pi N} \rangle$ at a pion laboratory energy of 180 Mev (see Figure 7.2). For this case the forward scattered pions have an average πNCM collision energy that is below the resonance energy while backward scattered pions have an average collision energy that is above the resonance energy. The real part of the free scattering amplitude changes sign at the resonance energy, causing the real part of $\langle t_{\pi N} \rangle$ to be strongly distorted at backward angles. At other laboratory energies the effect is much less dramatic, but is still present.

Finally, it is interesting to note that although our parameterization of $\bar{t}_{\pi N}$ in equation (6.3) is a zero-range form, the effective impulse interaction $\langle t_{\pi N} \rangle$ has a finite range (which changes with the πNCM scattering energy ω°) due to the dependence of $\bar{\omega}_{cm}$ on $\underset{\sim}{p}_\pi$ and $\underset{\sim}{p}'_\pi$.

CHAPTER VIII

CORRECTIONS TO THE IMPULSE APPROXIMATION

Up to this point we have assumed the t-matrix for scattering of a pion from a bound nucleon is the same as the free pion-nucleon t-matrix, i.e., we have used the impulse approximation. We now consider corrections to the impulse approximation using a 3-body model.

The calculation described in this chapter was motivated by estimates given by Goldberger and Watson which indicated that binding effects in pion-nucleus scattering are large in the (3,3) resonance region (Gol64). Our calculations indicate that the effects are, in fact, not very large. Moreover, since the calculation of binding effects is very tedious even in a simple 3-body model, we have developed a fairly good approximation to our exact calculation.

Most of the work presented in this chapter was done some time before the calculation presented in previous chapters and, consequently, there are some minor differences between the model used here and the one used in previous chapters. In this chapter we assume an infinitely heavy nucleus and use a finite-range off-shell parameterization of the free pion-nucleon t-matrix. Our experience indicates that these two factors do not significantly affect the results. Since the binding correction itself turned out to be fairly small, it was not necessary to modify this early model.

1. A 3-Body Model

Instead of treating the complete problem of a pion and A target nucleons, we consider the interaction of a pion with a single nucleon which is bound in a fixed potential well.[1] We shall assume in this chapter that our 3-body model is a reasonable approximation for the (A + 1)-body problem. In Appendix E we give a theoretical justification for the model.

In our model the incident pion interacts only with the nucleon and not with the potential well itself, so the model Hamiltonian is

$$H = K_\pi + H_N + V_{\pi N} \quad . \tag{8.1}$$

Here K_π is the relativistic pion kinetic energy, H_N is the Hamiltonian for the bound nucleon and $V_{\pi N}$ is the potential between the pion and the target nucleon. The nucleon Hamiltonian H_N is taken to be

$$H_N = K_N + U_N \tag{8.2}$$

---

[1] We note that since the potential well is fixed in space, nuclear recoil effects are neglected and the πN CM coordinates are identical to the laboratory coordinates.

where K_N is the nucleon kinetic energy and U_N is a single particle binding potential. Our 3-body Hamiltonian is formally similar to the original (A + 1)-body problem in that the nuclear Hamiltonian H_ν is replaced with H_N .

By replacing H_ν with H_N in the formalism of Chapter II, we can easily obtain the t-matrix for scattering of a pion from a bound nucleon in terms of the free pion-nucleon t-matrix.[1]

$$(8.3)\quad \hat{T}_{\pi N}(E) = t_{\pi N}(E') + t_{\pi N}(E')\left[g(E) - g_0(E')\right]\hat{T}_{\pi N}(E)$$

Here $t_{\pi N}$ is the free pion-nucleon t-matrix and g and g_0 are given by

$$(8.4)\quad g(E) = (E - K_\pi - K_N - U_N + i\epsilon)^{-1}$$

$$(8.5)\quad g_0(E') = (E' - K_\pi - K_N + i\epsilon)^{-1} .$$

---

[1] We thus replace the nuclear degrees of freedom with the degrees of freedom associated with a single bound nucleon.

The propagator $g(E)$ can be written as

$$g(E) = g_0(E) + g_0(E) R_N g_0(E) \tag{8.6}$$

where R_N is defined as

$$R_N = U_N + U_N g_0(E) R_N \,. \tag{8.7}$$

That is, R_N is the t-matrix associated with the potential U_N. We can now write $\uparrow_{\pi N}$ as

$$\uparrow_{\pi N}(E) = t_{\pi N}(E') + t_{\pi N}(E') \left[g_0(E) - g_0(E') + g_0(E) R_N g_0(E) \right] \uparrow_{\pi N}(E) \tag{8.8}$$

In Chapter II it was stated that the energy E' in $t_{\pi N}(E')$ is an arbitrary parameter. Several authors have suggested that E' can be chosen so as to minimize the second term in equation (8.8) (Sch72, Lan73). We intend to calculate the second term explicitly so we simply take $E' = E$. Setting $E' = E$ in equation (8.8) we obtain for $\uparrow_{\pi N}$

$$(8.9)\quad \hat{T}_{\pi N}(E) = t_{\pi N}(E) + t_{\pi N}(E)\, g_0(E)\, R_N\, g_0(E)\, \hat{T}_{\pi N}(E) .$$

Rather than attempting to solve the full integral equation for $\hat{T}_{\pi N}$, we calculate the first two terms in the series. It turns out that the second term is small compared to the first term, so our procedure is reasonable. We also assume that $t_{\pi N}$ acts only in the (3,3) channel (i.e., $t_{\pi N} = t_{33}$), so we want to calculate

$$(8.10)\quad \hat{T}_{\pi N}(E) = t_{33}(E) + t_{33}(E)\, g_0(E)\, R_N\, g_0(E)\, t_{33}(E) .$$

The separable parameterization of Appendix B is used for t_{33}. The off-shell factor $g(k)$ used in the separable parameterization (see Appendix B) was taken to be $k/(1 + k^2 r_0^2)\,\omega(k)$ rather than unity[1]. The t-matrix R_N is assumed to have a single s - wave bound state at $E_N = -20$ MeV.

Equation (8.10) can be thought of in terms of multiple scattering and represented diagrammatically as in Figure 8.1.

---

[1] In previous chapters a zero-range force was used so that the off-shell factor was one. The off-shell factor given here was taken from the work of Charlton and Eisenberg (Cha71). The factor $\omega(k)$ is $(\hbar^2 c^2 k^2 + m_\pi^2 c^4)^{1/2}$ and r_0 was taken to be .5 fm. We have found the elastic cross sections to be relatively insensitive to the form of the off-shell factor.

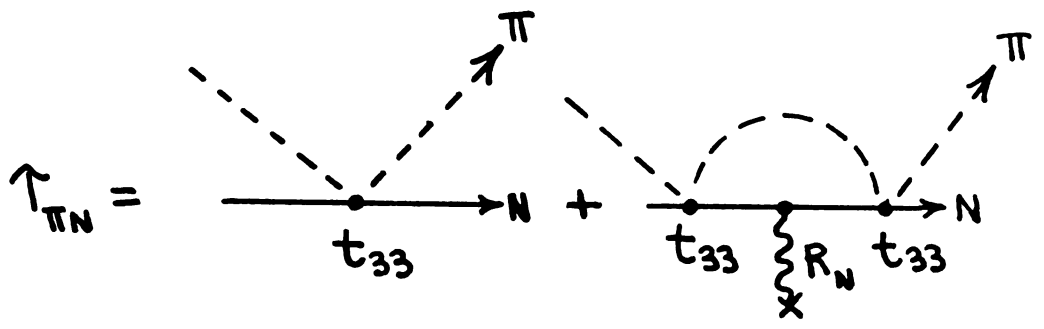

Figure 8.1 - Diagrammatic representation of equation (8.10).

The first diagram is the impulse term and the second is a correction to the impulse term. In the second diagram the nucleon is scattered by the potential well (via R_N) between scatterings with the pion. The interaction of the nucleon with the potential well causes the nucleon wave function to be "distorted" in the intermediate states. Thus, our 3-body model takes into account multiple interaction of the pion with the same nucleon and the distortion of the nucleon's wave function by the binding potential.

In preliminary calculations using a square well for U_N , the main contribution from R_N appeared to be coming from the bound state pole. It is well known that near a bound state pole a one-term separable potential gives a good approximation for a local potential (Lov64). Also, a separable potential for U_N considerably simplifies the calculation, so the binding potential was taken to be an s -wave separable potential of the form

$$(8.11) \quad U_N(\underset{\sim}{p}'_N, \underset{\sim}{p}_N) = \lambda u_N(p'_N) u_N(p_N)$$

where $u_N(p_N) = (\alpha^2 + p_N^2)^{-1}$, $\alpha = 3.17\ fm^{-1}$ and $\lambda = 38935\ MeV \cdot fm^{-1}$. These values for α and λ give a bound state at -20 MeV with an RMS radius of 1.61 fm. (A one-term separable potential can produce only one bound state.) The t-matrix associated with the above separable potential is

$$(8.12)\quad R_N(E; p_N', p_N) = \lambda u_N(p_N')\, r_N(E)\, u_N(p_N) .$$

The energy factor $r_N(E)$ is given by

$$(8.13)\quad r_N(E) = \left[1 + \left(\frac{\lambda m_N}{8\pi^2\hbar^2}\right) \frac{1}{2\alpha(\alpha + i p_E)}\right]^{-1}$$

where $p_E = (2 m_N E / \hbar^2)^{1/2}$.

The matrix elements for the binding correction term were calculated using the vector bracket method as described in Chapter III for the impulse term. The binding correction term considered here is considerably more complicated than the impulse term, so instead of giving a detailed derivation we indicate schematically the procedure. A more complete development is given in Appendix F.

We want to calculate

$$(8.14)\quad \Delta t_{\pi N} \equiv \langle \underset{\sim}{p}'_{\pi} | \langle 0 | t_{33} g_0 R_N g_0 t_{33} | 0 \rangle | \underset{\sim}{p}_{\pi} \rangle \ .$$

Denoting a complete set of two-body states for the pion-nucleon C.M. frame as $|\pi N CM\rangle\int\langle\pi N CM|$ and a complete set for the pion-nucleus C.M. frame as $|\pi\nu CM\rangle\int\langle\pi\nu CM|$ we calculate

$$(8.15)\quad \Delta t_{\pi N} = \langle \underset{\sim}{p}'_{\pi} | \langle 0 | \pi\nu CM\rangle\int\langle\pi\nu CM|\pi N CM\rangle\int\langle\pi N CM|$$
$$\times t_{33}|\pi N CM\rangle\int\langle\pi N CM|\pi\nu CM\rangle\int\langle\pi\nu CM|$$
$$\times g_0 R_N g_0 |\pi\nu CM\rangle\int\langle\pi\nu CM|\pi N CM\rangle\int\langle\pi N CM|$$
$$\times t_{33}|\pi N CM\rangle\int\langle\pi N CM|\pi\nu CM\rangle\int\langle\pi\nu CM|0\rangle|\underset{\sim}{p}_{\pi}\rangle \ .$$

2. Numerical Results for $\hat{T}_{\pi N}$

We have calculated exactly the L = 0 and L = 1 components of $\langle \underset{\sim}{p}'_{\pi} | \langle 0 | \hat{T}_{\pi N} | 0 \rangle | \underset{\sim}{p}_{\pi} \rangle$ for energies between 31 and 373 MeV $(p^0_{\pi} = .5\ fm^{-1}$ to $2.5\ fm^{-1})$. In Figure 8.2 the result for L = 1 is plotted on an argand diagram. The solid line is the impulse result and the dashed line is the impulse result

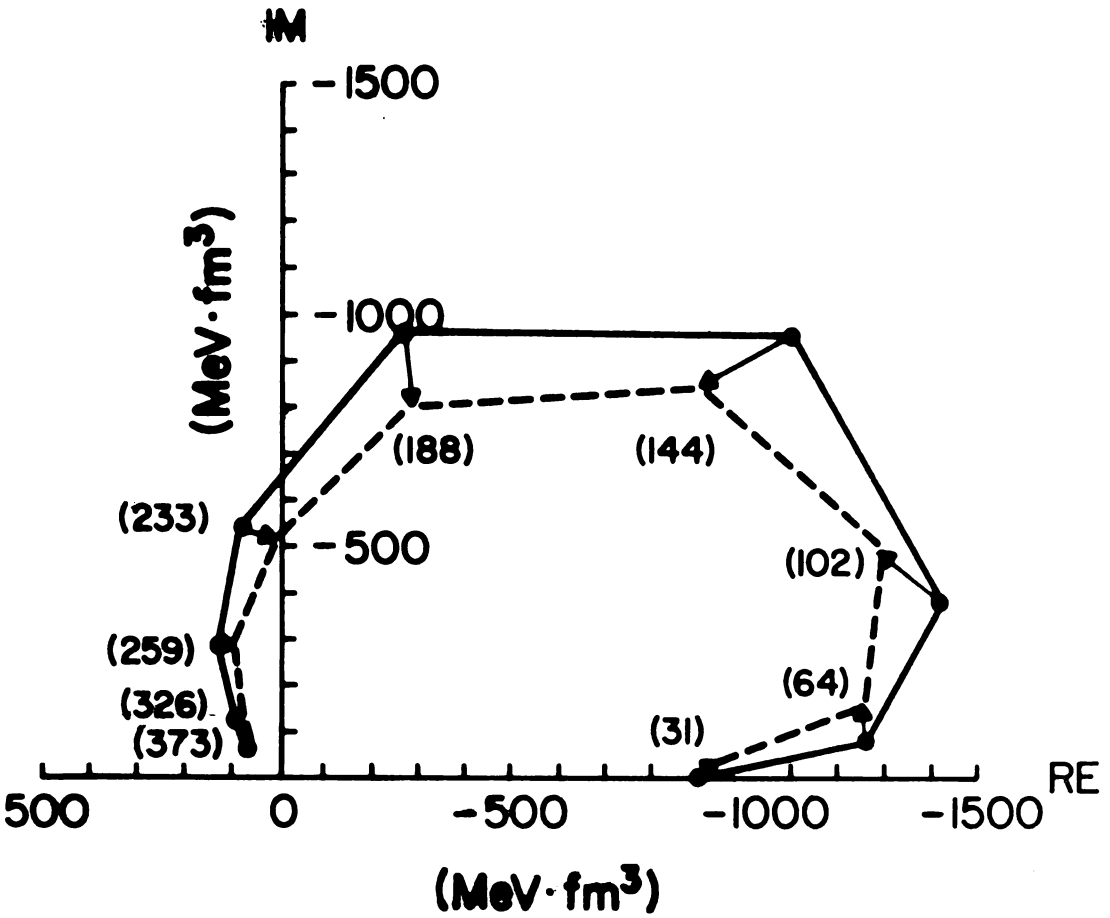

FIGURE 8.2--An Argand diagram of the L = 1 component of

$\langle \underset{\sim}{p}'_{\pi} | \langle 0 | t_{\pi N} | 0 \rangle | \underset{\sim}{p}_{\pi} \rangle$ (impulse result)

and

$\langle \underset{\sim}{p}'_{\pi} | \langle 0 | T_{\pi N} | 0 \rangle | \underset{\sim}{p}_{\pi} \rangle$ (impulse plus binding effects).

The solid line is the impulse result and the dashed line is the impulse result plus the binding correction. At a given energy, the arrow connecting the solid line and the dashed line is the binding correction itself.

plus the binding correction. At a particular energy, the arrow connecting the solid line and the dashed line is the binding correction itself. The real and imaginary part of the binding correction (i.e., the arrow) is shown as a function of energy in Figure 8.3.

One immediately apparent feature in Figure 8.2 is that the binding correction term (i.e., the arrow) is small and "rotates" about twice as fast as the impulse term. A more careful study indicates that the binding correction term varies approximately as (-i) times the square of the impulse term. The simple relationship between the binding correction term and the impulse term prompted us to look for some simple approximation which we could justify theoretically. In the next section we derive an approximation for the binding correction term.

3. A Single State Approximation for Binding Effects

As we mentioned in the previous section, the main contribution from the t-matrix R_N comes in vicinity of the bound state pole, i.e., $R_N(e)$ is the largest for $e \cong E_B$. We want to consider now a simple model which takes into account just the bound state pole contribution.

The one-body t-matrix associated with a potential V can be written

$$T = V + V(E - K + i\epsilon)^{-1} T \tag{8.16}$$

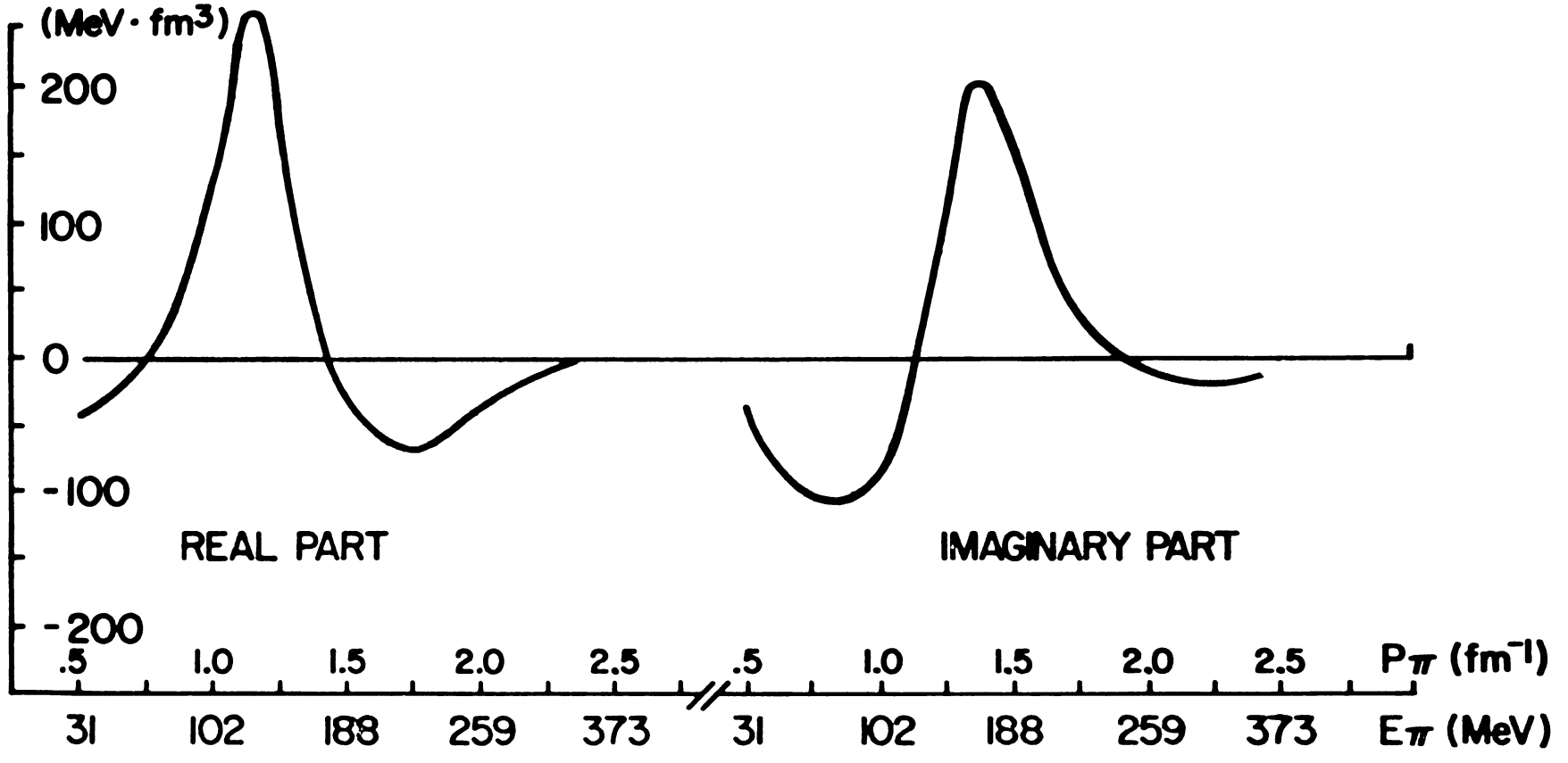

FIGURE 8.3--The real and imaginary parts of the binding correction shown in Figure 8.2 (i.e., the arrow in Figure 8.2). These curves result from an exact numerical evaluation of $\langle \underset{\sim}{P}' K o | t_{33} g_o R_4 g_o t_{33} | o \rangle | \underset{\sim}{P} \rangle$ Note that the binding correction is only 10-20% of the impulse term.

where K is the kinetic energy operator. We can also write T as

$$T = V + V \sum_m \frac{|m\rangle\langle m|}{E - E_m + i\epsilon} V \tag{8.17}$$

where the kets $|m\rangle$ are the eigenstates of K + V and include the continuum. Near a bound state with energy E_i the i^{th} term dominates so we can approximate the t-matrix there by

$$T \cong \frac{V|i\rangle\langle i|V}{E - E_i + i\epsilon} . \tag{8.18}$$

This form, which is discussed in some detail by Lovelace (Lov64), is the form we will take for R_N . However, in our problem R_N is given by equation (8.7) which includes the pion kinetic energy operator in the propagator. Writing out the propagator g_0 explicitly, we have for R_N

$$R_N = U_N + U_N (E - K_\pi - K_N + i\epsilon)^{-1} R_N . \tag{8.19}$$

An equivalent equation, analogous to equation (8.17), is

$$R_N = U_N + U_N \sum_i \frac{|i\rangle\langle i|}{E - K_\pi - E_i + i\epsilon} U_N \tag{8.20}$$

where $|i\rangle$ are the eigenstates of $K_N + U_N$, including the continuum states. We assume the potential U_N has only one bound state and use the form in equation (8.18) to obtain an approximate form for R_N near this single pole.

$$(8.21)\quad R_N \cong U_N \frac{|0\rangle\langle 0|}{E - K_\pi - E_B + i\epsilon} U_N$$

Here E_B is the energy of the bound state $|0\rangle$. Now the energy E is $E = E_B + E_\pi$ where E_π is the kinetic energy of the pion. The denominator in equation (8.21) hence is

$$(E_B + E_\pi) - K_\pi - E_B + i\epsilon = E_\pi - K_\pi + i\epsilon \quad .$$

Thus, in our single pole approximation, we have for R_N

$$(8.22)\quad R_N = U_N \frac{|0\rangle\langle 0|}{E_\pi - K_\pi + i\epsilon} U_N \quad .$$

Also, we take for the pion-nucleon t-matrix the spin-isospin averaged (3,3) channel component of t_{33} which we denote as $\bar{t}_{33}$. Then using equation (8.22) for R_N we have for the binding correction term

$$(8.23)\quad \Delta t_{\pi N} = \langle \underset{\sim}{p}'_\pi | K_0 | \bar{t}_{33} g_0 \frac{U_N |0\rangle\langle 0| U_N}{E_\pi - K_\pi + i\epsilon} g_0 \bar{t}_{33} | 0 \rangle | \underset{\sim}{p}_\pi \rangle \quad .$$

Inserting a complete set of pion states on both sides of $g R_N g_0$ and remembering that g_0 and R_N are diagonal with respect to the pion momentum we obtain

$$(8.24)\quad \Delta t_{\pi N} = \int \frac{d^3 p_\pi''}{(2\pi)^3} \langle \underset{\sim}{p}_\pi' | \langle 0 | \bar{t}_{33} | \underset{\sim}{p}_\pi'' \rangle \times g_0 \frac{U_N |0\rangle\langle 0| U_N}{E_\pi - K_\pi'' + i\epsilon} g_0 \langle \underset{\sim}{p}_\pi'' | \bar{t}_{33} | 0 \rangle | \underset{\sim}{p}_\pi \rangle .$$

The denominator $E_\pi - K_\pi'' + i\epsilon$ can be written

$$(8.25)\quad (E_\pi - K_\pi'' + i\epsilon)^{-1} = \frac{PP}{E_\pi - K_\pi''} - i\pi \delta(E_\pi - K_\pi'') .$$

Since $K_\pi'' = (\hbar^2 c^2 p_\pi''^2 + m_\pi^2 c^4)^{1/2} - m_\pi c^2$ we can write the δ-function in terms of the momentum

$$(8.26)\quad (E_\pi - K_\pi'' + i\epsilon)^{-1} = \frac{PP}{E_\pi - K_\pi''} - \frac{i\pi \omega_\pi^0}{\hbar^2 c^2 p_\pi^0} \delta(p_\pi^0 - p_\pi'')$$

where $E_\pi = (\hbar^2 c^2 p_\pi^{0 2} + m_\pi^2 c^4)^{1/2} - m_\pi c^2 \equiv \omega_\pi^0 - m_\pi c^2$.

Remembering that d^3p_π'' means $p_\pi''^2 dp_\pi'' d\Omega_{p_\pi''}$ and keeping just the δ-function contribution from R_N we have after the integration over p_π''

$$(8.27)\quad \Delta t_{\pi N} = \int \frac{d\Omega_{p_\pi''}}{(2\pi)^3} \langle \underset{\sim}{p}_\pi' | \langle 0 | \bar{t}_{33} | \underset{\sim}{p}_\pi^{0\,''} \rangle \times \left(\frac{-i\pi \omega_\pi^0 p_\pi^0}{\hbar^2 c^2} \right) g_0 U_N |0\rangle \langle 0| U_N g_0 \times \langle \underset{\sim}{p}_\pi^{0\,''} | \bar{t}_{33} | 0 \rangle | \underset{\sim}{p}_\pi \rangle .$$

In equation (8.27) the notation $|\underset{\sim}{p}_\pi^{0\,''}\rangle$ means a state where $|\underset{\sim}{p}_\pi''| = p_\pi^0$ but the direction of $\underset{\sim}{p}_\pi^{0\,''}$ is still an integration variable. We can further simplify $\Delta t_{\pi N}$ by noting the form that g_0 now has. Before we took the $i\delta$ part of R_N, g_0 was given by

$$(8.28)\quad g_0 = (E_B + E_\pi - K_\pi - K_N + i\epsilon)^{-1} .$$

Taking the $i\delta$ part of R_N puts $|\underset{\sim}{p}_\pi''| = p_\pi^0$ so $K_\pi = E_\pi$ and g_0 becomes

$$(8.29)\quad g_0 = (E_B - K_N + i\epsilon)^{-1} .$$

Now by definition $(E_B - K_N + i\epsilon)^{-1} U_N |0\rangle = |0\rangle$

so we can write equation (8.27) as

$$(8-30)\quad \Delta t_{\pi N} = \frac{-i\omega_\pi^0 p_\pi^0}{8\pi^2 \hbar^2 c^2} \int d\Omega_{p_\pi''} \langle \underset{\sim}{p_\pi'} | \langle 0 | \bar{t}_{33} | 0 \rangle | \underset{\sim}{p_\pi^{0''}} \rangle$$

$$\times \langle \underset{\sim}{p_\pi^{0''}} | \langle 0 | \bar{t}_{33} | 0 \rangle | \underset{\sim}{p_\pi} \rangle .$$

The quantity $\langle \underset{\sim}{p_\pi'} | \langle 0 | \bar{t}_{33} | 0 \rangle | \underset{\sim}{p_\pi^{0''}} \rangle$ is the same matrix element that was calculated for the optical potential in our independent particle model for ^{4}He, i.e., we wrote in earlier chapters (for just the (3,3) channel):

$$(8.31)\quad U_{\pi\nu}(\underset{\sim}{p_\pi'}, \underset{\sim}{p_\pi^{0''}}) = (A-1) \langle \underset{\sim}{p_\pi'} | \langle 0 | \bar{t}_{33} | 0 \rangle | \underset{\sim}{p_\pi^{0''}} \rangle$$

so we can write equation (8.22) as

$$(8.32)\quad \Delta t_{\pi N} = \frac{1}{(A-1)^2} \left(\frac{-i\omega_\pi^0 p_\pi^0}{8\pi^2 \hbar^2 c^2} \right)$$

$$\times \int d\Omega_{p_\pi''} U_{\pi\nu}(\underset{\sim}{p_\pi'}, \underset{\sim}{p_\pi^{0''}}) U_{\pi\nu}(\underset{\sim}{p_\pi^{0''}}, \underset{\sim}{p_\pi}) .$$

Making a partial-wave expansion of $U_{\pi N}$ we obtain[1]

$$(8.33)\quad \Delta t_{\pi N} = \frac{1}{(A-1)^2}\left(\frac{-i\,\omega_\pi^0 p_\pi^0}{8\pi^2\hbar^2c^2}\right) \times \sum_L \frac{2L+1}{4\pi} U^L_{\pi N}(p'_\pi p_\pi^0) U^L_{\pi N}(p_\pi^0 p_\pi) P_L(\hat{p}'_\pi \cdot \hat{p}_\pi).$$

In Figure 8.4 we compare the approximation for $\Delta t_{\pi N}$ given in equation (8.33) with the exact result for $L = 1$. Our approximation is fairly accurate and since the binding correction is small, we felt that the approximate form was adequate for our purposes.

Our approximation allows us to understand the main features of $\Delta t_{\pi N}$ in a simple way. The fact that the bound state pole of R_N contributes strongly means that the factor $q_0 R_N q_0$ is largely imaginary and the pion momentum is on-shell so that $\langle \underset{\sim}{p}'_\pi | \langle 0 | \bar{t}_{33} q_0 R_N q_0 \bar{t}_{33} | 0 \rangle | \underset{\sim}{p}_\pi \rangle$ varies approximately as $-i[\langle \underset{\sim}{p}'_\pi | \langle 0 | \bar{t}_{33} | 0 \rangle | \underset{\sim}{p}_\pi \rangle]^2$. This relationship between the phase of the impulse term and the phase of the binding correction causes the impulse + binding term to lie "inside" the impulse term on a argand diagram (see Figure 8.2). In the resonance region the binding correction term is approximately 180° out of phase with the impulse term so that

---

[1] In equation (8.33) the partial-wave components are defined by the expansion

$$U_{\pi N}(\underset{\sim}{p}'_\pi \underset{\sim}{p}_\pi) = \sum_L \frac{2L+1}{4\pi} U^L_{\pi N}(p'_\pi p_\pi) P_L(\hat{p}'_\pi \cdot \hat{p}_\pi).$$

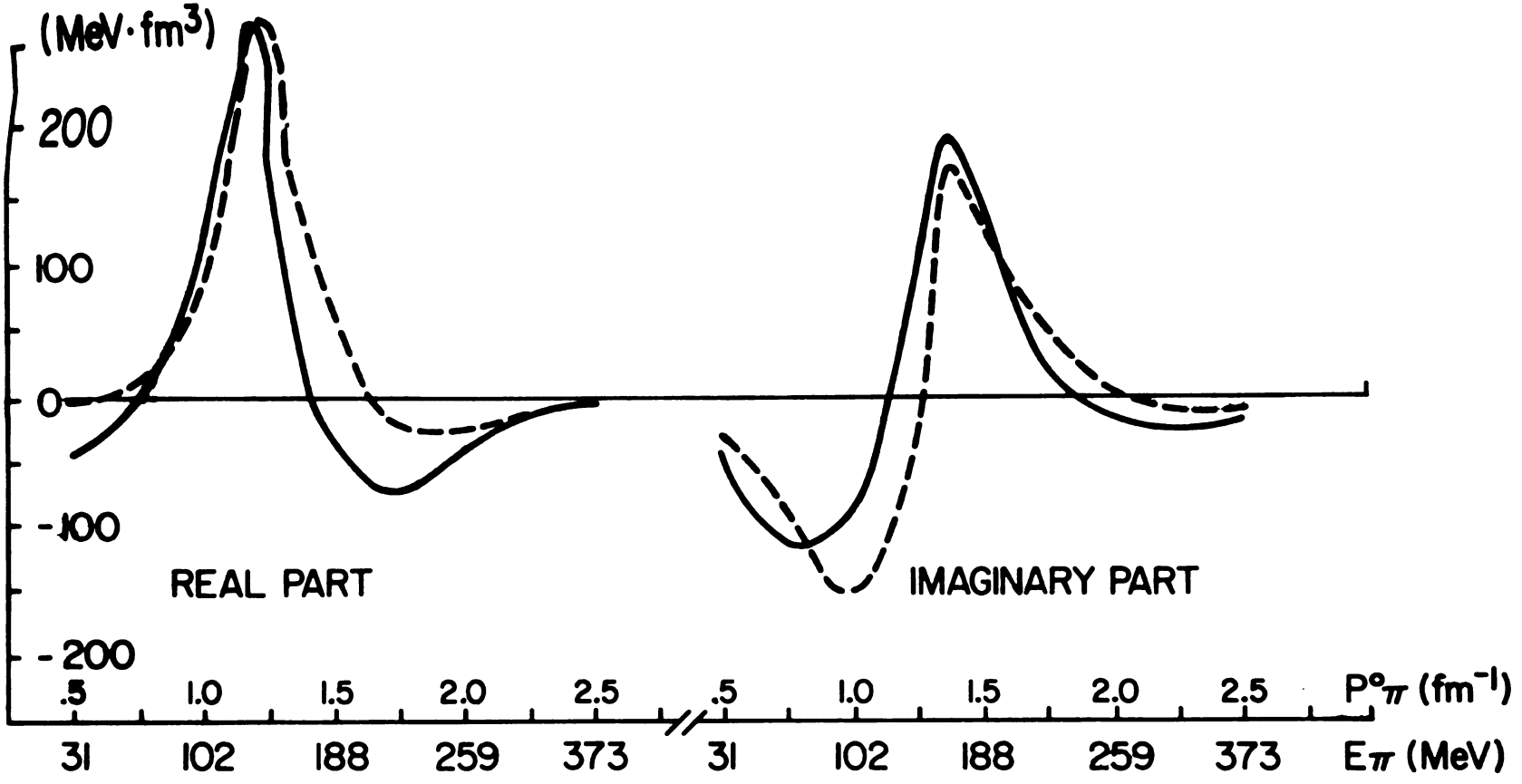

FIGURE 8.4--The real and imaginary parts of $\langle \tilde{p}' | \langle 0 | t_{33} g_0 R_N g_0 t_{33} | 0 \rangle | \tilde{p} \rangle$ for (L=1) calculated two ways: (a) (solid line) the exact result using vector brackets; (b) (dashed line) the single state approximation from equation (8.33). The solid line is the same as in Figure 8.3.

the imaginary part of the pion-nucleon interaction strength is reduced by 10 - 20 % . Above and below the resonance, the phase is such that the real part is decreased.

The bound t-matrix $\tau_{\pi N}$ is now obtained using our approximation for $\Delta t_{\pi N}$. (We also write the impulse term in terms of $U_{\pi\nu}$.)

$$(8.34)\quad \langle \underset{\sim}{p}'_\pi | \langle 0 | \tau_{\pi N} | 0 \rangle | \underset{\sim}{p}_\pi \rangle$$
$$= \frac{1}{A-1} \sum_L \frac{2L+1}{4\pi} \Big[U^L_{\pi\nu}(p'_\pi p_\pi) + \frac{-i}{A-1} \Big(\frac{\omega^\circ_\pi p^\circ_\pi}{8\pi^2 \hbar^2 c^2} \Big) U^L_{\pi\nu}(p'_\pi p^\circ_\pi) U^L_{\pi\nu}(p^\circ_\pi p_\pi) \Big]$$
$$\times P_L(\hat{p}'_\pi \cdot \hat{p}_\pi)$$

If we extend our approximation to include all terms in the series implied by equation (8.9), we obtain

$$(8.35)\quad \langle \underset{\sim}{p}'_\pi | \langle 0 | \tau_{\pi N} | 0 \rangle | \underset{\sim}{p}_\pi \rangle =$$
$$\frac{1}{(A-1)} \sum_L \frac{2L+1}{4\pi} \Big[U^L_{\pi\nu}(p'_\pi p_\pi) \frac{-i}{(A-1)} \Big(\frac{\omega^\circ_\pi p^\circ_\pi}{8\pi^2 \hbar^2 c^2} \Big) \frac{U^L_{\pi\nu}(p'_\pi p^\circ_\pi) U^L_{\pi\nu}(p^\circ_\pi p_\pi)}{1 + \frac{i}{A-1} \Big(\frac{\omega^\circ_\pi p^\circ_\pi}{8\pi^2 \hbar^2 c^2} \Big) U^L_{\pi\nu}(p^\circ_\pi p^\circ_\pi)} \Big]$$
$$\times P_L(\hat{p}'_\pi \cdot \hat{p}_\pi) .$$

We shall refer to the above approximation as the "single state approximation" for the t-matrix $\uparrow_{\pi N}$ since we have assumed a single bound state for the nucleon. Equation (8.35) is used in the actual calculations of the cross sections. The numerical differences between equations (8.34) and (8.35) are very small.

4. A Closure Limit

In order to estimate an upper limit on binding effects of the sort we discussed in the previous sections, we now consider a model where there are an infinite number of bound states (as in a harmonic oscillator potential). We want to emphasize that our aim is only to estimate an upper bound for binding effects and not to represent any physical system.

We generalize equation (8.22) to represent an infinite number of bound states by taking R_N to be of the form

$$(8.36)\quad R_N(E) = \sum_m \frac{U_N |m\rangle\langle m| U_N}{E - E_m + i\epsilon}$$

so that equation (8.30) for $\Delta t_{\pi N}$ becomes

$$(8.37)\quad \Delta t_{\pi N} = \frac{-i\omega_\pi^0 p^0}{8\pi^2\hbar^2c^2} \sum_m \int d\Omega_{p_\pi''} \langle p_\pi' | K_0 | t_{33} | m \rangle | p_\pi^{0''} \rangle$$

$$\times \langle p_\pi^{0''} | K_m | \bar{t}_{33} | 0 \rangle | p_\pi \rangle .$$

Using the factored form as was done in the optical potential calculation (see Chapter VI) we can write equation (8.37) as

(8.38)

$$\Delta t_{\pi N} = \sum_m \int d\Omega_{p_\pi^m} \left(\frac{i\pi \omega_\pi^m p_\pi^m}{8\pi^2 \hbar^2 c^2} \right) \langle t_{33}(p_\pi', p_\pi^m) \rangle$$

$$\times \rho_{om}(p_\pi' - p_\pi^m) \rho_{mo}(p_\pi^m - p_\pi) \langle t_{33}(p_\pi^m, p_\pi) \rangle$$

where $\omega_\pi^m = \omega_\pi^o + E_o - E_m$ and p_π^m is defined by the relation $\omega_\pi^m = (m_\pi^2 c^4 + \hbar^2 c^2 (p_\pi^m)^2)^{1/2}$. The vector p_π^m has fixed magnitude p_π^m but the direction is variable. Since the energy ω_π^o is much larger than $E_o - E_m$ we set ω_π^m to ω_π^o and p_π^m to p_π^o obtaining

(8.39)

$$\Delta t_{\pi N} = \left(\frac{-i\omega_\pi^o p_\pi^o}{8\pi^2 \hbar^2 c^2} \right) \int d\Omega_{p_\pi^o} \langle t_{33}(p_\pi', p_\pi^o) \rangle$$

$$\times \langle t_{33}(p_\pi^o, p_\pi) \rangle \sum_m \rho_{om}(p_\pi' - p_\pi^o) \rho_{mo}(p_\pi^o - p_\pi) .$$

Now the form factors ρ_{m0} are given by

$$\rho_{m0}(q_\gamma) = \int \psi_m^*(p+q_\gamma)\psi_0(p)\frac{d^3p}{(2\pi)^3} \tag{8.40}$$

so that using closure we have

$$\sum_m \rho_{0m}(p_\pi' - p_\pi^0)\rho_{m0}(p_\pi^0 - p_\pi) = \rho_{00}(p_\pi' - p_\pi). \tag{8.41}$$

The quantity $\rho_{00}(p_\pi' - p_\pi)$ is just what we have been calling $\rho(q_\gamma)$ so equation (8.39) can be written

$$\Delta t_{\pi N} = \left(\frac{-i p_\pi^0 \omega_\pi^0}{8\pi^2 \hbar^2 c^2}\right)\rho(q_\gamma) \tag{8.42}$$

$$\times \int d\Omega_{p_\pi^0} \langle \bar{t}_{33}(p_\pi' p_\pi^0)\rangle \langle \bar{t}_{33}(p_\pi^0 p_\pi)\rangle .$$

Making a partial-wave expansion of $\langle \bar{t}_{33}(p_\pi' p_\pi^0)\rangle$ and $\langle \bar{t}_{33}(p_\pi^0 p_\pi)\rangle$ we obtain the result

(8.43)

$$\Delta t_{\pi N} = \left(\frac{-i p_\pi^0 \omega_\pi^0}{8\pi^2 \hbar^2 c^2}\right) \rho(q_0)$$

$$\times \sum_L \frac{2L+1}{4\pi} \langle \bar{t}_{33}(p_\pi' p_\pi^0) \rangle_L \langle \bar{t}_{33}(p_\pi^0 p_\pi) \rangle_L P_L(\hat{p}_\pi' \cdot \hat{p}_\pi) .$$

Extending our result to include all terms implied by equation (8.9) we have

(8.44)

$$\Delta t_{\pi N} = \left(\frac{-i p_\pi^0 \omega_\pi^0}{8\pi^2 \hbar^2 c^2}\right) \rho(q_0)$$

$$\times \sum_L \frac{2L+1}{4\pi} \frac{\langle \bar{t}_{33}(p_\pi' p_\pi^0) \rangle_L \langle \bar{t}_{33}(p_\pi^0 p_\pi) \rangle_L}{1 + \frac{i \omega_\pi^0 p_\pi^0}{8\pi^2 \hbar^2 c^2} \langle t_{\pi N}(p_\pi^0 p_\pi^0) \rangle_L} P_L(\hat{p}_\pi' \cdot \hat{p}_\pi) .$$

Using this approximation we obtain for the closure limit form of $\tau_{\pi N}$

(8.45)

$$\langle \underset{\sim}{p}_\pi' | \langle 0 | \hat{T}_{\pi N} | 0 \rangle | \underset{\sim}{p}_\pi \rangle = \rho(q) \sum_L \frac{2L+1}{4\pi} \times$$

$$\left[\langle \bar{t}_{33}(p_\pi' p_\pi) \rangle_L - \left(\frac{i p_\pi^0 \omega_\pi^0}{8\pi^2 \hbar^2 c^2} \right) \frac{\langle \bar{t}_{33}(p_\pi' p_\pi^0) \rangle_L \langle \bar{t}_{33}(p_\pi^0 p_\pi) \rangle_L}{1 + \frac{i \omega_\pi^0 p_\pi^0}{8\pi^2 \hbar^2 c^2} \langle \bar{t}_{33}(p_\pi^0 p_\pi^0) \rangle_L} \right] P_L(\hat{p}_\pi' \cdot \hat{p}_\pi).$$

The closure limit varies with energy in roughly the same way as the single state approximation, but the effect is about twice as large. For example, near the (3,3) resonance the single state approximation reduces the imaginary part of the impulse term by about 10 - 20 % in the forward direction while the closure approximations reduces it by about 30 - 40 % .

The results we obtain for $\Delta t_{\pi N}$ in the closure limit are in good agreement with results given by Goldberger and Watson (Gol64) who estimate the binding correction term to be about 2/3 of the impulse term near the (3,3) resonance. Goldberger and Watson do not sum the binding correction series so their result corresponds to the result we obtain in equation (8.43). Our equation (8.43) gives the binding correction at $\theta_{\pi N} = 0^\circ$ to be about 60 % of the impulse term near the (3,3) resonance, but after the series is summed in equation (8.44) the correction is only about 30 - 40 % of the impulse term.

In Figures 8.5 - 8.7 we show the effective impulse interactions given by the single state approximation and the closure limit.

FIGURE 8.5--Three different versions of the effective pion-nucleon interaction: (a) (solid line) the fully-integrated impulse result (FIA); (b) (dashed line) the single state approximation for binding effects (SSAB); (c) (dot-dash line) the closure limit for binding effects (CAB). The laboratory kinetic energy of the pion is 110 MeV.

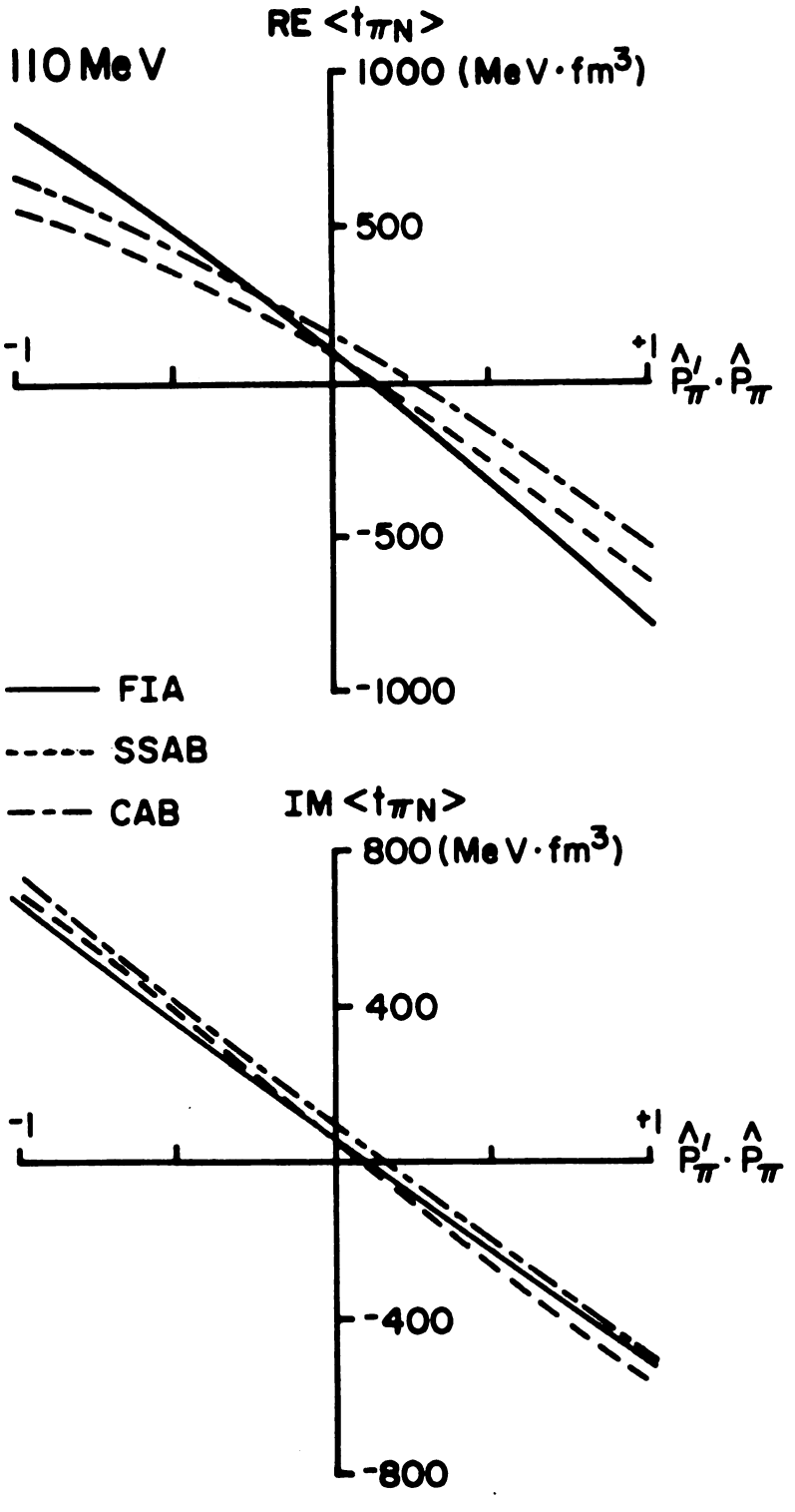
RE $<t_{\pi N}>$
110 MeV
1000 (MeV·fm^3)
500
-500
-1000
-1
+1
$\hat{P}'_\pi \cdot \hat{P}_\pi$
FIA
SSAB
CAB
IM $<t_{\pi N}>$
800 (MeV·fm^3)
400
-400
-800
-1
+1
$\hat{P}'_\pi \cdot \hat{P}_\pi$

FIGURE 8.5.

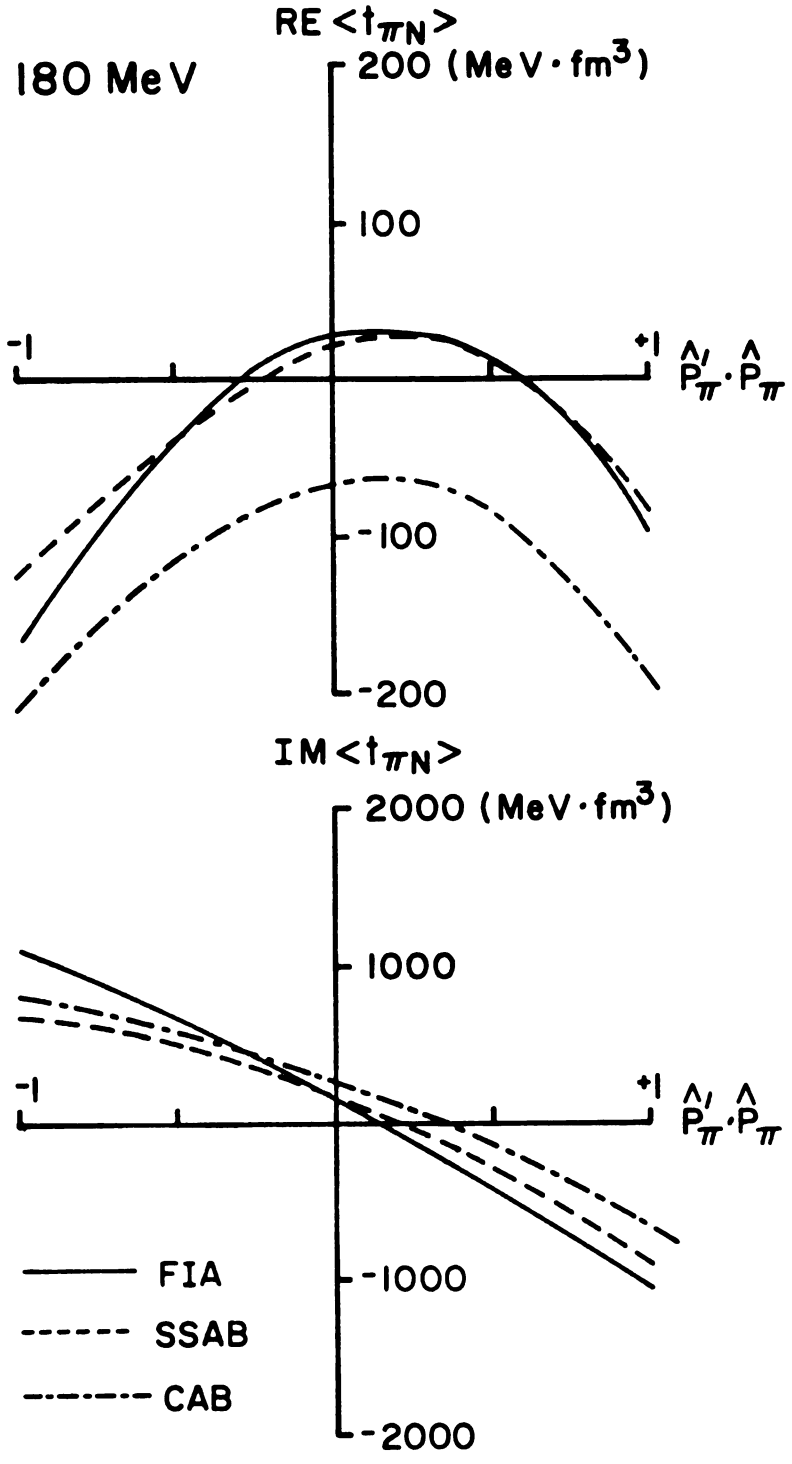

FIGURE 8.6--As in Figure 8.5 except at 180 MeV.

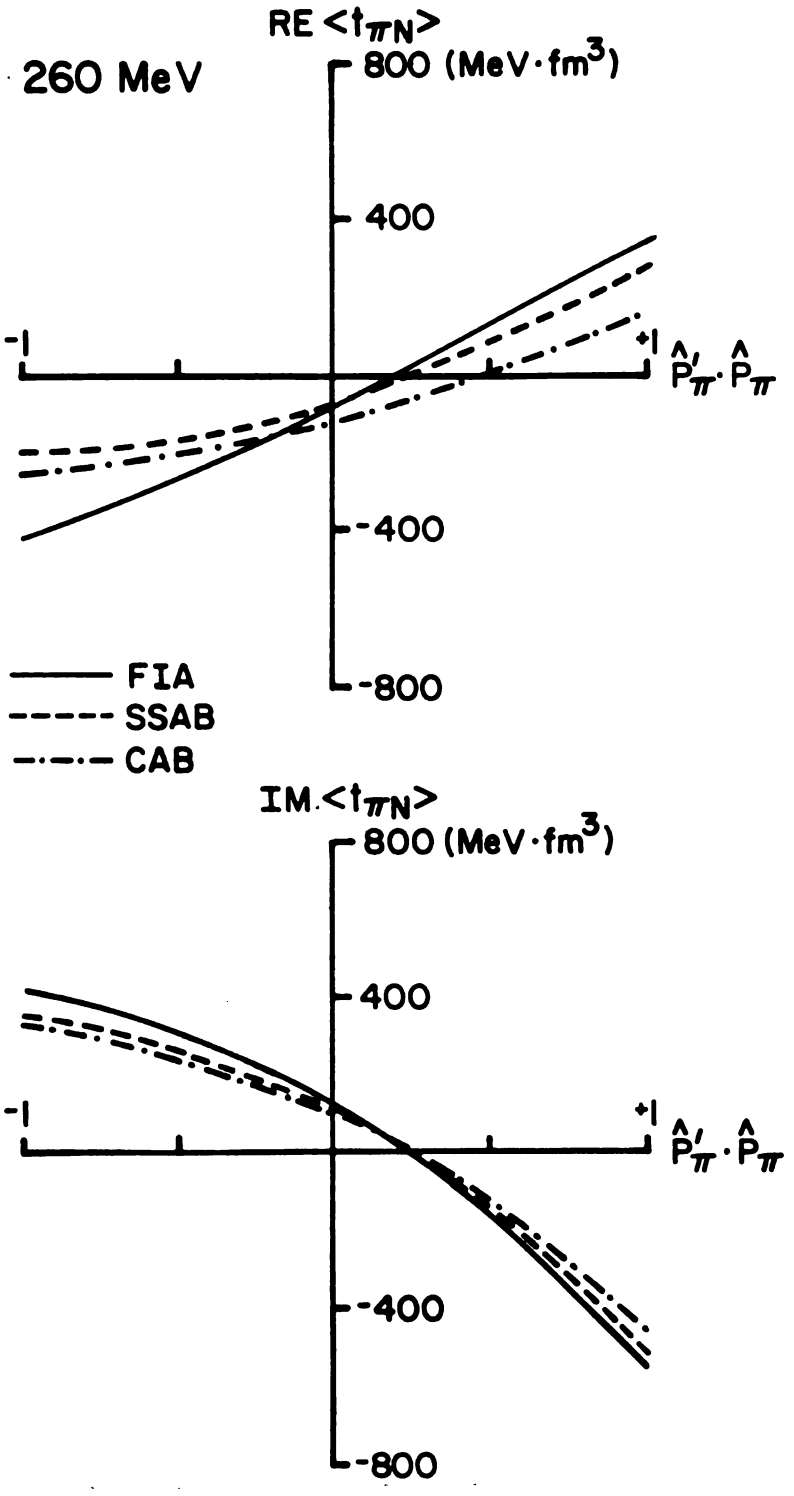

FIGURE 8.7--As in Figure 8.5 except at 260 Mev.

CHAPTER IX

CALCULATION OF THE ELASTIC SCATTERING CROSS SECTIONS

In previous chapters the calculation of the pion-nucleus optical potential was discussed; in this chapter we discuss the calculation of elastic cross sections from the pion-nucleus optical potential.

1. Relation of the Cross Section to the Pion-Nucleus t-Matrix

The elastic differential cross section is related to the elastic scattering amplitude $f(\theta_{\pi\nu})$ by

$$(9.1) \quad d\sigma/d\Omega = \left|f(\theta_{\pi\nu})\right|^2$$

and the elastic scattering amplitude in related to the pion-nucleus t-matrix $T_{\pi\nu}$ by

$$(9.2) \quad f(\theta_{\pi\nu}) = -\frac{1}{2\pi\hbar^2c^2}\,\frac{\omega_\pi^0\,\omega_\nu^0}{\omega_\pi^0+\omega_\nu^0}\,T_{\pi\nu}(\underset{\sim}{p}_\pi^{0\prime},\underset{\sim}{p}_\pi^{0})$$

where $|\underset{\sim}{p}_\pi^{0\prime}| = |\underset{\sim}{p}_\pi^0| = p_\pi^0$, p_π^0 being the incident pion momentum in the $\pi\nu$CM frame. The energies ω_π^0 and ω_ν^0 are given by $\omega_\pi^0 = (m_\pi^2 c^4 + \hbar^2 c^2 p_\pi^{0\,2})^{1/2}$ and $\omega_\nu^0 = (m_\nu^2 c^4 + \hbar^2 c^2 p_\pi^{0\,2})^{1/2}$

Defining the partial wave components of $T_{\pi\nu}(\underset{\sim}{p}_\pi' \underset{\sim}{p}_\pi)$ as

$$(9.3)\quad T_{\pi\nu}^L(p_\pi' p_\pi) = 2\pi \int_{-1}^{1} T_{\pi\nu}(\underset{\sim}{p}_\pi' \underset{\sim}{p}_\pi) P_L(\hat{p}_\pi' \cdot \hat{p}_\pi)\, d(\hat{p}_\pi' \cdot \hat{p}_\pi)$$

so that

$$(9.4)\quad T_{\pi\nu}(\underset{\sim}{p}_\pi' \underset{\sim}{p}_\pi) = \sum_L \left(\frac{2L+1}{4\pi}\right) T_{\pi\nu}^L(p_\pi' p_\pi) P_L(\hat{p}_\pi' \cdot \hat{p}_\pi)$$

we easily obtain for the total elastic cross section,

$$(9.5)\quad \sigma_{TOT}^E = \int |f(\theta_{\pi\nu})|^2 d\Omega = \left(\frac{1}{2\pi} \frac{\omega_\pi^0 \omega_\nu^0}{\omega_\pi^0 + \omega_\nu^0}\right)^2 \sum_L \left(\frac{2L+1}{4\pi}\right) T_{\pi\nu}^L(p_\pi^0 p_\pi^0) .$$

Using the Optical Theorem, we have for the total cross section,

$$(9.6)\quad \sigma_{TOT} = \frac{4\pi}{p_\pi^0} \, IM\left[f(\theta_{\pi\nu} = 0)\right] .$$

The reaction cross section is then given by

$$\sigma_{TOT}^{R} = \sigma_{TOT} - \sigma_{TOT}^{E} \quad . \tag{9.7}$$

2. Calculation of the Pion-Nucleus t-Matrix

The auxillary pion-nucleus t-matrix $T'_{\pi\nu}$ was defined in Chapter II using a relativistic Lippmann-Schwinger equation of the form

$$T'_{\pi\nu}(\underset{\sim}{p}'_{\pi}\,\underset{\sim}{p}_{\pi}) = U_{\pi\nu}(\underset{\sim}{p}'_{\pi}\,\underset{\sim}{p}_{\pi}) + \int \frac{U_{\pi\nu}(\underset{\sim}{p}'_{\pi}\,\underset{\sim}{p}''_{\pi})\,T_{\pi\nu}(\underset{\sim}{p}''_{\pi}\,\underset{\sim}{p}_{\pi})}{\omega_0 - \omega(p''_{\pi}) + i\epsilon}\,\frac{d^3p''_{\pi}}{(2\pi)^3} \tag{9.8}$$

with the actual pion-nucleus t-matrix being given by

$$T_{\pi\nu}(\underset{\sim}{p}'_{\pi}\,\underset{\sim}{p}_{\pi}) = \left(A/A-1\right)T'_{\pi\nu}(\underset{\sim}{p}'_{\pi}\,\underset{\sim}{p}_{\pi}) \quad . \tag{9.9}$$

In order to actually solve for $T'_{\pi\nu}$ we must first reduce equation (9.8) to a one-dimensional integral equation. We define the partial wave components of $T'_{\pi\nu}$ and $U_{\pi\nu}$ using the same definition as for $T_{\pi\nu}$ (see equation (9.3)) and obtain a one-dimensional Lippmann-Schwinger equation for $T'^{L}_{\pi\nu}$

(9.10)

$$T'^{L}_{\pi\nu}(p'_\pi p_\pi) = U^{L}_{\pi\nu}(p'_\pi p_\pi) + \int_0^\infty \frac{U^{L}_{\pi\nu}(p'_\pi p''_\pi)\, T'^{L}_{\pi\nu}(p''_\pi p_\pi)}{\omega_0 - \omega(p''_\pi) + i\epsilon} \frac{p''^{2}_\pi dp''_\pi}{(2\pi)^3} .$$

The above integral equation for $T'^{L}_{\pi\nu}$ is solved numerically using matrix inversion techniques. The method is discussed in Appendix G.

3. Partial-Wave Decomposition of the Optical Potential

As discussed in the previous section, a partial wave decomposition of the 3-dimensional optical potential is needed for the solution of the scattering equation. In this section we discuss the procedure for obtaining such a partial wave decomposition.

We always assume a 3-dimensional pion-nucleus optical potential of the form

$$(9.11)\quad U_{\pi\nu}(\underset{\sim}{p}'_\pi \underset{\sim}{p}_\pi) = (A-1)\langle t_{\pi N}\rangle \rho(q)$$

where A is the number of target nucleons and $\rho(q)$ is an <u>empirical</u> ground state form factor.

When we have an explicit 3-dimensional form for $\langle t_{\pi N}\rangle$ (as in the quadratic approximation, for example), it is simple to obtain the partial wave components of $U_{\pi\nu}$. We first write $\rho(q)$ as

$$(9.12)\quad \rho(q) = \sum_L \rho_L(p'_\pi p_\pi) P_L(\hat{p}'_\pi \cdot \hat{p}_\pi) .$$

Then we write $\langle t_{\pi N}\rangle$ as

$$(9.13)\quad \langle t_{\pi N}\rangle = \sum_L \left(\frac{2L+1}{4\pi}\right)\langle t_{\pi N}\rangle_L P_L(\hat{p}'_\pi \cdot \hat{p}_\pi) .$$

So we have

$$(9.14)$$

$$U_{\pi\nu}(\underset{\sim}{p}'_\pi \underset{\sim}{p}_\pi) = \sum_{L'} \left(\frac{2L'+1}{4\pi}\right) U^{L'}_{\pi\nu}(p'_\pi p_\pi) P_{L'}(\hat{p}'_\pi \cdot \hat{p}_\pi)$$

$$= (A-1)\sum_{L''L'''} \left(\frac{2L''+1}{4\pi}\right)\langle t_{\pi N}\rangle_{L''} \rho_{L'''}(p'_\pi p_\pi) P_{L''}(\hat{p}'_\pi \cdot \hat{p}_\pi) P_{L'''}(\hat{p}'_\pi \cdot \hat{p}_\pi) .$$

Multiplying equation (9.14) by $P_L(\hat{P}'_\pi \cdot \hat{P}_\pi)$ and integrating over $\hat{P}'_\pi \cdot \hat{P}_\pi$ we obtain

(9.15)

$$U^L_{\pi\nu}(P'_\pi P_\pi) =$$

$$(A-1)\sum_{L''L'''}\left(\frac{2L''+1}{2L+1}\right)\langle L''L'''00|L0\rangle^2\langle t_{\pi N}\rangle_{L''}\rho_{L'''}(P'_\pi P_\pi).$$

When we obtain $\langle t_{\pi N}\rangle$ numerically by calculating the ^{4}He optical potential using a gaussian ground state wave function and the definition in equation (6.2), we calculate $U^L_{\pi\nu}$ in a slightly different way. The definition in equation (6.2) gives us

$$(9.16)\quad \langle t_{\pi N}\rangle = \frac{1}{3} U_g(P'_\pi P_\pi)/\rho_g(q)$$

where $U_g(P'_\pi P_\pi)$ is the numerically computed <u>gaussian</u> ^{4}He optical potential and $\rho_g(q)$ is the associated gaussian form factor. The numerical calculation of U_g automatically gives us the partial wave components U^L_g so it is convenient to use these components directly in the calculation of the partial wave components of $U_{\pi\nu}$. The general optical potential $U_{\pi\nu}$ is given by

(9.17)

$$U_{\pi\nu}(\underset{\sim}{p}'_\pi \underset{\sim}{p}_\pi) = (A-1)\langle t_{\pi N}\rangle \rho(q)$$

$$= (A-1)\left[\frac{1}{3} U_g(\underset{\sim}{p}'_\pi \underset{\sim}{p}_\pi)/\rho_g(q)\right]\rho(q)$$

or

(9.18)

$$U_{\pi\nu}(\underset{\sim}{p}'_\pi \underset{\sim}{p}_\pi) =$$

$$(A-1)\left[\frac{1}{3}\sum_L \left(\frac{2L+1}{4\pi}\right) U_g^L(p'_\pi p_\pi) P_L(\hat{p}'_\pi \cdot \hat{p}_\pi)\right]\rho(q)/\rho_g(q) .$$

We now define a "reduced" form factor $\rho(q)/\rho_g(q)$ and make a partial wave decomposition of this reduced form factor.

(9.19)

$$\hat{\rho}(q) \equiv \rho(q)/\rho_g(q) = \sum_L \hat{\rho}_L(p'_\pi p_\pi) P_L(\hat{p}_\pi \cdot \hat{p}_\pi)$$

Then following the same procedure as in equations (9.14) and (9.15), we obtain for the partial wave components of the pion-nucleus optical potential

(9.20)

$$U^{L}_{\pi\nu}(p'_{\pi} p_{\pi}) =$$

$$\left(\frac{A-1}{3}\right) \sum_{L''L'''} \left(\frac{2L''+1}{2L+1}\right) \langle L''L''' 00 | L0 \rangle^{2} U^{L''}_{g}(p'_{\pi} p_{\pi}) \hat{\rho}_{L}(p'_{\pi} p_{\pi}) .$$

The above method thus allows us to calculate optical potentials with realistic form factors directly from the fully integrated gaussian ^{4}He optical potential. We note that even for ^{4}He this method is necessary since the empirical ^{4}He form factor is not purely gaussian (Fro67).

4. The Form Factors

In calculating elastic cross sections for ^{4}He, ^{12}C, and ^{16}O the form factor in the relation $U_{\pi\nu}(\underset{\sim}{p'_{\pi}} \underset{\sim}{p_{\pi}}) = (A-1)\langle t_{\pi N} \rangle \rho(q_{0})$ is always a ground state form factor compatible with electron scattering experiments.

The ground state form factor is defined as

(9.21) $$\rho(q_{0}) = \rho_{Q}(q_{0}) / \rho_{P}(q_{0})$$

where ρ_Q is the nuclear charge form factor obtained from electron scattering and ρ_p is the charge form factor for a proton. The division of ρ_Q by ρ_p is intended to remove the effect of the finite proton size so ρ_Q / ρ_p is the form factor for an ensemble of point particles.[1] We take ρ_p to be

$$\rho_p(q) = \exp(-r_p^2 q^2/6) \tag{9.22}$$

where r_p = .76 fm. (Ehr59).

For ^{4}He we take ρ_Q from the work of Frosch et.al. (Fro67), so using equation (9.21), we have for the ^{4}He ground state form factor

$$\rho(q) = [1 - (a^2 q^2)^6] \exp(-b^2 q^2) \tag{9.23}$$

where a = .316 fm and b = .606 fm .

For ^{12}C and ^{16}O we use the parameterization of Ehrenberg et. al. (Ehr59) for ρ_Q . The resulting ground state form factor is

---

[1] The finite nucleon size is already contained in the pion-nucleon t-matrix so it should not be included in the nuclear form factor.

(9.24)

$$\rho(q) = \left[1-\alpha(qa_{cm})^2/2(2+3\alpha)\right]\exp\left[-(qa_{ch})^2/4\right]$$

where $a_{cm} = 1.66$ fm, $a_{ch} = 1.59$ fm, $\alpha = (A-4)/6$.

5. Treatment of the Non-Resonant Channels

In calculating nucleon motion effects and binding effects we assumed the pion-nucleon interaction is in the (3,3) channel only. In the actual calculation of elastic cross sections we include the non-resonant parts of the optical potential via the simple static approximation. Consequently, whenever nucleon motion or binding effects are taken into account the optical potential is the sum of two parts: A "resonant" part which includes nucleon motion and/or binding effects and a "nonresonant" part obtained from the simple static approximation. This procedure is adequate since the non-resonant part of the optical potential is relatively small at the energies we consider.

6. Coulomb Effects

Finally, the coulomb potential is neglected in this calculation. The work of Lee and McManus (Lee71) indicates that coulomb effects are unimportant in the (3,3) resonance region.

CHAPTER X

COMPARISON OF THE CALCULATED CROSS SECTIONS WITH EXPERIMENT

1. Impulse Approximation Results for ^{4}He

The results for ^{4}He given by the fully-integrated impulse approximation (FIA), the simple static approximation (SSA), and the modified static approximation (MSA) are compared to the experimental data in Figure 10.1. The results for the quadratic approximation are shown in Figure 10.2 and for the Kujawski-Miller-Landau (KML) approximation in Figure 10.3.

We shall be mainly concerned with the predictions of the FIA (or its equivalent) since this model is preferred on theoretical grounds. However, in order to show the consequences of using ad hoc models which are poor approximations to the FIA optical potential, we also discuss the predictions of the SSA and MSA.

a. The First Minimum in ^{4}He:

The first minimum in ^{4}He is apparently due to the p -wave pion-nucleon resonance and is approximately stationary at $\sim 77^\circ$ in the πNCM system. The correct prediction of this minimum is an important test of any $\pi^- - ^4$He optical potential.

FIGURE 10.1--The elastic π^- - ^{4}He differential cross sections resulting from three different effective pion-nucleon impulse interactions: (a) (solid line) the fully-integrated impulse result (FIA); (b) (short dash line) the simple static approximation (SSA); (c) (dot-dash line) the modified static approximation (MSA). The energies shown are the laboratory kinetic energy of the pion.

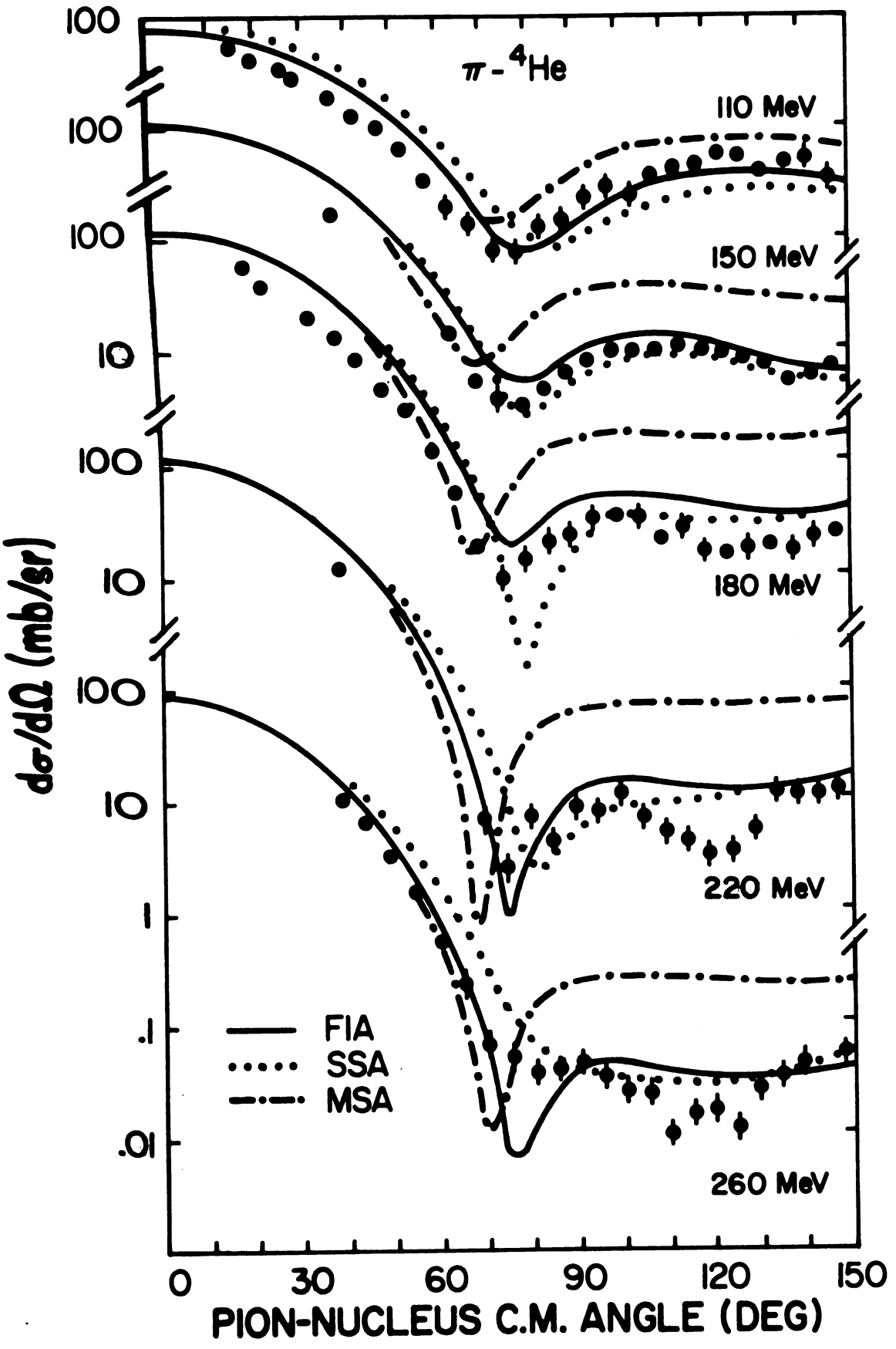
π - 4He
110 MeV
150 MeV
180 MeV
220 MeV
260 MeV
FIA
SSA
MSA
dσ/dΩ (mb/sr)
100
100
100
10
100
10
100
10
1
.1
.01
0
30
60
90
120
150
PION-NUCLEUS C.M. ANGLE (DEG)

FIGURE 10.1.

As can be seen in Figure 10.1, the FIA correctly predicts the location and relative depth of the first minimum at all energies except 260 MeV where the experimental minimum is somewhat weak. At 260 Mev the predicted minimum is too far forward by 5^{o} and too deep.

The SSA and MSA do not fit the first minimum in ^{4}He nearly as well as the FIA. The MSA gives the first minimum too far forward at all energies and the SSA gives the first minimum at too large an angle at all energies except 150 MeV. For most energies, the relative depth is too large with the MSA. The SSA generally gives a more accurate depth for the first minimum, but fails badly at 180 MeV.

The first minimum becomes considerably weaker at 260 MeV. All three models indicate a decreasing depth for energies above 220 MeV, but none of the models have the proper degree of weakening at 260 MeV. The FIA and MSA minima are too deep, and the minimum vanishes completely with the SSA.

The predictions of the various models for the first minima in ^{4}He are directly related to the angle transformations involved (i.e., the

relationship between $\cos\theta_{\pi N}$ and $\cos\theta_{\pi\gamma}$). These angle transformations will be discussed in detail in a later section.

b. The Second Minimum in ^{4}He:

At 180 MeV, a second minimum appears and is quite prominent at 220 and 260 MeV, moving toward smaller angles with increasing incident pion energy. This second minimum is consistent with the experimentally observed zero in the ^{4}He form factor (Fro67). Although we use form factors compatible with electron scattering in all our models, we still fail to predict the second minimum. Our form factors are obtained by dividing the electron scattering nuclear charge form factor by the proton charge form factor. This procedure is intended to remove the effect of the finite proton size so that we are left with the nuclear form factor for an ensemble of point nucleons. For an independent particle model and harmonic oscillator wave functions, our procedure is valid (Ehr59). However, for ^{4}He it is an approximation of questionable validity since the nucleons are highly correlated and hence only approximately described by single particle wave functions.

It may be that a more accurate treatment of nucleon size effects is necessary for a correct prediction of the second minimum.

c. The Discrepancy at Forward Angles:

At all energies, except 260 MeV, the predicted cross section is too large for all the impulse models. The binding correction, which we discuss later on, weakens the pion-nucleus optical potential somewhat and thus gives improvement in the forward direction.

At 180 MeV, the FIA is too large at forward angles and also at backward angles, although the overall shape is good. The weakening effect of the binding correction improves the agreement with experiment at both forward and backward angles.

d. Relation of the ^{4}He Cross Sections to the Angle Transformation:

Single scattering dominates in ^{4}He so that the cross sections vary with angle approximately as $|U_{\pi y}|^2$. Hence, the features of the cross sections are closely connected to the features of the effective interaction $\langle t_{\pi N} \rangle$ used in each model. Since most of the larger effects in $\langle t_{\pi N} \rangle$ can be related to the angle

transformation, it is simpler to discuss the features of $d\sigma/d\Omega$ in relation to the features of the various angle transformations. The angle transformations shown in Figure 5.1 can be used to understand most of the effects. The KML curve in Figure 5.1 can be taken to represent the angle transformations of the FIA and quadratic approximation since they all are the same (on-shell) to order $(\omega_\pi^\circ/\omega^\circ)^2 \cong 1/25$.[1]

For a given model, the predicted position of the first minimum in ^{4}He is directly related to the zero in the corresponding $\cos\theta_{\pi N}$ vs $\cos\theta_{\pi N}$ curve in Figure 5.1. For example, the MSA minimum in $d\sigma/d\Omega$ is at the smallest angle and SSA is at the largest angle with the FIA in between the MSA and SSA. Looking at Figure 5.1, we see the same relation exists for the zeros of the various angle transformations. The features of the three angle transformations (SSA, MSA, KML) are also clearly seen in the backward scattering. The FIA and SSA are not too different at backward angles, with the FIA generally being slightly higher. At backward

---

[1] There is no explicit analytic form for the FIA angle transformation since the FIA result is obtained numerically.

angles, the MSA cross sections are larger than the FIA and SSA cross sections (and also the data) by a factor of 4 to 6. This large discrepancy in the MSA arises from the MSA angle transformation which allows $|\cos\theta_{nn}|$ to exceed one at backward angles.

e. The Quadratic Approximation and the Kujawski-Miller-Landau Approximation:

The ^{4}He results for the quadratic approximation are shown in Figure 10.2. The quadratic approximation results from a systematic approximation to the fully-integrated impulse model (see Chapter VII). It is evident that the quadratic approximation gives a very good representation of the fully-integrated impulse approximation (FIA).

In Figure 10.3 we show the results for ^{4}He using the Kujawski-Miller-Landau (KML) model. The agreement with the FIA results is essentially the same as that obtained with the quadratic approximation. Hence, we see that a proper angle transformation is essential for a good representation of the FIA[1]. However,

---

[1]Again, recall that the angle transformation in the KML model is essentially the same as the one in the FIA.

FIGURE 10.2--The elastic π^--^{4}He differential cross sections calculated by two methods: (a) (solid line) the fully-integrated impulse result (FIA); (b) (dashed line) the quadratic approximation (QA) to case (a). The energies shown are the laboratory kinetic energy of the pion.

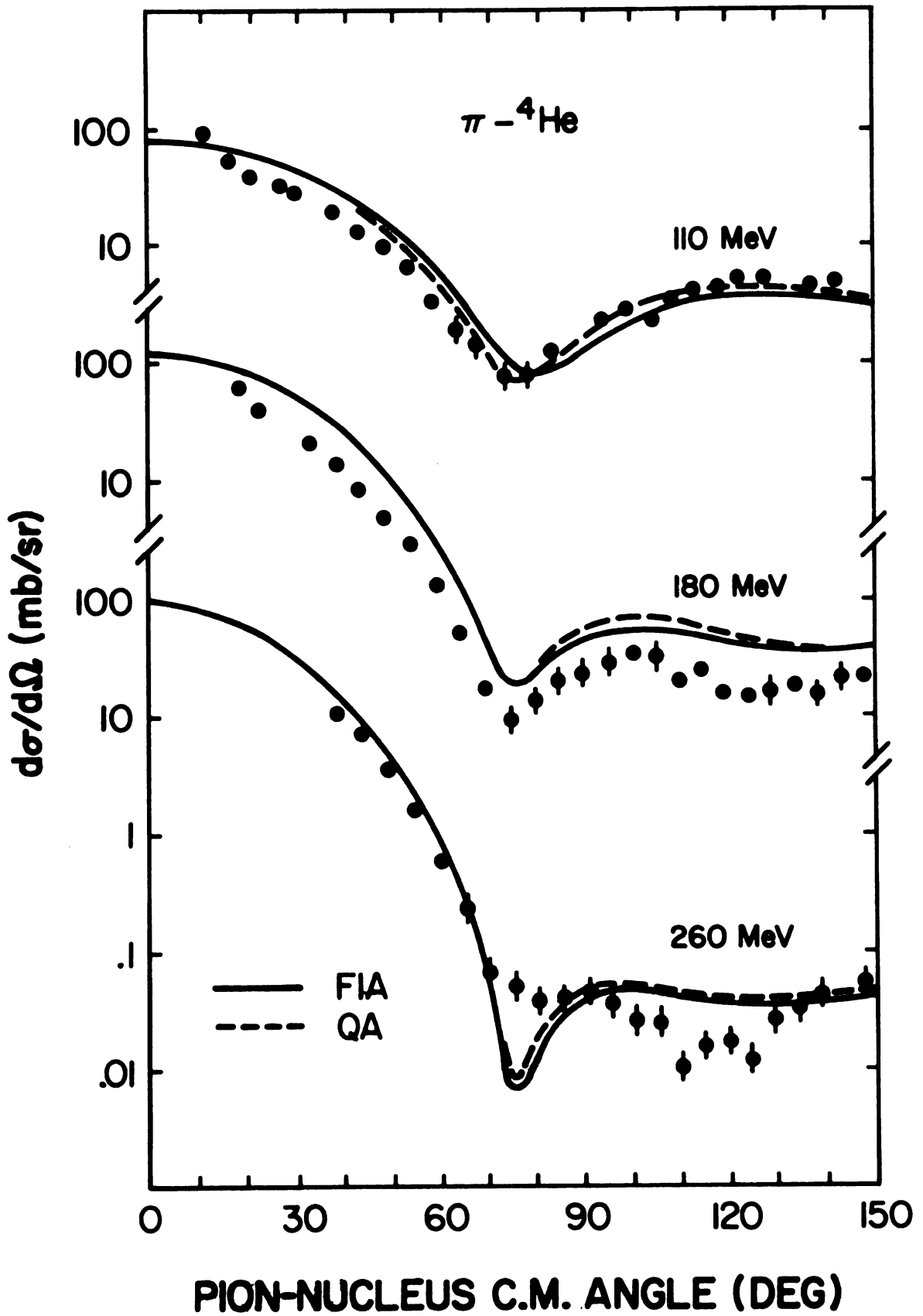

ons cal-
rated
proximat
kinetic

FIGURE 10.2.

FIGURE 10.3--The elastic π^- - ^{4}He differential cross sections calculated by two methods: (a) (solid line) the fully-integrated impulse result (FIA); (b) (dashed line) the Kujawski-Miller-Landau (KML) approximation. The energies shown are the laboratory kinetic energy of the pion.

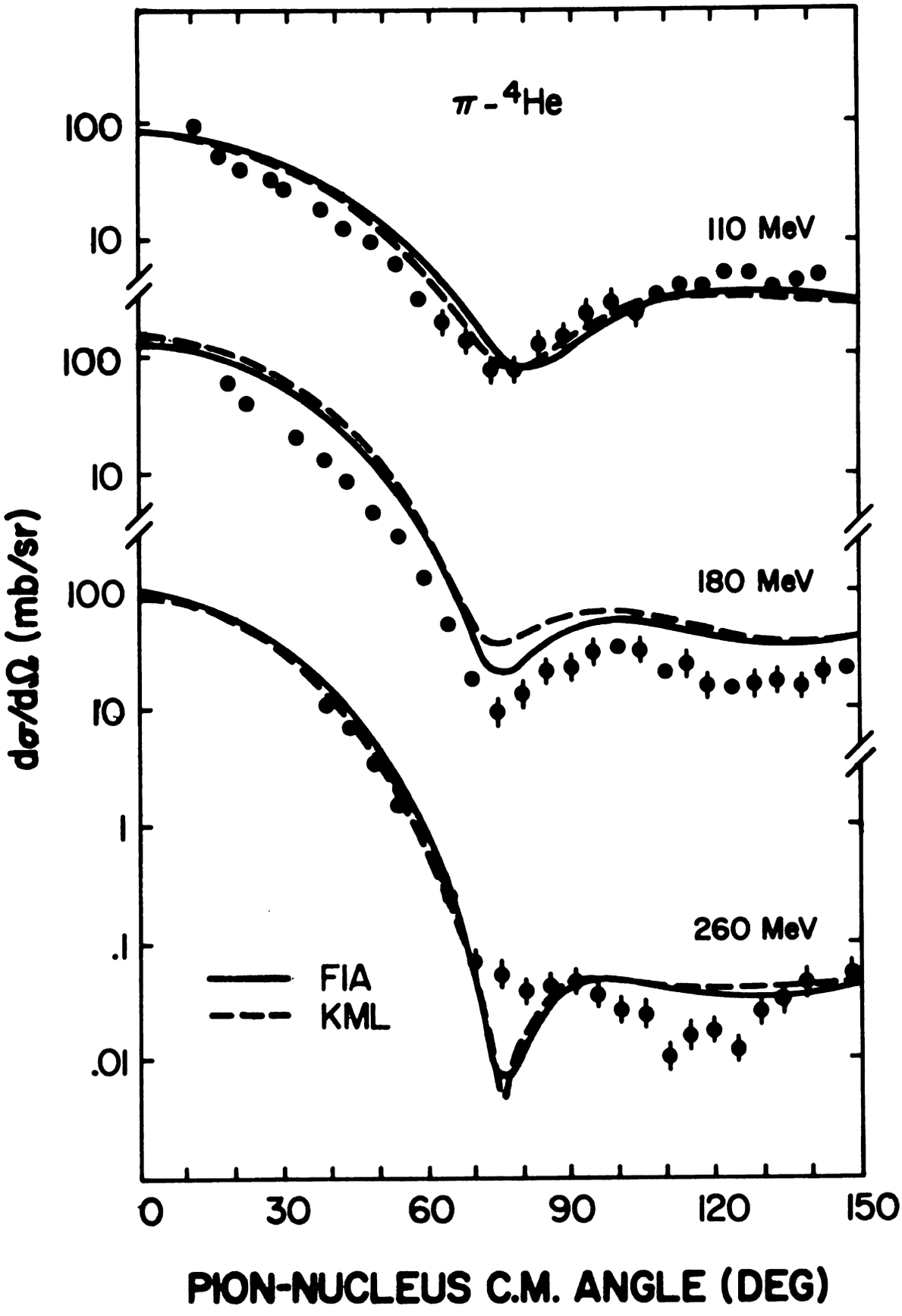
π - 4He
110 MeV
180 MeV
260 MeV
FIA
KML
dσ/dΩ (mb/sr)
100
10
100
10
100
10
1
.1
.01
0
30
60
90
120
150
PION-NUCLEUS C.M. ANGLE (DEG)

FIGURE 10.3.

we should point out that at lower energies the angle transformation effects and collision energy effects (i.e., ω_{cm} effects) are comparable although neither is a dominant effect. For example, at 110 and 150 MeV, the simple static approximation (which contains no angle transformation or collision energy effects) gives cross sections which are not too different from the FIA result. Angle transformation effects, which vary as $\omega_\pi^\circ / \omega^\circ$, become increasingly important at higher energies while collision energy effects remain about the same as at lower energies. Hence, the angle transformation gives the dominant effect for the energy region above the (3,3) resonance.

2. Impulse-plus-Binding Correction Results for ^{4}He

We now consider the results obtained for ^{4}He with the following models: 1) the fully-integrated impulse approximation (FIA); 2) the single state approximation for binding effects (SSAB); 3) the closure approximation for binding effects (CAB). The results for all three cases are shown in Figure 10.4.

a. The Single State Approximation for Binding Effects:

Due to the weakening of the optical potential produced with SSAB, the SSAB cross

FIGURE 10.4--The elastic π^- - ^{4}He differential cross sections resulting from three different effective pion-nucleon interactions: (a) (solid line) the fully-integrated impulse result (FIA); (b) (short dash line) the single state approximation for binding effects (SSAB); (c) (dot-dash line) the closure limit for binding effects (CAB). The energies shown are the laboratory kinetic energy of the pion.

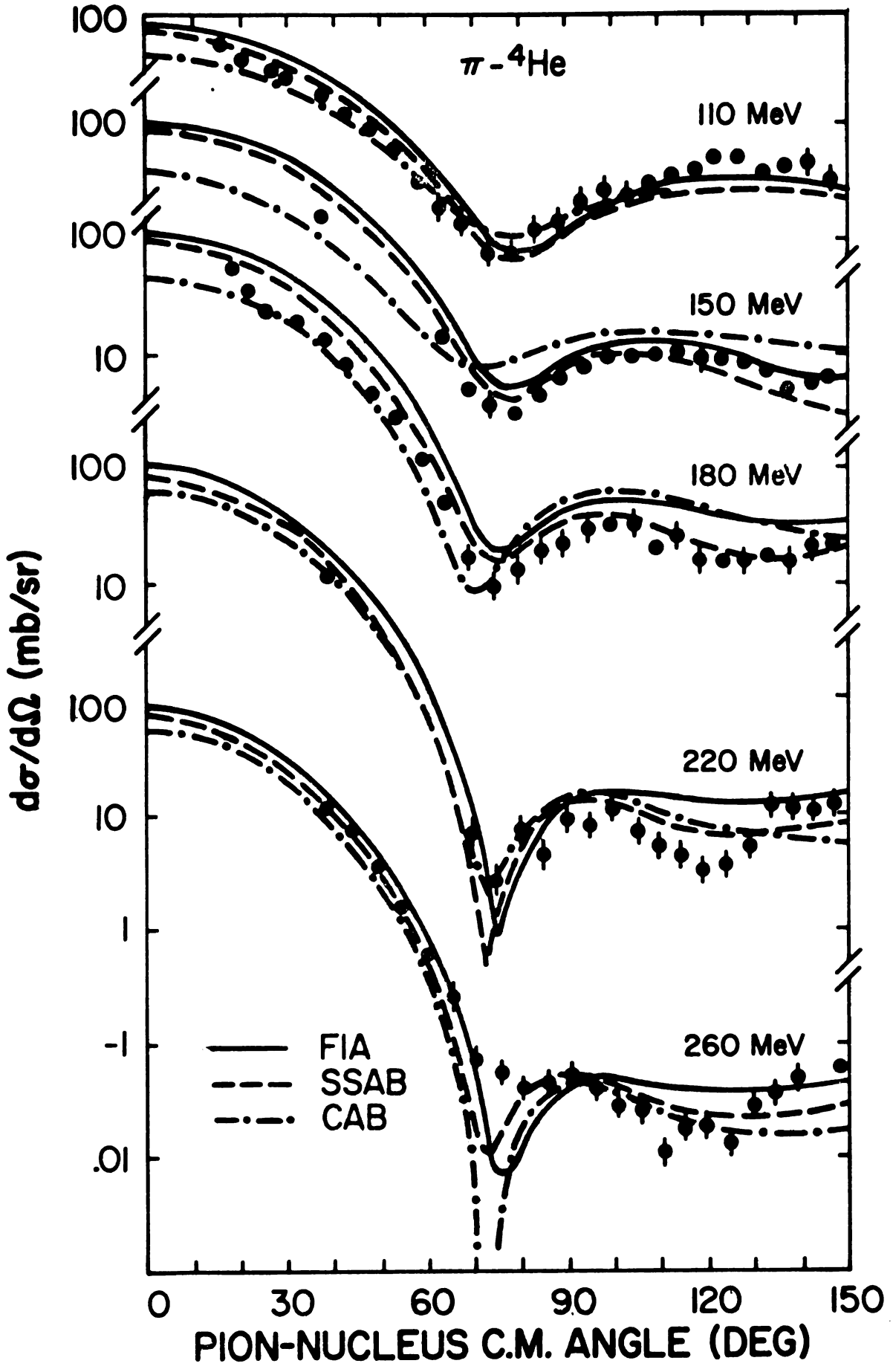
π - 4He
110 MeV
150 MeV
180 MeV
220 MeV
260 MeV
FIA
SSAB
CAB
dσ/dΩ (mb/sr)
100
10
1
-1
.01
0
30
60
90
120
150
PION-NUCLEUS C.M. ANGLE (DEG)

FIGURE 10.4.

sections are lower than those given by the FIA. At 110 and 150 MeV the reduction is fairly small, giving a slight improvement at forward angles and a slight worsening at backward angles. At 180 and 220 MeV the forward angle cross section is improved some and the backward angle cross section is improved significantly. At 260 MeV the forward angle cross section is not improved (or perhaps is slightly worsened), but the backward angle cross section is improved noticeably. At 110, 150, and 180 MeV the position of the first minimum is not changed by the binding correction, but at 220 and 260 MeV the minimum is shifted forward by a few degrees. Thus, the overall result of the SSAB is to noticeably improve the agreement with the ^{4}He data.

b. The Closure Approximation for Binding Effects:

The CAB affects the ^{4}He cross section a good deal more than does the SSAB, with the effect being greatest at 150 and 180 MeV. Generally, the CAB overestimates the binding correction. At 110 MeV the forward angle

result of the CAB is as much too low as the SSAB result is too high. The fit at the minimum is considerably worsened, but the backward angle result is left unchanged. At 150 MeV the CAB gives very poor results, being too low at forward angles and too high at backward angles. The first minimum at 150 MeV is too far forward and too shallow. The forward angle result at 180 MeV is as good as the SSAB result, but the first minimum is too far forward and the cross section at backward angles is too high. At 220 MeV the CAB result goes through the one data point at forward angles and is comparable to the SSAB at backward angles. The 260 MeV result is somewhat too low at forward angles but comparable to the SSAB result at backward angles. Also, the CAB minimum at 260 MeV is far too deep.

The overall effect of the CAB is to worsen the agreement with experiment. This result is not surprising since the CAB is only intended to give an estimate of an upper limit on the binding correction and is not intended to be a realistic model.

3. Impulse Approximation Results for ^{12}C

We now consider the impulse approximation cross sections for ^{12}C using the same models as used for ^{4}He. The results are shown in Figures 10.5 - 10.8. Again, we are mainly interested in the FIA result (and good approximations to the FIA), but we discuss the other models in order to show the sensitivity of the elastic cross sections to the features of the optical potential.

a. Nature of the Minima in ^{12}C:

In ^{4}He, single scattering dominated so we could identify the first minima as coming from the pion-nucleon p-wave resonance and the second minima as being diffractive in character. In ^{12}C, such an identification is not possible because multiple scattering strongly affects the shape of the elastic cross section and masks the features of the single scattering term. For example, one of the models studied by Lee and McManus (Lee71) is a simple local optical potential which completely neglects the p-wave nature of the pion-nucleon interaction. Although this crude model does not give a satisfactory fit to the data, it nevertheless is capable of reproducing the gross features of pion-^{12}C data (i.e., two minima). Hence, it is pointless to try to relate the features of $d\sigma/d\Omega$ directly to the details of the optical potential.

However, the main differences between the various optical potentials are usually reflected in some way in the elastic cross sections, even though for ^{12}C the general shape of $d\sigma/d\Omega$ is independent of the details of $U_{\pi y}$.

b. The Fully-Integrated Impulse Approximation (FIA) Results for ^{12}C:

The FIA results for ^{12}C are shown in Figures 10.5 - 10.8. At forward angles the agreement of the FIA with the data is good. In particular, the first minimum and first maximum are described fairly accurately up to 260 MeV. The agreement at the second minimum and second maximum is only fair, with the cross section at backward angles being underestimated at all energies. The tendency to underestimate the large angle cross sections in ^{12}C seems common to many models (Lan73, Lee71, Kuj74) including models with the optical potential parameters adjusted for a best fit (Ste70). Lee and McManus (Lee71) have suggested that ground state deformation effects are possibly important in ^{12}C so it may be that a more sophisticated treatment is required for ^{12}C. Nevertheless, the fit obtained with the FIA is as good or better than any so far published.

FIGURE 10.5--The elastic $\pi^- - {}^{12}C$ differential cross sections resulting from three different effective pion-nucleon impulse interactions: (a) (solid line) the fully-integrated impulse result (FIA); (b) (short dash line) the simple static approximation (SSA); (c) (dot-dash line) the modified static approximation (MSA). The energies shown are the laboratory kinetic energy of the pion.

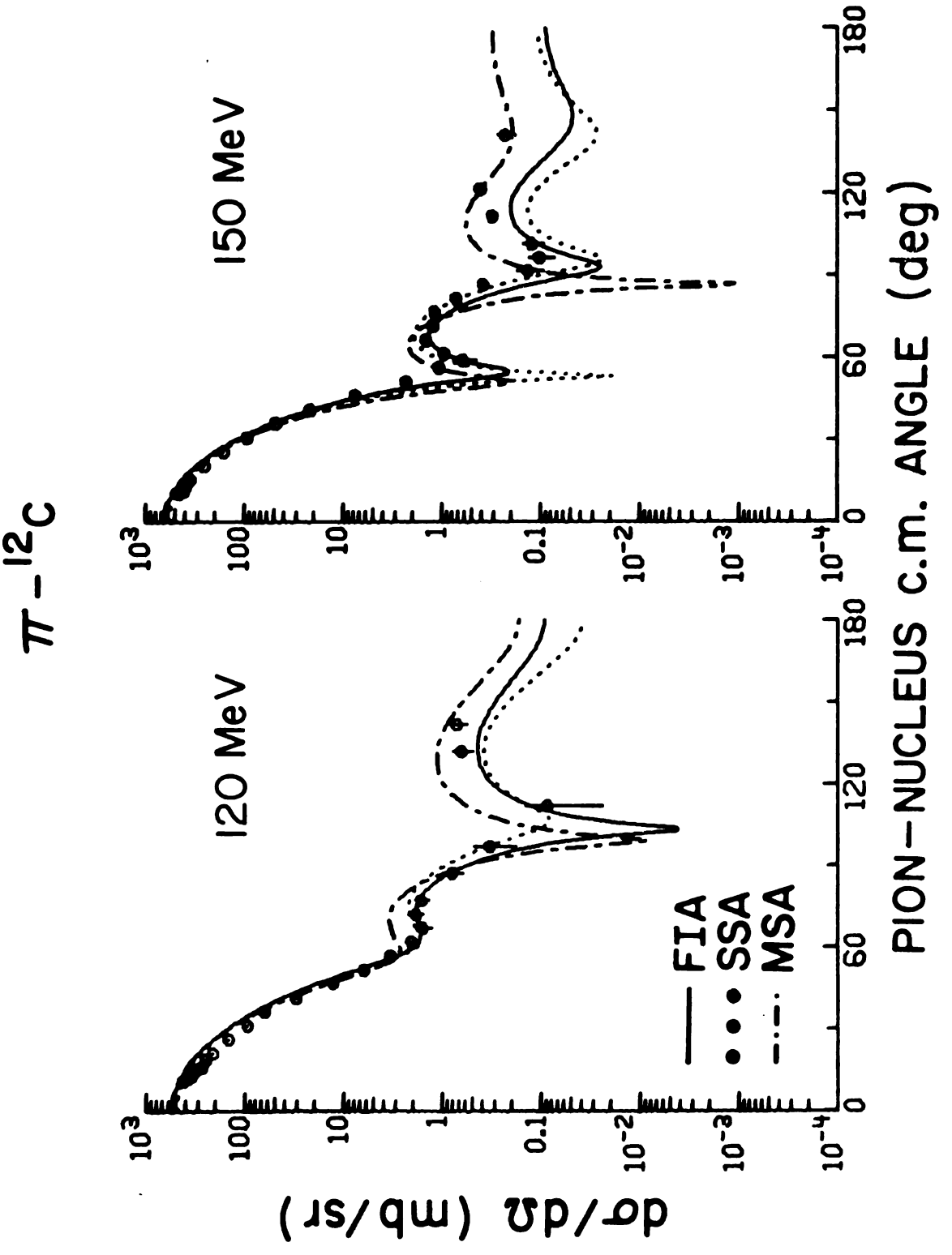
π⁻ ¹²C
120 MeV
150 MeV
dσ/dΩ (mb/sr)
PION–NUCLEUS c.m. ANGLE (deg)
FIA
SSA
MSA
10³
100
10
1
0.1
10⁻²
10⁻³
10⁻⁴
0
60
120
180

FIGURE 10.5

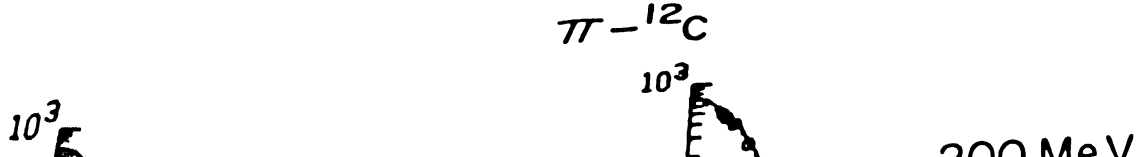
$\pi^- {}^{12}C$
10^3
200 MeV

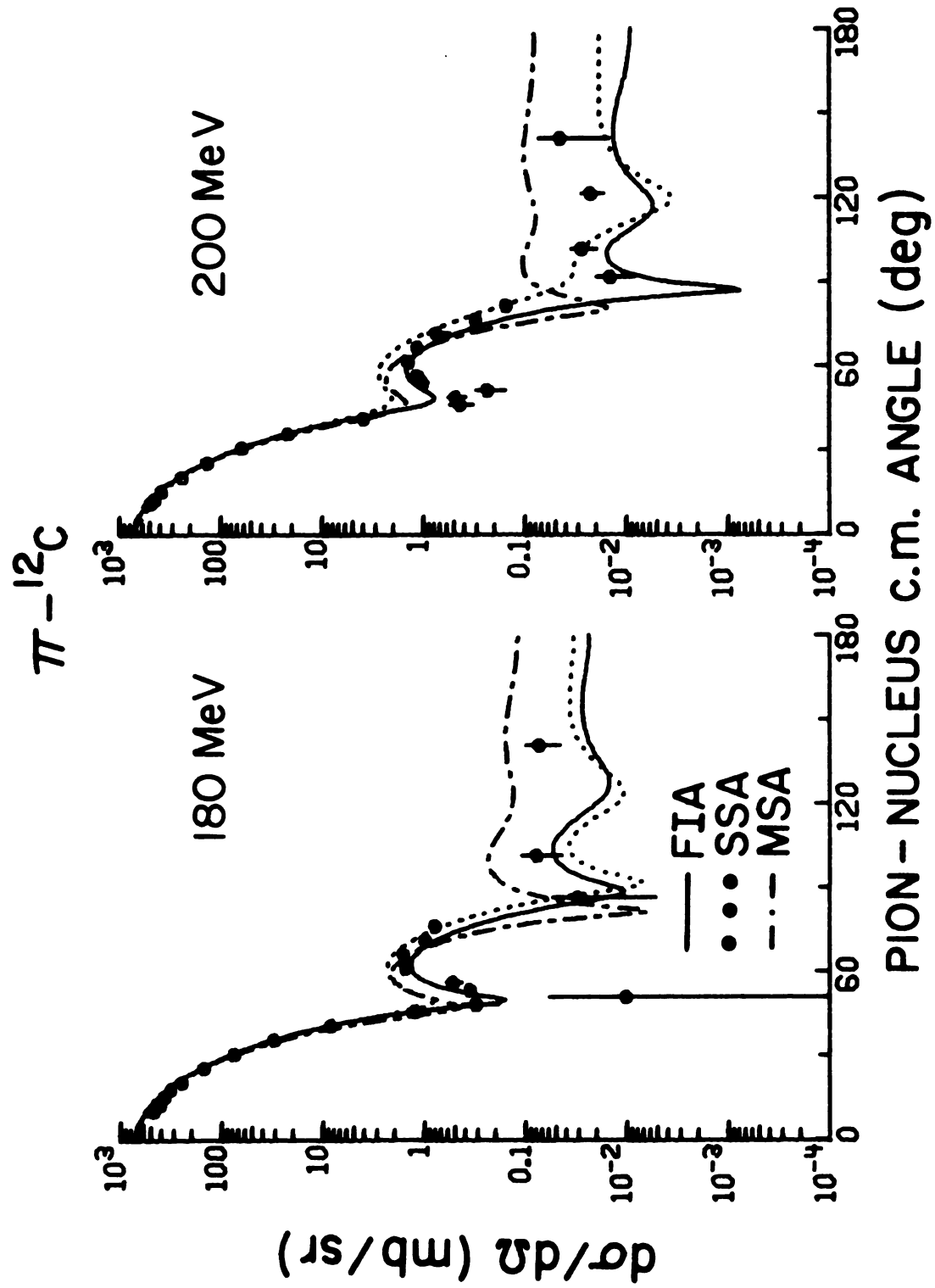

FIGURE 10.6--As in Figure 10.5.

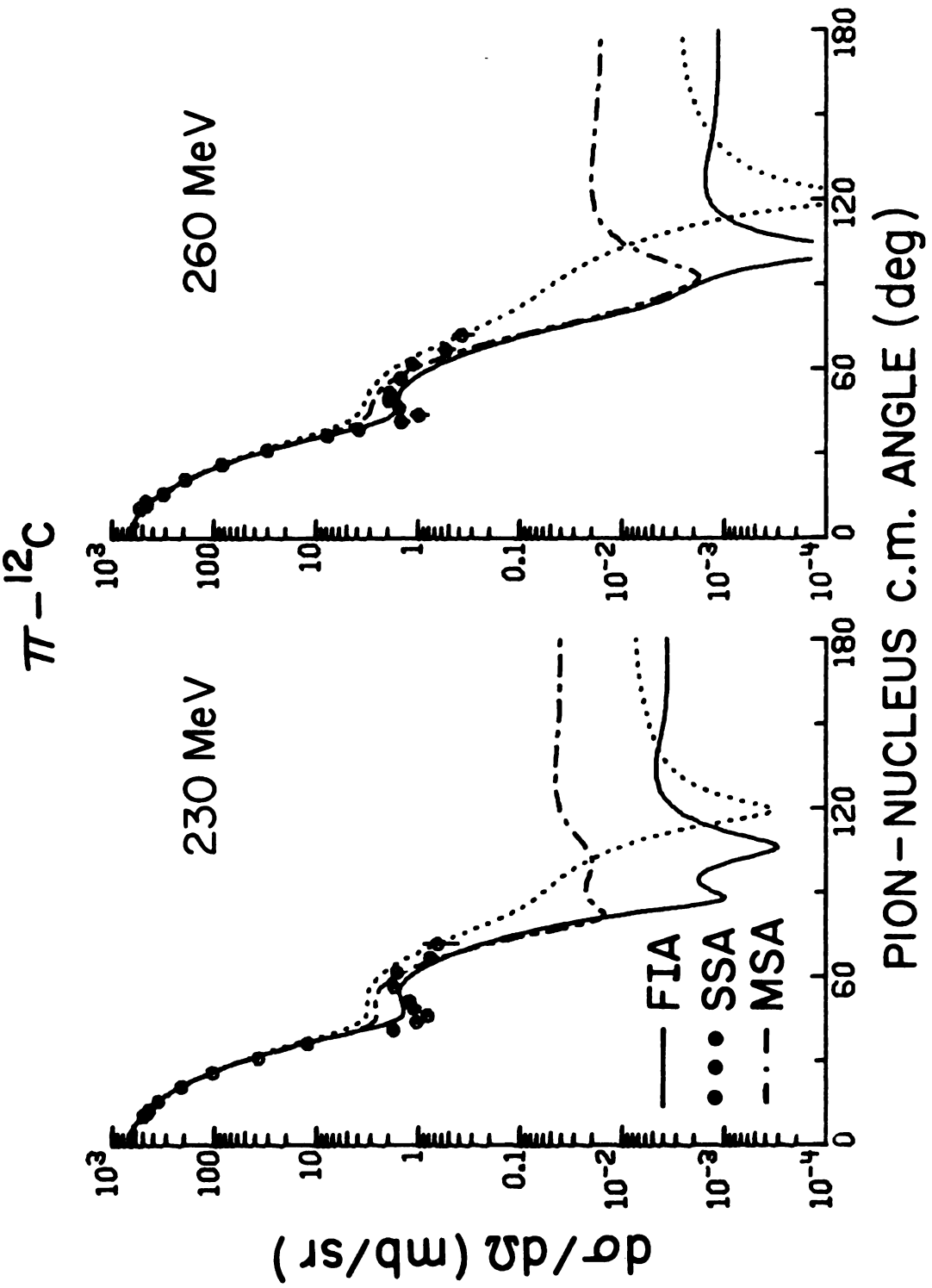

FIGURE 10.7--As in Figure 10.5.

FIGURE 10.8--As in

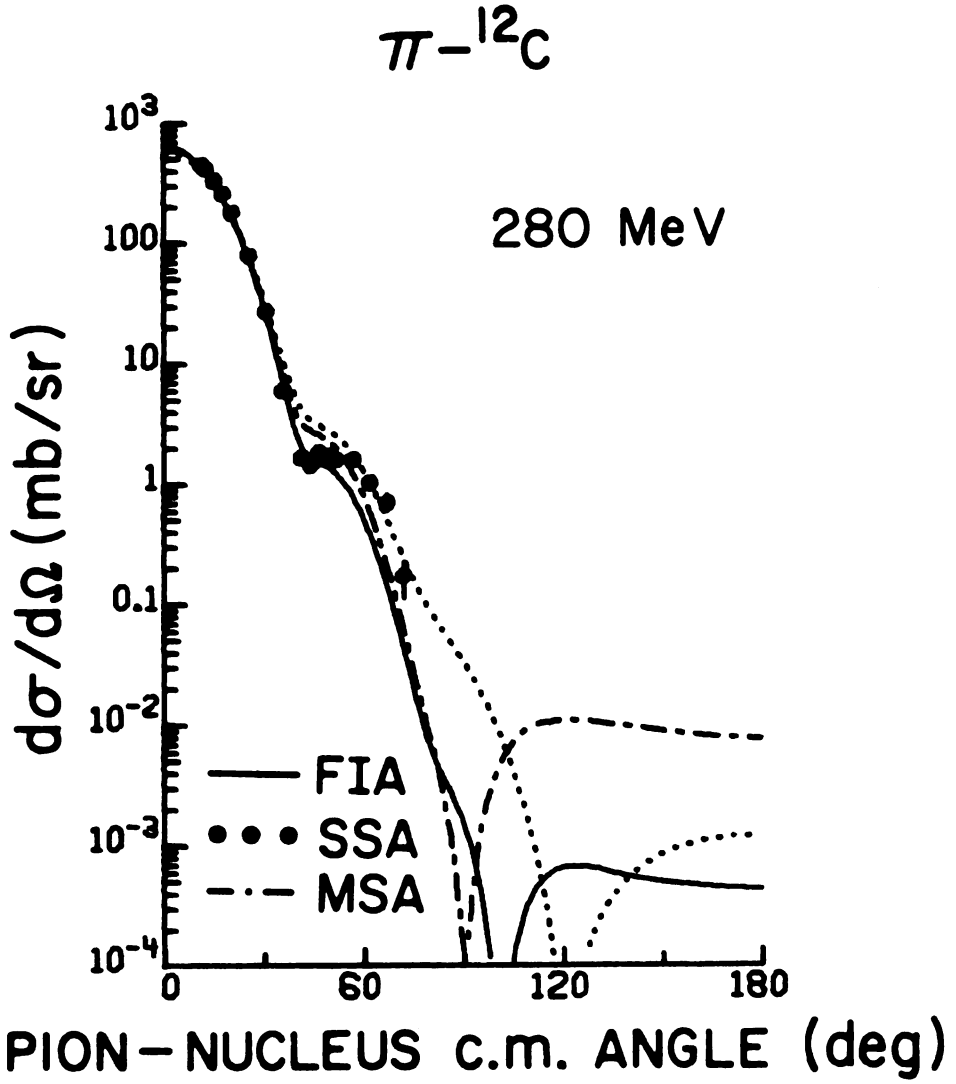

FIGURE 10.8--As in Figure 10.5.

c. Compa
(MSA)
the F

not as
the gr
depend
rather
sparse
to rea
model

the M
minima
whole
parab
diffe
some
too h

the F
At le
first
FIA a
conti
havi
shoul
has d
bette

c. Comparison of the Modified Static Approximation (MSA) and Simple Static Approximation (SSA) to the Fully-Integrated Impulse Approximation (FIA):

For ^{12}C the differences in the models are not as clear-cut as in ^{4}He. As already mentioned, the gross shape of the ^{12}C cross section does not depend much on the details of the model. A rather model-independent shape, together with sparse backward angle data, makes it difficult to reach any definite conclusions as to which model is to be preferred.

Except for the 260 and 280 MeV results, the MSA does not fit the ^{12}C data near the first minima and maxima as well as the FIA. On the whole, the MSA fit at backward angles is comparable to the FIA even though the MSA and FIA differ by as much as an order of magnitude at some energies. The MSA is generally as much too high at backward angles as the FIA is too low.

At 120 MeV the SSA is actually better than the FIA and at 150 MeV the fit is comparable. At 180 and 200 MeV the SSA is too large at the first minima and maxima, but is as good as the FIA at backward angles. Beyond 200 MeV the SSA continues to be too large at the first minimum having only a "shoulder" where the first minimum should be. However, at 280 MeV the FIA fit has degenerated to the point that it is no better than the SSA.

Although we cannot clearly distinguish between the FIA, SSA, and MSA on the basis of the ^{12}C, it is evident that the calculated ^{12}C cross sections are still somewhat dependent on the model, even though the general shape of $d\sigma/d\Omega$ is the same for all the models. For example, the depth and position of the second minima is quite sensitive to the model and at backward angles the differences in the different models are quite large. In ^{12}C, as in ^{4}He, the unphysical values of $\cos\theta_{\pi N}$ in the MSA show up rather dramatically in the large angle cross section. Moreover, the difference between the FIA and SSA at higher energies and backward angles is even greater in ^{12}C than in ^{4}He.

d. The Quadratic Approximation and the Kujawski-Miller-Landau (KML) Approximation in ^{12}C:

The quadratic approximation (discussed in Chapter VII) is compared to the fully-integrated impulse approximation (FIA) in Figures 10.9 - 10.12. The quadratic approximation obviously provides an excellent approximation to the FIA, although there are a few small differences at backward angles at some energies.

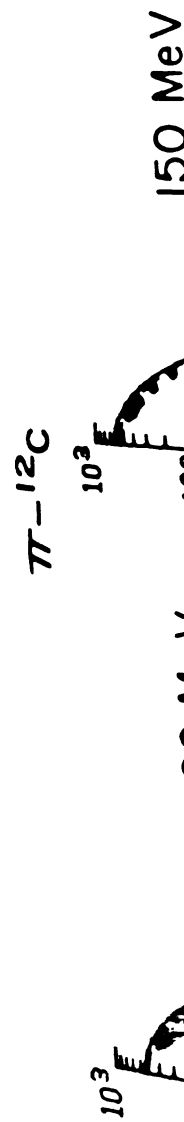

FIGURE 10.9--The elastic $\pi^- - {}^{12}C$ differential cross sections calculated by two methods: (a) (solid line) the fully-integrated impulse result (FIA); (b) (dashed line) the quadratic approximation (QA) to case (a). The energies shown are the laboratory kinetic energy of the pion.

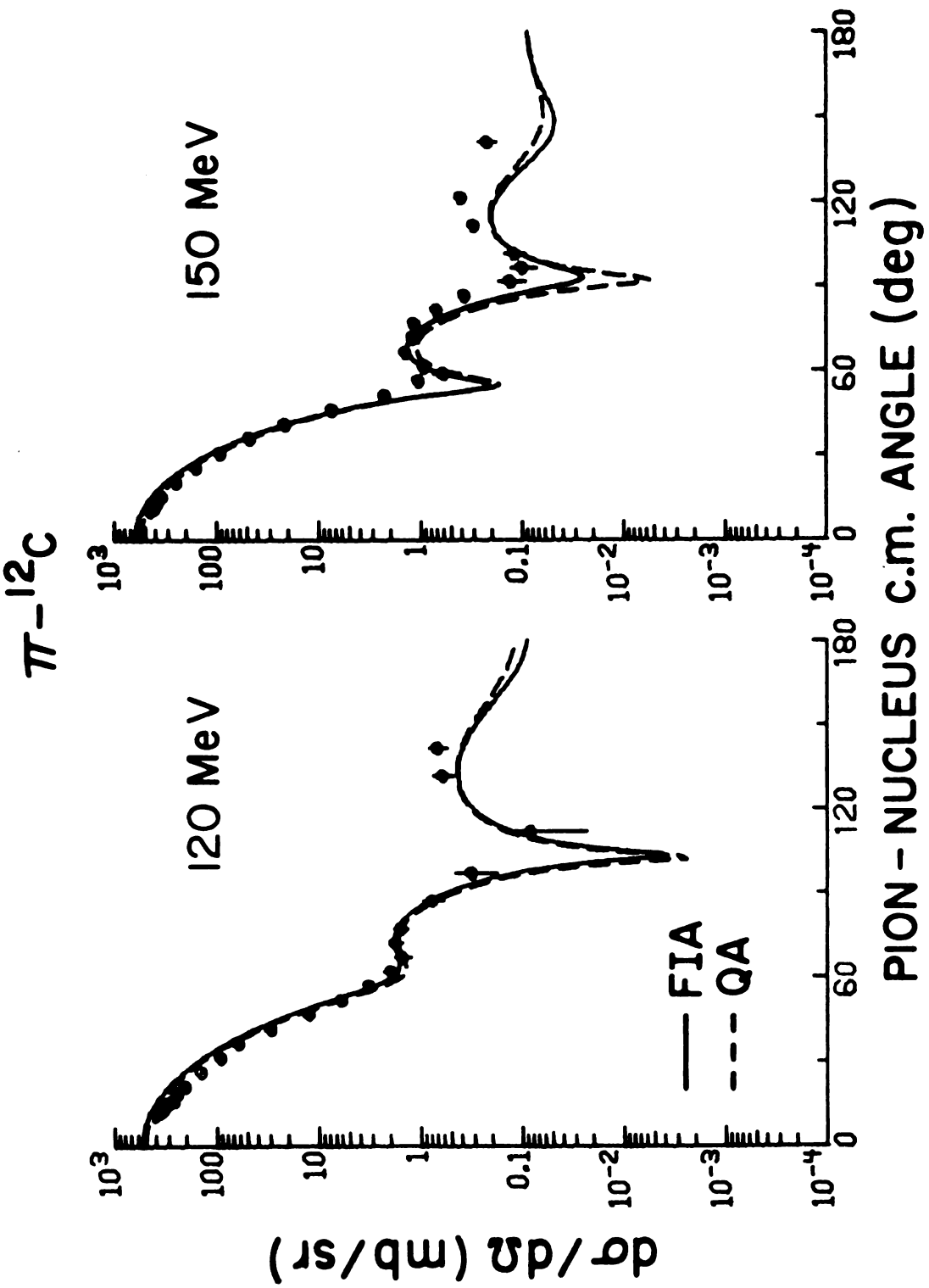
π−12C
150 MeV
120 MeV
FIA
QA
dσ/dΩ (mb/sr)
PION–NUCLEUS c.m. ANGLE (deg)
10^3
100
10
1
0.1
10^-2
10^-3
10^-4
0
60
120
180

FIGURE 10.9

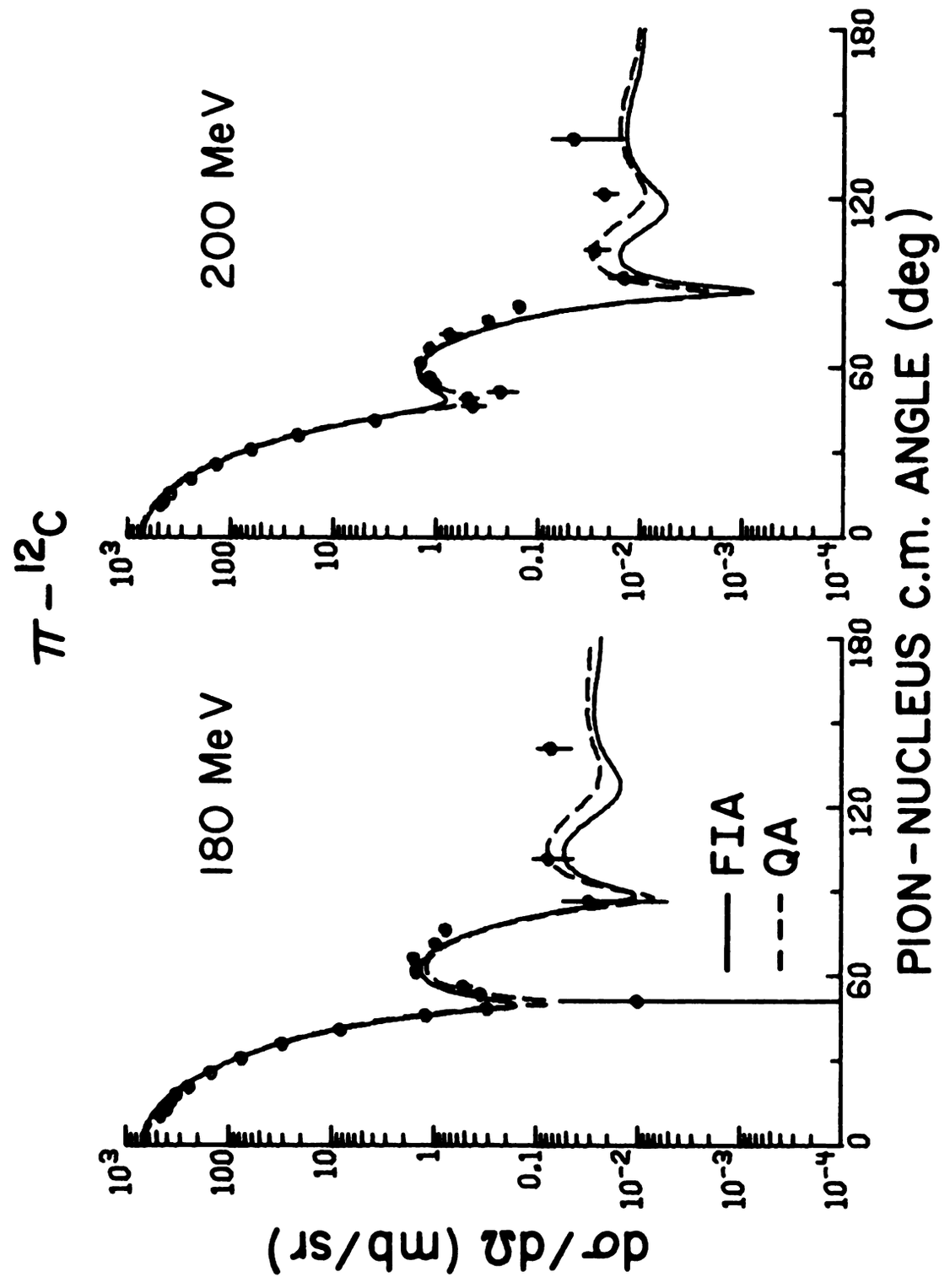

FIGURE 10.10--As in Figure 10.9.

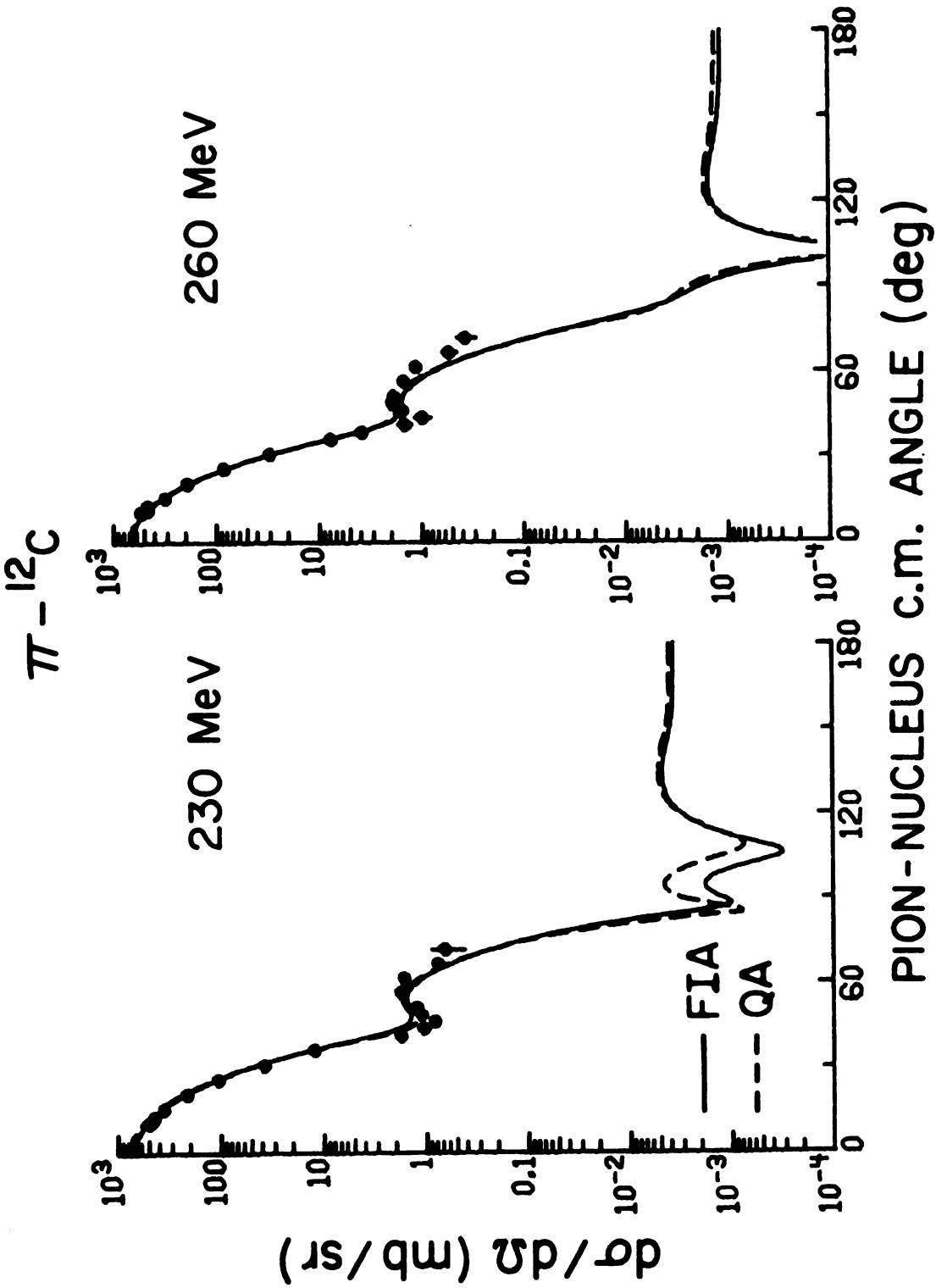

FIGURE 10.11--As in Figure 10.9.

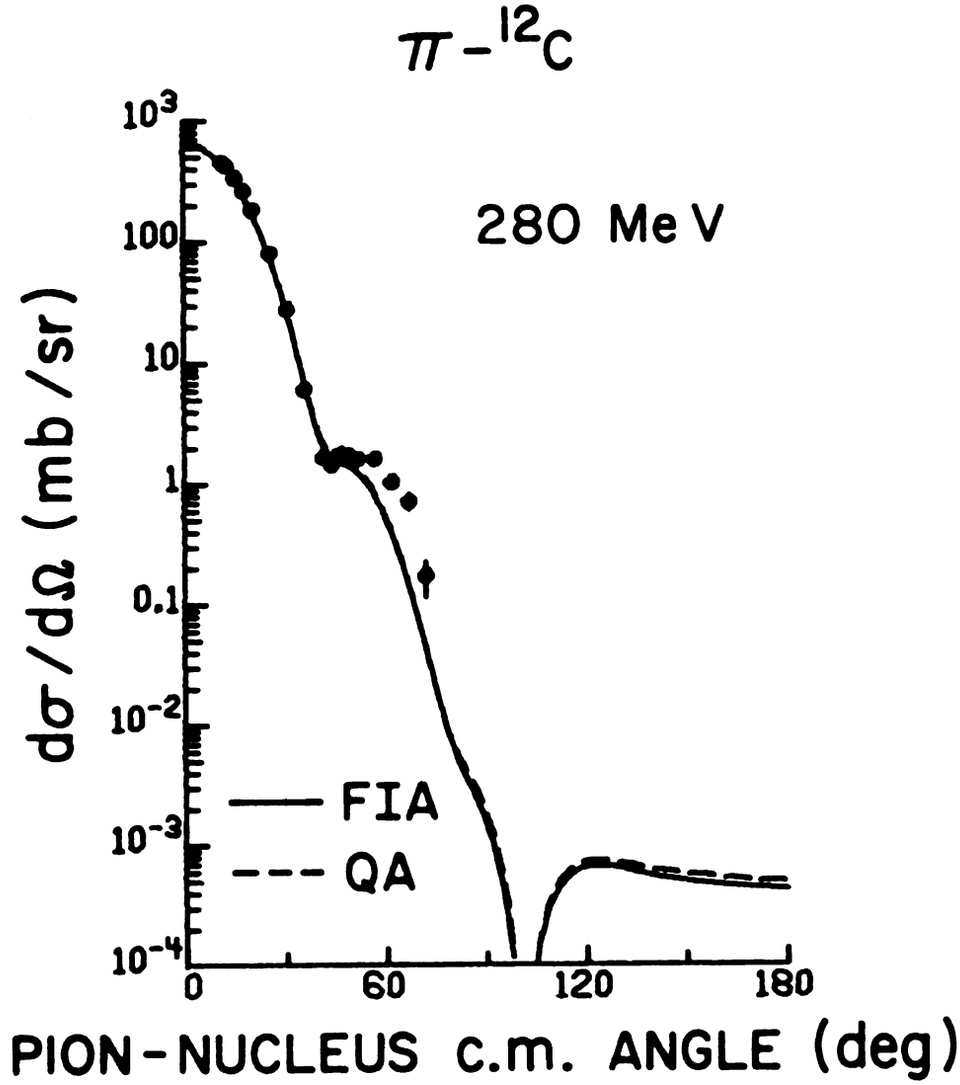

FIGURE 10.12--As in Figure 10.9.

FIGURE 10.13--The elastic π^- -^{12}C differential cross sections calculated by two methods: (a) (solid line) the fully-integrated impulse result (FIA); (b) (dashed line) the Kujawski-Miller-Landau (KML) approximation. The energies shown are the laboratory kinetic energy of the pion.

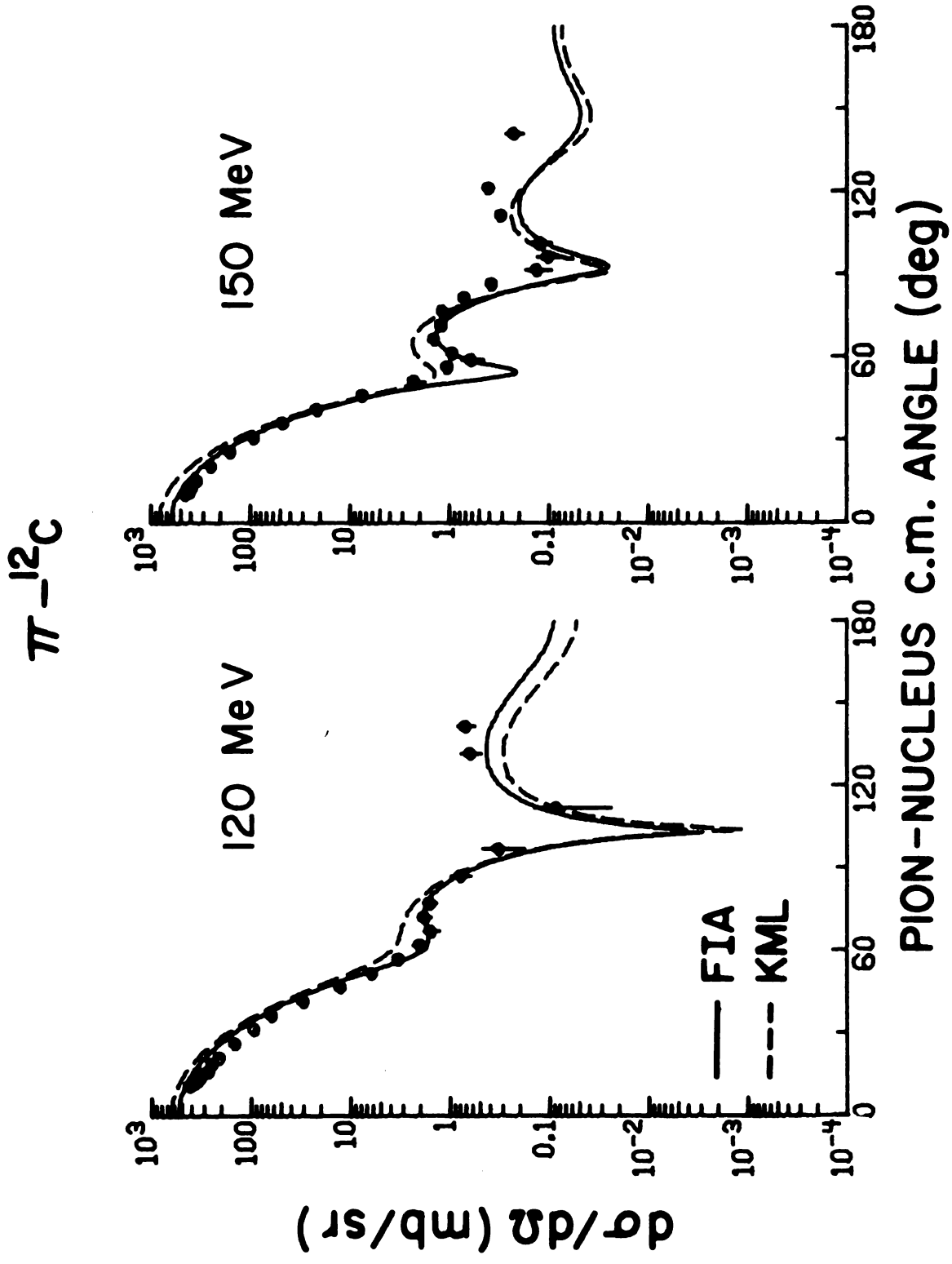
π⁻ ¹²C
150 MeV
120 MeV
FIA
KML
dσ/dΩ (mb/sr)
PION-NUCLEUS c.m. ANGLE (deg)
10³
100
10
1
0.1
10⁻²
10⁻³
10⁻⁴
0
60
120
180

FIGURE 10.13

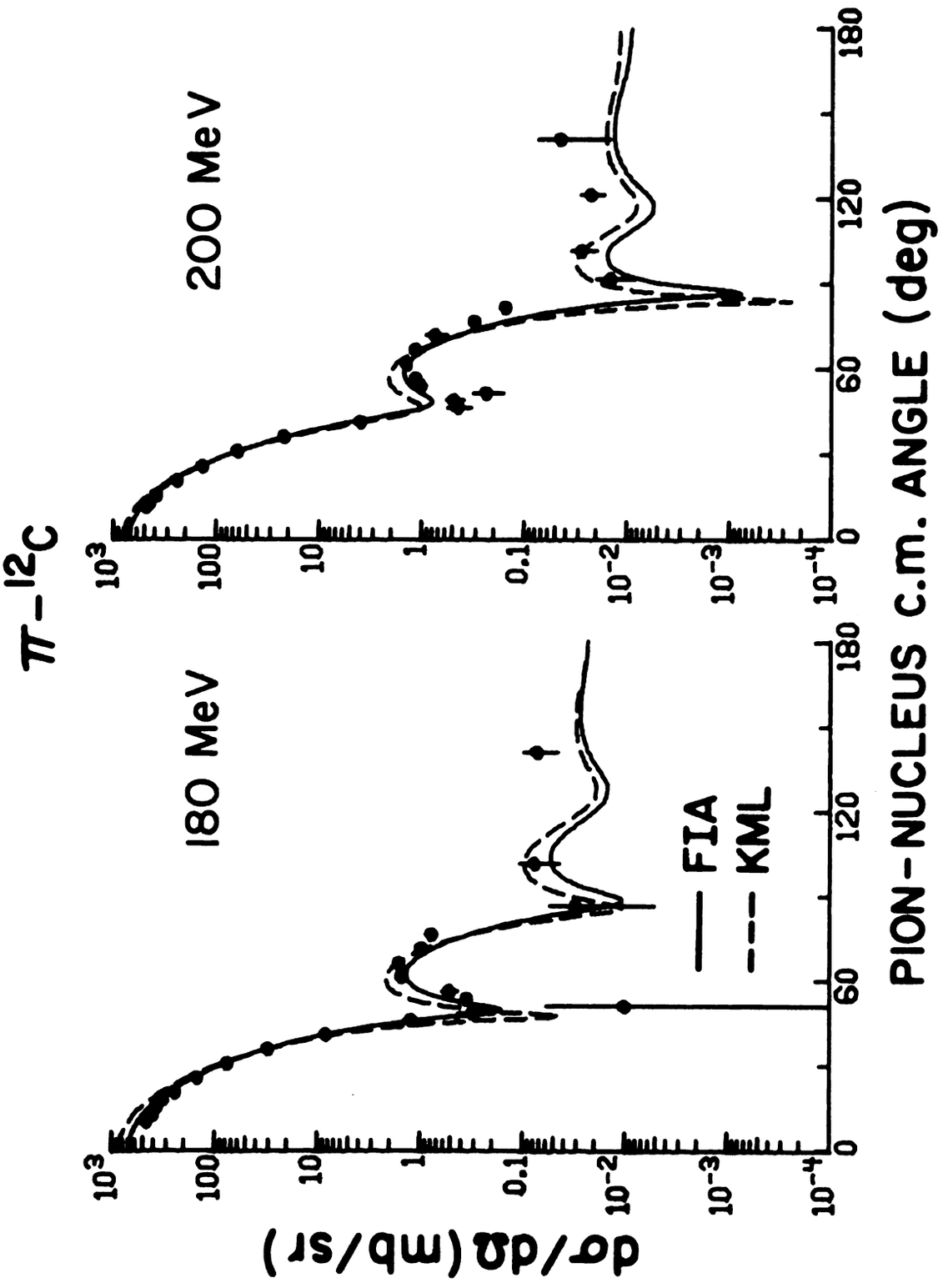

FIGURE 10.14--As in Figure 10.13.

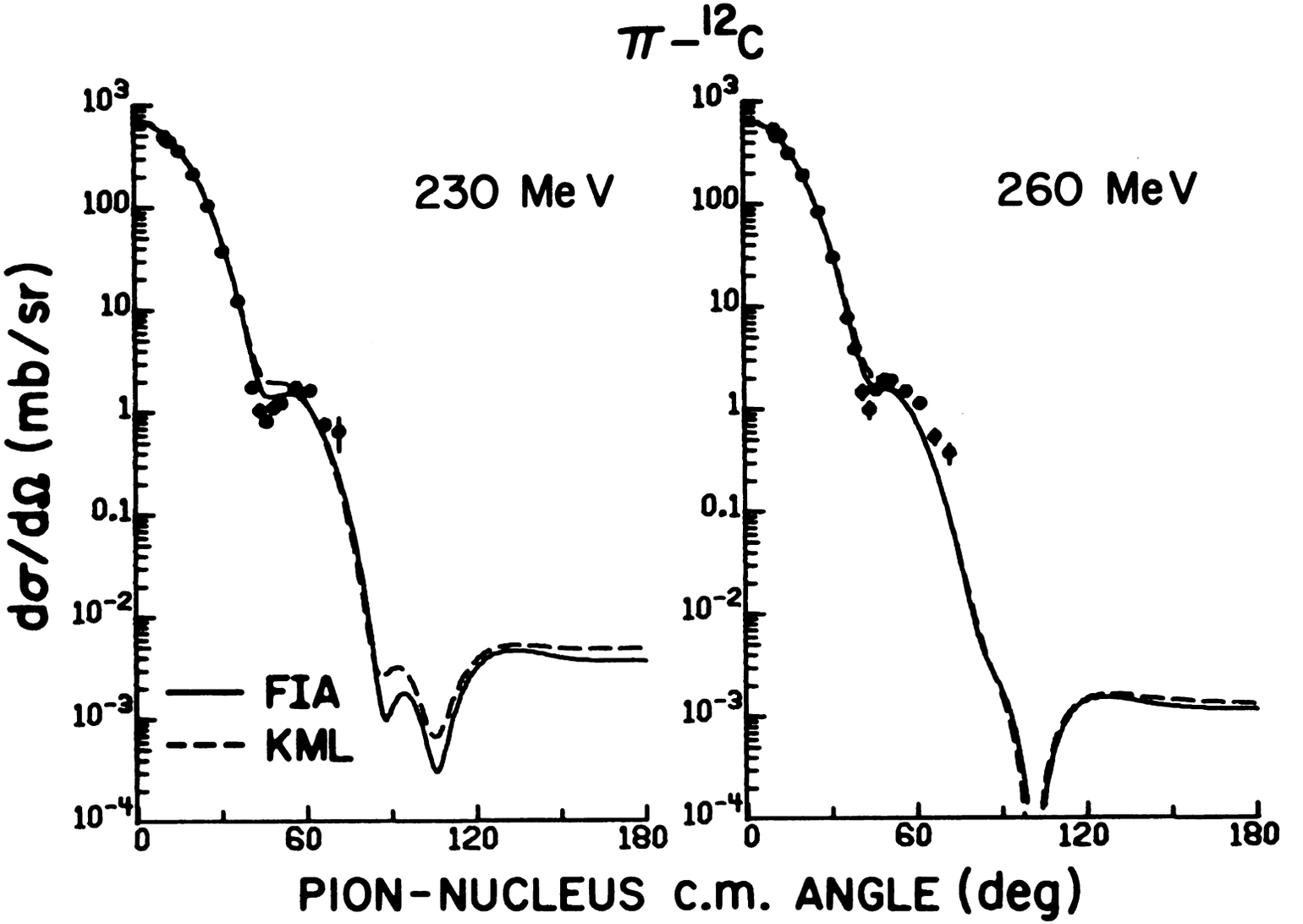

FIGURE 10.15--As in Figure 10.13.

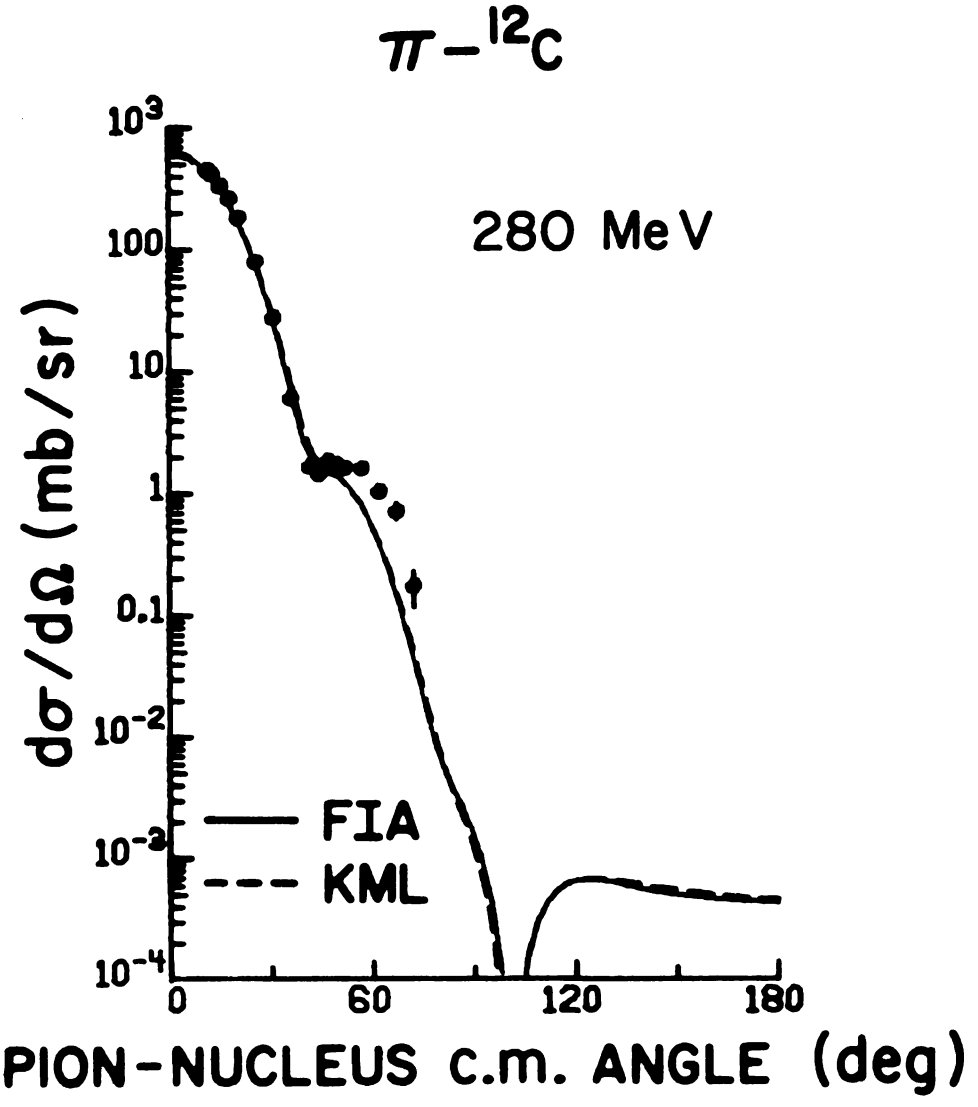

FIGURE 10.16--As in Figure 10.13.

The KML approximation for ^{12}C is shown in Figures 10.13 - 10.16. At lower energies, the KML approximation is not as close to the FIA as is the quadratic approximation because of the neglect of collision energy effects in the KML model. At higher energies, where angle transformation effects dominate, the KML model is just as good as the quadratic model.

4. Impulse-plus-Binding Correction Results for ^{12}C

In Figures 10.17 - 10.20, we show the ^{12}C results obtained using the single state approximation for binding (SSAB) along with the closure approximation for binding (CAB).

In ^{4}He, the SSAB gave noticeably improved agreement with experiment, but in ^{12}C the SSAB leaves the (fairly good) FIA result essentially unchanged.

In ^{12}C, the CAB causes some rather drastic changes in the cross section. The largest effect occurs at 150 MeV where the CAB result at $\theta \approx 0^{\circ}$ is too low by a factor of 3. Even at 280 MeV, where the CAB binding correction is smallest, the CAB result underestimates the first maximum by a factor of 3 or 4. In ^{12}C, as in ^{4}He, the CAB model evidently gives much too large an effect.

5. Impulse Approximation Results for ^{16}O

The results for ^{16}O using the fully-integrated impulse approximation (FIA), simple static approximation (SSA), and modified static approximation (MSA) are shown in Figures 10.21 - 10.23.

FIGURE 10.17--The elastic $\pi^- - {}^{12}C$ differential cross sections resulting from three different effective pion-nucleon interactions: (a) (solid line) the fully-integrated impulse result (FIA); (b) (short dash line) the single state approximation for binding effects (SSAB); (c) (dot-dash line) the closure limit for binding effects (CAB). The energies shown are the laboratory kinetic energy of the pion.

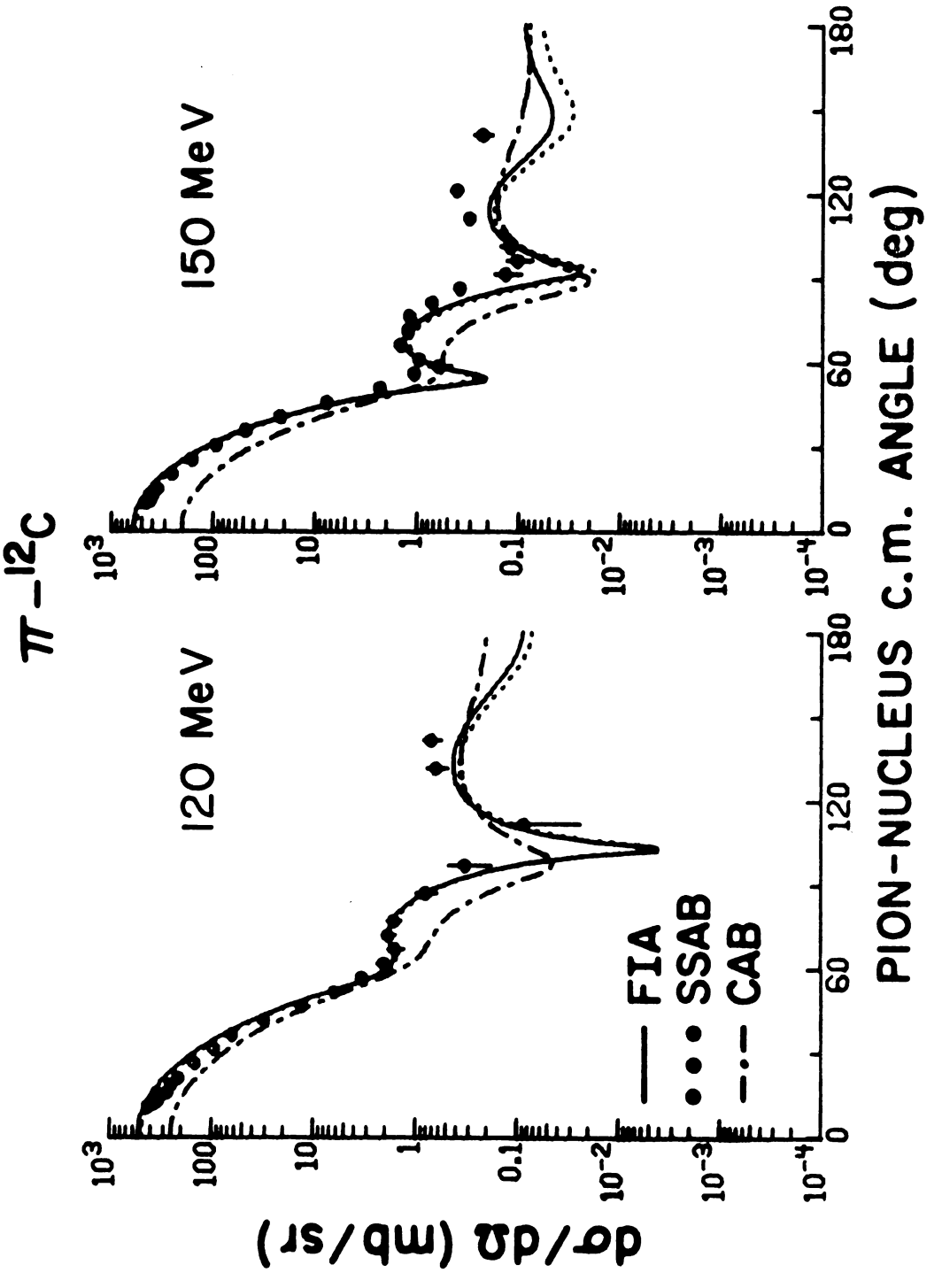
π⁻ ¹²C
120 MeV
150 MeV
dσ/dΩ (mb/sr)
PION-NUCLEUS c.m. ANGLE (deg)
FIA
SSAB
CAB
10³
100
10
1
0.1
10⁻²
10⁻³
10⁻⁴
0
60
120
180

FIGURE 10.17

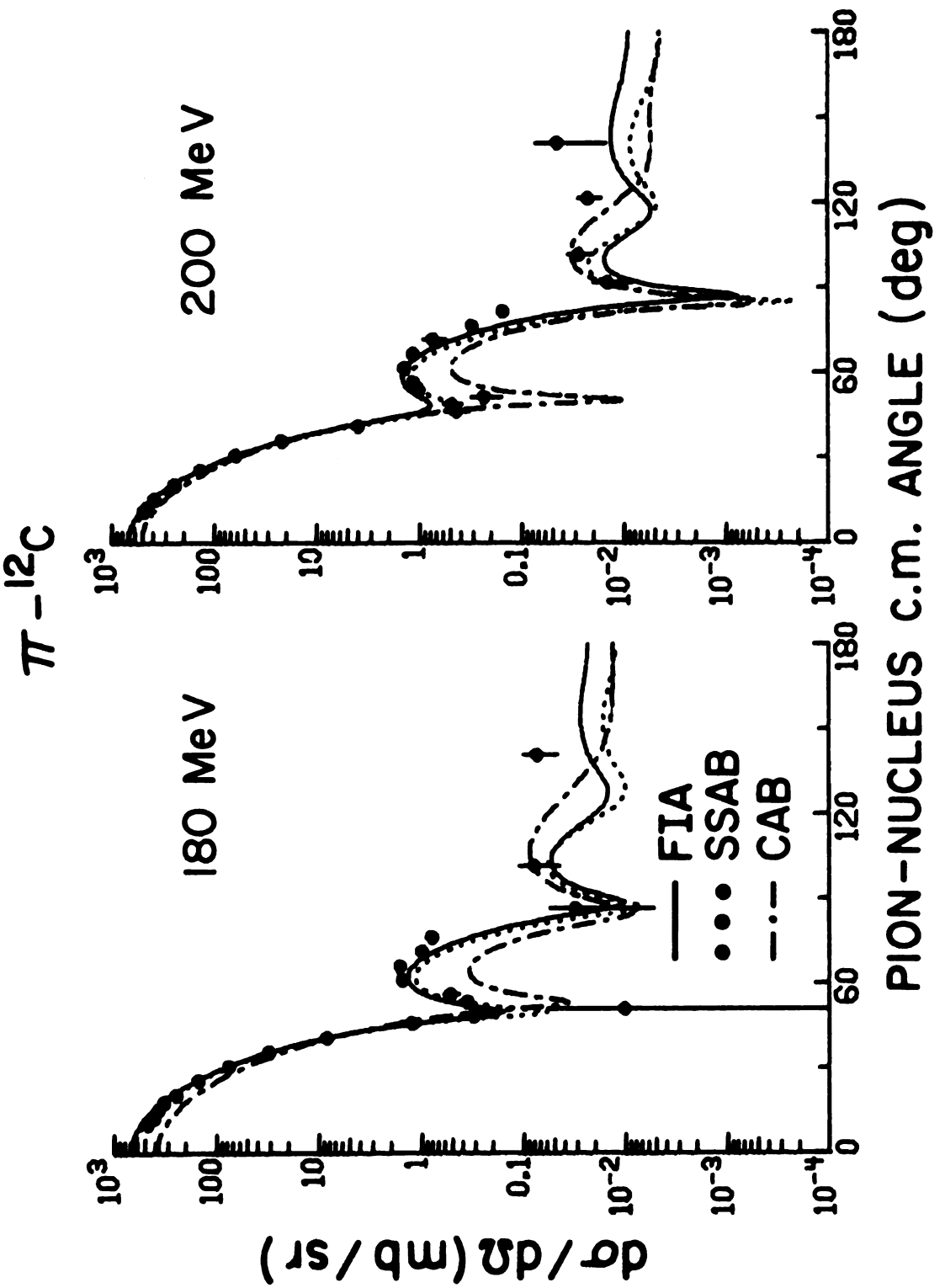

FIGURE 10.18--As in Figure 10.17.

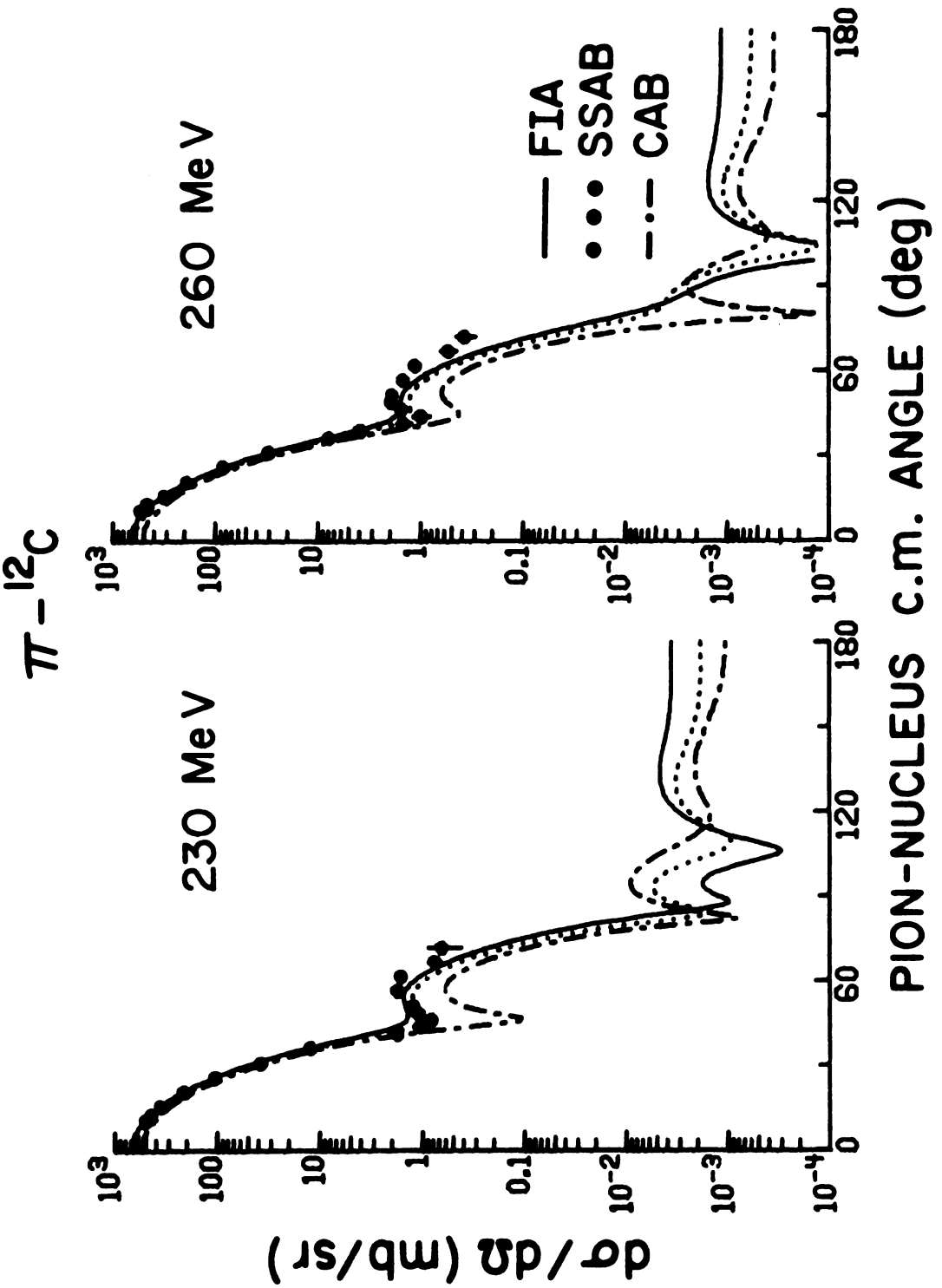

FIGURE 10.19--As in Figure 10.17.

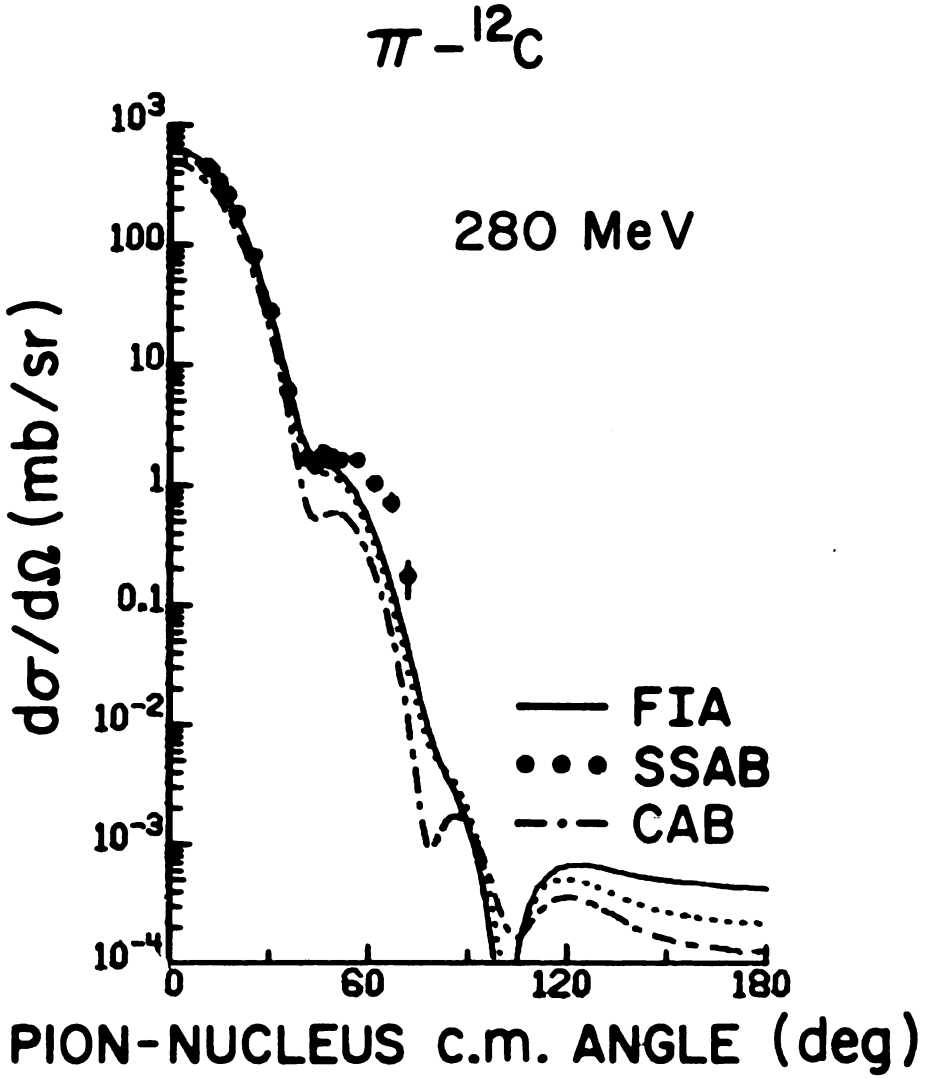

FIGURE 10.20--As in Figure 10.17.

The quadratic approximation is shown in Figures 10.24 - 10.26, and the Kujawski-Miller-Landau (KML) approximation is shown in Figures 10.27 - 10.29.

a. The Fully-Integrated Impulse Approximation (FIA) Results for ^{16}O:

In ^{16}O, as in ^{12}C, the FIA gives a good description of the data. Although the FIA cross sections are quite similar in ^{16}O and ^{12}C, there is one interesting difference. In ^{12}C the FIA generally was too low starting at about 60° or 70° and got worse toward larger angles. The ^{16}O results do not show the same tendency to underestimate the data. Since ^{16}O is a spherical nucleus, these results lend some support to the suggestion of Lee and McManus (Lee71) that the backward angle discrepancy in ^{12}C is a result of ground state deformation effects. However, since the ^{16}O data only extends to about 75°, definite conclusions on this point must await further large angle data.

b. Comparison of the MSA and SSA to the FIA for ^{16}O:

The FIA gives a somewhat better account of the region around the first minimum in ^{16}O than the SSA or MSA. This feature is the same as in ^{12}C, although in ^{16}O there seems to be less dependence on the model. At 230 MeV, for example,

FIGURE 10.21--The elastic $\pi^- - {}^{16}O$ differential cross sections resulting from three different effective pion-nucleon impulse interactions: (a) (solid line) the fully-integrated impulse result (FIA); (b) (short dash line) the simple static approximation (SSA); (c) (dot-dash line) the modified static approximation (MSA). The energies shown are the laboratory kinetic energy of the pion.

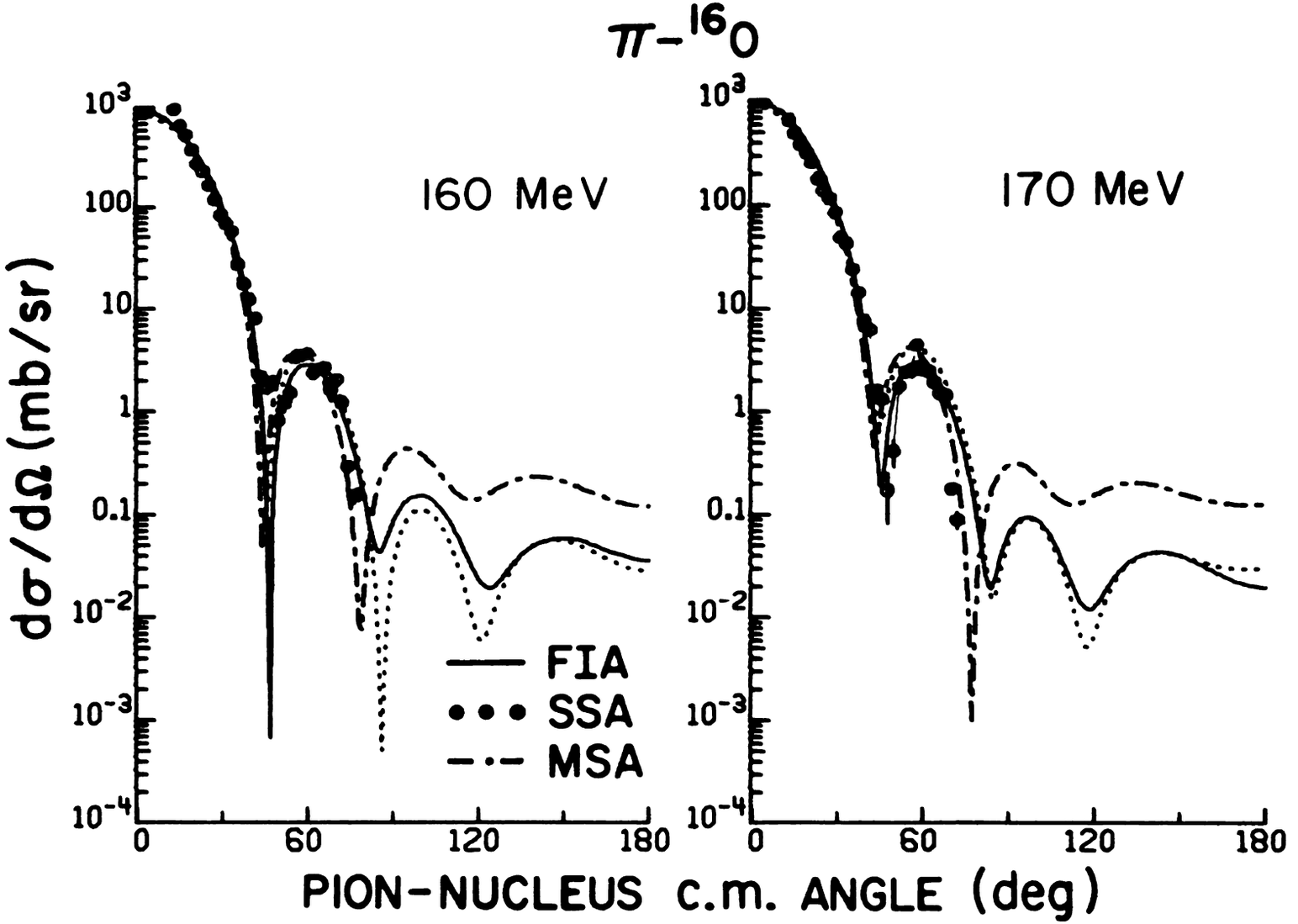
π-16O
160 MeV
170 MeV
dσ/dΩ (mb/sr)
FIA
SSA
MSA
PION-NUCLEUS c.m. ANGLE (deg)

FIGURE 10.21

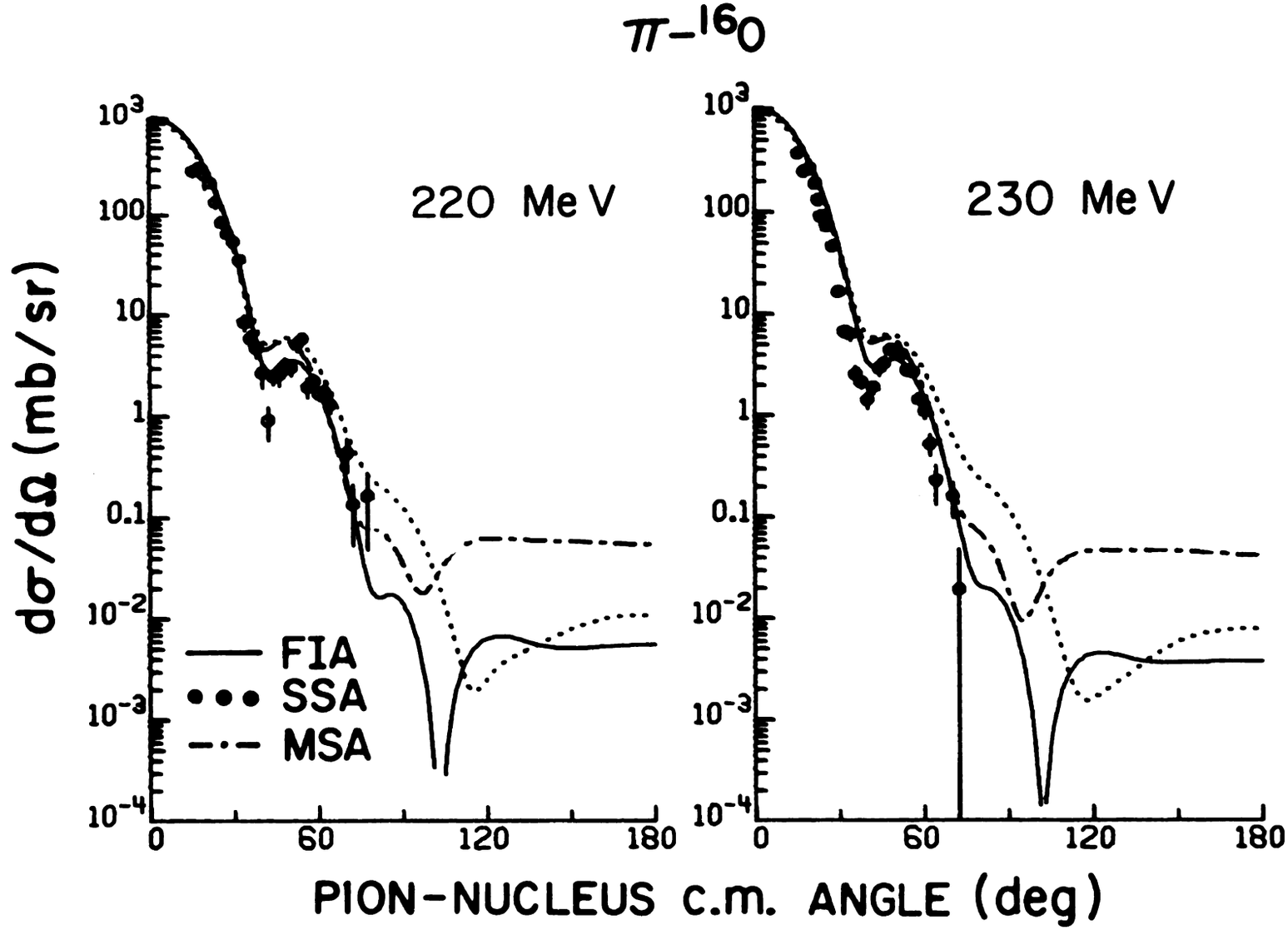

FIGURE 10.22--As in Figure 10.21.

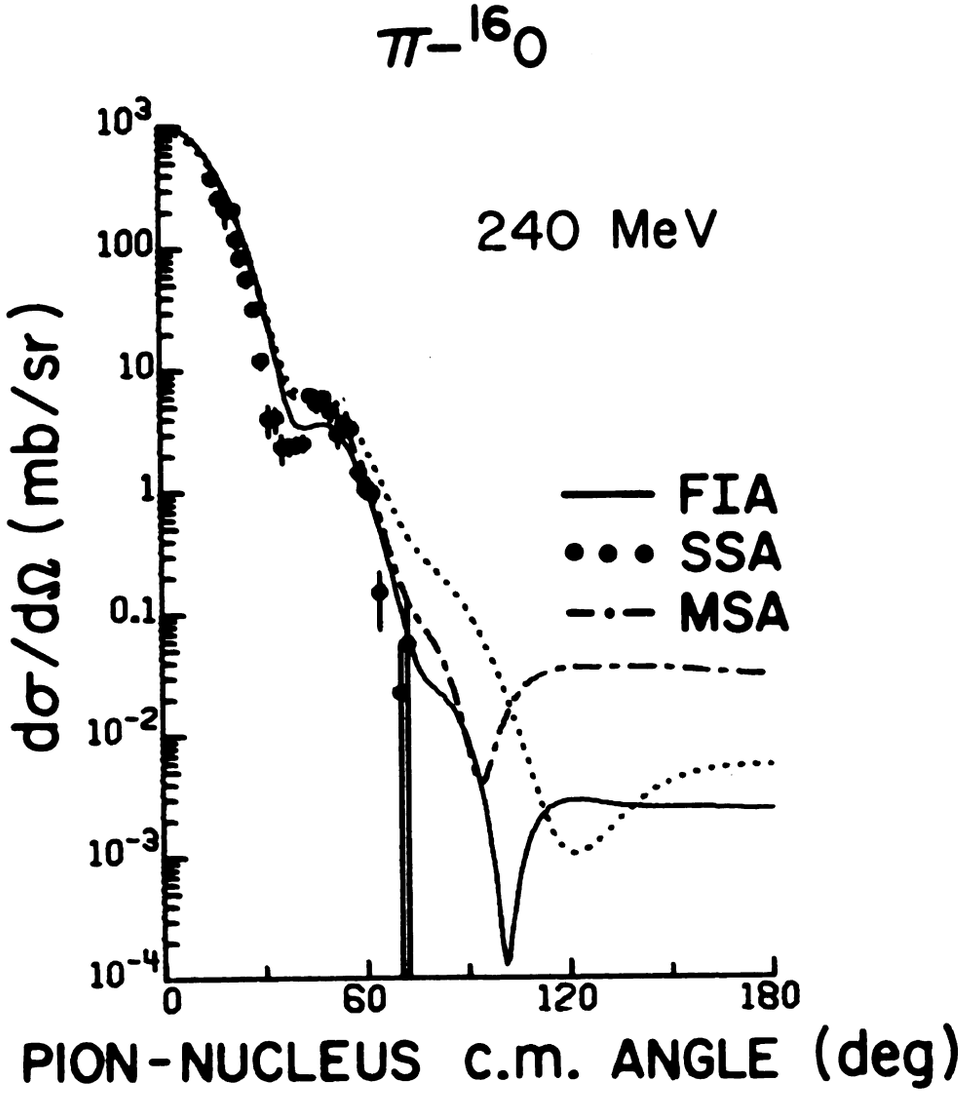

FIGURE 10.23--As in Figure 10.21.

FIGURE 10.24--The elastic $\pi^- - {}^{16}O$ differential cross sections calculated by two methods: (a) (solid line) the fully-integrated impulse result (FIA); (b) (dashed line) the quadratic approximation (QA) to case (a). The energies shown are the laboratory kinetic energy of the pion.

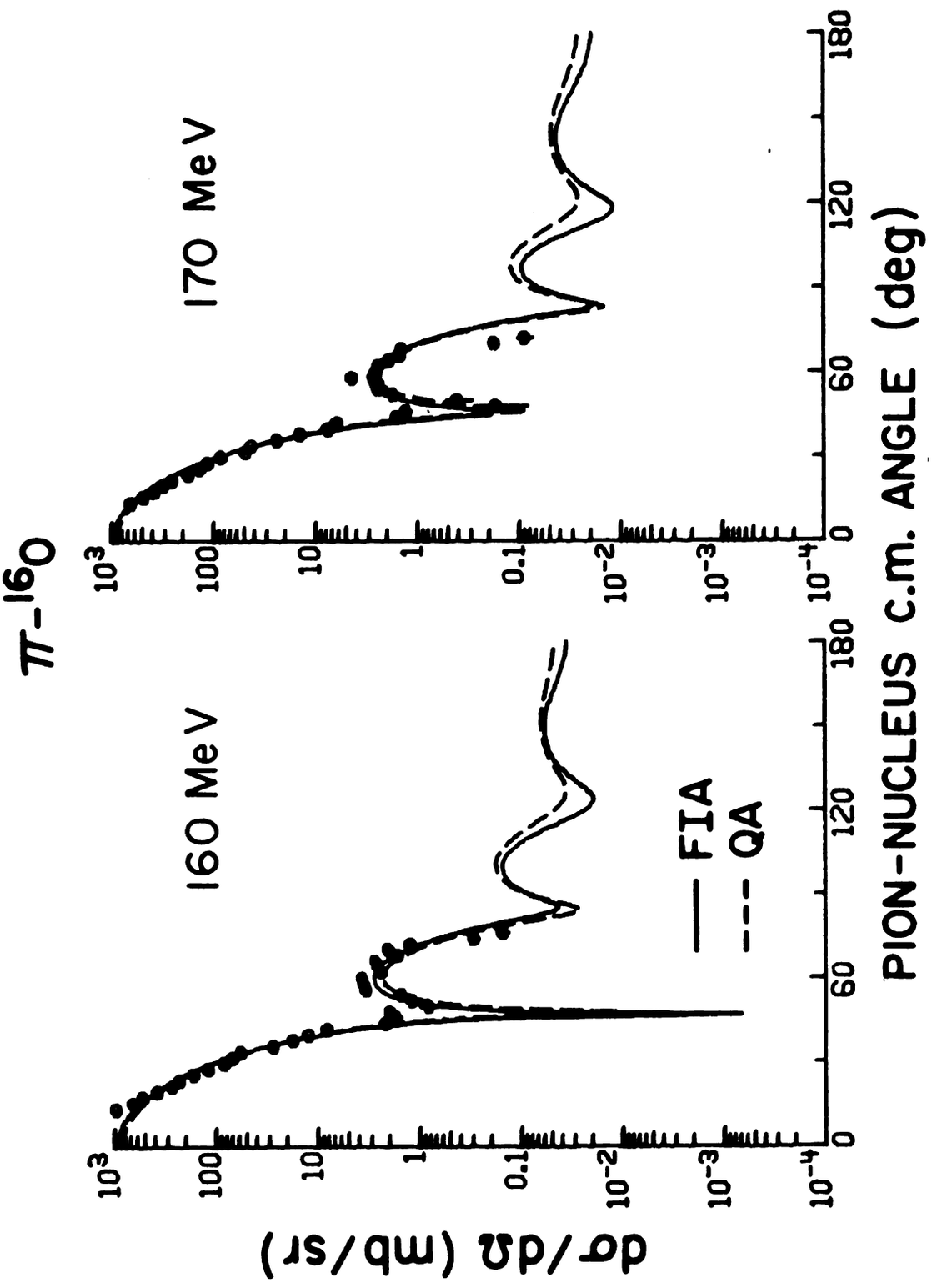
π⁻-¹⁶O
160 MeV
170 MeV
FIA
QA
dσ/dΩ (mb/sr)
PION-NUCLEUS c.m. ANGLE (deg)
10³
100
10
1
0.1
10⁻²
10⁻³
10⁻⁴
0
60
120
180

FIGURE 10.24

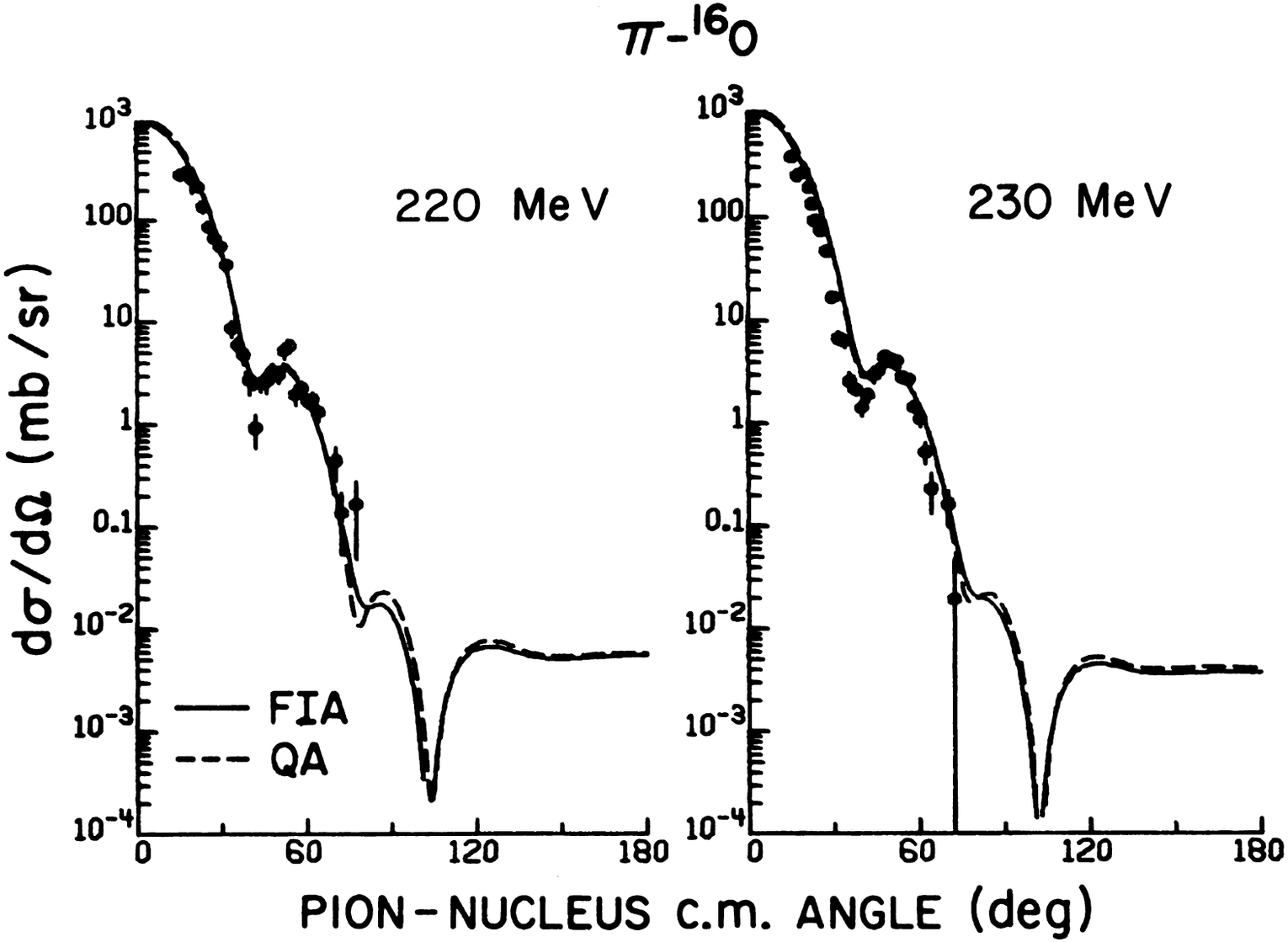

FIGURE 10.25--As in Figure 10.24.

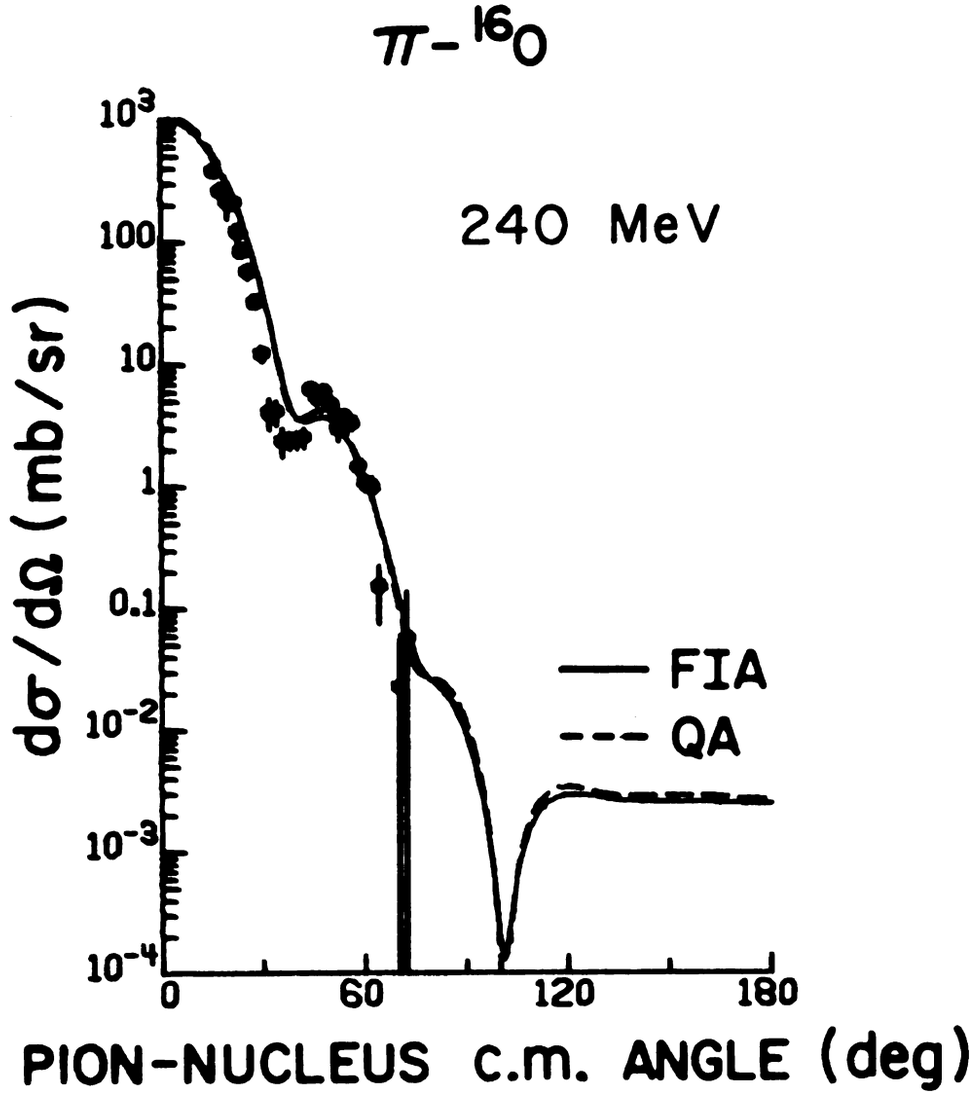

FIGURE 10.26--As in Figure 10.24.

FIGURE 10.27--The elastic π^--^{16}O differential cross sections calculated by two methods: (a) (solid line) the fully integrated impulse result (FIA); (b) (dashed line) the Kujawski—Miller-Landau (KML) approximation. The energies shown are the laboratory kinetic energy of the pion.

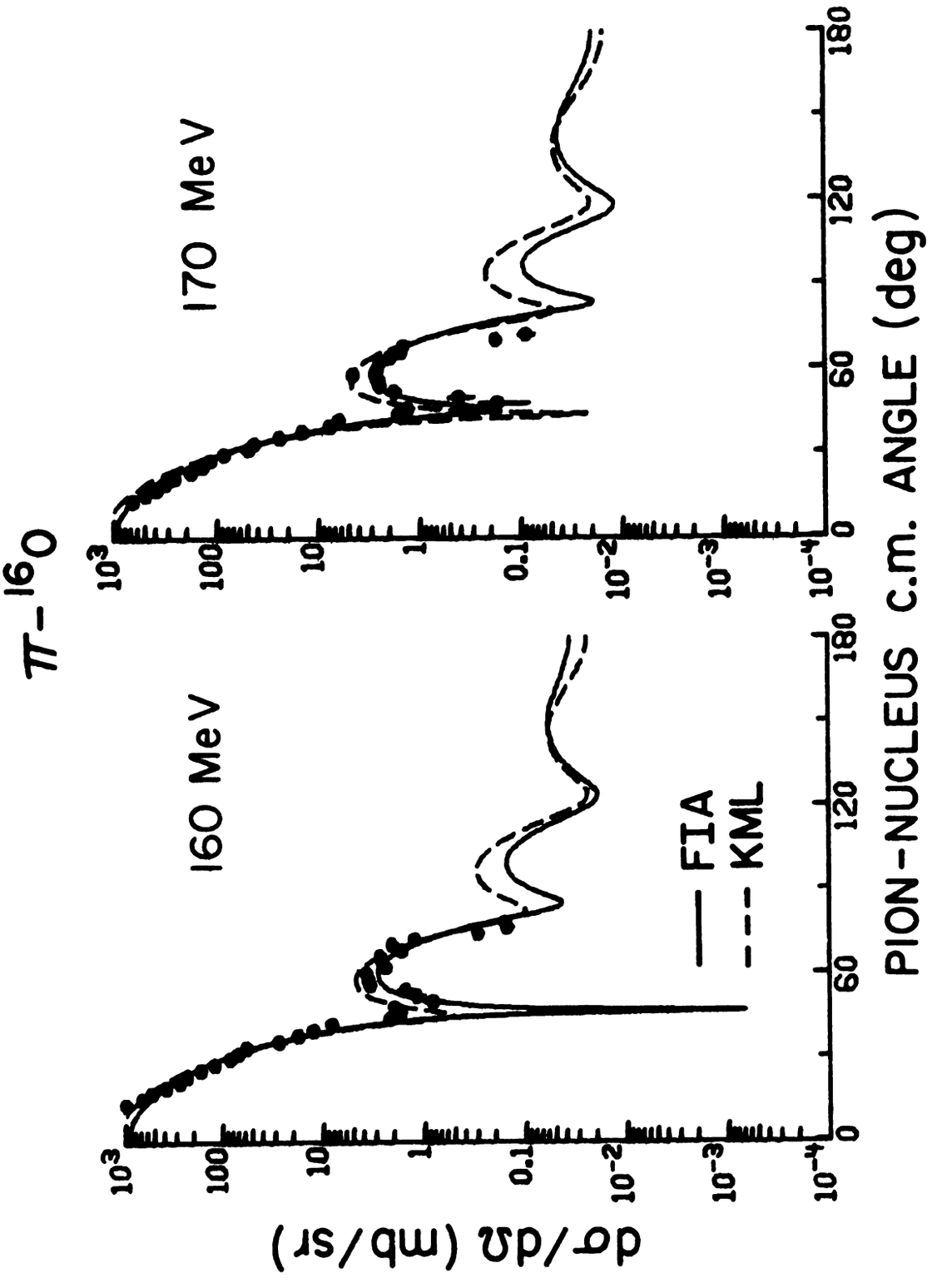
π−16O
170 MeV
160 MeV
FIA
KML
dσ/dΩ (mb/sr)
PION-NUCLEUS c.m. ANGLE (deg)
10^3
100
10
1
0.1
10^-2
10^-3
10^-4
0
60
120
180

FIGURE 10.27

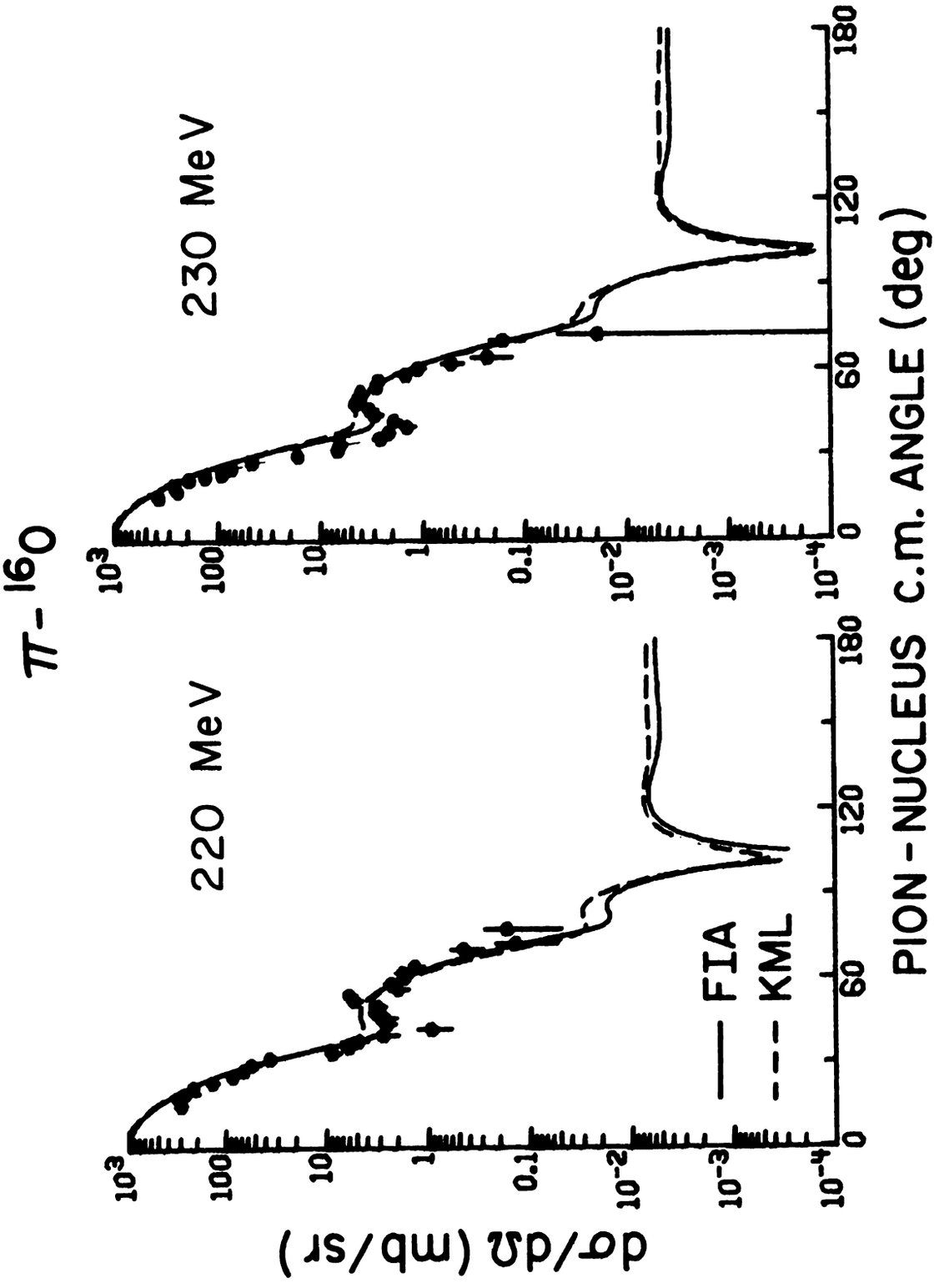

FIGURE 10.28--As in Figure 10.27.

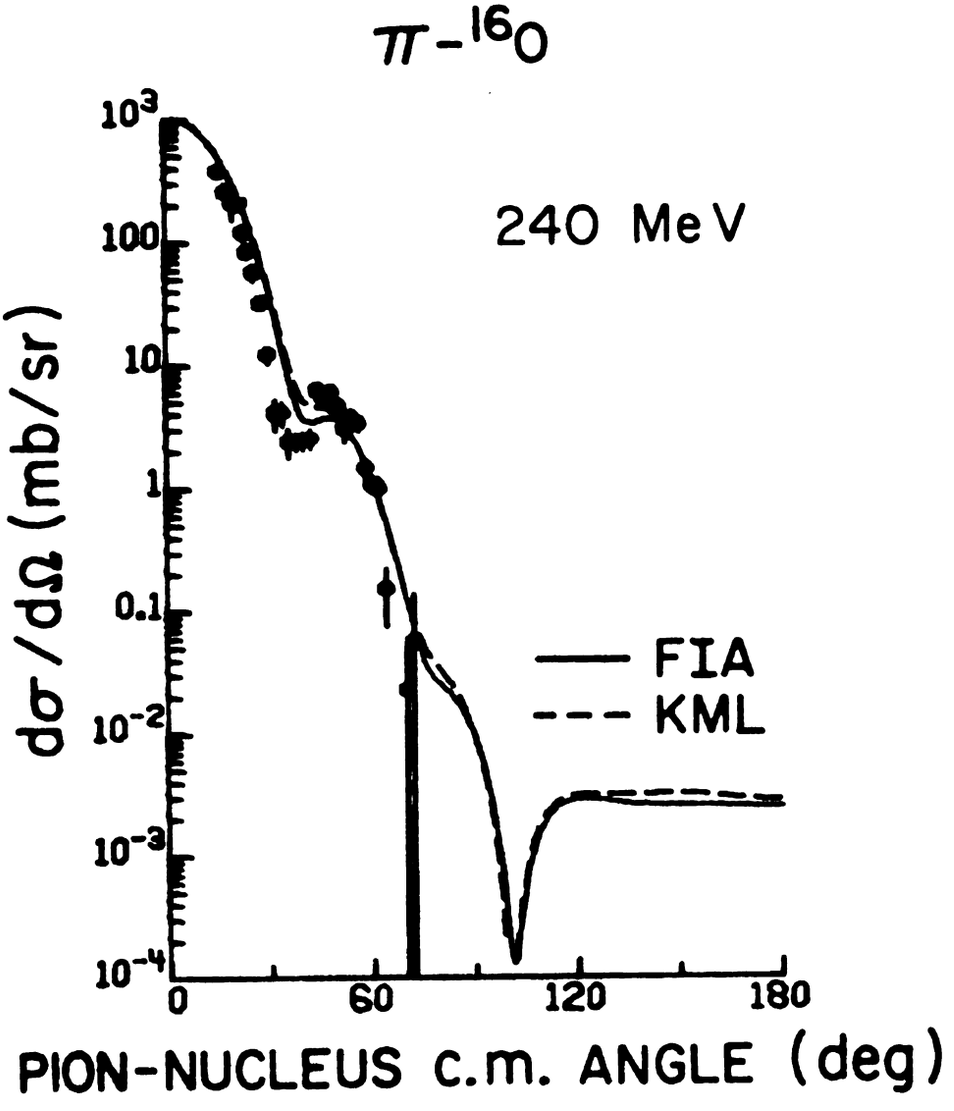

FIGURE 10.29--As in Figure 10.27.

a comparison of the results near the first minimum shows the models in noticeably closer agreement in ^{16}O than in ^{12}C. The backward angle results, however, are just as sensitive to the details of the models.

c. The Quadratic Approximation and the Kujawski-Miller-Landau (KML) Approximation in ^{16}O:

The quadratic approximation gives an accurate representation of the FIA in ^{16}O just as in ^{4}He and ^{12}C. There are again some small differences at backward angles.

The ^{16}O results for the KML approximation are also similar to the KML results in ^{12}C. At lower energies the neglect of collision energy effects causes some significant differences between the KML approximation and the FIA. However, at higher energies the differences are quite small.

6. Impulse-plus-Binding Correction Results for ^{16}O

The ^{16}O results for the single state approximation for binding (SSAB) and closure approximation for binding (CAB) are shown in Figures 10.30 - 10.32.

In ^{16}O the small change in $d\sigma/d\Omega$ given by the SSAB is entirely compatible with the data. (In ^{12}C the SSAB worsened the fit by a small amount.) The SSAB is hence compatible with the experimental results for all the nuclei we have studied.

FIGURE 10.30--The elastic $\pi^- - {}^{16}O$ differential cross sections resulting from three different effective pion-nucleon interactions: (a) (solid line) the fully-integrated impulse result (FIA); (b) (short dash line) the single state approximation for binding effects (SSAB); (c) (dot-dash line) the closure limit for binding effects (CAB). The energies shown are the laboratory kinetic energy of the pion.

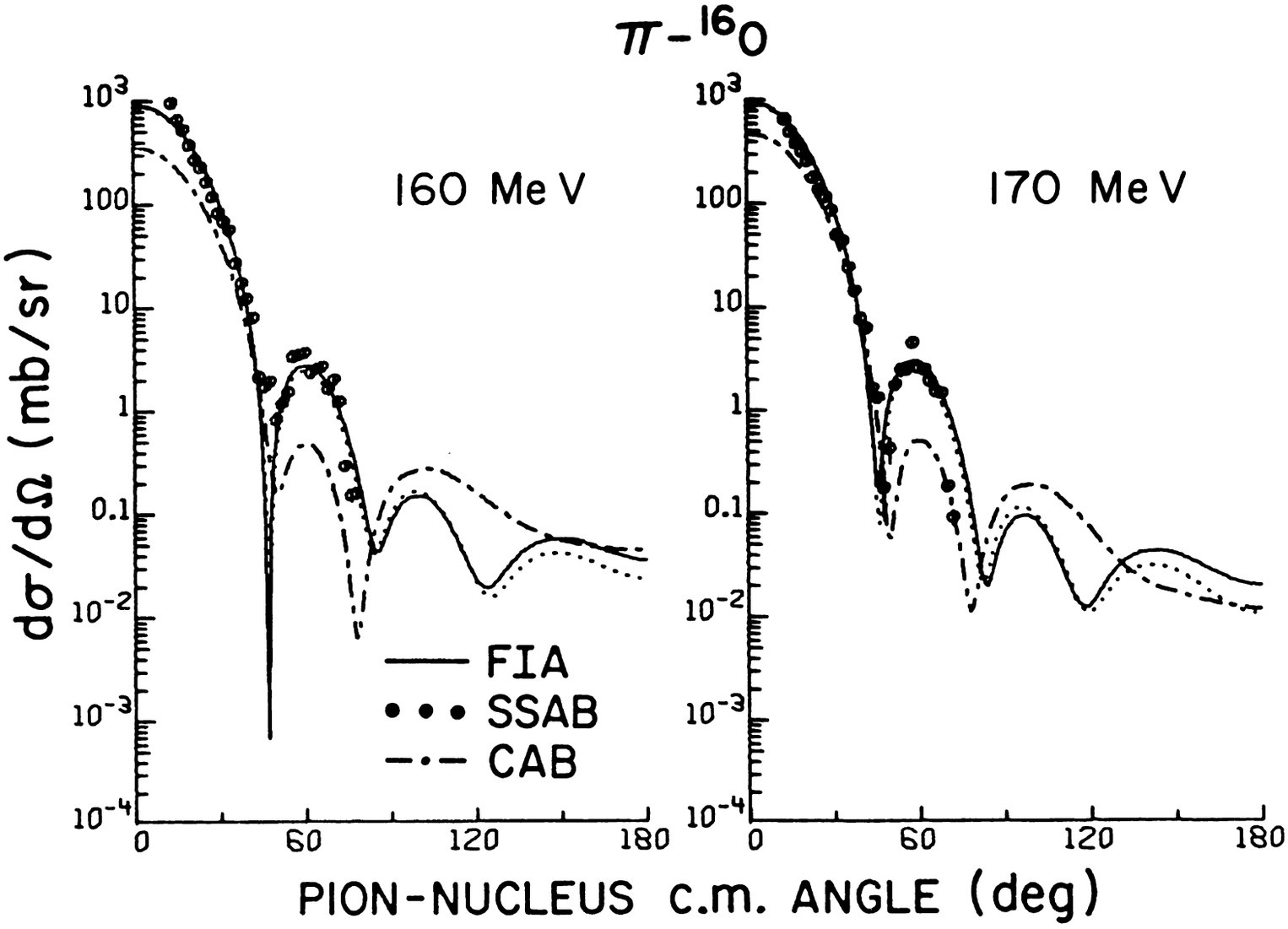
π-16O
160 MeV
170 MeV
dσ/dΩ (mb/sr)
FIA
SSAB
CAB
PION-NUCLEUS c.m. ANGLE (deg)

FIGURE 10.30

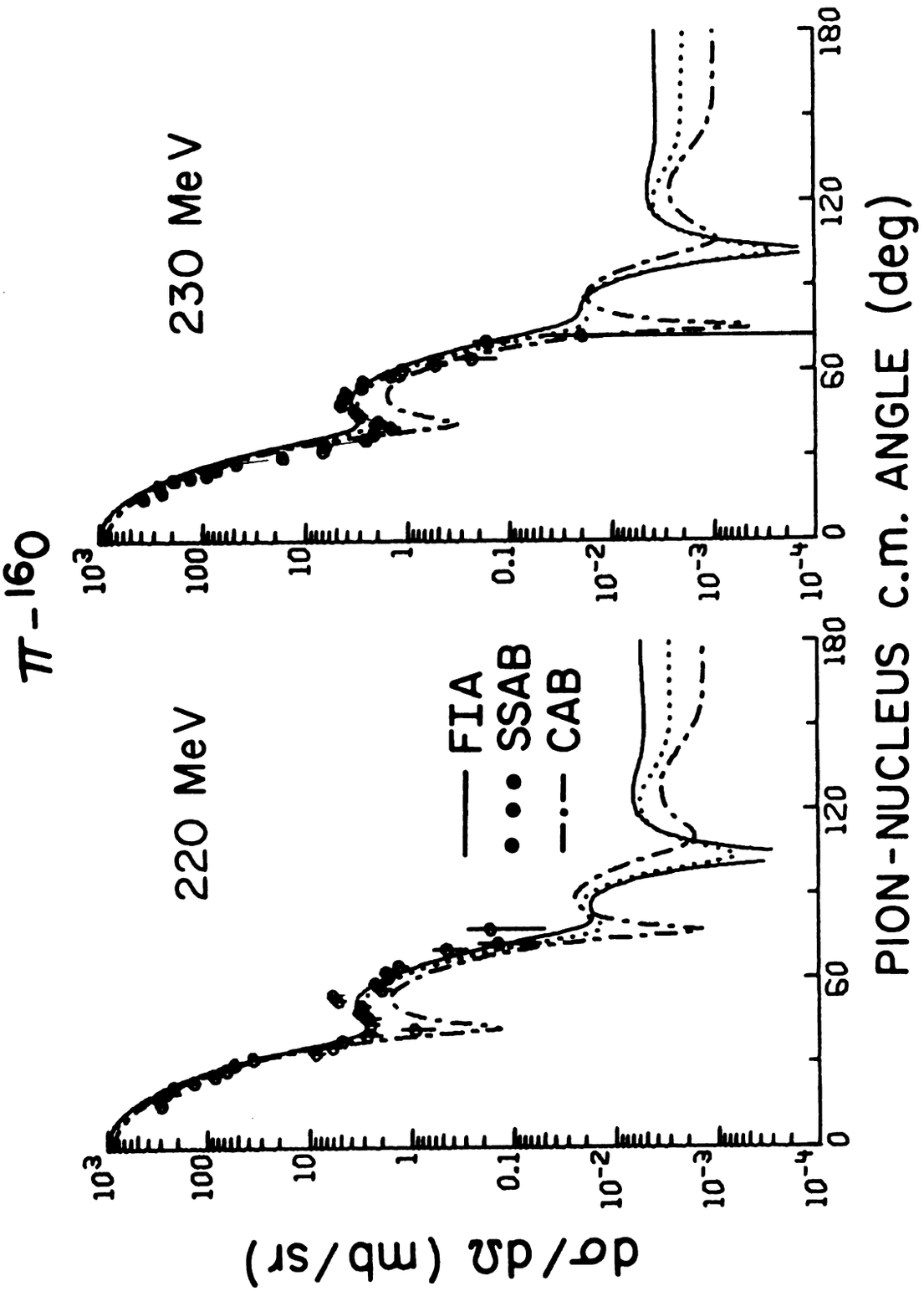

FIGURE 10.31--As in Figure 10.30.

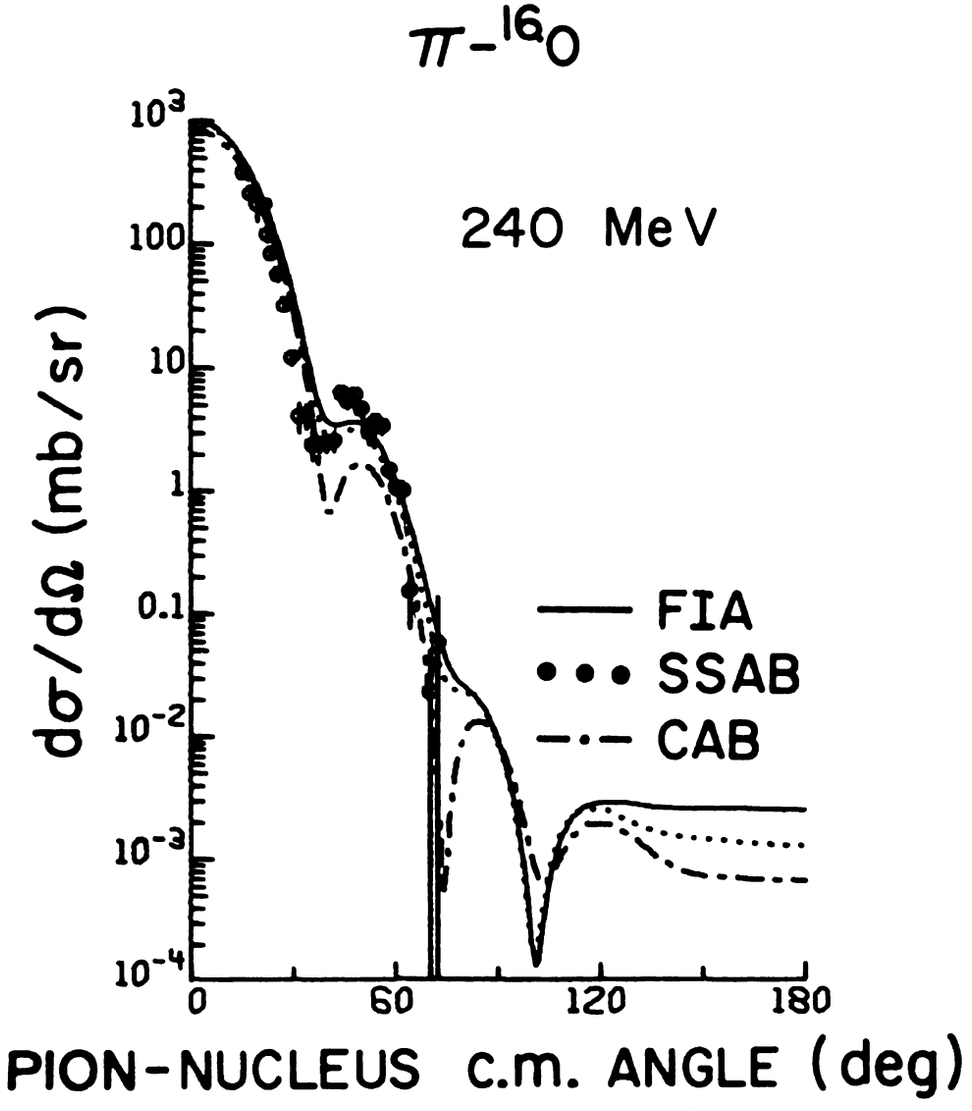

FIGURE 10.32--As in Figure 10.30.

The CAB results for ^{16}O are the same as in ^{12}C; the CAB overestimates the binding correction by a considerable amount.

CHAPTER XI

SUMMARY AND CONCLUSIONS

We have studied elastic scattering of pions from ^{4}He, ^{12}C and ^{16}O in the 100-300 MeV region. We began our study by calculating an optical potential for ^{4}He which was based on the impulse approximation and a harmonic oscillator shell model. The integration over the nucleon momenta was carried out exactly. We defined an effective pion-nucleon impulse interaction as the fully-integrated π^{-}-^{4}He optical potential divided by the associated harmonic oscillator form factor. Because we calculated the scattering in momentum space, it was not necessary to put the effective interaction or the associated optical potential into a coordinate space form.

We next studied three ad hoc models for the effective impulse interaction, two of which gave poor agreement with the fully-integrated version. The third ad hoc model, which took into account nucleon recoil, gave much better agreement with the fully-integrated results, although there were still serious discrepancies.

By systematically approximating the integrals over the nucleon momenta, we developed our own simple but accurate approximation to the fully-integrated impulse interaction. Our systematic approximation provided some insight into the effects of nucleon motion in the effective impulse interaction.

We found that the optical potentials based on the fully-integrated impulse approximation (FIA), or its equivalent, gave a satisfactory account of the data for ^{4}He, ^{12}C and ^{16}O. The ad hoc models which were not good approximations to the FIA (such as the modified static approximation) gave poor agreement with the ^{4}He data. No definite conclusions could be reached for ^{12}C and ^{16}O due to the lack of sufficient backward angle data.

On the basis of the ^{4}He results, and on theoretical grounds, we conclude that it is important to accurately approximate the integrals over the nucleon momenta. We further conclude that an accurate approximation can be made by evaluating the free pion-nucleon t-matrix at certain "effective" values of the pion-nucleon C.M. momenta and energy. The prescription we give in the "quadratic" approximation (Chapter VII) provides an accurate representation of the fully-integrated impulse interaction and is as easy to use in momentum-space calculations as any of the conventional ad hoc models.

Corrections to the impulse approximation (which we call "binding" corrections) were studied using a 3-body model where the pion scatters from a single target nucleon which is bound in a potential well. Using a separable s-wave binding potential, we exactly calculated the first correction to the impulse approximation and found it to be relatively small. A simple approximation (called the single state approximation) was developed which gave fairly good agreement with the exact result. In order to estimate an upper limit on binding corrections, the single state approximation was

extended to include an infinite number of bound states. This extended approximation, (called the closure approximation) was found to give a binding correction which is approximately twice as large as in the single state approximation. We found for ^{4}He that the single state approximation gave noticeable improvement but that the closure approximation (which was not intended to be physically realistic) made the agreement with experiment somewhat worse. For ^{12}C and ^{16}O, the single state approximation was essentially the same as the impulse approximation, but the closure approximation overestimated the binding correction by a large amount. We thus found the ^{4}He, ^{12}C and ^{16}O data to be compatible with the relatively small binding correction of the single state approximation but not compatible with the larger correction of the closure approximation.

We conclude, therefore, that binding effects are relatively small in the (3,3) resonance region. We expect other effects (neglected here) such as physical absorption of the pion and excitation of virtual nuclear states (dispersive effects) to be as important as the binding effect considered here.

Representing the pion-nucleus optical potential in momentum space and solving a momentum-space Lippmann-Schwinger equation for the elastic scattering proved to be a useful and convenient approach. This method enabled us to easily study the sensitivity of the cross sections to various kinematical and dynamical factors. For example, we easily verified by direct calculation that in the (3,3) resonance region the elastic cross sections are not very sensitive to the details of the off-shell parameterization. As a result, we were able to use a simple zero-range t-matrix with confidence.

We feel that this work provides a useful approach for obtaining an accurate impulse-type pion-nucleus optical potential, thus making it possible to obtain meaningful estimates of higher order corrections from a comparison of impulse approximation results with experiment. We also feel that our single state estimate of binding effects is reasonable and shows that such effects do not greatly change the predictions of the impulse approximation in the (3,3) resonance region.

BIBLIOGRAPHY

BIBLIOGRAPHY

Ade72 M. L. Adelberg and A. M. Saperstein, Phys. Rev. C5 (1972) 1180.

Bal69 R. Balian and E. Brézin, Nuovo Cimento 61 (1969) 403.

Ber72 R. W. Bercaw, J. S. Vincent, E. T. Boschitz, M. Blecher, K. Gotow, D. K. Anderson, R. Kerns, R. Minehart, K. Ziock, and R. Johnson, Phys. Rev. Letters 29 (1972) 1031.

Bin70 F. Binon, et. al., Nucl. Phys. B17 (1970) 168-188.

Bin71 F. Binon, et. al., preprint CERN, submitted to the 4th Int. Conf. on high-energy physics and nuclear structure Dubna, 7-11 September 1971.

Cer74 CERN 74-8, 10 April 1974: Proceedings from "Topical Meeting on Intermediate Energy Physics," Lyceum Alpinum Zuoz, Engadin, Switzerland, 4-13 April 1973.

Cha71 L. A. Charlton and J. M. Eisenberg, Ann. Phys. (N.Y.) 63 (1971) 286-308.

Ded71 J. P. Dedonder, Nucl. Phys. A174 (1971) 251-272.

Doe73 R. R. Doering, A. I. Galonsky and R. A. Hinrichs, Jour. of Comp. Phys. 12 (1973) 498.

Ehr59 H. F. Ehrenberg, R. Hofstadter, U. Meyer-Borkhout, D. G. Ravenhall and S. E. Sobottka, Phys. Rev. 113 (1959) 666.

Fal72 Goran Faldt, Phys. Rev C5 (1972) 400.

Fra74 Victor Franco, Phys. Rev. C5 (1974) 1690.

Fro67 R. F. Frosch, J. S. McCarthy, R. E. Rand and M. R. Yearian, Phys. Rev. 160 (1967) 874.

Ger73 J. F. Germond and J. P. Amiet, Nucl. Phys. A216 (1973) 157.

Gla67 R. J. Glauber, High Energy Physics and Nuclear Structure, (G. Alexander, ed.), p. 311, John Wiley and Sons, New York (1967).

Haf70 M. I. Haftel and F. Tabakin, Nucl. Phys. A158 (1970) 1.

Hag64 R. Hagedorn, Relativistic Kinematics, (W. A. Benjamin, Inc., New York, 1964).

Her70 D. H. Herndon, A. Barbaro-Galtieri, and A. H. Rosenfeld, LRL Report No. UCRL-20030 (1970), (unpublished).

Het65 J. H. Hetherington and L. H. Schick, Phys. Rev. 137 (1965) B935.

Gol64 M. L. Goldberger and K. M. Watson, Collision Theory, (Wiley, New York, 1964).

Ker59 A. K. Kerman, H. McManus and R. M. Thaler, Ann. Phys. (N. Y.) 8 (1959) 551.

Kis55 L. S. Kisslinger, Phys. Rev. 98 (1955) 761.

Kis74 L. S. Kisslinger and F. Tabakin, Phys. Rev. C9 (1974) 188.

Kol70 D. S. Kolton, "Interaction of Pions with Nuclei," Advances in Nuclear Physics, Vol. 3, (Academic Press, New York, 1970).

Kow63 K. L. Kowalski and D. Feldman, Phys. Rev. 130 (1963) 276.

Kuj74 E. Kujawski and G. A. Miller, Phys. Rev. C9 (1974) 1205.

Lan72 R. H. Landau and F. Tabakin, Phys. Rev. D5 (1972) 2746.

Lan73 R. H. Landau, S. C. Phatak and F. Tabakin, Ann. Phys. (N. Y.) 78 (1973) 299.

Lan74a R. H. Landau, Private Communication

Lan74b R. H. Landau and F. Tabakin, Nucl. Phys A231 (1974)445-454.

Lee71 H. K. Lee and H. McManus, Nucl. Phys. A167 (1971) 257.

Lov64 C. Lovelace, Phys. Rev. 5 (1964) B1225.

Mac73 R. Mach, Nucl. Phys. A205 (1973) 56-72.

Mil74 G. A. Miller, Phys. Rev. C10 (1974) 1242.

Mos59 M. Moshinsky, Nucl. Phys. 13 (1959) 104.

Pha73 S. C. Phatak, F. Tabakin and R. H. Landau, Phys. Rev. C7 (1973) 1803.

Rod67 Leonard S. Rodberg and R. M. Thaler, Introduction to the Quantum Theory of Scattering, (Academic Press, New York, 1967).

Sch72 C. Schmit, Nucl. Phys. A197 (1972) 449.

Ste70 M. M. Sternheim and E. H. Auerbach, Phys. Rev. Let. 25 (1970) 1500.

Wat53 K. M. Watson, Phys. Rev. 89 (1953) 575; N. Francis and K. M. Watson, Phys. Rev. 92 (1953) 291; W. B. Riesenfeld and K. M. Watson, Phys. Rev. 102 (1956) 1157; K. M. Watson, Revs. Modern Phys. 30 (1958) 565.

Won72 C. W. Wong and D. M. Clement, Nucl. Phys. A183 (1972) 210.

APPENDICES

APPENDIX A

REFERENCE FRAMES AND KINEMATICS

At a laboratory kinetic energy of 100 - 300 MeV, a pion is quite relativistic, so at first glance it seems necessary to use fully relativistic kinematics. However, due to the fact that $m_\pi / m_N \cong 1/7$, it is possible to use essentially nonrelativistic kinematics except for the pion energy.

The primary reason for developing "quasi-relativistic" kinematics is to allow a straightforward application of the vector bracket method which is discussed in Appendix D. The vector bracket method was originally constructed for nonrelativistic problems where the various momenta are related via linear equations. Fully relativistic kinematics involve nonlinear relations; but as shown in this appendix, we can linearize the relations at the energies we consider. A secondary reason for quasi-relativistic kinematics is to make contact with the nonrelativistic forms so we can use our physical intuition more effectively.

Experimental pion-nucleon phase shifts give us information about pion-nucleon scattering in the pion-nucleon C.M. frame ($\pi N CM$ frame); however, the pion-nucleus scattering calculation is usually done in the pion-nucleus C.M. frame ($\pi \nu CM$ frame), so we must make a transformation between the two frames. Even though the pion is relativistic in both the $\pi N CM$ frame and the $\pi \nu CM$ frame, the transformation between the two frames is not very relativistic because the $\pi N CM$ frame is moving at a

nonrelativistic velocity with respect to the πNCM frame.[1] First order relativistic effects can be taken into account without losing the simplicity of nonrelativistic kinematics. We present both the relativistic and nonrelativistic equations and then show how to construct a simple formalism that is nonrelativistic in form but that agrees to within a few percent with the relativistic formalism.[2]

We first define the momentum and energy variables that we will deal with.

$\underset{\sim}{p}_\pi$: pion momentum in the πNCM frame.

$\underset{\sim}{p}_N$: nucleon momentum in the πNCM frame.

$\underset{\sim}{\kappa}$: total pion-nucleon momentum in the πNCM frame; $\underset{\sim}{\kappa} = \underset{\sim}{p}_\pi + \underset{\sim}{p}_N$.

ω_π : pion energy in the πNCM frame.

ω_N : nucleon energy in the πNCM frame.

ω° : scattering energy in the πNCM frame; $\omega^\circ = \omega_\pi + \omega_N$.

$\underset{\sim}{k}$: pion momentum in the πNCM frame (the nucleon momentum is $-\underset{\sim}{k}$).

ω_{cm} : scattering energy in the πNCM frame.

(Our "momenta" here are actually wavenumbers in fm^{-1}.)

---

[1] Due to the fairly small ratio m_π/m_N , the velocity of the πNCM frame relative to the πNCM frame is less than $\sim .3c$ at the energies we consider.

[2] The transformation between laboratory and πNCM coordinates presents no problems, so it is not discussed here. The lab-πNCM transformations used in this calculation are fully relativistic.

The nonrelativistic kinematics are given by (Rod67):

$$\omega_\pi = m_\pi c^2 + \hbar^2 \underset{\sim}{p}_\pi^2 / 2m_\pi \tag{A.1}$$

$$\omega_N = m_N c^2 + \hbar^2 \underset{\sim}{p}_N^2 / 2m_N \tag{A.2}$$

$$\underset{\sim}{k} = (m_N \underset{\sim}{p}_\pi - m_\pi \underset{\sim}{p}_N)/(m_\pi + m_N) = \underset{\sim}{p}_\pi - \frac{m_\pi}{m_\pi + m_N} \underset{\sim}{\kappa} \tag{A.3}$$

$$\omega_{cm} = \omega_\pi + \omega_N - \hbar^2 \underset{\sim}{\kappa}^2 / 2(m_N + m_\pi) \tag{A.4}$$

and the relativistic kinematics are given by (Hag64):

$$\omega_\pi = (m_\pi^2 c^4 + \hbar^2 c^2 \underset{\sim}{p}_\pi^2)^{1/2} \tag{A.5}$$

$$\omega_N = (m_N^2 c^4 + \hbar^2 c^2 \underset{\sim}{p}_N^2)^{1/2} \tag{A.6}$$

$$\underset{\sim}{k} = \underset{\sim}{p}_\pi + \hbar^2 c^2 [\omega_{cm}(\omega_{cm} + \omega^0)]^{-1} [\underset{\sim}{p}_\pi \cdot \underset{\sim}{\kappa}] \underset{\sim}{\kappa} - (\omega_\pi / \omega_{cm}) \underset{\sim}{\kappa} \tag{A.7}$$

$$\omega_{cm} = [\omega^{0\,2} - \hbar^2 c^2 \kappa^2]^{1/2}. \tag{A.8}$$

Since the target nucleons move at nonrelativistic velocities we can write equation (A.6) as

$$\omega_N \cong m_N c^2 + \hbar^2 \underset{\sim}{p}_N^2 / 2 m_N \quad . \tag{A.9}$$

Also, in the 100 - 300 MeV region we have $|\underset{\sim}{p}_\pi| \cong 1\text{-}2\ \text{fm}^{-1}$, $\underset{\sim}{\kappa} \cong 0\text{-}3\ \text{fm}^{-1}$, $\omega_\pi \cong 300$ MeV, and $\omega^\circ \cong \omega_{cm} \cong 1200$ MeV. Using these values in equation (A.7), we find the leading term is about 1.5 fm^{-1}, the second term is about .05 fm^{-1}, and the third term is about .5 fm^{-1}. Hence, the second term, which is complicated, can be dropped without any significant loss in accuracy. Further, since $\hbar^2 c^2 \kappa^2 << \omega^{\circ 2}$ and $\omega_{cm} \cong \omega^\circ$ we can write equation (A.7) and (A.8) as

$$\underset{\sim}{k} \cong \underset{\sim}{p}_\pi - (\omega_\pi / \omega^\circ)\, \underset{\sim}{\kappa} \tag{A.10}$$

$$\omega_{cm} \cong \omega^\circ - \frac{\hbar^2 c^2}{2\omega^\circ} \kappa^2 \quad . \tag{A.11}$$

The above equations for $\underset{\sim}{k}$ and ω_{cm} can be obtained from the nonrelativistic equations (A.3) and (A.4) simply by making the replacements $m_\pi \rightarrow \omega_\pi / c^2$, and $m_N \rightarrow \omega_N / c^2$ where ω_π is calculated from equation (A.5). We will use this prescription unless stated otherwise.

Sometimes it will be useful to call $\underset{\sim}{k}$ the relative pion-nucleon momentum and $\underset{\sim}{K}$ the center-of-mass momentum. Then our transformation can be regarded as a transformation from $\pi N CM$ coordinates to relative and center-of-mass coordinates.

The momentum and energy transformations we have given thus far are all that is needed if the initial and final states of the nucleon are free particle states. If the nucleon is bound in a nucleus we need to consider a third frame, the C.M. frame of the nucleus alone, since we use single particle ground state wave functions which depend on the nucleon momentum in the nuclear center-of-mass frame. We shall refer to the nuclear C.M. frame as the $4NCM$ frame since we mainly consider π - ^{4}He scattering in our derivations. However, we shall leave the number of target nucleons, A, arbitrary in our equations in order to obtain a more general result.

The initial and final momentum of the ^{4}He nucleus in the frame are respectively $-\underset{\sim}{p}_\pi$ and $-\underset{\sim}{p}'_\pi$. We show the situation schematically in Figure A.1. In Figure A.1, the symbol $\otimes$ denotes the ^{4}He center-of-mass. Using $\underset{\sim}{p}_{4N}$ to indicate the nucleon momentum in the $4NCM$ frame, we have for the nucleon momentum in the πNCM frame

$$\underset{\sim}{p}_N = \underset{\sim}{p}_{4N} - (M_N / M_{He})\,\underset{\sim}{p}_\pi \cong \underset{\sim}{p}_{4N} - (1/A)\,\underset{\sim}{p}_\pi \quad . \tag{A.12}$$

(Before collision)

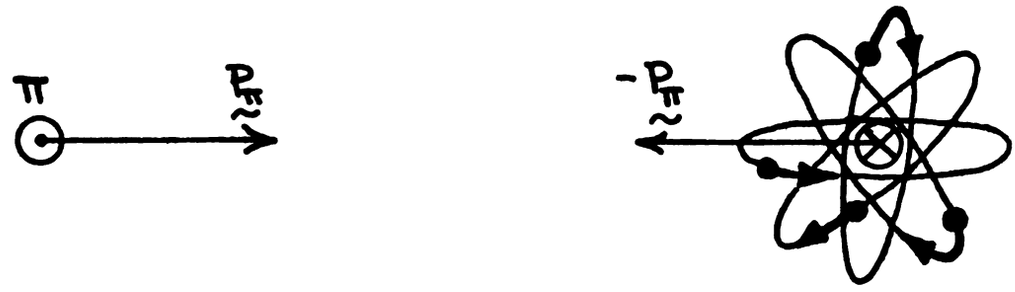

(After collision)

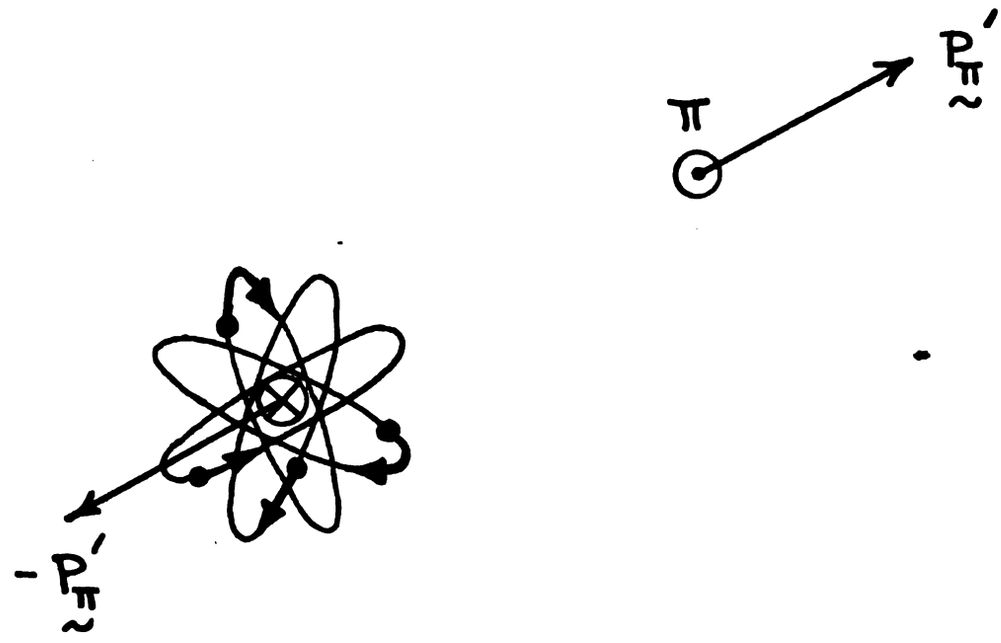

Figure A.1 - Schematic representation of an elastic $\pi - {}^4He$ scattering. The symbol ⊗ denotes the ${}^4He$ center of mass.

We can now write the πNCM frame variables in terms of the variables and 4NCM variables.

$$(A.13)\quad \underset{\sim}{k} = \underset{\sim}{p}_{\pi}\left[1 - \left(\frac{A-1}{A}\right)\frac{\omega_{\pi}}{\omega^{o}}\right] - \frac{\omega_{\pi}}{\omega^{o}}\ \underset{\sim}{P}_{4N}$$

$$(A.14)\quad \underset{\sim}{K} = \left(\frac{A-1}{A}\right)\underset{\sim}{p}_{\pi} + \underset{\sim}{P}_{4N}$$

It should be noted that there are actually two 4NCM frames involved (the initial and final) since the nuclear center-of-mass itself is deflected by the collision with the pion. We ignore this point in our discussions and speak of "the" 4NCM frame as if there were only one.

Finally, in pion-nucleus scattering, it is necessary to distinguish between on-shell and off-shell kinematical variables. On-shell variables are fixed whenever the πNCM scattering energy is fixed so we write them with an "o". For example, we write the on-shell value of ω_{π} as ω_{π}^{o} .

APPENDIX B

PARAMETERIZATION OF THE OFF-SHELL PION-NUCLEON t-MATRIX

In pion-nucleus scattering we need the entire (on-shell and off-shell) pion-nucleon t-matrix in the pion-nucleus C.M. frame ($\pi\nu CM$ frame). The experimental pion-nucleon phase shifts give us the pion-nucleon t-matrix only on the energy shell and in the pion-nucleon C.M. frame (πNCM frame) so that we must first make some parameterization for the off-shell part of the t-matrix and then transform to the $\pi\nu CM$ frame.

The on-shell pion-nucleon t-matrix in the πNCM frame is related to the pion-nucleon phase shifts by

$$(B.1)\quad t_{IJL}(\omega_{cm}, k_o, k_o) = \frac{-8\pi^2\hbar^2c^2}{\mu_R}\left[\frac{\eta_{IJL}\, e^{2i\delta_{IJL}} - 1}{2ik_o}\right]$$

where I, J, L denote respectively the pion-nucleon eigenchannel isospin, total angular momentum, and orbital angular momentum. The quantity δ_{IJL} is the eigenchannel phase shift and η_{IJL} is the eigenchannel absorption parameter. The on-shell momentum in the πNCM frame is k_o, and μ_R is the relativistic reduced mass, which is defined as

$$(B.2)\quad \mu_R = \left[\frac{\omega_\pi(k_o)\,\omega_N(k_o)}{\omega_\pi(k_o) + \omega_N(k_o)}\right]^{1/2}$$

where $$\omega_\pi(k_0) = \left(m_\pi^2 c^4 + \hbar^2 c^2 k_0^2\right)^{1/2}$$

and $$\omega_N(k_0) = \left(m_N^2 c^4 + \hbar^2 c^2 k_0^2\right)^{1/2} .$$

The phase shifts and absorption parameters were taken from the CERN theoretical fit as tabulated in Her70.

There are several popular off-shell parameterizations for the pion-nucleon t-matrix (Lan73), but the one best suited to our purpose is the separable parameterization used by Landau and Tabakin (Lan72).

$$(B.3)\quad t_{IJL}(\omega_{cm}, k', k) = t_{IJL}(\omega_{cm}, k_0, k_0)\frac{g_{IJL}(k')\, g_{IJL}(k)}{g^2_{IJL}(k_0)}$$

Landau and Tabakin obtain the g's in equation (B.3) by solving an inverse scattering problem so that $g_{IJL}(k') \times g_{IJL}(k)$ defines a separable potential which reproduces the on-shell pion-nucleon t-matrix. We have found our pion-nucleus scattering results to be relatively insensitive to the choice of the g's (for smooth nondivergent forms) so we take the g's to be unity.

In part of our pion-nucleus scattering calculation we need the spin-isospin averaged form of the pion-nucleon t-matrix. Using the parameterization of equation (B.3) and averaging over spin and isospin we obtain for the 3-dimensional t-matrix in the πNCM frame

(B.4) $$\bar{t}_{\pi N}(\omega_{CM}, \underset{\sim}{k}, \underset{\sim}{k'}) =$$

$$\frac{1}{12\pi}\sum_{IJL}(I+\tfrac{1}{2})(J+\tfrac{1}{2})\,t_{IJL}(\omega_{CM}, k, k')\,P_L(\hat{k}'\cdot\hat{k}).$$

In order to insure Lorentz invariance of probability we must make a transformation of the pion-nucleon scattering operator itself. The scattering operator in the $\pi N CM$ frame is related to the scattering operator in the $\pi N CM$ frame by

(B.5) $$(t_{\pi N})_{\pi N CM} = \gamma\,(t_{\pi N})_{\pi N CM}$$

where γ is given by

(B.6) $$\gamma = \left[\frac{\omega_\pi(k')\,\omega_N(k')\,\omega_\pi(k)\,\omega_N(k)}{\omega_\pi(p_\pi')\,\omega_N(p_N')\,\omega_\pi(p_\pi)\,\omega_N(p_N)}\right]^{1/2}.$$

In equation (B.6) the unprimed momenta and primed momenta refer respectively to momenta before and after the collision. The energies are defined as $\omega_\pi(x) = (m_\pi^2 c^4 + \hbar^2 c^2 x^2)^{1/2}$

and $\omega_N(x) = \left(m_N^2 c^4 + \hbar^2 c^2 x^2\right)^{1/2}$.

The transformation in equation (B.5) is a purely relativistic effect and should not be confused with the momentum and energy transformations discussed in Appendix A. In a completely nonrelativistic formalism we would have $(t_{\pi N})_{\pi N CM} = (t_{\pi N})_{\pi N CM}$ even though momentum and energy transformations would still be necessary.

There is a minor point we have so far glossed over. When equation (B.5) is used for the pion-nucleon t-matrix in the $\pi N CM$ frame, the γ factor gives rise to a form that is a function of the $\pi N CM$ nucleon momentum $\underset{\sim}{p}_N$ and $\underset{\sim}{p}_N'$ and the $\pi N CM$ pion momentum $\underset{\sim}{p}_\pi$ and $\underset{\sim}{p}_\pi'$ as well as ω_{CM}, $\underset{\sim}{k}$ and $\underset{\sim}{k}'$. However, since the kinetic energy of the nucleon is always much less than its rest mass energy, the dependence of γ on $\underset{\sim}{p}_N$ and $\underset{\sim}{p}_N'$ is very weak. Further, $\underset{\sim}{p}_\pi$ and $\underset{\sim}{p}_\pi'$ are fixed in the integral over nucleon momentum (see equation (3.2)) so that for convenience we write the $\pi N CM$ t-matrix as a function of just ω_{CM}, $\underset{\sim}{k}$ and $\underset{\sim}{k}'$ just as we would in a completely nonrelativistic theory. In the actual calculations the dependence of the $\pi N CM$ pion-nucleon t-matrix on $\underset{\sim}{p}_\pi$, $\underset{\sim}{p}_\pi'$, $\underset{\sim}{p}_N$ and $\underset{\sim}{p}_N'$ is taken into account properly.

APPENDIX C

NOTATION

We denote the state vector of a particle with definite momentum as $|\underset{\sim}{p}\rangle$. The normalization is taken to be $\langle \underset{\sim}{p}' | \underset{\sim}{p} \rangle = (2\pi)^3 \delta(\underset{\sim}{p}' - \underset{\sim}{p})$. The coordinate representation of $|\underset{\sim}{p}\rangle$ is

$$\text{(C.1)} \quad \langle \underset{\sim}{r} | \underset{\sim}{p} \rangle = e^{i \underset{\sim}{p} \cdot \underset{\sim}{r}} = 4\pi \sum_{LM} Y_{LM}(\hat{r}) Y^*_{LM}(\hat{p}) i^L j_L(pr)$$

where we define

$$\text{(C.2)} \quad \langle \underset{\sim}{r} | \underset{\sim}{p} \rangle \equiv \sum_{LM} Y^*_{LM}(\hat{p}) \langle \underset{\sim}{r} | PLM \rangle$$

so that

$$\text{(C.3)} \quad |\underset{\sim}{p}\rangle \equiv \sum_{LM} Y^*_{LM}(\hat{p}) |PLM\rangle \ .$$

The state $|PLM\rangle$ is a state of definite angular momentum and kinetic energy. The normalization is $\langle P'L'M' | PLM \rangle = (2\pi)^3 \delta(L', L) \delta(M', M) \delta(P' - P) / p^2$.

A two particle state for particles of definite momentum is written $|\underset{\sim}{p}_1\rangle|\underset{\sim}{p}_2\rangle = |\underset{\sim}{p}_1\,\underset{\sim}{p}_2\rangle$ or

$$(C.4)\quad |\underset{\sim}{p}_1\,\underset{\sim}{p}_2\rangle = \sum_{\substack{L_1M_1\\L_2M_2}} Y^*_{L_1M_1}(\hat{p}_1)\,Y_{L_1M_1}(\hat{p}_2)\,|p_1L_1M_1\rangle|p_2L_2M_2\rangle\ .$$

We often need to couple the angular momentum of particles 1 and 2. We write such a "coupled" state as

$$(C.5)\quad |p_1p_2\ell m L_1L_2\rangle = \sum_{M_1M_2} \langle L_1L_2M_1M_2|\ell m\rangle \times |p_1L_1M_1\rangle|p_2L_2M_2\rangle\ .$$

If one of the particles has spin, say particle 1, we can couple the spin to $\underset{\sim}{L}_1$ and write (we assume a spin of 1/2 so $\underset{\sim}{j}_1 = \underset{\sim}{L}_1 + \underset{\sim}{1/2}$)

$$(C.6)\quad |p_1j_1j_{1z}L_1\rangle = \sum_{M_1S_{1z}} \langle L_1S_1M_1S_{1z}|j_1j_{1z}\rangle \times |p_1L_1M_1\rangle|S_{1z}\rangle\ .$$

Then this state can be coupled to the angular momentum of particle 2 to obtain

$$(C.7)\quad |P_1 P_2 \mathcal{J}\mathcal{J}_z j_1 L_1 L_2\rangle = \sum_{j_{1z}, M_2} \langle j_1 L_2 j_{1z} M_2 | \mathcal{J}\mathcal{J}_z\rangle \times |P_1 j_1 j_{1z}\rangle |P_2 L_2 M_2\rangle \,.$$

If more convenient, we could of course use a different order for the coupling.

Since the states $|\underset{\sim}{P_1}\rangle|\underset{\sim}{P_2}\rangle$ are complete we have that

$$(C.8)\quad |\underset{\sim}{P_1}\rangle|\underset{\sim}{P_2}\rangle \int \frac{d^3P_1}{(2\pi)^3}\int \frac{d^3P_2}{(2\pi)^3} \langle \underset{\sim}{P_1}|\langle \underset{\sim}{P_2}| = 1 \,.$$

Similarly we can write

$$(C.9)\quad |P_1 P_2 \mathcal{L}\mathcal{M} L_1 L_2\rangle \sum_{\substack{\mathcal{L}\mathcal{M}\\ L_1 L_2}} \iint \frac{P_1^2 dP_1}{(2\pi)^3} \frac{P_2^2 dP_2}{(2\pi)^3} \langle P_1 P_2 \mathcal{L}\mathcal{M} L_1 L_2| = 1$$

and

$$(C.10)\quad |P_1 P_2 \mathcal{J}\mathcal{J}_z j_1 L_1 L_2\rangle \sum_{\substack{\mathcal{J}\mathcal{J}_z \\ j_1 L_1 L_2}} \int \frac{P_1^2 dP_1}{(2\pi)^3} \int \frac{P_2^2 dP_2}{(2\pi)^3} \langle P_1 P_2 \mathcal{J}\mathcal{J}_z j_1 L_1 L_2| = 1 .$$

Suppose now $\underset{\sim}{P_1}$ and $\underset{\sim}{P_2}$ are related to two other vectors $\underset{\sim}{k}$ and $\underset{\sim}{K}$ by the relations

$$(C.11)\quad \underset{\sim}{P_1} = a_1 \underset{\sim}{k} + b_1 \underset{\sim}{K}$$

$$(C.12)\quad \underset{\sim}{P_2} = a_2 \underset{\sim}{k} + b_2 \underset{\sim}{K}$$

where we assume the Jacobian $|a_1 b_2 - a_2 b_1|$ is equal unity. For example, $\underset{\sim}{k}$ might be the relative momentum and $\underset{\sim}{K}$ the center-of-mass momentum (see Appendix A). The state $|\underset{\sim}{k}\rangle|\underset{\sim}{K}\rangle$ is then equivalent to the state $|\underset{\sim}{P_1}\rangle|\underset{\sim}{P_2}\rangle$. We can now define as before

$$(C.13)\quad |\underset{\sim}{k}\rangle = \sum_{l_k m_k} Y^*_{l_k m_k}(\hat{k}) \, |k \, l_k \, m_k\rangle$$

$$(C.14)\quad |\underset{\sim}{\kappa}\rangle = \sum_{l_\kappa m_\kappa} Y^*_{l_\kappa m_\kappa}(\hat{\kappa})\,|\kappa\, l_\kappa\, m_\kappa\rangle$$

$$(C.15)\quad |k\kappa\, \ell m\, l_k\, l_\kappa\rangle =$$

$$\sum_{m_k m_\kappa} \langle l_k\, l_\kappa\, m_k\, m_\kappa | \ell m\rangle\, |k\, l_k\, m_k\rangle |\kappa\, l_\kappa\, m_\kappa\rangle .$$

The spin can be included as before

$$(C.16)\quad |k\, j_k\, j_{kz}\, l_k\rangle =$$

$$\sum_{m_k s_z} \langle l_k\, s\, m_k\, s_z | j_k\, j_{kz}\rangle\, |k\, l_k\, m_k\rangle |s\, s_z\rangle .$$

And as before, we can further couple the two single particle states

$$(C.17)\quad |k\kappa\, j j_z\, j_k\, l_k\, l_\kappa\rangle =$$

$$\sum_{j_{kz}\, m_\kappa} \langle j_k\, l_\kappa\, j_{kz}\, m_\kappa | j j_z\rangle\, |k\, j_k\, j_{kz}\, l_k\rangle |\kappa\, l_\kappa\, m_\kappa\rangle .$$

The states $|\underset{\sim}{k}\rangle|\underset{\sim}{\kappa}\rangle$ also form a complete set of states so we can write

$$(C.18)\qquad |\underset{\sim}{k}\rangle|\underset{\sim}{\kappa}\rangle\int\frac{d^3\kappa}{(2\pi)^3}\int\frac{d^3k}{(2\pi)^3}\langle\underset{\sim}{\kappa}|\langle\underset{\sim}{k}| = 1$$

or

$$(C.19)\qquad |k\kappa\, l m\, l_k\, l_\kappa\rangle\sum_{\substack{l m\\ l_k\, l_\kappa}}\iint\frac{k^2dk}{(2\pi)^3}\,\frac{\kappa^2d\kappa}{(2\pi)^3}\langle k\kappa\, l m\, l_k\, l_\kappa|$$

$$= 1$$

or

$$(C.20)\qquad |k\kappa\, j j_z\, j_k\, l_k\, l_\kappa\rangle\sum_{\substack{j j_z\\ j_k\, l_k\, l_\kappa}}\iint\frac{k^2dk}{(2\pi)^3}\,\frac{\kappa^2d\kappa}{(2\pi)^3}\langle k\kappa\, j j_z\, j_k\, l_k\, l_\kappa|$$

$$= 1\ .$$

The completeness relations given in this appendix are useful when we want the matrix elements of a two-body operator in terms of some "unnatural" coordinates and the operator has a simple known form in terms of "natural" coordinates. In such a case the unit operators in terms of the natural states can be inserted in the proper places so that the operator is "sandwiched" between natural states. Then we need only the overlaps between the natural and unnatural states. This procedure is discussed in detail in Appendix D.

APPENDIX D

VECTOR BRACKETS

"Vector brackets" can be used in scattering problems in the same way Moshinsky or oscillator brackets (Mos59) are used in bound state problems. The purpose of both types of brackets is to provide a more convenient and systematic method for evaluation of certain matrix elements. Oscillator brackets are generally used to calculate state "overlaps" for two independent particles moving in a harmonic oscillator well so that the coordinate-space radial wave functions involved are proportional to $\exp(-\alpha^2 r^2) \times$ (Laguerre polynomial). Vector brackets, on the other hand, are related to overlaps between free particle states so that the associated radial wave functions are proportional to spherical Bessel functions. Except for the different associated radial wave functions, oscillator brackets and vector brackets are identical. However, it is possible to obtain an explicit expression for vector brackets while oscillator brackets usually must be tabulated in numerical form or evaluated on a computer. We give a general expression for the vector bracket in this appendix.

Vector brackets have been used in various forms in 3-body theory for quite some time. We thank Dr. Nancy Larson for introducing us to these overlaps and for providing notes which made it possible to derive results appropriate for 2-body states. Balian and Brezin (Bal69) give a derivation which leads to a more useful form than we derived originally. Recently, Wong and Clement (Won72) generalized the overlap and introduced the name "vector bracket" into

the literature. The general expression obtained by Wong and Clement is given here. Suppose we want to calculate

$$\text{(D.1)}\quad \langle P_1' P_2' \mathcal{L}' \mathcal{M}' l_1' l_2' | Q | P_1 P_2 \mathcal{L} \mathcal{M} l_1 l_2 \rangle$$

where $\underset{\sim}{l}_1 + \underset{\sim}{l}_2 = \underset{\sim}{\mathcal{L}}$ and $\underset{\sim}{l}_1' + \underset{\sim}{l}_2' = \underset{\sim}{\mathcal{L}}'$

(See Appendix C for notation).

Also, suppose we know Q in terms of the $\underset{\sim}{k}$, $\underset{\sim}{\mathcal{K}}$ coordinates (for example, $\underset{\sim}{k}$ and $\underset{\sim}{\mathcal{K}}$ might be the relative and center-of-mass momenta). That is, we know

$$\text{(D.2)}\quad \langle k' \mathcal{K}' \mathcal{L}' \mathcal{M}' l_{k'} l_{\mathcal{K}'} | Q | k \mathcal{K} \mathcal{L} \mathcal{M} l_k l_{\mathcal{K}} \rangle .$$

We can evaluate the expression in equation (D.1) by inserting the unit operator

(D.3)

$$|k'' \mathcal{K}'' \mathcal{L}'' \mathcal{M}'' l_{k''} l_{\mathcal{K}''}\rangle \sum_{\substack{\mathcal{L}'' \mathcal{M}'' \\ l_{k''} l_{\mathcal{K}''}}} \iint \frac{k''^2 dk''}{(2\pi)^3} \frac{\mathcal{K}''^2 d\mathcal{K}''}{(2\pi)^3} \langle k'' \mathcal{K}'' \mathcal{L}'' \mathcal{M}'' l_{k''} l_{\mathcal{K}''} |$$

$$= 1$$

on both sides of Q in equation (D.1) and performing the sums and integrals, provided we have an expression for overlaps of the form

$$\text{(D.4)}\quad \langle \mathrm{I}|\mathrm{II}\rangle = \langle P_1' P_2' \mathcal{L}' \mathcal{M}' l_1' l_2' | k'' \chi'' \mathcal{L}'' \mathcal{M}'' l_{k''} l_{\chi''} \rangle .$$

The expression in equation (D.4) is the so-called "vector bracket." When $\underset{\sim}{k}''$ and $\underset{\sim}{\chi}''$ are related to $\underset{\sim}{P}_1'$ and $\underset{\sim}{P}_2'$ by

$$\text{(D.5)}\quad \underset{\sim}{k}'' = a_1 \underset{\sim}{P}_1' + a_2 \underset{\sim}{P}_2'$$

$$\text{(D.6)}\quad \underset{\sim}{\chi} = b_1 \underset{\sim}{P}_1' + b_2 \underset{\sim}{P}_2' .$$

Wong and Clement show that the expression in equation (D.4) is given by

(D.7)

$$\langle \mathrm{I}|\mathrm{II}\rangle = N^2 (4\pi)^2 \delta(\mathcal{L}'\mathcal{L}'')\delta(\mathcal{M}'\mathcal{M}'')\delta(W)$$

$$\times \Theta(1-x_1^2)\Theta(1-x_2^2)\frac{1}{2\mathcal{L}+1}\frac{1}{P_1' P_2' k'' \chi''} A_{\mathrm{I,II}}$$

where

(D.8) N^2 = a normalization factor (we use $N = (2\pi)^3$)

(D.9) $$W = b_1 b_2 k''^2 + a_1 a_2 \kappa''^2 + (a_2 b_1 - b_2 a_1)(a_1 b_1 P_1'^2 - a_2 b_2 P_2'^2)$$

(D.10) $$X_1 = (k''^2 - a_1^2 P_1'^2 - a_2^2 P_2'^2) / (2 a_1 a_2 P_1' P_2')$$

(D.11) $$X_2 = (\kappa''^2 - b_1^2 P_1'^2 - b_2^2 P_2'^2) / (2 b_1 b_2 P_1' P_2') .$$

The variables X_1 and X_2 are expressions for the cosine of the angle between $\underset{\sim}{P_1}$ and $\underset{\sim}{P_2}$. The functions which are defined as

(D.12) $$\theta(x_i) = \begin{cases} 1 & 0 \le x_i \le 1 \\ 0 & x_i > 1 \end{cases} \qquad (i = 1, 2)$$

just insure that $|X_1|$ and $|X_2|$ are less than or equal 1 . The symbol $A_{I,II}$ is

$$(D.13)\quad A_{I,II} = \sum_{m=-\ell'}^{\ell'} \left\{ \left[\sum_{m_1 m_2} \langle \ell_1' \ell_2' m_1 m_2 | \ell' m \rangle Y_{\ell_1' m_1}(\hat{P}_1') Y_{\ell_2' m_1}(\hat{P}_2') \right]^* \times \left[\sum_{m_k m_\chi} \langle \ell_{k''} \ell_{\chi''} m_k m_\chi | \ell' m \rangle Y_{\ell_{k''} m_k}(\hat{k}'') Y_{\ell_{\chi''} m_\chi}(\hat{\chi}'') \right] \right\}.$$

The vectors $\underset{\sim}{P}_1'$, $\underset{\sim}{P}_2'$, $\underset{\sim}{k}''$ and $\underset{\sim}{\chi}''$ all lie in a plane and the relative angles between the vectors are fixed by the magnitudes of the vectors. The orientation of the plane itself is arbitrary. For computational purposes it is useful to take the vectors to lie in the X-Y plane so that $Y_{LM}(\theta = \pi/2, \varphi) \to \Gamma_{LM} e^{im\varphi}$ where

$$(D.14)\quad \Gamma_{LM} = \begin{cases} \dfrac{(-1)^{(\ell+m)/2}}{2^\ell \left(\frac{\ell+m}{2}!\right)\left(\frac{\ell-m}{2}!\right)} \left[\dfrac{2\ell+1}{4\pi} (\ell+m)!(\ell-m)! \right]^{1/2} & \text{for } (\ell-m) \text{ even} \\ 0 \quad \text{for } (\ell-m) \text{ odd} \end{cases}$$

The factor $\delta(W)$ expresses conservation of kinetic energy. For example, for the familiar transformation

$$\underset{\sim}{k}'' = (m_2 \underset{\sim}{P}_1' - m_1 \underset{\sim}{P}_2')/(m_1 + m_2) \,, \quad \underset{\sim}{\chi}'' = \underset{\sim}{P}_1'' + \underset{\sim}{P}_2''$$

we obtain the result

(D.15) $$\delta(W) = (1/2\mu)\delta(k''^2/2\mu + \chi''^2/2m - p_1'^2/2m_1 - p_2'^2/2m_2)$$

where $\mu = m_1 m_2/(m_1+m_2)$ and $m = m_1 + m_2$.

Finally, we note that parity conservation requires

$$(\ell_1' + \ell_2' + \ell_{k''} + \ell_{\chi''}) \longrightarrow \text{even}$$

The inclusion of spin is straight forward. We shall list some results for the case where one of the particles has spin 1/2.

First, some useful expansions:

(D.16) for $\underset{\sim}{j}_1' = \underset{\sim}{\ell}_1' + \underset{\sim}{1/2}$, $\underset{\sim}{j}' = \underset{\sim}{j}_1' + \underset{\sim}{\ell}_2'$

and

$$\underset{\sim}{\mathcal{L}}' = \underset{\sim}{\ell}_1' + \underset{\sim}{\ell}_2' \quad , \underset{\sim}{\mathcal{J}}' = \underset{\sim}{\mathcal{L}}' + \underset{\sim}{1/2}$$

$$|p_1' p_2' j' j_2' j_1' \ell_1' \ell_2'\rangle$$

$$= \sum_{\mathcal{L}'} \begin{Bmatrix} 1/2 & \ell_1' & j_1' \\ \ell_2' & j' & \mathcal{L}' \end{Bmatrix} [(2\mathcal{L}'+1)(2j_1'+1)]^{1/2} (-1)^{1/2+\ell_1'+\ell_2'+j'}$$

$$\times |p_1' p_2' j' j_2' \mathcal{L}' \ell_1' \ell_2'\rangle$$

(D.17) for $\underset{\sim}{j}_{k''} = \underset{\sim}{l}_{k''} + \underset{\sim}{1/2}$, $\underset{\sim}{j}'' = \underset{\sim}{j}_{k''} + \underset{\sim}{l}_{x''}$

$\underset{\sim}{\lambda}'' = \underset{\sim}{l}_{k''} + \underset{\sim}{l}_{x''}$, $\underset{\sim}{j}'' = \underset{\sim}{\lambda}'' + \underset{\sim}{1/2}$

$$|k''x''j''j_z''\, j_{k''}\, l_{k''}\, l_{x''}\rangle$$

$$= \sum_{\lambda''} \begin{Bmatrix} 1/2 & l_{k''} & j_{k''} \\ l_{x''} & j'' & \lambda'' \end{Bmatrix} \left[(2\lambda''+1)(2j_{k''}+1)\right]^{1/2} (-1)^{1/2 + l_{k''} + l_{x''} + j''}$$

$$\times |k''x''j''j_z''\lambda''\, l_{k''}\, l_{x''}\rangle$$

(D.18) For the simple case

$\underset{\sim}{\lambda}'' = \underset{\sim}{l}_{k''} + \underset{\sim}{l}_{x''}$ $\qquad$ $\underset{\sim}{j}'' = \underset{\sim}{\lambda}'' + \underset{\sim}{1/2}$

$\underset{\sim}{\lambda}' = \underset{\sim}{l}_1' + \underset{\sim}{l}_2'$ $\qquad$ $\underset{\sim}{j}' = \underset{\sim}{\lambda}' + \underset{\sim}{1/2}$

$$\langle k''x''j''j_z''\lambda''\, l_{k''}\, l_{x''} | P_1' P_2' j' j_z' \lambda' l_1' l_2'\rangle$$

$$= \delta(j''j')\delta(j_z''j_z')\delta(\lambda''\lambda')$$

$$\times \langle k''x''\lambda' m'=0\, l_{k''}\, l_{x''} | P_1' P_2' \lambda' m'=0\, l_1' l_2'\rangle$$

The simple case in (D.18) together with the expansions in equations (D.16) and (D.17) can be used to obtain

(D.19) $\underset{\sim}{j}_{k''} = \underset{\sim}{l}_{k''} + \underset{\sim}{1/2} \qquad \underset{\sim}{J}'' = \underset{\sim}{j}_{k''} + \underset{\sim}{1/2}$

$\underset{\sim}{L}' = \underset{\sim}{l}_1' + \underset{\sim}{l}_2' \qquad \underset{\sim}{J}' = \underset{\sim}{L}' + \underset{\sim}{1/2}$

$$\langle k'' x'' J'' J_z'' j_{k''} l_{k''} l_{x''} | P_1' P_2' J' J_z' L' l_1' l_2' \rangle$$

$$= \delta(J'' J') \delta(J_z'' J_z') \begin{Bmatrix} 1/2 & l_{k''} & j_{k''} \\ l_{x''} & J' & L' \end{Bmatrix} \left[(2L'+1)(2j_{k''}+1)\right]^{1/2}$$

$$\times (-1)^{1/2 + l_{k''} + l_{x''} + J'} \langle k'' x'' L' M'=0 \, l_{k''} l_{x''} | P_1' P_2' L' M'=0 \, l_1' l_2' \rangle$$

(D.20)

$$\underset{\sim}{j}_{k''} = \underset{\sim}{l}_{k''} + \underset{\sim}{1/2} \;, \quad \underset{\sim}{J}'' = \underset{\sim}{l}_{x''} + \underset{\sim}{j}_{k''}$$

$$\underset{\sim}{j}_1' = \underset{\sim}{l}_1' + \underset{\sim}{1/2} \;, \quad \underset{\sim}{J}' = \underset{\sim}{l}_2' + \underset{\sim}{j}_1'$$

$$\langle k'' x'' J'' J_z'' j_{k''} l_{k''} l_{x''} | P_1' P_2' J' J_z' j_1' l_1' l_2' \rangle$$

$$= \delta(J'' J') \delta(J_z'' J_z')$$

$$\times \sum_{L'} \begin{Bmatrix} 1/2 & l_{k''} & j_{k''} \\ l_{x''} & J' & L' \end{Bmatrix} \begin{Bmatrix} 1/2 & l_1 & j_1 \\ l_2' & J' & L' \end{Bmatrix} (2L'+1) \left[(2j_{k''}+1)(2j_1'+1)\right]^{1/2}$$

$$\times (-1)^{l_{k''} + l_{x''} + l_1' + l_2'} \langle k'' x'' L' M'=0 \, l_{k''} l_{x''} | P_1' P_2' L' M'=0 \, l_1' l_2' \rangle$$

APPENDIX E

THEORETICAL JUSTIFICATION OF THE 3-BODY MODEL IN PION-NUCLEUS SCATTERING

In Chapter VIII we obtained the t-matrix for scattering of a pion from a single nucleon which is bound in a potential well. This 3-body t-matrix was later used in place of the free pion-nucleon t-matrix in the calculation of elastic pion scattering from ^{4}He, ^{12}C, and ^{16}O. In this appendix we give a theoretical justification for the use of the 3-body t-matrix in pion-nucleus scattering.

In the development of the optical potential formalism in Chapter II, we eliminated the pion-nucleon potential, $\tilde{v}_{\pi N}$, by writing $\tilde{v}_{\pi N}$ in terms of the t-matrix $\hat{t}_{\pi N}$ where we defined

$$\text{(E.1)} \quad \hat{t}_{\pi N} = \tilde{v}_{\pi N} + \tilde{v}_{\pi N} G \hat{t}_{\pi N} .$$

The propagator G was given as

$$\text{(E.2)} \quad G = \mathcal{A} (E - E_{\nu} - K_{\pi} + i\epsilon)^{-1}$$

where $\mathcal{A}$ is a projection operator for completely antisymmetric states. The elimination of $\tilde{v}_{\pi N}$ using equation (E.1) is clearly an arbitrary step. Any operator equation containing $\tilde{v}_{\pi N}$ could have been used to eliminate $\tilde{v}_{\pi N}$. However, the resulting equations for the optical potential do not have conventional forms for some choices.

Kerman, McManus, and Thaler (Ker59) give a systematic way for eliminating $v_{\pi N}$ in their Appendix IV. Their approach is completely general and shows the conditions necessary to end up with a conventional Schroedinger (or Lippmann-Schwinger) scattering equation. We first present their approach and then we apply the result to our 3-body model.

Kerman, McManus, and Thaler (KMT) point out that we can define a whole series of scattering operators t_σ

$$t_\sigma = v_{\pi N} + v_{\pi N} G_\sigma t_\sigma \tag{E.3}$$

which can be used to eliminate $v_{\pi N}$. The propagator G_σ is completely arbitrary; however, as we shall see, there is only a certain class which lead to a final scattering equation of conventional form. Our objective here is to show that we can make a consistent definition of the pion-nucleus optical potential when G_σ is the propagator used in our 3-body model.

If we use equation (E.3) to eliminate $v_{\pi N}$, we obtain for any choice of G_σ

$$T_{\pi\nu} = \left[A/(A-1)\right] T'_{\pi\nu} \tag{E.4}$$

$$T'_{\pi\nu} = (A-1)\, t_\sigma \left(1 + \tilde{G}_\sigma T'_{\pi\nu}\right) \tag{E.5}$$

$$\text{(E.6)}\quad \tilde{G}_\sigma = \left[A/(A-1)\right]\left[G - G_\sigma/A\right] .$$

Equations (E.4) - (E.6) are the same results we obtained in Chapter II, except now we have $\tilde{G}_\sigma$ instead of G and t_σ instead of $\uparrow_{\pi N}$. Defining the first order optical potential as

$$\text{(E.7)}\quad U^{o}_{\pi\nu} = (A-1)t_\sigma$$

and the complete optical potential as

$$\text{(E.8)}\quad U_{\pi\nu} = U^{o}_{\pi\nu} + U^{o}_{\pi\nu}\left(1 - |0\rangle\langle 0|\right)\tilde{G}_\sigma U_{\pi\nu}$$

the equation for $T'_{\pi\nu}$ becomes

$$\text{(E.9)}\quad T'_{\pi\nu} = U_{\pi\nu} + U_{\pi\nu}|0\rangle\langle 0|\tilde{G}_\sigma|0\rangle\langle 0|T'_{\pi\nu} .$$

Further, the t-matrix t_σ can be written in terms of the free pion-nucleon t-matrix

$$t_\sigma = t_{\pi N} + t_{\pi N}\,(G_\sigma - g_o)\,t_\sigma \tag{E.10}$$

where, as before, $t_{\pi N}$ is given by

$$t_{\pi N} = v_{\pi N} + v_{\pi N}\, g_o\, t_{\pi N} \,. \tag{E.11}$$

In order for equation (E.9) to be the conventional one-body Lippmann-Schwinger equation we must have [1]

$$\langle o | \tilde{G}_\sigma | o \rangle = (E_\pi - K_\pi + i\epsilon)^{-1} \tag{E.12}$$

or equivalently,

$$\langle o | G_\sigma | o \rangle = \langle o | G | o \rangle \,. \tag{E.13}$$

(Recall that $\langle o | G | o \rangle = (E_\pi - K_\pi + i\epsilon)^{-1}$.)

---

[1] We assume an infinitely heavy nucleus here so the nuclear kinetic energy terms are not present.

The Hamiltonian for the bound nucleon in our 3-body problem was $H_N = K_N + U_N$. If we use an independent particle model for the nucleus and single out one of the nucleons (call it nucleon #1), we obtain the one-particle Hamiltonian $H_1 = K_1 + U_1$. We therefore define a t-matrix $t_1 \equiv t_{3B}$ in terms of H_1 and $v_{\pi N}$

$$t_{3B} = v_{\pi N} + v_{\pi N} G_1 t_{3B} \tag{E.14}$$

where $G_1 = (E_1 + E_\pi - K_1 - U_1 - K_\pi + i\epsilon)^{-1}$.

The t-matrix t_{3B} is the same t-matrix that was calculated in Chapter VIII. (In Chapter VIII we denote the 3-body t-matrix as $T_{\pi N}$. Here we use the notation t_{3B} to avoid confusion with the t-matrix in equation (E.1) .) Hence, we now want to see if $\langle 0|G_1|0\rangle \stackrel{?}{=} \langle 0|G|0\rangle = (E_\pi - K_\pi + i\epsilon)^{-1}$.

Since G_1 is a one-nucleon operator and $|0\rangle$ is an antisymmetric nuclear (many-body) state, we have

$$\langle 0|G_1|0\rangle = \frac{1}{A}\sum_{\alpha=1}^{A} \frac{1}{E_\pi - K_\pi + (E_1 - E_\alpha) + i\epsilon} \tag{E.15}$$

Where α indicates the occupied single-particle states and E_α is the single-particle energy. In an independent-particle picture of the ^{4}He ground state, all the occupied single particle states have

the same energy E_1 , so for that case we have the required result:

$$\langle 0|G_1|0\rangle_{^4He} = (E_\pi - K_\pi + i\epsilon)^{-1}.$$

Hence, for ^{4}He, we end up with the usual Lippmann-Schwinger equation for $T'_{\pi\nu}$ when we use the 3-body t-matrix, t_{3B} , to obtain the (first order) optical potential. For ^{12}C and ^{16}O, we have that

$$\langle 0|G_1|0\rangle \cong (E_\pi - K_\pi + i\epsilon)^{-1}$$

since we consider energies where $E_\pi >> (E_1 - E_d)$.

Further, in equation (E.6) the G_σ term is multiplied by 1/A . Hence, for ^{12}C and ^{16}O, we obtain an ordinary Lippmann-Schwinger equation to a very good approximation.

Thus we have shown that it is <u>possible</u> to use the 3-body t-matrix in the definition of the optical potential, but we have not shown that this procedure makes the first order optical potential (which is what we use for $U_{\pi\nu}$) a better approximation to the complete optical potential. To show that there is an improvement would require showing that the higher order terms are smaller for $U^0_{\pi\nu} = (A-1)\,t_{3B}$ than for $U^0_{\pi\nu} = (A-1)\,t_{\pi N}$. We therefore take a "try and see" attitude in this work, and require that the final justification come from a comparision with experiment.

APPENDIX F

CALCULATION OF BINDING CORRECTIONS USING VECTOR BRACKETS

The first binding correction term is given in our 3-body model by

$$\text{(F.1)}\quad \Delta t_{\pi N} = t_{33} g_0 R_N g_0 t_{33} .$$

In Chapter VIII we showed in a schematic way how this term is calculated. In this appendix we discuss the details of the calculation.

We want to calculate the matrix elements of $\Delta t_{\pi N}$ and average over the z-components of spin and isospin of target nucleon. Hence, we want to evaluate (we use $\langle \Delta t_{\pi N} \rangle$ to denote the matrix elements of $\Delta t_{\pi N}$)

$$\text{(F.2)}\quad \langle \Delta t_{\pi N} \rangle = \frac{1}{(2s^N+1)} \frac{1}{(2i^N+1)} \sum_{i_z^N s_z^N} \langle p_\pi' i_z^\pi | \langle \psi\, i_z^N s_z^N | \Delta t_{\pi N} | \psi\, i_z^N s_z^N \rangle | p_\pi i_z^\pi \rangle .$$

In equation (F.2), $|\psi i_z^N s_z^N\rangle \equiv |\psi\rangle |i_z^N\rangle |s_z^N\rangle$ where $|\psi\rangle$ denotes the wavefunction for the bound (s-wave) nucleon; s_z^N and i_z^N are the z-components of the nucleon

spin and isospin respectively. The initial and final pion momenta are $\underset{\sim}{p}_\pi$ and $\underset{\sim}{p}'_\pi$ respectively and i^π_z is the z-component of the pion isospin; also we define $|\underset{\sim}{p}_\pi i^\pi_z\rangle \equiv |\underset{\sim}{p}_\pi\rangle |i^\pi_z\rangle$. Since all the operators in $\Delta t_{\pi N}$ are diagonal with respect to the total isospin $\underset{\sim}{I} = \underset{\sim}{i}^\pi + \underset{\sim}{i}^N$, we can easily sum on i^N_z. We first write the isospin state $|i^\pi i^\pi_z\rangle |i^N i^N_z\rangle$ as

$$(F.3)\quad |i^\pi i^\pi_z\rangle |i^N i^N_z\rangle = \sum_{I I_z} \langle I I_z | i^\pi i^N i^\pi_z i^N_z\rangle |I I_z\rangle .$$

Then we calculate

$$(F.4)\quad \langle \Delta t_{\pi N}\rangle = \frac{1}{2\Delta^N+1}\frac{1}{2i^N+1}\sum_{I I_z}\sum_{i^N_z \Delta^N_z} \langle I I_z | i^\pi i^N i^\pi_z i^N_z\rangle^2 \langle I I_z | K \underset{\sim}{p}'_\pi K \psi \Delta^N_z | \Delta t_{\pi N} | \psi \Delta^N_z\rangle |\underset{\sim}{p}_\pi\rangle |I I_z\rangle .$$

The matrix elements of $\Delta t_{\pi N}$ are independent of I_z and

$$\text{(F.5)}\quad \sum_{I_z i^N_z} \langle i^\pi\, i^N\, i^\pi_z\, i^N_z \,|\, I I_z\rangle^2 = \frac{2I+1}{2i^\pi+1} \,.$$

So taking $I_z = 0$ we have

(F.6)

$$\langle \Delta t_{\pi N}\rangle = \sum_I \frac{2I+1}{(2i^N+1)(2i^\pi+1)} \sum_{\Delta^N_z} \frac{1}{2\Delta^N+1}$$

$$\times \langle I\, I_z=0 | \langle P'_{\underset{\sim}{\pi}} | \langle \psi\, \Delta^N_z | \Delta t_{\pi N} | \psi\, \Delta^N_z\rangle | P_{\underset{\sim}{\pi}}\rangle | I\, I_z=0\rangle$$

We assume the pion-nucleon interaction is only in the (3,3) channel so $I = 3/2$. Hence, we want

(F.7)

$$\langle \Delta t_{\pi N}\rangle = (2/3)\frac{1}{2\Delta^N+1} \sum_{\Delta^N_z} \langle P'_{\underset{\sim}{\pi}} | \langle \psi\, \Delta^N_z | \Delta t_{\pi N} | \psi\, \Delta^N_z\rangle | P_{\underset{\sim}{\pi}}\rangle$$

The sum over the nucleon spin can also be easily done, but it is not quite as straightforward as for the isospin. First, we write the state $|\psi_0\, \Delta^N_z\rangle | P_{\underset{\sim}{\pi}}\rangle$ as

(F.8)

$$|\psi\, A^N_z\rangle |p_{\pi}\rangle = \sum_{\substack{jj_z \\ L_\pi M_\pi A^N_z}} \langle jj_z | L_\pi A^N M_\pi A^N_z \rangle \times \int \frac{p_N'^2 dp_N'}{(2\pi)^3} R_{00}(p_N') |p_\pi p_N' jj_z \mathcal{L} L_\pi L_N = 0\rangle$$

In equation (F.8), $\mathcal{L} = L_\pi$ since $L_N = 0$. (We use this redundant notation in order to be consistent with the notation in Appendix D.) The function $R(p_N')$ is defined by

$\psi(p_N') = R(p_N') Y_{00}(\hat{p}_N)$, i.e., $R(p_N')$ is the "radial" part of the momentum space wavefunction. Using the expansion in equation (F.8) we have

$$\text{(F.9)}\quad \langle \Delta t_{\pi N} \rangle = \frac{2}{3} \frac{1}{2A^N + 1} \sum_{\substack{jj_z \\ L_\pi M_\pi \\ L'_\pi M'_\pi \\ A^N_z}} \langle L'_\pi A^N M'_\pi A^N_z | jj_z \rangle \langle jj_z | L_\pi A^N M_\pi A^N_z \rangle \times Y_{L'_\pi M'_\pi}(\hat{p}'_\pi) Y^*_{L_\pi M_\pi}(\hat{p}_\pi) \int \frac{p_N'^2 dp_N}{(2\pi)^3} \int \frac{p_N^2 dp_N}{(2\pi)^3} R(p_N') R(p_N) \times \langle p'_\pi p_N' jj_z \mathcal{L}' L'_\pi L'_N = 0 | \Delta t_{\pi N} | p_\pi p_N jj_z \mathcal{L} L_\pi L_N = 0 \rangle$$

Now conservation of total angular momentum and conservation of parity require $L'_\pi = L_\pi = \ell = \ell'$ (Recall the nucleon wavefunction is s-wave.) Also, $\langle \Delta t_{\pi N} \rangle$ is independent of j_z, so using the fact that

$$\text{(F.10)} \quad \sum_{\substack{\Lambda_z^N \\ j_z}} \left| \langle L_\pi \Lambda^N M_\pi \Lambda_z^N | j j_z \rangle \right|^2 = \frac{2j+1}{2L_\pi+1}$$

and

$$\text{(F.11)} \quad \sum_{M_\pi} Y_{L_\pi M_\pi}(\hat{p}_\pi) Y_{L_\pi M_\pi}(\hat{p}'_\pi) = \frac{2L_\pi+1}{4\pi} P_{L_\pi}(\hat{p}_\pi \cdot \hat{p}'_\pi)$$

we have

$$\text{(F.11)} \quad \langle \Delta t_{\pi N} \rangle = \frac{1}{12\pi} \sum_{j L_\pi} (2j+1) P_{L_\pi}(\hat{p}'_\pi \cdot \hat{p}_\pi)$$

$$\times \int \frac{p_N'^2 dp'_N}{(2\pi)^3} \int \frac{p_N^2 dp_N}{(2\pi)^3} R_{00}(p'_N) R_{00}(p_N)$$

$$\times \langle p'_\pi p'_N j j_z \mathcal{I} L_\pi L_N = 0 | \Delta t_{\pi N} | p_\pi p_N j j_z \mathcal{I} L_\pi L_N = 0 \rangle$$

At this point we take advantage of the separable form for R_N (see Chapter VIII) by writing $g_0 R_N g_0$ as

(F.13)

$$g_0 R_N g_0 = \sum_{\substack{J'' L_\pi'' \\ \gamma'' \gamma_2''}} \int \frac{p_\pi''^2 dp_\pi''}{(2\pi)^3} \frac{p_N''^2 dp_N''}{(2\pi)^3} \frac{p_N'''^2 dp_N'''}{(2\pi)^3}$$

$$\times |p_\pi'' p_N'' \gamma'' \gamma_2'' J'' L_\pi'' L_N'' = 0\rangle g_0(E, p_\pi'', p_N'') \mathcal{U}_N(p_N'')$$

$$\times \lambda r_N(E - K_\pi(p_\pi'')) \times \mathcal{U}_N(p_N''') g_0(E, p_\pi''', p_N''')$$

$$\times \langle p_\pi'' p_N'' \gamma'' \gamma_2'' J'' L_\pi'' L_N'' = 0 |$$

(Note: $J'' = L_\pi''$ since $L_N'' = 0$)

Inserting the above form for $g_0 R_N g_0$ we obtain

(Again, by conservation of angular momentum and parity, $L_\pi = L_\pi''$.)

(F.14)

$$\langle \Delta t_{\pi N} \rangle = \frac{1}{12\pi} \sum_{\gamma L_\pi} (2\gamma + 1) \int \frac{p_\pi''^2 dp_\pi''}{(2\pi)^3} \lambda r_N(E - K_\pi(p_\pi''))$$

$$\times B(p_\pi' p_\pi'' \gamma L_\pi) B(p_\pi p_\pi'' \gamma L_\pi)$$

where

$$(F.15)\quad B(P_\pi P_\pi'' \mathcal{J} L_\pi) =$$

$$\int_0^\infty \frac{P_N'^2 dP_N}{(2\pi)^3} \int_0^\infty \frac{P_N''^2 dP_N''}{(2\pi)^3} R(P_N') g_0(E, P_\pi'', P_N'') \mathcal{U}_N(P_N'')$$

$$\times \langle P_\pi' P_N' \mathcal{J} J_z \mathcal{J} L_\pi L_N = 0 | t_{33} | P_\pi'' P_N'' \mathcal{J} J_z \mathcal{J} L_\pi L_N'' = 0 \rangle$$

The expression for $B(P_\pi P_\pi'' \mathcal{J} L_\pi)$ is quite similar to the impulse term calculated in Chapter III. Instead of $R(P_N') R(P_N'')$ we have $R(P_N') g_0(E, P_\pi'', P_N'') \mathcal{U}_N(P_N'')$ and we have t_{33} instead of $\bar{t}_{33}$. As with the impulse term in Chapter III, we insert a complete set of πNCM states on each side of t_{33}, i.e., we insert the unit operator

(F.16)

$$|k'' \chi'' \mathcal{J}'' J_z'' j_{k''} l_{k''} l_{\chi''}\rangle \sum_{\mathcal{J}'' J_z''} \iint \frac{k''^2 dk''}{(2\pi)^3} \frac{\chi''^2 d\chi''}{(2\pi)^3}$$

$$j_{k''} l_{k''} l_{\chi''}$$

$$\times \langle k'' \chi'' \mathcal{J}'' J_z'' j_{k''} l_{k''} l_{\chi''} | = 1$$

where $\mathcal{J}'' = \underset{\sim}{j}_{k''} + \underset{\sim}{l}_{\chi''}$ and $\underset{\sim}{j}_{k''} = \underset{\sim}{l}_{k''} + \underset{\sim}{1/2}$

The matrix elements of t_{33} for the above states are

(F.17)

$$\langle k'' \chi'' \gamma'' \gamma_z'' \, j_{k''} l_{k''} l_{\chi''} | t_{33} | k''' \chi''' \gamma''' \gamma_z''' \, j_{k'''} l_{k'''} l_{\chi'''} \rangle$$

$$= (2\pi)^3 \frac{\delta(\chi'' - \chi''')}{\chi''^2} \delta(\gamma'' \gamma''') \delta(\gamma_z'' \gamma_z''') \delta(j_{k''} j_{k'''}) \delta(j_{k''} 3/2)$$

$$\times \delta(l_{k''} l_{k'''}) \delta(l_{k''} 1) \delta(l_{\chi''} l_{\chi'''}) \times t_{33}(\omega_{cm} k'' k''')$$

where from Appendix B we have

(F.18)

$$t_{33}(\omega_{cm} k'' k''') = \gamma \, t_{33}(\omega_{cm} k_0 k_0) \frac{g_{33}(k'') g_{33}(k''')}{g_{33}^2(k_0)}$$

and

(F.19)

$$t_{33}(\omega_{cm} k_0 k_0) = \frac{-8\pi^2 \hbar^2 c^2}{\mu_R} \left(\frac{\eta_{33} e^{i\delta_{33}} - 1}{2i k_0} \right).$$

(See Appendix B for the details. The off-shell factor g_{33} should not be confused with the free particle propagator g_0 .) Using the separable form in equation (F.18) for t_{33} we obtain for B

(F.20)

$$B(p_\pi p_\pi'' J L_\pi) = \int \frac{x''^2 dx''}{(2\pi)^3} \frac{t_{33}(\omega_{CM}, k_0 k_0)}{g_{33}^2(k_0)}$$

$$\times B_1(p_\pi x'' J L_\pi) B_2(p_\pi'' x'' J L_\pi)$$

where

(F.21)

$$B_1(p_\pi x'' J L_\pi) =$$

$$\sum_{l_{x''}} \int \frac{k''^2 dk''}{(2\pi)^3} \int \frac{p_N'^2 dp_N'}{(2\pi)^3} R(p_N') g_{33}(k'')$$

$$\times \langle p_\pi p_N' J j_z = 0 \; J L_\pi L_N = 0 \; | k'' x'' J j_z \; j_{k''} = 3/2 \; l_{k''} = 1 \; l_{x''} \rangle$$

and

$$(F.22)\quad B_2(P_\pi'' \chi'' j L_\pi)$$

$$\sum_{l_\chi'''} \int \frac{k'''^2 dk'''}{(2\pi)^3} \int \frac{P_N''^2 dP_N''}{(2\pi)^3} u_N(P_N'') g_0(E\, P_\pi'' P_N'') g_{33}(k''')$$

$$\times \langle P_\pi'' P_N'' j j_z l L_\pi L_N'' = 0 \,|\, k''' \chi'' j j_z j = 3/2\; l_{k''} = 1\; l_{\chi'''} \rangle$$

The vector bracket expression in equation (F.21) and (F.22) is given in equation (D.19) of Appendix D. The quantities B_1 and B_2 are evaluated in the same way as the $\mathcal{F}_{IJl_k}$ factor of the impulse term (see section 3 of Chapter III). Proceeding as in the impulse term we obtain for B_1 and B_2

$$(F.23)\quad B_i(P_\pi \chi j L_\pi) = -(4\pi)^2 \sum_{l_\chi} (-1)^{j + l_\chi + 1/2}$$

$$\times \begin{Bmatrix} 1/2 & 1 & 3/2 \\ l_\chi & j & L_\pi \end{Bmatrix} \frac{1}{\sqrt{2L_\pi + 1}} \int_{-1}^{1} dx\, f_i \left[\frac{\omega_\pi(k)\omega_N(k)}{\omega_\pi(P_\pi)\omega_N(P_N)} \right]^{1/2}$$

$$\times \sum_{m=-L_\pi}^{L_\pi} \left\{ \left[\sum_{\substack{m_k \\ m_\chi}} \langle 1\, l_\chi\, m_k\, m_\chi | L_\pi m \rangle\, Y_{1 m_k}(\hat{k}) Y_{l_\chi m_\chi}(\hat{\chi}) \right]^* \times \left[Y_{L_\pi m}(\hat{P}_\pi)\, Y_{00}(\hat{P}_N) \right] \right\}$$

Where f_i is $R(P_N) g_{33}(k)$ for $i=1$ and $u_N(P_N) g_0(E P_\pi P_N) g_{33}(k)$ for $i=2$. The variable x is $\hat{P}_\pi \cdot \hat{k}$.

Using the results from equations (F.14), (F.20) and (F.23) and regrouping some of the factors, we have finally for $\langle \Delta t_{\pi N} \rangle$

$$(F.24)\quad \langle \Delta t_{\pi N} \rangle = \frac{32}{3\pi^2} \sum_{\substack{L_\pi j \\ l_x l_{x'}}} \frac{2j+1}{(2L_\pi+1)^2} P_{L_\pi}(\hat{P}'_\pi \cdot \hat{P}_\pi)$$

$$\times \begin{Bmatrix} 1/2 & 1 & 3/2 \\ l_x & j & L_\pi \end{Bmatrix}^2 \begin{Bmatrix} 1/2 & 1 & 3/2 \\ l_{x'} & j & L_\pi \end{Bmatrix} \int_0^\infty P''^2_\pi \, dP''_\pi \, \lambda r(E - K_\pi(P''_\pi))$$

$$\times \beta(P_\pi P''_\pi L_\pi l_x) \beta(P'_\pi P''_\pi L_\pi l_{x'})$$

The function β is given by

(F.25)

$$\beta(P_\pi P''_\pi L_\pi l_x) = \int_0^\infty x''^2 \, dx'' \, \frac{t_{33}(\omega_{cm} k_0 k_0)}{g^2_{33}(k_0)}$$

$$\times \Gamma_1(P_\pi x'' L_\pi l_x) \Gamma_2(P''_\pi x'' L_\pi l_x)$$

where

(F.26)

$$\Gamma_i(P_\pi \chi'' L_\pi l_\chi) = \int_{-1}^{1} dx\, f_i \left[\frac{\omega_\pi(k)\omega_N(k)}{\omega_\pi(P_\pi)\omega_N(P_N)}\right]$$

$$\times \sum_{m=-L_\pi}^{L_\pi} \left\{ \left[\sum_{m_k m_\chi} \langle 1\, l_\chi\, m_k\, m_\chi | L_\pi m \rangle Y_{1 m_k}(\hat{k}) Y_{l_\chi m_\chi}(\hat{\chi}) \right]^* \left[Y_{L_\pi m}(\hat{P}_\pi) Y_{00}(\hat{P}_N) \right] \right\}$$

As before, $f_1 = R(P_N) g_{33}(k)$ and $f_2 = u_N(P_N) g_0(E P_\pi P_N) g_{33}(k)$. The integration variable x is $\hat{P}_\pi \cdot \hat{\chi}''$.

In order to avoid the singularities on the real axis, the integrals over P_π'' and χ are taken along complex contours by making the substitution $P_\pi'' \rightarrow P_\pi'' e^{i\varphi}$ and $\chi'' \rightarrow \chi'' e^{i\varphi}$. The validity of this procedure is discussed by Hetherington and Schick (Het65).

APPENDIX G

SOLUTION OF THE

LIPPMANN-SCHWINGER EQUATION

Haftel and Tabakin have developed a simple matrix method for solving the Lippman-Schwinger equation in momentum space (Haf70). We present here a modified version of their method. Our method does not involve "subtracting out" the singularity in the free two-particle green function and produces the transition matrix itself rather than the phase shifts.

The Lippmann-Schwinger equation for two spinless particles interacting via an arbitrary potential V is given by

$$(G.1)\quad T(\omega_0, \underset{\sim}{p}', \underset{\sim}{p}) = V(\underset{\sim}{p}', \underset{\sim}{p}) + \int \frac{V(\underset{\sim}{p}', \underset{\sim}{p}'') T(\omega_0, \underset{\sim}{p}'', \underset{\sim}{p})}{\omega_0 - \omega(\underset{\sim}{p}'') + i\epsilon} \frac{d^3 p''}{(2\pi)^3}$$

where $\underset{\sim}{p}$ and $\underset{\sim}{p}'$ are respectively the initial and final momenta[1] in the two particle center-of-mass frame. The energy variable $\omega(p'')$ is given by

$$(G.2)\quad \omega(\underset{\sim}{p}'') = m_1 c^2 + m_2 c^2 + \hbar^2 \underset{\sim}{p}''^2 / 2m_1 + \hbar^2 \underset{\sim}{p}''^2 / 2m_2$$

for the nonrelativistic case and by

---

[1] As in previous sections, the momenta here are actually wave numbers.

$$\omega(\underset{\sim}{p}'') = \left(m_1^2c^4 + \hbar^2c^2\,\underset{\sim}{p}''^2\right)^{1/2} + \left(m_2^2c^4 + \hbar^2c^2\,p''^2\right)^{1/2} \tag{G.3}$$

in the relativistic case. The energy parameter ω_0 is related to the on-shell momentum $\underset{\sim}{p}_0$ by

$$\omega_0 = \omega(\underset{\sim}{p}_0) \tag{G.4}$$

where $\omega(p_0)$ is given by equation (G.2) for the nonrelativistic case and by equation (G.3) for the relativistic case.

For a central potential, we have after a partial wave expansion

$$T_L(\omega_0, p'p) = V_L(p'p) + \int_0^\infty \frac{V_L(p'p'')\,T_L(\omega_0, p''p)}{\omega_0 - \omega(p'') + i\epsilon}\,\frac{p''^2 dp''}{(2\pi)^3} \tag{G.5}$$

where

$$V(\underset{\sim}{p}'\underset{\sim}{p}) = \sum_L \left(\frac{2L+1}{4\pi}\right) V_L(p'p)\,P_L(\hat{p}'\cdot\hat{p}) \tag{G.6}$$

$$T(\omega_0, \underset{\sim}{p}'\underset{\sim}{p}) = \sum_L \left(\frac{2L+1}{4\pi}\right) T_L(\omega_0, p'p)\,P_L(\hat{p}'\cdot\hat{p}) \tag{G.7}$$

The momentum variables without $\sim$ in equations (G.5) - (G.7) denote the magnitudes of the vector momenta.

By rationalizing the denominator of the integral in equation (G.5) we obtain

$$(G.8)\quad T_L(\omega_0, p'p) = V_L(p'p) + \int_0^\infty \frac{\beta(p_0 p'') V_L(p'p'') T_L(\omega_0, p''p)}{p_0^2 - p''^2 + i\epsilon} \frac{p''^2 dp''}{(2\pi)^3}$$

where

$$(G.9)\quad \beta(p_0 p'') = \frac{2 m_1 m_2}{m_1 + m_2} \frac{1}{\hbar^2}$$

for the nonrelativistic case and

$$(G.10)\quad \beta(p_0 p'') = \left[\frac{(\omega_1(p_0) + \omega_1(p''))(\omega_2(p_0) + \omega_2(p''))}{\omega_1(p_0) + \omega_1(p'') + \omega_2(p_0) + \omega_2(p'')}\right] \frac{1}{\hbar^2 c^2}$$

for the relativistic case.

In equation (G.10) the energies ω_1 and ω_2 are given by

$$(G.11)\quad \omega_i(p) = \left(m_i^2 c^4 + \hbar^2 c^2 p^2\right)^{1/2} \qquad i = 1, 2$$

Using the identity

$$\text{(G.12)}\quad \frac{dx}{x-x_0-i\epsilon} = PP\ \frac{dx}{x-x_0} + i\pi\,\delta(x-x_0)$$

we can write equation (G.8) as

(G.13)

$$T_L(\omega_0, p'p) = V_L(p'p) - \frac{i\pi p_0}{2(2\pi)^3}\beta(p_0 p_0) V_L(p' p_0) T_L(\omega_0, p_0 p)$$

$$- PP\int_0^\infty \frac{\beta(p_0 p'') V_L(p' p'') T_L(\omega_0, p'' p)}{p''^2 - p_0^2}\ \frac{p''^2 dp''}{(2\pi)^3}$$

We now obtain a finite integral by making the substitution $p'' = p_0\left(\frac{1+x}{1-x}\right)$. Also, we are interested only in the half-off-shell t-matrix, $T(\omega_0, p', p_0)$, so we consider the equation

(G.14)

$$T_L(\omega_0, p' p_0) = V_L(p' p_0) + \frac{i\pi p_0}{2(2\pi)^3}\beta(p_0 p_0) V_L(p p_0) T_L(\omega_0, p_0\ p_0)$$

$$- \frac{1}{2p_0} PP\int_{-1}^{1} \frac{\beta(p_0 p'') V_L(p' p'') T_L(\omega_0, p'' p_0)}{x}\ \frac{p''^2 dx}{(2\pi)^3}$$

Let us now digress for a moment and consider just the principal-value integral in equation (G.14). In a Gaussian formulation of numerical integration we have the quadrature rule

$$\text{(G.15)} \quad \int_A^B \Omega(x) f(x) dx \cong \sum_{i=1}^{N} W_i f(x_i)$$

where $f(x)$ is an arbitrary function to be integrated and $\Omega(x)$ is a preassigned weight function. The weights W_i and points x_i are found by requiring the moments $\mathcal{M}_m$

$$\text{(G.16)} \quad \int_A^B \Omega(x) x^m dx = \sum_{i=1}^{N} W_i x_i^m \equiv \mathcal{M}_m$$

be exact for m equal zero to $2N-1$ so that equation (G.16) is exact if $f(x)$ is a polynomial of order $\leq 2N-1$. For Gauss-Legendre integration we would take $\Omega(x)=1$ and $[A, B] = [-1, 1]$. In our principal-value integral in equation (G.14) we can choose the weight function to be $1/x$. With this weight function and N even, we obtain the result[1]

$$\text{(G.17)} \quad x_i^{PV} = x_i^{GAUSS}$$

---

[1] For N odd, the "center" x_i is zero, so the center weight is not defined.

$$(G.18)\quad W_i^{PV} = W_i^{GAUSS} / X_i^{GAUSS}$$

where "PV" refers to $\Omega(x) = 1/x$ and "Gauss" refers to $\Omega(x) = 1$.

Thus, an N-point Gauss-Legendre evaluation of integrals of the form $\int f(x)\,dx/x$ is exact if $f(x)$ is a polynomial of order $\leq 2N-1$ (N even), provided the points are taken symmetrically about $x = 0$.

For convenience, we now make the following definitions:

$$(G.19)\quad T_L(\omega_0, P_i P_0) \equiv T_i$$

$$(G.20)\quad V_L(P_i P_j) \equiv V_{ij}$$

$$(G.21)\quad \beta(P_0, P_i) \equiv \beta_i$$

where $P_i = P_0(1 + X_i^{GAUSS})/(1 - X_i^{GAUSS})$.

We call P_0 the $N + 1$ point, and write equation (G.14) as

(G.22)

$$T_i = V_{i,N+1} - \frac{\sqrt{-1}\,\pi P_{N+1}}{2(2\pi)^3}\,\beta_{N+1}\,V_{i,N+1}\,T_{N+1}$$

$$- \frac{1}{2P_{N+1}} \sum_{j=1}^{N} \left(P_j^2 / (2\pi)^3 \right) \beta_j V_{ij} T_j W_j^{GAUSS} / X_j^{GAUSS}$$

We further define weights

$$W_j = \begin{cases} - \dfrac{1}{2P_{N+1}} \dfrac{P_j^2}{(2\pi)^3}\,\beta_j \left(W_j^{GAUSS} / X_j^{GAUSS} \right) & j = 1,N \\ - \dfrac{\sqrt{-1}\,\pi P_{N+1}}{2(2\pi)^3}\,\beta_j & j = N+1 \end{cases} \tag{G.23}$$

so that equation (G.22) can be written

$$T_i = V_{i,N+1} + \sum_{j=1}^{N+1} W_j V_{ij} T_j \,. \tag{G.24}$$

Or equivalently,

$$(G.25)\quad \sum_{j=1}^{N+1} (\delta_{ij} - W_j V_{ij}) T_j = V_{i,N+1} .$$

Equation (G.25) defines a system of complex equations which we solve by Gauss elimination.

In order to check the accuracy of our method we calculated differential elastic cross sections for several different local optical potentials using our method and the optical potential code GIBELUMP (Doe73). We found that 16 points gave results that agreed with the GIBELUMP results to 3 digits. In addition, the pion-nucleus differential cross sections calculated with 16 and 24 points agreed with each other to three digits. Hence, we feel that our code produces reliable results for the cases calculated in this work.